

Deep Australia

**Understanding plate architecture and evolution
of the transition between Proterozoic Australia
and the eastern margin of Gondwana**

by

Giovanni Pietro Tommaso Spampinato, MSc

A thesis submitted for the degree of

DOCTOR OF PHILOSOPHY

at

Monash University

School of Earth, Atmosphere and Environment

2014

Copyright Notices

Notice 1

Under the Copyright Act 1968, this thesis must be used only under the normal conditions of scholarly fair dealing. In particular no results or conclusions should be extracted from it, nor should it be copied or closely paraphrased in whole or in part without the written consent of the author. Proper written acknowledgement should be made for any assistance obtained from this thesis.

Notice 2

I certify that I have made all reasonable efforts to secure copyright permissions for third-party content included in this thesis and have not knowingly added copyright content to my work without the owner's permission.

To my mother and father

To Clara

To Dana

TABLE OF CONTENTS

LIST OF FIGURES	11
ACKNOWLEDGEMENTS	17
ABSTRACT.....	23
THESIS OUTLINE.....	27
1. Chapter 1 - Introduction.....	31
1.1 Study area	32
1.2 Aim	34
1.3 Publication arising from this research	36
1.3.1 Journal articles	36
1.3.2 Conference abstracts	37
1.3.3 Seminars.....	37
1.3.4 Manual	37
2. Chapter 2 - Methodology	39
2.1 Potential field data	40
2.2 Gravity data.....	40
2.2.1 Latitude correction	41
2.2.2 Tides and instrumental drift.....	41
2.2.3 Free air anomaly	42
2.2.4 Bouguer Anomaly.....	42
2.2.5 Applications and limitations of gravity data.....	44
2.3 Magnetic Data.....	44
2.3.1 Magnetic susceptibility	45
2.3.2 Curie Temperature	47

2.3.1	Remanent magnetization	48
2.3.1	Total magnetic field	48
2.3.2	Applications and limitations of magnetic data	49
2.4	Geophysical coverage	50
2.4.1	Mount Isa terrane	50
2.4.2	Thomson Orogen	51
2.5	Image processing	52
2.6	Image interpretation	53
2.7	Geological constraints	54
2.7.1	Deep Seismic Surveys	55
2.7.2	Drillholes	55
2.7.3	Other geophysical constraints	56
2.8	Forward modelling	56
Declaration for Thesis Chapter 3		59
3.	Chapter 3: Structural architecture of the southern Mount Isa terrane in Queensland inferred from Magnetic and Gravity data	63
ABSTRACT		64
3.1	Introduction	65
3.2	Regional geology	67
3.2.1	Ca. 1900 – 1840 Ma crystalline basement	67
3.3	Pre - 1600 Ma Basinal Evolution	70
3.3.1	1790 - 1730 Ma Leichhardt Superbasin	70
3.3.2	1725 - 1690 Ma Calvert Superbasin	71
3.3.3	1675 – 1595 Ma Isa Superbasin	74
3.3.4	The Isan Orogeny	75

3.4 Previous geophysical surveys	78
3.5 Methods	82
3.5.1 Rock Properties.....	83
3.6 Observations and results	84
3.6.1 Geophysical boundaries	85
3.6.2 Leichhardt River Domain	86
3.6.3 Kalkadoon-Leichhardt Domain	88
3.6.4 Mitakoodi Domain.....	89
3.6.5 Kuridala - Selwyn Domain	91
3.6.6 Soldiers Cap Domain.....	92
3.7 Discussion.....	94
3.8 Interpretation of the geophysical signature of the southern Mount Isa terrane	95
3.8.1 Leichhardt River Domain	95
3.8.2 Kalkadoon-Leichhardt Domain	99
3.8.3 Mitakoodi Domain.....	101
3.8.4 Kuridala - Selwyn Domain	104
3.8.5 Soldiers Cap Domain.....	106
3.8.6 Cork Fault Zone	110
3.9 Conclusions.....	112
Declaration for Thesis Chapter 4	115
4. Chapter 4: Early tectonic evolution of the Thomson Orogen in Queensland inferred from constrained magnetic and gravity data.....	119
ABSTRACT	120
4.1 Introduction.....	121
4.2 Geological setting	123

4.3 Previous geophysical surveys	129
4.4 Methods	133
4.5 Observations and results	134
4.5.1 Cork Fault	134
4.5.2 Diamantina River Domain	135
4.5.3 Maneroo Platform	135
4.5.4 Southeast Thomson Orogen	136
4.5.5 Canaway Ridge	136
4.5.6 Adavale Basin	137
4.5.7 Nebine Ridge	137
4.5.8 Westgate Trough	138
4.5.9 Cooladdi Trough	139
4.5.10 Cheepie Shelf	139
4.5.11 Quilpie Trough	139
4.5.12 Warrabin Trough	140
4.5.13 Barcoo Trough	140
4.5.14 Western Thomson Orogen	141
4.5.15 Barrolka Trough and Cooper Basin	141
4.6 Interpretation	142
4.6.1 Cork Fault	142
4.6.2 Diamantina River Domain	143
4.6.3 Maneroo Platform	145
4.6.4 Canaway Ridge	145
4.6.5 Eastern Thomson Orogen	146
4.6.6 Devonian sedimentary basins	146

4.6.7	Western Thomson Orogen	147
4.6.8	Regional interpretation	147
4.7	Late Proterozoic to Middle Palaeozoic tectonic evolution of the Thomson Orogen.....	149
4.7.1	The Rodinia break-up	149
4.7.2	Middle Cambrian to Late Silurian	153
4.7.3	Devonian extension.....	156
4.8	A global perspective	158
4.9	Conclusions.....	160
	Declaration for Thesis Chapter 5	163
5.	Chapter 5: Crustal architecture of the Thomson Orogen in Queensland inferred from forward modelling technique	167
	ABSTRACT	168
5.1	Introduction.....	168
5.2	Geological background.....	170
5.3	Previous geophysical surveys	173
5.3.1	Nebine Ridge	176
5.3.2	Magnetotelluric survey	176
5.3.3	Tomographic data	177
5.4	Evolutionary models	177
5.5	Method.....	178
5.6	Observation and results.....	179
5.6.1	Regional geophysical signature of the Thomson Orogen	179
5.7	Forward models	182
5.7.1	Forward model n. 1	182
5.7.2	Forward model n. 2.....	185

5.7.3	Forward model n. 3.....	188
5.7.4	Forward model n. 4.....	191
5.8	Regional architecture of the Thomson Orogen.....	194
5.9	Crustal architecture of the Thomson Orogen.....	194
5.9.1	The Thomson Orogen as a single feature	195
5.9.2	Thomson Orogen Vs. Lachlan Orogen.....	196
5.9.3	Thomson Orogen Vs. Mount Isa terrane	197
5.10	The crustal nature of the lower crust	198
5.11	Conclusions.....	199
	Declaration for Thesis Chapter 6.....	203
6.	Chapter 6: Imaging the basement architecture across the Cork Fault in Queensland using magnetic and gravity data.....	207
	ABSTRACT.....	208
6.1	Introduction.....	208
6.2	Regional geology.....	210
6.2.1	The Mount Isa terrane.....	210
6.2.2	The Thomson Orogen	213
6.3	Previous geophysical surveys	215
6.3.1	The Mount Isa terrane.....	215
6.3.2	The Thomson Orogen	217
6.3.3	The Cork Fault zone	218
6.4	Methods	220
6.4.1	Image interpretation.....	220
6.4.2	Forward modelling.....	221
6.5	Geophysical signature of the region	222

6.6 Regional interpretation	225
6.7 Forward models	228
6.7.1 Forward model n. 1	229
6.7.2 Forward model n. 2	231
6.7.3 Forward model n. 3	234
6.8 Validity of the interpretation.....	236
6.9 Discussion.....	237
6.9.1 Timing of initiation and reactivation of the Cork Fault.....	237
6.10 Conclusions.....	242
7. Chapter 7: Synthesis and Conclusion	247
7.1 Chapter 3 – Tectonic evolution of the southern Mount Isa terrane	247
7.2 Chapter 4 – Tectonic evolution of the Thomson Orogen	249
7.3 Chapter 5 – Nature of the lower crust of the Thomson Orogen	251
7.4 Chapter 6 – The tectonic significance of the Cork Fault	252
REFERENCES	257
Appendix A.....	277
Appendix B.....	285

LIST OF FIGURES

Fig 2.1 Densities of common rocks and ore minerals.....	43
Fig 2.2 Magnetic susceptibilities of common rocks and ores.....	51
Fig 2.3 Regional (400 m or better line spacing) state and federal airborne geophysical coverage in the area of study.....	51
Fig. 3.1 Simplified tectonic map showing the exposed Mount Isa Inlier, the Mount Isa Geophysical Domain and some of the surrounding geological provinces.....	66
Fig. 3.2 Tectonic framework of the exposed Mount Isa Inlier	69
Fig. 3.3 Stratigraphic space - plot showing the timing of major depositional packages and major deformation and magmatic events	73
Fig. 3.4 Map of the geological domains and major structural features of the southern Mount Isa terrane	77
Fig. 3.5 Location of the 2006 Deep Seismic Transects across the Mount Isa terrane and rock magnetic property data from hand samples and drillholes over a TMI map	78
Fig. 3.6 Deep Seismic Transects N. 06GA-M6	80
Fig. 3.7 Southwest end of the Deep Seismic Profile 07GA-IG1	81
Fig. 3.8 Major Rock type densities and susceptibilities of the Mount Isa region.....	84
Fig. 3.9 Context map showing the geological provinces surrounding the Mount Isa Geophysical Domain and major structures within the area of study over a a) RTP map and b) Bouguer Gravity map.....	85
Fig. 3.10 RTP magnetic map of the southern Mount Isa terrane along with its geophysical sub-domains.....	86
Fig. 3.11 Bouguer gravity map of the southern Mount Isa terrane along with its geophysical sub-domains.....	87
Fig. 3.12 composite RTP and tilt derivative magnetic map of the southern Mount Isa terrane along with its geophysical subdomains.	91

Fig. 3.13 Tilt derivative Bouguer map of the southern Mount Isa terrane along with its geophysical sub-domains.....	93
Fig. 3.14 Fault architecture of the southern Mount Isa Geophysical Domain constrained by the Deep Seismic Transect 06GA-M6 over a RTP and tilt derivative magnetic map.....	95
Fig. 3.15 Map showing some structure active during the ca. 1870–1850 Ma Barramundi Orogeny	99
Fig. 3.16 Map showing major structures that accommodated the ca. 1800 – 1740 Ma Leichhardt Superbasin sedimentation	103
Fig. 3.17 Map showing major structures active during the ca. 1720 – 1600 Ma Calvert to Isa Superbasin extension	106
Fig. 3.18 Map showing major structures active during the ca. 1570 – 1550 Ma Middle Isan Orogeny	109
Fig. 3.19 Map showing some structures active during the ca. 1550 – 1540 Ma wrenching phase of the Isan Orogeny	109
Fig. 3.20 Lithological interpretation map of the southern Mount Isa terrane.....	111
Fig. 4.1 Area of study over a Bouguer gravity map of the Australian continent.....	122
Fig. 4.2 Sketch showing the distribution of major geological features and the extension of the geological provinces surrounding the Thomson Orogen.....	125
Fig 4.3 Map of the geological domains and major structures of the Thomson Orogen.....	126
Fig. 4.4 Time – space diagram illustrating the major depositional units of the Thomson Orogen	128
Fig. 4.5 Location of the BMR deep seismic profiles and drill holes along with major known structures over a composite RTP and tilt derivative magnetic map of the Central Eromanga Basin.	130
Fig. 4.6 Interpreted seismic zones along the traverses 1 and 9 of the BMR seismic sections.....	131
Fig. 4.7 Fault architecture along the Deep Seismic section n. 6.....	131
Fig. 4.8 Seismic reflection sections showing the structural setting of the Quilpie, Warrabin and Barcoo troughs.....	132

Table 1 Major filters used in geophysical processing and their effect on the filtered grid	134
Fig 4.9 Map of the regional RTP magnetic anomalies of the Thomson Orogen and surrounding regions.....	136
Fig. 4.10 Map of the regional Bouger gravity anomalies in the Central Thomson Orogen	138
Fig. 4.11 Greyscale tilt derivative map of the Thomson Orogen and surrounding regions.....	140
Fig. 4.12 Composite map of the regional Bouger gravity anomalies, tilt derivative and vertical derivative magnetic anomalies of the southern Mount Isa terrane and the Thomson Orogen	142
Fig. 4.13 Interpreted shear zone in the eastern part of the Diamantina River Domain	144
Fig. 4.14 Lithological interpretation map of the Thomson Orogen.....	148
Fig. 4.15 Major structures from Greene (2010) and this study on a RTP magnetic map of the Thomson Orogen, Mount Isa terrane and eastern Arunta Province	150
Fig. 4.16 Tectonic setting of the Thomson Orogen during the Neoproterozoic Rodinia Break-up.	151
Fig. 4.17 RTP magnetic map of the Bourke – Brewarrina area with location of the drill holes ACDWE008 and ACDWE009	152
Fig. 4.18 Inferred tectonic setting of the Thomson Orogen during the Late Neoproterozoic to Early Cambrian.....	153
Fig. 4.19 Inferred Delamerian shortening.....	154
Fig. 4.20 Reconstruction of the Tasmanides accretionary event	155
Fig. 4.21 Interpreted Devonian tectonic evolution of the Thomson Orogen.....	157
Fig. 4.22 Alternative interpretations of extension direction postulated during the Neoproterozoic Rodinia break-up.....	158
Fig. 5.1 Location map showing the distribution of some of the eastern Australian orogens	169
Fig. 5.2 Time - space diagram illustrating the major depositional sequences along the Thomson Orogen and the Anakie Inlier during the Palaeozoic.....	172
Fig. 5.3 Map of the geological domains and major structural features of the Central Thomson Orogen	173

Fig. 5.4 Location of the BMR Central Eromanga Deep Seismic Transects and drill holes intersecting the basement in the Central Eromanga Basin over a composite Bouguer and tilt derivative magnetic map.....	174
Fig. 5.5 Traverses 1 and 9 of the BMR seismic sections along with the main structures	175
Fig. 5.6 Traverses 6 and 2 of the BMR seismic sections along with the main structures	176
Fig. 5.7 Images of the tomographic S-wave velocity models at 100 and 150 km depth over a map of the geological provinces of the Australian continent	177
Fig. 5.8 Bouguer gravity map of the Thomson Orogen and surrounding provinces	180
Fig. 5.9 RTP magnetic map of the Thomson Orogen and surrounding provinces	181
Fig 5.10 Forward model n. 1 along the Deep Seismic Transects n. 1 and 9.....	184
Fig 5.11 Forward model n. 2 along the Deep Seismic Transect n 3.....	187
Fig 5.12 Forward model n. 3 along the Deep Seismic Transects n . 6 and 2.....	190
Fig. 5.13 Forward model n. 4 along the Deep Seismic Transects n. 11	193
Fig. 5.14 Inferred nature of the crust under the Thomson and Lachlan orogens as proposed by A) Glen et al. (2013) and B) Musgrave (2013).....	196
Fig. 6.1 Area of study over a TMI magnetic grid.....	209
Fig. 6.2 a) Simplified tectonic setting of the exposed southern Mount Isa Inlier b) Simplified tectonic map showing the position and extent of the Mount Isa Inlier along with its geophysical domain; c) Distribution of some of the central and eastern Australian orogens.	211
Fig. 6.3 Time - space diagram illustrating the major depositional sequences along the Mount Isa terrane and the Thomson Orogen from the Palaeoproterozoic to Late Palaeozoic	214
Fig. 6.4 Map of the geological domains and major structural features of the southern Mount Isa terrane and the Thomson Orogen	215
Fig. 6.5 interpreted seismic transects 06GA-M6.....	216
Fig. 6.6 Deep Seismic Traverse n. 3 of the BMR Central Eromanga deep seismic sections along with the main structures.....	217

Fig. 6.7 Location of some of the 2006 Deep Seismic Transects crossing the Mount Isa terrane; 1980-1984 BMR Central Eromanga deep seismic reflection profiles; constraining drill holes over a composite RTP and tilt derivative magnetic map	218
Fig. 6.8 Approximate location of 4 seconds seismic surveys for oil exploration purpose	219
Fig. 6.9 RTP magnetic map of Central Queensland	223
Fig. 6.10 Bouguer gravity map of the boundary between the Mount Isa terrane and the Thomson Orogen	224
Fig. 6.11 Vertical derivative Bouguer gravity map over a grey tilt and vertical derivative magnetic map of the boundary between the Mount Isa terrane and the Thomson Orogen	225
Fig. 6.12 Lithological map at the junction of the Proterozoic Mount Isa terrane and the Phanerozoic Thomson Orogen.....	227
Fig. 6.13 Location of the forward models and constraining drill holes over a composite RTP and vertical derivative map.....	229
Fig. 6.14 Forward model n. 1.....	230
Fig. 6.15 Forward model n. 2.....	233
Fig. 6.16 Forward model n. 3.....	235
Fig. 6.17 Mid-Proterozoic Reconstruction of the Australian continent after a) Giles et al. (2004); b) Henson (2011) c) Gibson et al. (2008) d) Betts & Giles (2006)	239
Fig. 6.18 Sketch showing the inferred Early Cambrian shortening event within the Diamantina River Domain.....	241

ACKNOWLEDGEMENTS

I wish to express my sincere gratitude for all those who contributed in many ways to the success of this study and made it an unforgettable experience for me.

I would like to express my special appreciation and thanks to my supervisors Dr. Laurent Ailleres and Associate Professor Peter Betts for their support and friendship. With your patience and guidance you allowed me to grow as a research scientist. Pete, I owe you.

Professor Sandy Cruden, Dr. Fabio Capitanio and Dr. Andy Tomkins are thanked for serving as my panel members and for brilliant comments and suggestions.

I would like to thank Professor Chris Fergusson of Wollongong University for his valuable advice, constructive criticism and extensive discussions around my work.

The School of Geoscience and Monash University are gratefully acknowledged for providing financial support, infrastructure and resources to accomplish my research work.

Administrative and technical assistance was provided by Meghan Hough, Florita Henricus, Draga Gelt, Robert Douglass, Petrina Soh, Tien Chin Chen, Silvana Cifaratti, Dr. Massimo Raveggi and various staff at science faculty IT. A special thanks to Rob Oakley who has been a very supportive friend during my candidature.

Teagan Blaikie and Dr. Caroline Venn are thanked for contributing to the improvement of my chapters and for their constructive comments. Brenton Crawford, Tom Carmichael, Antoinette Stryk, David Moore, Mark Lindsay and the Structural Geophysics Group are thanked for their constant support.

Thanks to my office mate Roland Seubert for his friendship and many insightful discussions and suggestions.

A very special mention to Robin Armit. You have been a mentor and a friend. You gave me constant guidance and support over the years, I am indebted to you. You are a great geologist, a kind person and a true friend.

I would also like to thank all of my friends, with a special mention to Morena Salerno, who supported me in writing, and incited me to strive towards my goal.

I owe a lot to my parents. I miss my father Tommaso Spampinato who is not with me to share this joy. My mother Anna Spampinato gave me the strenght to achieve my goals over the years, thank you.

I would like express appreciation to the love of my life, Clara Marri who was always my support in the moments when there was no one to answer my queries. This is a piece of work of yours too, thank you.

General Declaration

Monash University

Declaration for thesis based or partially based on conjointly published or unpublished work

General Declaration

In accordance with Monash University Doctorate Regulation 17.2 Doctor of Philosophy and Research Master's regulations the following declarations are made:

I hereby declare that this thesis contains no material which has been accepted for the award of any other degree or diploma at any university or equivalent institution and that, to the best of my knowledge and belief, this thesis contains no material previously published or written by another person, except where due reference is made in the text of the thesis.

This thesis includes four unpublished publications. The core theme of the thesis is deciphering the crustal architecture of the concealed southern Mount Isa terrane and the Thomson Orogen using geophysical data. The ideas, development and writing up of all the papers in the thesis were the principal responsibility of myself, the candidate, working within the Monash University - School of Earth, Atmosphere and Environment under the supervision of Dr. Laurent Ailleres and Associate Professor Peter Betts.

In the case of four chapters my contribution to the work involved the following:

Thesis chapter	Publication title	Publication status*	Nature and extent of candidate's contribution
3	Structural architecture of the southern Mount Isa terrane in Queensland inferred from magnetic and gravity data	To be submitted	Processing and interpretation of gravity and aeromagnetic data; manuscript preparation (90%)
4	Early tectonic evolution of the Thomson Orogen in Queensland inferred from constrained magnetic and gravity data	To be submitted	Processing and interpretation of gravity and aeromagnetic data; manuscript preparation (90%)
5	Crustal architecture of the Thomson Orogen in Queensland inferred from forward modelling technique	To be submitted	Interpretation of gravity and magnetic data; 2D forward modelling; manuscript preparation (90%)
6	Imaging the basement architecture across the Cork Fault in Queensland using magnetic and gravity data	To be submitted	Interpretation of gravity and magnetic data; 2D forward modelling; manuscript preparation (90%)

I have / have not (circle that which applies) renumbered sections of submitted or published papers in order to generate a consistent presentation within the thesis.

Signed:

Date:

ABSTRACT

The basement rocks in central Queensland are largely obscured by the Phanerozoic sedimentary succession and the basement geology is known from limited drill holes. Constrained regional potential field analysis is applied to unveil the crustal architecture of the Proterozoic southern Mount Isa terrane and the Phanerozoic Thomson Orogen in Queensland.

The Mount Isa terrane forms part of the Palaeoproterozoic North Australian Craton. The exposed Mount Isa Inlier preserves geological record that spans more than 350 million years between ca. 1870 and 1500 Ma. An early cycle of a ca. 1870 Ma orogenesis and ca. 1870 Ma - 1850 Ma extensive batholith emplacement was succeeded by ca. 1800 - 1600 Ma superimposed rifting and subsidence. This was followed by major period of Mesoproterozoic orogeny. Constrained aeromagnetic and gravity data indicate that the depositional sequences and the regional architecture of the Mount Isa terrane extend for ~250 km south of the exposed Inlier, beneath Palaeozoic cover. In the southern parts of the Mount Isa terrane, Palaeoproterozoic sedimentation and volcanism were controlled by NNW-trending structures in half graben setting, resulting in complex superimposed and stacked basins prior to intense basin inversion associated with the Isan Orogeny. Petrophysically constrained geophysical interpretation indicates that prominent regional magnetic and gravity anomalies of the region reflect shallowing of the Pre-1800 Ma crystalline basement and the distribution of meta-sedimentary and meta-volcanic rocks deposited during the development of the ca. 1790 Ma to 1730 Ma Leichhardt Superbasin. Regional low magnetic and low gravity responses coincide with sedimentary successions deposited during the development of the Calvert and Isa superbasins. The ca. 1600 - 1500 Ma Isan Orogeny reactivated the existing extensional fault network and determined the current regional architecture. Extensive low density batholith emplacement occurred at that time.

The Thomson Orogen forms the northern extent of the eastern Australian Tasmanides. The region records a protracted tectonic evolution that spans the Neoproterozoic to Triassic and is coincident with one of the largest period of continental growth of the Australian continent. Combined potential field and seismic interpretation indicates that NE- and NW-trending high angle reverse thrusts represent the main crust-scale structural elements in the mid- to lower crust. Gravity data indicate that the eastern and western portions of the Thomson Orogen have a

different crustal architecture. The eastern Thomson Orogen is characterized by a regional NE trend and a network of orthogonal faults resulting in a series of troughs and highs. The negative gravity anomalies reflect mostly the distribution of the basinal sequences inferred from drill holes and deep seismic surveys. The western part appears as a series of NW-trending structures interpreted to reflect reverse thrust faults. The smooth magnetic signature of the Thomson Orogen is interpreted to represent source bodies at mid- to lower crustal level. Seismic profiles and forward models consistently indicate that the upper and lower crusts show different geophysical properties. The Thomson Orogen can be distinctly divided in a non-magnetic to weakly magnetic upper crust and a magnetic lower crust. Long wavelength magnetic anomalies are inferred to reflect the topography of the magnetic lower basement. Forward modelling indicates that the western and eastern parts of the Thomson Orogen are petrophysically indistinguishable and the region is interpreted to be a single terrane. The constrained geophysical interpretation indicates that lower basement consists of attenuated Precambrian and mafic enriched continental crust.

The Cork Fault is a continental scale structure that defines the boundary between the Proterozoic Mount Isa terrane and the Phanerozoic Thomson Orogen. The Cork Fault coincides with one of the most distinguishable geophysical features of the Australian continent. The prominent geophysical signature of the Cork Fault reflects the abrupt termination of positive NNW-trending geophysical features of the Mount Isa terrane against NE-trending low gravity and low magnetic anomalies of the Thomson Orogen. 2D forward modelling indicates that the lower basement crust of the Thomson Orogen is petrophysically indistinguishable from the Proterozoic crust of the Mount Isa terrane. Best fit reconstruction suggests that high angle listric faults offset the magnetic crust which regionally deepens toward the Thomson Orogen. The prominent potential field gradients associated with the Cork Fault are interpreted to represent the displacement and burying of the Mount Isa terrane crust under the Thomson Orogen basement rocks.

The geophysical interpretation indicates that the timing of initiation of the Cork Fault postdates the Isa Orogeny. Initiation of the Cork Fault may be consistently dated to the Mesoproterozoic and may be related to the continental re-organization of the Australian continent that led to the separation of the Mount Isa terrane from the Curnamona Province. The mechanism of separation envisages initial N-S- to NNW-directed extension and development of normal faults. The Cork Fault formed part of a network of major north-dipping and south-dipping normal

faults active at that time. Constrained aeromagnetic and gravity data provide support for a Neoproterozoic extensional event in the Thomson Orogen which was controlled by NW-oriented rift segments and occurred in a continental setting as a distal response to the E-W to NE Rodinia break-up.

A tectonic model is proposed in which the Thomson Orogen represents the interior extensional architecture during the Rodinia break-up, which is recorded further east in the Anakie Inlier and south in the Koonenberry Belt and the Adelaide Fold Belt in south Australia. This implies that the continental break-up did not occur along the Cork Fault. Instead during the Rodinia break-up, the Cork Fault may have been reactivated as a strike-slip fault, being in a favourable orientation, and formed part of the NE-striking strike-slip faults and NW-oriented normal faults that accommodated the deposition of the Late Neoproterozoic to Middle Cambrian stratigraphy in the Thomson Orogen. Alternatively, at ca. 580 Ma the Thomson Orogen may have switched to a continental back-arc setting driven by the roll-back of a NW-dipping subduction zone. Renewed deposition and volcanism occurred during the Ordovician that may have continued into the Late Silurian, resulting in thinned Proterozoic basement crust and extensive basin systems that formed in a distal continental back-arc environment. The Devonian extensional basinal system in the Thomson Orogen formed in a continental setting. At this time, the extension was controlled by the existing NE- and NW-trending fault architecture. The basin is interpreted to record a distal back-arc basin in the interior of the Australian continent.

The Early Palaeozoic tectonic evolution of the continental crust of the Thomson Orogen differs from that of the oceanic crust of the Lachlan Orogen to the south and amalgamation of the two geological terranes might have occurred during Middle Palaeozoic. Thinned Precambrian crust of the Thomson Orogen may be representative of an Early Palaeozoic continental margin or back-arc setting whereas the Lachlan Orogen formed via incorporation of arc type, oceanic and continental rocks.

These results demonstrate that regional potential field datasets are a valuable tool in the comprehension of regional geology of tectonic systems with little or no geological exposure.

THESIS OUTLINE

This thesis is organized as a collection of research articles, which will be submitted to peer review journals. The core chapters (3 - 6) are structured as stand-alone manuscripts and their format reflects peer-reviewed journal guidelines. The reader will therefore encounter some repetition in the introductory section of each core chapter, which describes the geological background of the study region, as well as in the methodology section. The thesis is structured in seven chapters and two appendices that follow Monash University guidelines and policies.

Chapter 1 consists in an introduction to the main theme of the research project. It includes a general overview of the study area which is covered in details in the core chapters (3 - 6). The chapter contains a section that outlines the current understanding of the region and specifies the the research questions covered by this research project.

The methodologies used to address the objectives are described in each core chapter (3 - 6). However, the methodologies are not addressed in details due to word limits imposed by peer-reviewed journals. Chapter 2 appropriately covers the methodologies and techniques used in this research project.

Chapter 3 presents the results of constrained potential field interpretation of the southern Mount Isa terrane. Although the region is totally concealed under younger sedimentary sequences, well defined geophysical anomalies extend north and south of the exposed Inlier and define the extent of the Mount Isa Geophysical Domain. Therefore, the Mount Isa terrane represents an ideal 'laboratory' for testing the effectiveness of potential field method in resolving the basement architecture and interpreting discrete tectonic events of poorly exposed regions. The chapter consists of a detailed analysis of the known depositional sequences and mechanism of major tectonic processes that affected the Proterozoic Mount Isa Inlier. Then geological correlations between the exposed inlier and the concealed southern part of the Mount Isa terrane are inferred based on the geophysical expression of rocks and mapped structures undercover. The geophysical data are constrained by the great amount of geological information gained from the exposed Mount Isa Inlier. Rocks are petrophysically characterized by a compilation of rock property data, which further constrains the interpretation of the area. The results of this study provide insights into the Proterozoic tectonic evolution of the Mount Isa terrane and might have

implications in understanding the distribution of economically significant depositional systems across the province.

Chapter 4 investigates the crustal architecture of the Thomson Orogen using high resolution regional potential field datasets. This study presents also a synthesis of the timing and kinematics of major tectonic events that affected the region during the Neoproterozoic until the Devonian. This chapter illustrates the role played by major structures during the Rodinia break-up and the inferred tectonic setting of the Thomson Orogen at that time. At the conclusion, the case study presents a global overview of the Neoproterozoic to Phanerozoic tectonic processes that affected the eastern Australian continent and provides insights into the timing of interaction between the Thomson Orogen and surrounding geological provinces. This case study would have major implications on reconstructing the post - Rodinia evolution of the Australian continent as well as determining the time of amalgamation of the Tasmanides of Eastern Australia.

In chapter 5, I present the results of constrained potential field data interpretation to determine the source to the regional geophysical anomalies that characterize the Thomson Orogen. Gravity and magnetic data are analysed quantitatively and 2D profiles are forward modelled to infer the presence of attenuated continental crust that floors the region. The implications of this study is that the crust of the Thomson Orogen might have Precambrian affinities and thus differs from most of the Tasmanides of Eastern Australia. The outcome of this study provides insights to better understand the geodynamic evolution of the eastern Australian continent as well as determine the timing of amalgamation with the Phanerozoic Lachlan Orogen.

Chapter 6 describes a case study in which interpretation of regional aeromagnetic and Bouguer gravity data have been used to investigate the crustal architecture at the junction of the Proterozoic Mount Isa terrane and the Phanerozoic Thomson Orogen. Forward modelling of potential fields has been used to validate the geophysical interpretation. It is interpreted that Precambrian continental crust of the Mount Isa terrane continues undercover beneath the Central Thomson Orogen. The results provide insights in understanding the Precambrian tectonic evolution of the Eastern Australian continent and have implications for unraveling the nature of the deep crust of the Thomson Orogen.

Chapter 7 is an overview of the results and conclusions of each case study and consists of an integrative discussion that emphasizes the contribution that each chapter makes towards a better

understanding of the geodynamic evolution of the area of study, followed by concluding remarks.

Appendix A is a compilation of geological maps that have been built from image interpretation in ArcGis and Oasis MontajTM environment. Appendix B consists in a manual for students in order to acquire familiarity with image processing in Oasis MontajTM environment.

References that have been cited in this thesis are listed at the back of this document.

Chapter 1 - Introduction

The Neoproterozoic break-up of the supercontinent Rodinia occurred during a protracted period of crustal extension, which is now preserved along the eastern edge of the Proterozoic provinces of Australia (Glen, 2005; Powell et al., 1994; Williams et al., 2002; Wingate et al., 1998). In eastern Australia, the Rodinia break-up boundary is largely obscured by thick Phanerozoic sedimentary sequences, resulting in the lack of exposed piercing points (Glen, 2005). Moreover, the intense reworking that the Australian continent underwent adds ambiguities in understanding the transition from the Neoproterozoic break-up of Rodinia to the subsequent Phanerozoic evolution of east Gondwana. As a result, the configuration of the Proterozoic supercontinent Rodinia as well as the nature and position of the Neoproterozoic supercontinent break-up are still partly unresolved.

In Queensland, the Mount Isa terrane is characterized by Precambrian continental crust and forms part of the North Australian Craton (Betts et al., 2006; Blake, 1987; O'Dea et al., 1997b). Further south, the Thomson Orogen records multiple phases of tectonism and magmatism that spans the Neoproterozoic to Triassic and are associated with continental growth of the eastern Australian continent (Glen, 2005; Murray and Kirkegaard, 1978). Such as the majority of ancient basement terranes of the Australian continent, the Mount Isa terrane (Betts et al., 2006; O'Dea et al., 1997b) and the Thomson Orogen (Glen, 2005; Murray and Kirkegaard, 1978) are poorly exposed. No basement rocks outcrop within the research area because they are concealed under a thick Phanerozoic sedimentary succession (Betts et al., 2006; Fergusson and Henderson, 2013; Glen, 2005; Murray and Kirkegaard, 1978; O'Dea et al., 1997b). Sparse drillholes and geophysical investigations provided information about the geology of the two regions. However, the lack of a regional tectonic framework of the southern Mount Isa terrane and the poor understanding of the crustal architecture of the Thomson Orogen represent a limitation to an adequate geodynamic/tectonic model. This research project investigates the tectonic significance of a continental scale geophysical lineament that separates the Proterozoic Mount Isa terrane from the Phanerozoic Thomson Orogen. Determining the architecture and the kinematic evolution of this major boundary is essential to understand the tectonic evolution of the northern Tasmanides and has major implications for understanding the nature of the break-up of Australia in the context of Rodinia.

Regional gravity and aeromagnetic data has been used to map rocks in regions with limited geological coverage (Aitken and Betts, 2009; Stewart and Betts, 2010a; Wellman, 1992). In regional gravity and aeromagnetic datasets, source bodies having different petrophysical properties are reflected by variation of amplitudes and texture of geophysical responses, resulting in gradients, lineaments and discontinuities that define the architecture of the region. The method is effective for constraining the three dimensional geometry of the subsurface as well as identifying source bodies at different crustal levels (Aitken and Betts, 2009; Austin and Blenkinsop, 2008; Betts et al., 2004; Crawford et al., 2010; McLean et al., 2010; Williams et al., 2009). Potential field method is also effective for constraining relative overprinting relationships (Betts et al., 2003; McLean and Betts, 2003) and kinematics of faults and discontinuities reflected in the geophysical data (Betts et al., 2007). Recently Geoscience Australia has released high resolution aeromagnetic and gravity datasets of both the Mount Isa terrane and the Thomson Orogen providing the unique opportunity to define the regional scale structural architecture of the region. Potential field analysis and interpretation is therefore the primary tool to accomplish this research project.

1.1 Study area

The Proterozoic Mount Isa terrane in Queensland represents a continental crustal fragment that amalgamated to the North Australian Craton during the Palaeoproterozoic (Betts et al., 2006; Bierlein and Betts, 2004; Giles et al., 2006a; MacCready, 2006a; Spikings et al., 2001). The Mount Isa terrane developed through poly-cyclic tectonic events. Intra-continental rift evolution, basin inversions, intra-plate igneous activity, high pressure - low temperature metamorphism, poly-phase deformation and extensive metasomatism have been extensively recorded throughout the region (Betts et al., 2006; Edmiston et al., 2008; Eriksson et al., 1994; Geological_Survey_of_Queensland, 2010; Giles et al., 2006a; Giles et al., 2006b; O'Dea et al., 1997b; Wellman, 1992). The Mount Isa Geophysical Domain is defined by prominent N-S- to NNW-trending geophysical anomalies which extend for at least 200 km north and 250 km south of the exposed Mount Isa Inlier (Betts et al., 2006; Drummond et al., 1998; Giles et al., 2006b; Wellman, 1992). Recent deep seismic reflection surveys covered the northern and central parts of the Mount Isa terrane providing great contribution to the understanding of the crustal architecture, tectonic styles, and geodynamic evolution of the region (Betts et al., 2006; MacCready, 2006a; O'Dea et al., 1997b). However, the concealed southern Mount Isa terrane is

not so well understood and the regional tectonic pattern observed in the geophysical dataset remains substantially poorly resolved.

The Thomson Orogen lies to the immediate south of the Mount Isa terrane. The Thomson Orogen represents the largest tectonic domain of the eastern Australian Tasmanides (Glen, 2005; Glen et al., 2006) and records a protracted tectonic evolution that spans the Neoproterozoic to Triassic (Glen, 2005). The basement rocks of the Thomson Orogen lie beneath Middle Palaeozoic to Mesozoic sedimentary systems (Murray and Kirkegaard, 1978) and its geology is only known from limited drill holes. Deep seismic reflection data imaged major features and provided insights into the intra-basins setting (Finlayson, 1990, 1993; Finlayson and Collins, 1987; Finlayson et al., 1988; Finlayson et al., 1989; Finlayson et al., 1990b; Finlayson et al., 1990c; Leven and Finlayson, 1987; Leven et al., 1990; Spence and Finlayson, 1983). However, the architecture of the underlying basement is still poorly resolved because of the lack of seismic reflectors. The nature of the crust at mid to low crustal level is also enigmatic. Finlayson et al. (1990c) and Glen et al. (2005) interpreted that the Thomson Orogen is floored by thinned and seismically reflective continental crust. Glen et al. (2013) suggested that the western part of the Thomson Orogen developed on Neoproterozoic to Early Cambrian oceanic crust, supporting the early work of Harrington (1974). In their view, the seismically reflective lower crust may represent igneous oceanic crust extending from the western edge of the Tasmanides to Central Thomson Orogen. Forward modelled seismic profiles crossing the Thomson and the Lachlan orogens indicate that an eastwards-rifted Precambrian continental sliver forms the southern extension of the Thomson Orogen (Glen et al., 2013). The sliver may link to inferred continental crust forming the eastern part of the Thomson Orogen (Glen et al., 2013). Musgrave (2013) also indicated that the Thomson Orogen may not be a single terrane. In his view, the regional magnetic signature of the Thomson Orogen suggests that the region may be formed by two distinctive crustal domains. In this interpretation, the Thomson Orogen formed as attenuated continental/arc crust to the east and accreted oceanic crust to the west. In this context, there are uncertainties whether the Thomson Orogen was built on extended continental crust (Fergusson et al., 2007a; Fergusson et al., 2009; Finlayson et al., 1989; Finlayson et al., 1990c; Glen, 2005), oceanic crust (Harrington, 1974) or both (Glen et al., 2013; Musgrave, 2013). Understanding the nature of the basement crust of the Thomson Orogen is a fundamental issue that needs to be addressed to determine the evolution of the Gondwanan margin in Australia.

The Cork Fault divides the Proterozoic Mount Isa terrane from the Phanerozoic Thomson Orogen (Finlayson et al., 1988; Glen, 2005; Murray and Kirkegaard, 1978) and is one of the most distinguishable geophysical features at a continental scale (Wellman, 1990; Wellman, 1992). Because of its geophysical prominence, some authors interpreted that the Cork Fault represents the break-up of the supercontinent Rodinia (Finlayson et al., 1988; Gunn et al., 1997; Murray and Kirkegaard, 1978; Shaw et al., 1996; Veevers and Powell, 1984). Finlayson et al. (1988) suggested that the Cork Fault initiated during the Late Neoproterozoic as a NE-oriented rift segment associated with the NW-directed Rodinia break-up. Greene (2010) suggested that during the Rodinia break-up the Cork Fault developed as NE-trending transform fault offsetting NW-trending rift segments. In this context, the Cork Fault forms a segment of the much debated ‘Tasman Line’ (Direen and Crawford, 2003) which is widely intended as a structure, or a series of structures, that broadly divides the Proterozoic provinces of the Australian continent from Phanerozoic rocks of the Tasmanides (Fergusson et al., 2007b; Glen, 2005; Murray and Kirkegaard, 1978; Veevers, 2000a) and also separate two continental-scale regions showing different geophysical signature (Glen, 2005; Wellman, 1992). Other authors suggested that the continental break-up occurred east of the Cork Fault (Fergusson et al., 2009; Hill, 1951). Therefore, the role and kinematics of the Cork Fault during the Rodinia Break-up remain unclear. Nevertheless, understanding the architecture at the junction of the Mount Isa terrane and the Thomson Orogen would have major implications in determining the evolution of the eastern Australian continent as well as assessing potential links between the two regions.

1.2 Aim

The main aim of this project is to establish a tectonic framework of the southern Mount Isa terrane and the Thomson Orogen and determine the tectonic processes responsible for the crustal architecture of this large and relatively poorly resolved part of the Australian continent. The project will also address the architecture and the tectonic significance of the boundary that divides Palaeoproterozoic rocks of the Mount Isa terrane from Neoproterozoic to Triassic rocks of the Thomson Orogen. This boundary is critical to resolve the tectonic evolution of the northern Tasmanides and the break-up of the Australian component of Rodinia.

In the context of these major aims, there are a number of secondary objectives:

- 1. To define the architecture and kinematics of major structures and to determine the nature of the crust and geological bodies at different crustal levels*

The geophysical anomalies reflect the lithospheric structure of a geological region. Gravity and magnetic data allow 3D mapping of the regional architecture and determining fault kinematics through overprinting relationships and the apparent offset of magnetic markers (See chapter 2 section 2.6). Characterizing the fault kinematics and the internal architecture at different scales is essential for understanding the regional tectonic setting, determining the deformation style under a given stress regimes and defining the major tectonic processes that affected the area.

2. *To asses how major features might have controlled the architecture of the region*

The inherited fault architecture tends to control the location and geometries during subsequent tectonic deformations (Lechler and Greene, 2006; White et al., 1986). This occurs because pre-existing geological structures form planes of weakness that can be repeatedly utilized under a favourable stress regime (White et al., 1986). Particularly, during basin inversion pre-existing normal faults may concentrate stress and localise future thrust ramps or may be reactivated as reverse thrusts (Blenkinsop et al., 2008; Bonini et al., 2012; Giles et al., 2006a; Letouzey et al., 1990). In the context of this research project, some structures have been demonstrated to exhibit a long lived tectonic history developed through multiple reactivations, with a kinematic sense appropriate to the stress field, during discrete tectonic events (Betts, 1999; Betts et al., 2004; Betts et al., 2006; Blenkinsop et al., 2008; Finlayson, 1993; Finlayson and Leven, 1987; Finlayson et al., 1988; Giles et al., 2006a; O'Dea et al., 2006; O'Dea et al., 1997b). Determining reactivation episodes has major implications in reconstructing the tectonic setting as well as understanding how the inherited faults system controlled the architecture of the region.

3. *To identify the potential relationships between the mapped structures in the exposed Mount Isa Inlier and the geophysical features evident in the concealed southern Mount Isa terrane*

The area of the concealed southern Mount Isa terrane is almost as extensive as the exposed inlier (Wellman, 1992). It is nevertheless poorly understood. Geophysical mapping and interpretation will provide insights into the extent and deformation style of the tectonic processes that affected the region and will inform about the distribution and geometries of the rock packages overlying the crystalline basement. This will also set the basis for a better understanding of the boundary between the Mount Isa terrane and the Thomson Orogen, represented by the Cork Fault.

4. *To establish the tectonic setting of the Thomson Orogen during the Neoproterozoic Rodinia break-up and its relationship with the rest of the Tasmanides*

The Neoproterozoic represents one of the most critical periods of the Australian Continent because it defines a period of major break-up of the supercontinent Rodinia (Direen and Crawford, 2003; Glen, 2005; Powell et al., 1994; Preiss, 2000; Wingate et al., 1998). The Neoproterozoic rocks represent a transitional zone between the Proterozoic craton of Australia and the Tasmanides. Determining the tectonic setting of this transitional zone in the Thomson Orogen will allow greater understanding of the nature of the break-up of Australia in the context of Rodinia and will elucidate the tectonic regime of this major event.

- 5. To develop a more comprehensive understanding of the architecture and the kinematic evolution of the region and to provide insights for a continental scale model for the geodynamic evolution of the area*

Understanding the kinematics and the tectonic processes that occurred at the boundary between the Precambrian and the Phanerozoic crust of the Australian continent has major implications in reconstructing the assembly, re-organization and dispersal of continents and supercontinents.

1.3 Publication arising from this research

A number of journal articles, conference abstracts and seminars have already been submitted or presented during this research project.

1.3.1 Journal articles

Spampinato, G.P.T., Betts, P.G. and Ailleres, L. (to be submitted to Precambrian Research): Structural architecture of the southern Mount Isa terrane in Queensland inferred from magnetic and gravity data (Chapter 3 of this Thesis).

Spampinato, G.P.T., Ailleres, L. and Betts, P.G. (to be submitted to Gondwana Research): Early tectonic evolution of the Thomson Orogen in Queensland inferred from constrained magnetic and gravity data (Chapter 4 of this Thesis).

Spampinato, G.P.T., Betts, P.G. and Ailleres, L. (to be submitted to Gondwana Research): Crustal architecture of the Thomson Orogen in Queensland inferred from forward modelling technique (Chapter 5 of this Thesis).

Spampinato, G.P.T., Ailleres, L. and Betts, P.G. (to be submitted to Interpretations): Imaging the basement architecture across the Cork Fault in Queensland using magnetic and gravity data (Chapter 6 of this Thesis).

1.3.2 Conference abstracts

Spampinato, G.P.T., Betts, P.G. and Ailleres, L., 2012. Deep Australia - Understanding plate architecture and its evolution. SGTSG, 29 January - 3rd February 2012, Waratah Bay, (VIC, Australia).

Spampinato, G.P.T., Betts, P.G. and Ailleres, L., 2012. Tectonic evolution of the SE Mount Isa Inlier; 34th IGC, 5 - 10 August 2012, Brisbane (Queensland, Australia).

Spampinato, G.P.T., Betts, P.G. and Ailleres, L., 2014. Crustal architecture of the Central Thomson Orogen in Queensland inferred from magnetic and gravity data; SGTSG, 2 - 8 February 2014, Thredbo (NSW, Australia).

1.3.3 Seminars

Spampinato, G.P.T., 2014. Unraveling the architecture of buried terranes using magnetic and gravity data: an example from Central Queensland. University of New South Wales (NSW, Australia) and University of Wollongong (NSW, Australia).

Spampinato, G.P.T., 2014. Gravity and magnetic exploration principles: processing and interpretation of potential field datasets. University of Sydney (NSW, Australia).

Spampinato, G.P.T., 2014. Deep Australia - Understanding plate architecture and its evolution; an example from SE Mount Isa Inlier. Monash University (VIC, Australia).

1.3.4 Manual

Spampinato, G.P.T., 2012. Oasis MontajTM interactive filtering tool.

Chapter 2 - Methodology

The understanding of the architecture, tectonic setting and geodynamic history of a geological region is commonly based on the integration of a wide range of geological and geophysical methods. Although a variety of geological (direct observation, drill holes, structural analysis) and geophysical (seismic, geoelectric) techniques are commonly used in geological interpretation, the use of unintegrated data may provide information which is spatially limited or not sufficient for the understanding of extended or complex geological terranes. For example, drill holes and outcrops provide detailed information about the mineralogy, lithological contacts, metamorphic grades, degrees of alteration and geometries of rocks although the information might not be representative of the regional geological context and the data only constrain the shallower part of the crust. Geophysics including seismic, magnetotelluric, electrical, magnetic and gravity methods can be used to investigate the architecture of the subsurface. For example, seismic surveys produce detailed understanding of geology to considerable depth, although the method has its limitations including poor seismic response and access issues. Also, dense 3D coverage of seismic reflection data is often limited by the high costs. Seismic tomography provides continental-scale coverage of the lithosphere, however the method is characterized by a relatively coarse resolution and small-scale variations might not be imaged. Therefore, a single method approach may be insufficient when multiscale geological characterization is required.

Gravity and magnetic fields can provide information on the distribution and geometries of different rocks in the subsurface of the Earth and have been proved to be an effective tool in understanding the 3D architecture of buried terranes (Aitken and Betts, 2009; Betts et al., 2004; Crawford et al., 2010; McLean et al., 2010; Williams et al., 2009). Potential field method allows extrapolating sparse and/or small-scale geological information into a regional context (Aitken and Betts, 2009; Betts et al., 2003b; Stewart and Betts, 2010b) and provides insights into the crustal architecture (Stewart and Betts, 2010a), structural setting (Betts et al., 2003; McLean and Betts, 2003) and associated kinematics (Betts et al., 2007) in regions with little or poor geological exposure.

In this study, potential field method is used as a primary tool to address the aims described in chapter 1. Gravity and magnetic data are used to discriminate rocks of different densities and magnetic susceptibilities although this is not necessary diagnostic of particular rock types (see

Figs. 2.1 and 2.2.) (Clark, 1981), which makes the methodology subject to inherent geological ambiguity. However, the ambiguity can be significantly reduced when integrating geological data are available (Gunn et al., 1997). To minimize the ambiguity, this research project adopts a multidisciplinary approach and makes use of integrated analysis of different geological and geophysical methods to constrain the magnetic and gravity data.

2.1 Potential field data

Any field that satisfies Laplace's equation (Equation 1) is termed a potential field:

$$\nabla^2 U = \frac{\partial^2 U}{\partial x^2} + \frac{\partial^2 U}{\partial y^2} + \frac{\partial^2 U}{\partial z^2} = 0 \quad \text{Equation 1}$$

Where:

U = the potential; x,y,z = Cartesian coordinates

Potential fields are those in which the strength and direction of the force depend on the location of the observer and decrease for increasing distance from the source (Lowrie, 1997). The gravity and magnetic fields of the Earth satisfies Laplace's equation and are examples of potential fields.

2.2 Gravity data

Newton's Law of Gravitation (Equation 2) describes the force of attraction (F) between two objects, termed the gravity force:

$$F = G \frac{m_1 m_2}{r^2} \quad \text{Equation 2}$$

Where:

F = force of attraction between two objects (N)

G = Universal Gravitational Constant ($6.67 * 10^{-11} \text{ Nm}^2/\text{kg}^2$)

m1, m2 = mass of the two objects (Kg)

r = distance between the center of mass of the objects (m)

The gravitational acceleration (g) observed on (or above) Earth's surface is given by Equation 3:

$$g = \frac{GM}{R^2} \quad \text{Equation 3}$$

Where:

G = Universal Gravitational Constant ($6.67 * 10^{-11} \text{ Nm}^2/\text{kg}^2$)

M = mass of the Earth

R = distance from the observation point to the Earth's centre of mass

Excluding tidal effects, the gravity field is a time invariant monopolar field (Lillie, 1999; Lowrie, 1997). This implies that on Earth the gravity field is symmetric and lines of force are directed towards the center of the Earth (Lillie, 1999). In geophysical studies it is necessary to measure variations in the Earth's gravity field caused by contrasts in the density of rock in the subsurface. This requires reduction of non-geological components from the gravity field for the effects that result from latitude, elevation, tides and instrumental drift.

2.2.1 Latitude correction

On Earth, the observed gravity field has an added component due to the centrifugal acceleration (Lillie, 1999). Towards the equator, the centrifugal force produced by Earth's rotation is larger than at polar latitudes. Also, the Earth is not a perfect sphere and the polar radius is smaller than the equatorial radius (Lowrie, 1997). The latitude correction G_ϕ accounts for Earth's elliptical shape and rotation. The theoretical variation of normal gravity with latitude is expressed in Equation 4:

$$G_\phi = 9.780327 \text{ m s}^{-2} (1 + 0.0053024 \text{ Sin}^2\phi - 0.0000058 \text{ Sin}^22\phi) \quad \text{Equation 4}$$

Where:

ϕ = Latitude

The value of the gravitational acceleration on Earth's surface is $\sim 9.78 \text{ m s}^{-2}$ at the equator and $\sim 9.83 \text{ m s}^{-2}$ at the poles (Lillie, 1999; Lowrie, 1997; Milsom, 2003).

2.2.2 Tides and instrumental drift

The superimposed lunar and solar tides produce deformation on Earth that has effect on gravity measurements (Lillie, 1999; Lowrie, 1997; Milsom, 2003). Therefore it is necessary to compensate gravity measurements for the tidal effect caused by the change in the relative position of the Earth, moon and sun. Earth's tides are predictable and correction can be calculated for a given location at a given time (Milsom, 2003).

The instrumental drift is mostly due to thermally induced changes in the elastic properties of the gravimeter springs (Milsom, 2003). Moreover, the elastic properties of the springs change with time (Milsom, 2003). The effects are relatively small and can be compensated making a drift correction. Drift correction can be determined measuring the gravity response at an established base station at the start and the end of any gravity survey. Base station readings corrected for the tidal effect are used to determine the drift rate occurred during the measurement session, assuming that the drift rate is a linear function (Milsom, 2003).

2.2.3 Free air anomaly

Under the same boundary conditions, a gravity station located at a higher elevation will show a lower gravitational reading than a gravity station located at a relative lower elevation. The free air correction accounts for the local change in the gravity response due to variation in elevation of the gravity stations. The free air anomaly is the observed gravity anomaly corrected for the latitude and elevation.

$$\nabla g_{fa} = g - g_t + h * (0.308 \frac{\text{mgal}}{\text{m}}) \quad \text{Equation 5}$$

Where:

∇g_{fa} = free air gravity anomaly

$h * (0.308 \frac{\text{mgal}}{\text{m}})$ = free air correction

g = gravitational acceleration observed at the station

g_t = theoretical gravity

h = elevation of the station above the sea level datum (m)

2.2.4 Bouguer Anomaly

Further correction might be needed to account for the gravitational attraction of the excess mass above the sea level datum. The Bouguer gravity correction assumes an infinite slab having density ρ and thickness h equal to the elevation of the station. The attraction of such a slab is described in equation 6:

$$BC = 2\pi\rho Gh \quad \text{Equation 6}$$

Where:

BC = Bouguer correction

ρ = density of the slab

G = Universal Gravitational Constant

h = thickness of the slab

On land, the density of the slab is commonly taken as 2.67 g cm^{-3} and its thickness is equal to the station elevation. The simple Bouguer gravity anomaly Δg_b results from subtracting the effect of the infinite slab BC from the free air gravity anomaly (Equation 7):

$$\Delta g_b = \Delta g_{fa} - BC \quad \text{Equation 7}$$

Common Rocks	
Dry sand	1.4–1.65
Serpentinite	2.5–2.6
Wet sand	1.95–2.05
Gneiss	2.65–2.75
Granite	2.5–2.7
Dolerite	2.5–3.1
Salt	2.1–2.4
Basalt	2.7–3.1
Limestone	2.6–2.7
Gabbro	2.7–3.3
Quartzite	2.6–2.7
Peridotite	3.1–3.4
Ore minerals	
Galena	7.3–7.7
Chalcopyrite	4.1–4.3
Chromite	4.5–4.8
Pyrrhotite	4.4–4.7
Hematite	5.0–5.2
Pyrite	4.9–5.2
Magnetite	5.1–5.3

Fig 2.1 Densities of common rocks and ore minerals (g cm^{-3}); modified from Milsom (2003)

Variations in gravity anomalies are in the order of less than 1% and often in the order of parts per million. Thus in geophysical investigation the Gravity Unit (g.u) is commonly used where $\text{g.u.} = 10^{-6} \text{ m s}^{-2} = 1 \mu\text{n gk}^{-1}$. Alternatively, it is practical adopting the milligal (mgal) where $1 \text{ mgal} = 10^{-3} \text{ gal} = 10 \text{ g.u.}$

2.2.5 Applications and limitations of gravity data

Gravity method can measure the subtle variation in the Earth's gravity field caused by difference in the density of rocks (Nabighian et al., 2005a). Therefore, the method can be successfully applied to gain information for any targets for which there is a density contrast at depth, such as salt domes, orebodies, structures, and regional geology (Nabighian et al., 2005a). For example, in the mining industry gravity data are used as an exploration tool to map subsurface geology and to help estimate ore reserves (Cheng and Yin, 2011; Hinze, 1960). In oil exploration, gravity technique helps validating seismic data, narrow the search area in large fields and provides an independent corroboration of total volume and shape of salt bodies when investigating sub-salt hydrocarbon potential (Hamdi-Nasr et al., 2009; Pinto et al., 2005). Gravity data can be used for understanding the architecture of sedimentary basins (Chakravarthi et al., 2013; Chakravarthi and Sundararajan, 2004) and the regional architecture of buried terranes (this study). Gravity data are also increasingly used for environmental (Greco et al., 2012; Zerbini et al., 2001) and geothermal studies (Kohrn et al., 2011; Shoffner et al., 2011; Soengkono et al., 2013).

The gravity method is not suitable if there is no sufficient density contrast between rocks (see Fig. 2.1). Moreover, an infinite number of gravity models can be created to match the observed gravity signal (Skeels, 1947). To limit the degrees of freedom and minimize the ambiguity, the integration of gravity data with other geological (drill holes, outcrops) and geophysical (seismic, electric, magnetic) data is required to produce a consistent geological model.

2.3 Magnetic Data

The magnetic field is a time variant dipolar field and it varies in both strength and direction over time and location (Lillie, 1999; Lowrie, 1997). Magnetic field directions change from being nearly horizontal at the Earth's magnetic equator to vertical at the Earth's magnetic poles (Lillie, 1999; Lowrie, 1997). About 98% of Earth's magnetic field is thought to be caused by motion of liquid metal in the core and is therefore of internal origin (Campbell, 1997). About 2% is of external origin and is associated with solar wind (Campbell, 1997).

The Earth's magnetic field can be approximated to that of a bar magnet having the negative magnetic pole in the northern hemisphere and the positive magnetic pole in the southern hemisphere (Lillie, 1999; Lowrie, 1997). However, the heterogeneous sources that originate the Earth's magnetism produce lines of force that vary considerably from a simple dipole model. The

actual north and south magnetic poles are not 180° apart and deviate considerably from the north and south geographic poles (Lillie, 1999; Lowrie, 1997). A magnetic field is a vector quantity, having both magnitude and direction. The direction of the magnetic field is defined by its inclination and declination. The magnetic inclination is the angle between magnetic lines of force and the horizontal ground surface. The magnetic declination is the angle a compass needle deviates from geographic north.

The magnitude of the total magnetic field vector or total magnetic intensity (F) is:

$$F = \sqrt{F_h^2 + F_v^2} = \sqrt{F_n^2 + F_e^2 + F_v^2} \quad \text{Equation 8}$$

Where:

F = total magnetic field vector

F_h = horizontal component of total field vector

F_n = north component of horizontal vector

F_e = east component of horizontal vector

F_v = vertical component of total field vector

2.3.1 Magnetic susceptibility

Induced magnetization results from magnetization of a substance when an external magnetic field (for example the Earth's ambient field) is applied (Lillie, 1999; Lowrie, 1997). The induced magnetization (M) depends on the magnitude and direction of the external field (F_{amb}) and the magnetic susceptibility (k) of the rocks (Equation 9).

$$M = kF_{amb} \quad \text{Equation 9}$$

Where:

M = induced magnetization of the material

k = magnetic susceptibility of the material

F_{amb} = local magnitude and direction of the ambient field

Therefore:

$$k = \frac{M}{F_{amb}} \quad \text{Equation 10}$$

Equation 10 tells that the magnetic susceptibility is a measure of the degree to which a substance becomes magnetically induced from an application of an external magnetic field. The magnetic susceptibility is a dimensionless constant.

In geophysics, the magnetic susceptibility of rocks is their ability to become magnetically induced by the Earth's magnetic field (Milsom, 2003). Minerals forming rocks show three types of magnetic susceptibility:

- a) Diamagnetic minerals acquire an induced magnetization opposite in direction to an externally applied magnetic field. The weak magnetization results from alteration of electron orbitals as force from the external field is applied. Examples of common diamagnetic mineral are halite (rock salt), quartz and calcite (Lowrie, 1997; Milsom, 2003).
- b) Paramagnetic minerals create an induced magnetic field having the same direction as the inducing magnetic field. The magnetism occurs as the magnetic moments of atoms are partially aligned with the inducing field. The alignment is opposed by thermal energy and in absence of an external magnetic field the magnetic moments are oriented randomly. Therefore, once the external magnetic field is removed paramagnetic minerals do not retain their magnetism. Pyroxenes, micas and amphiboles are examples of paramagnetic minerals. Both diamagnetic and paramagnetic minerals have small magnetic susceptibility and have negligible effect on aeromagnetic surveys (Lowrie, 1997; Milsom, 2003).
- c) In some metals, including iron, the atoms occupy lattice positions close enough to allow the exchange of electrons between neighboring atoms. The exchange interaction determines a strong molecular field within the material which aligns the atomic magnetic moments. In pure ferromagnetism, the magnetic moments become aligned with an applied external field and are in the same direction, producing a large positive induced magnetic field (Lowrie, 1997). Therefore, ferromagnetic minerals are characterized by positive magnetic susceptibilities. Antiferromagnetism occurs when the magnetism of minerals is aligned to the external field but adjacent atomic magnetic moments display opposite direction resulting in very weak or zero magnetic susceptibility (Lowrie, 1997). Ferrimagnetism occurs when domains within the minerals produce magnetic fields in opposite directions. The domains polarized in the direction opposite to the external field are weaker in intensity because the exchange process involves antiparallel and unequal

magnetization of the magnetic sub-lattices. This happens because the population consists of different ions (Spaldin, 2010). As a result, the total induced field will be weakly positive. The induced magnetic field measured during the aeromagnetic survey is mostly due to the magnetic response of ferrimagnetic minerals such as magnetite, titanomagnetite, ilmenite and pyrrhotite. Magnetite is the most common naturally occurring magnetic mineral (Lowrie, 1997; Milsom, 2003; Nabighian et al., 2005b). Hematite is the most abundant iron mineral but has a very small susceptibility because of its antiferromagnetic behavior (Milsom, 2003; Nabighian et al., 2005b).

The magnetic susceptibility depends on bulk rock chemistry. The content of iron in the rocks, particularly in the form of mineral magnetite (Fe_3O_4) influences the magnetic susceptibility. Magnetic susceptibility is also strongly dependent on the oxidation state which in turn is influenced by the oxygen fugacity. At very low oxygen fugacity (equivalent to reduced chemical conditions) iron in native state (Fe^0) occurs. At higher oxygen fugacities Fe occurs in divalent (Fe^{2+}) and trivalent (Fe^{3+}) state and is incorporated into silicates and magnetite. At higher oxygen fugacity, ferric iron (Fe^{3+}) is incorporated into hematite. Therefore, under increasing oxidizing conditions the susceptibility decreases. Weathering generally reduces susceptibility because magnetite is oxidized to hematite. Therefore, the aeromagnetic response of different rock types mostly reflects their magnetite content and oxidation state (Whiting, 1986). The sulfur fugacity is an additional factor that determines the magnetic susceptibility. The increase in sulphidation in rocks results in a lowering of the magnetic susceptibility (Haggerty, 1979).

2.3.2 Curie Temperature

Under increasing temperature conditions the magnetization decreases. The point at which the magnetization is lost is referred to as the Curie temperature which varies from different minerals. Most common minerals lose their magnetization at $\sim 550\text{-}600^\circ$. Assuming an average geothermal gradient of 30° km^{-1} the crust loses its magnetization at ~ 20 km. However, the geothermal gradient varies on Earth. Ancient geological provinces tend to have a lower geothermal gradient while younger terranes show higher geothermal gradients. In this study, we refer to the geothermal gradients from Maule et al. (2009).

2.3.1 Remanent magnetization

Ferromagnetic minerals produce a strong induced magnetic field which can persist after the external field has been removed and is termed the remanent magnetization. Remanent magnetisation occurs due to several processes (e.g. Telford et al., 1990), including cooling below the Curie temperature in the presence of an external field (thermoremanent magnetisation), alignment of fine grained particles in the direction of the external field during sediment deposition (detrital remanent magnetisation) and chemical reactions or crystalization at temperatures below the Curie temperature in the presence of an external magnetic field (chemical remanent magnetisation). The variations in the magnetic field on Earth reflect a combination of induced and remanent magnetization. In most rocks the effect of the remanent magnetization is negligible if compared to the magnetization induced by the external magnetic field (Clark and Emerson, 1991; Nabighian et al., 2005b).

Common rocks	
Slate	0–0.002
Dolerite	0.01–0.15
Greenstone	0.0005–0.001
Basalt	0.001–0.1
Granulite	0.0001–0.05
Rhyolite	0.00025–0.01
Salt	0.0–0.001
Gabbro	0.001–0.1
Limestone	0.00001–0.0001
Ores	
Hematite	0.001–0.0001
Magnetite	0.1–20.0
Chromite	0.0075–1.5
Pyrrhotite	0.001–1.0
Pyrite	0.0001–0.005

Fig. 2.2 Magnetic susceptibilities of common rocks and ores (SI); modified from Milsom (2003)

2.3.1 Total magnetic field

Above the Curie depth, the Earth's magnetic field may induce a secondary field. When magnetized rocks occur in the subsurface, the direction and magnitude of the total magnetic field change and can be measured. In the absence of remanent magnetization, the total magnetic field

is the sum of the Earth's ambient field and the induced magnetic field. The total magnetic intensity F observed in the vicinity of a magnetized source body is the sum of the Earth's ambient field F_{amb} and the induced field F_{ind} of the magnetic body:

$$F = F_{amb} + F_{ind} \quad \text{Equation 11}$$

The magnetic field (F) is measured in Tesla (T). For geophysical investigation the nanoTesla (nT) is commonly used where $1 \text{ nT} = 10^{-9} \text{ T}$.

2.3.2 Applications and limitations of magnetic data

The magnetic properties of adjacent rock masses may differ by several orders of magnitude rather than a few percent if compared to the gravity method (Figs. 2.1 and 2.2). This allows mapping boundaries and source bodies with high level of confidence. The magnetic method is the primary exploration tool in the search for minerals such as base and precious metals, diamonds, molybdenum, and titanium as well as the detection of mineralization such as iron oxide–copper–gold (FeO-Cu-Au) deposits, skarns, massive sulfides, and heavy mineral sands (Ferraccioli et al., 2002; Nabighian et al., 2005b). The method is useful for mapping host rocks or environments such as carbonatites, kimberlites, porphyritic intrusions, and hydrothermal alteration (Nabighian et al., 2005b). Because igneous bodies are frequently associated with mineralization, a magnetic interpretation can be the first step in finding favourable areas for the existence of mineral deposits (Nabighian et al., 2005b). The magnetic method can be successfully used for oil exploration purpose (Kivior and Boyd, 1998). For example, it can be used to map salt domes in weakly magnetic sediments. Magnetic method can be used to determine the basin structure, estimate the depth to basement and quantitatively map basement structures (Prieto and Morton, 2003). Magnetic method is widely used for geologic mapping of prospective areas or for the understanding of crustal architecture of buried terranes (this study). The method is also increasingly used in water-resource assessment (Smith and Pratt, 2003), environmental contamination issues (Smith et al., 2000), geothermal resources (Smith et al., 2002) and archaeological mapping (Tsokas and Papazachos, 1992).

However, the magnetic susceptibility is not diagnostic for rock identification, as many rock types show a wide range of magnetic susceptibility (see Fig. 2.2) and can exhibit similar response on a survey grid. Magnetic rocks can retain part of the induced magnetization after the previous

external field has been removed (Lillie, 1999; Lowrie, 1997; Milsom, 2003). In most cases, it is assumed that there is no remanent magnetization and the direction of magnetization is the same as the current inducing field direction (Nabighian et al., 2005b). However, when the remanent magnetization is present, the total magnetization direction can be significantly different from that of the inducing field (Lillie, 1999; Lowrie, 1997; Milsom, 2003). As a result, both the magnitude and shape of magnetic anomalies are altered (Roest and Pilkington, 1993). Lastly both magnetic and gravity data suffer from a lack of sensitivity to the geometry of structures at depth (Nabighian et al., 2005a).

2.4 Geophysical coverage

Recently collected high resolution aeromagnetic and gravity data in the Mount Isa terrane and the Thomson Orogen has greatly improved the resolution and extent of prior surveys and provide the unique opportunity to understand the tectonic system of the two regions. Geophysical survey reports and data are sourced from Geoscience Australia.

2.4.1 Mount Isa terrane

Modern airborne surveys were completed in 2006 and were released over the same period. All surveys are carried out at a line spacing of 400 m and a nominal ground clearance of 80 m over almost 430,000 km² of north-western Queensland. The data further extend and refine the coverage done by BMR in 1958 and Mount Isa Mines Ltd in the 1990s.

The Isa West survey, to the west of Mount Isa, collected ~63,533 line km of new magnetic data over an area of approximately 21,937 km². It was completed in April 2006 and released in August 2006 (Fig. 2.3). ~101,200 line km have been collected in the Isa southeast survey (Fig. 2.3) which was completed in 2006 and released in 2007. The Isa southwest survey (Fig. 2.3) was undertaken in 2006 with ~140,068 line km collected. These surveys were carried out by Department of Natural Resources, Mines and Water (Qld) and the contractor was Fugro Airborne Surveys Pty Ltd. The East Isa – north survey was collected in 2007 and released in 2007. This survey comprises ~113,195 line km of data and was collected by UTS Geophysics Pty Ltd for the Geological Survey of Queensland (GSQ). The East Isa – south was completed and released in 2007 and covers ~51,373 line km (Fig. 2.3). It was collected by Fugro Airborne Surveys Pty Ltd for the GSQ.

Gravity data have been collected with a 4 km to 2 km station interval over the same areas. A total of 36,643 stations were collected.

2.4.2 Thomson Orogen

New data acquisition was undertaken under the Greenfields 2020 Program, which has extended coverage to 100% of the study area by medium to high resolution airborne magnetics at a

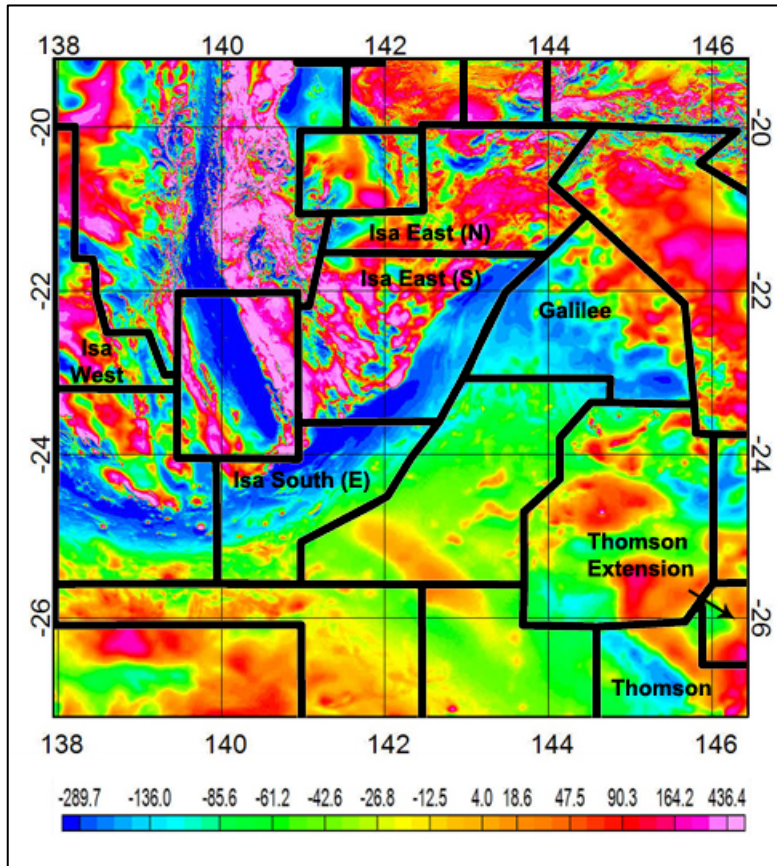


Fig 2.3 Regional (400 m or better line spacing) state and federal airborne geophysical coverage in the area of study

nominal 400 m line spacing and a nominal height of 80 m. Under Greenfield 2020 program, the airborne coverage was divided into three surveys - the Thomson survey, the Thomson extension survey and the Galilee survey (Fig. 2.3). The Thomson survey consists of ~299,000 line km of new magnetic data in the area bounded by St George in the east, Quilpie in the west and Charleville in the north. The Thomson extension survey consists of ~21,900 line km of new magnetic data collected in

the area around Augathella. The Galilee survey consists of ~124,400 line km of new magnetic data collected in central Queensland centred on Muttaborra. These new surveys bring the total coverage of Queensland at better than 400 m line spaced magnetic and radiometric data to just over 95%. Under Greenfield 2020 program, medium resolution ground gravity data were acquired as well. Data for the Thomson and Galilee gravity surveys were collected on a four km grid with each survey covering an area of approximately 100,000 km².

2.5 Image processing

In this study, image processing algorithms have been applied to the potential field data in order to enhance key features and improve the geophysical signal at different crustal levels. This allows the interpreter to explore shallowly sourced anomalies as well as deeply sourced components of the geophysical data, resolve the structural architecture of the region and link the upper crustal setting to the lower crustal architecture. A number of filters were used in order to correct the data with respect to their location on Earth and to highlight or remove anomalies having different wavelengths. Filtering was effective in enhancing variously oriented trends, gradients, boundaries and geometries of the source bodies not apparent in the original unfiltered datasets. The technical procedure and purpose of each filter have been described in the core chapter (3 - 6) for each study case. Appendix B is an integrated manual for students which describes the filtering procedure, the effects on the filtered spectrum and the main features of each filter in Oasis Montaj™ environment. It also includes a series of figures and explanatory notes in order to optimize filtering and imaging processing as well as useful tips. Filtering was undertaken using Geosoft's Oasis Montaj™ software. Geosoft's Oasis Montaj™ allows to view and process earth science datasets, grids and images within one integrated environment. It features a library of gridding utilities and plotting functionality in order to analyze and interpolate data.

Imaging coloring reflects the geophysical signal amplitude. Both unfiltered and processed images are assigned color range of red, green and blue tones where the blue represents lowest data values and red represents the highest data values. Coloring is normalized through histogram normalization so that the optimum amount of color contrast is achieved and enhances the degree of structural details. Greyscale tones have been assigned to selected grids (i.e. derivative filtered grids) because lineaments and gradients are best imaged if compared to the same pseudo-color images and provide greater contrast. Shaded illumination imaging technique has been applied to the images providing an artificial light source which illuminate the gravity and magnetic datasets from a selected azimuth and inclination. This casting shadows from high relief (highest amplitude values) providing an impression of depth and enhancing the perception of color intensity and saturation. As a result small amplitudes, short wavelength variations and structural trends orthogonal to the azimuth are enhanced.

ESRI ArcGIS™ has been used to assist in image interpretation and to build geological maps. The software allows visualizing multiple superimposed datasets (i.e. geophysical grids, location of outcrops, drill holes and seismic surveys) and facilitates integrated spatial analysis. As a result, it is possible to use the available geological information to constrain the interpretation of potential field data. In this study, some figures contain single filtered or unfiltered grids (e.g. total magnetic intensity grids, RTP magnetic grids or Bouguer grids) while other figures represent the superimposition of differently processed grids and constraining data to highlight key features and geological patterns.

2.6 Image interpretation

The lithospheric architecture of geological terranes is reflected in regional-scale geophysical anomalies. Geophysical interpretation uses a technique similar to that used in structural analysis and allows lithological mapping as well as the determination of overprinting relationships. Rock packages were assigned a lithology consistent with constraining geological data and their magnetic and gravity characters.

Basinal sequences are generally characterized by low gravity responses (see Fig. 2.1). The low magnetic signature (see Fig. 2.2) and smooth magnetic texture reflect the homogeneous distribution of the sparse magnetized minerals (Maidment et al., 2000; Nabighian et al., 2005b). Thickening of sedimentary packages is reflected as the decreasing in the amplitude of the long wavelength geophysical anomalies. Crystalline rocks show higher content of ferromagnetic minerals if compared to the overlying sedimentary deposit and are the main source of the magnetic anomalies (Crawford et al., 2010; Nabighian et al., 2005b). Shallowing or exposures of the crystalline basement is reflected in the geophysical grids as high geophysical responses and stippled texture. Burying of the basement instead is reflected by longer wavelength geophysical anomalies and decreasing amplitude values.

The aeromagnetic signature of igneous rocks reflects mostly their bulk composition, the variable oxidation state, and cooling history (Haggerty, 1979). Intrusive rocks can be distinguished from surrounding country rocks because of their distinctive geophysical anomalies. They are commonly associated with short wavelength, circular to elliptical shaped anomalies that truncate the long wavelength (regional) geophysical trend. Intrusions can be accompanied by contact metamorphic aureoles, which are associated with high linear magnetic anomalies. The positive anomalies reflect the combination of magnetite production which is due to contact metamorphic

processes and fluid migration at the pluton margin as the pluton solidifies. Granitic intrusions are characterized by low gravity anomalies whereas mafic bodies show high gravity anomalies and can be distinguishable. Granites derived from carbonaceous and metasedimentary rocks (S-Type) are commonly poorly magnetized while granites originated from melting of low-carbonaceous rocks (I-Type) are characterized by moderate to high magnetic responses. As a very general rule, short wavelength anomalies are related to shallower bodies while longer wavelength anomalies identify deeper structures. However, an extended superficial body can produce a long wavelength response as well.

In the geophysical grids, faults are commonly characterized by steep gradients and short wavelength linear anomalies. Faults, discontinuities and shear zones can be traced where the geophysical anomalies are a) truncated or displaced, b) regions showing a different geophysical character are juxtaposed and/or c) shear zones have undergone magnetite production or depletion as a result of fluid migration or metamorphic processes. Fault kinematics is interpreted through overprinting relationships and the apparent offset of geophysical markers. Dykes can be distinguished from faults because they do not truncate or offset the surrounding rock package. Excluding magnetite production, if the magnetic basement is not involved the fault may have discernible gravity signature but poor magnetic expression. Folds can be mapped when repetition of plunging or horizontal magnetic horizons are observed. Asymmetric curvature of magnetic bands or their horizontal gradients help in defining the geometries of the source bodies. Synforms produce low gravity anomalies and reflect the thickening of sedimentary rocks along the axis while antiforms show higher gravity anomalies which reflect the geometry of the positive structure and shallowing of the basement.

As a general and conclusive remark, the geophysical expression of lithologies is characterized by long wavelength responses while structures and shallow intrusions are associated with short wavelength anomalies. Juxtaposition of regions showing different geophysical signature reflect lithologic boundaries and may reflect facies transition (shallow gradients) or tectonic discontinuity (steep gradients).

2.7 Geological constraints

Gravity and magnetic data do not have unique solution and an infinite combination of geometries and petrophysical properties can be applied in order to match the observed geophysical signal (Betts et al., 2003b; Stewart and Betts, 2010b). However, the ambiguity can be significantly

reduced when the interpretation is constrained by additional geological and geophysical data. The geological interpretation in this study makes use of integrated geological and geophysical data which constrain the interpretation. Pre-existing geological and geophysical data from the published literature and unpublished documents have been integrated to obtain a geologically consistent interpretation.

2.7.1 Deep Seismic Surveys

Geophysical interpretation of the Mount Isa terrane is constrained by modern deep seismic reflection surveys conducted across North Queensland in a joint operation program that involved Geoscience Australia and the Geological Survey of Queensland (see Fig. 3.5 in chapter 3, section 3.4). A total of 2,287 km of seismic reflection data has been collected to 20s two way travel time equating to about 60 km in depth (Murray, 2007). The seismic data have been acquired and released between 2006 and 2007 and provide new insights to determine the geodynamic framework of North Queensland and to understand the tectonic style of major depositional systems (Murray, 2007). Two Mount Isa deep seismic lines shot by Australian Geological Survey Organisation in 1994 were reprocessed as well using the same standard methodology in order to present uniform data.

Magnetic and gravity interpretation in the Thomson Orogen has been constrained by the 1980 – 1986 Central Eromanga Deep Seismic Survey which covers a total linear distance of 1,400 km and join 5,000 km of older data, 2,300 km of which were reprocessed and digitalized (see Fig. 4.5 in chapter 4, section 4.3). The Central Eromanga Deep Seismic Survey provides insights into the crustal architecture and the distribution of the sedimentary sequences in the Thomson Orogen (Moss and Wake-Dyster, 1983; Wake-Dyster et al., 1983).

2.7.2 Drillholes

Shallow subsurface data have been provided by a number of drill holes. Although the coverage is not uniform, the drill holes provide constraints in defining the distribution of the basal sequences as well as the topography and nature of the upper crystalline basement. Isotopic analyses on samples collected from drill holes provide constraints for the timing and nature of some of the geological processes that affected the study area.

2.7.3 Other geophysical constraints

Geophysical mapping and interpretation of the southern Mount Isa terrane are largely based on the data released in the ‘Rock property data of the Mount Isa region’ report (Meixner, 2009) and the ‘Density and susceptibility characterization of major rock units and rock types of Mount Isa Inlier’ report (Barlow, 2004). The compilation of rock magnetic property data consists of 442 samples from the Mount Isa region from hand samples, drill cores and rock outcrops released by Geosciences Australia.

Modern surface wave tomography imaging has been performed to investigate the regional scale upper mantle structure and the contrast in lithospheric thickness across the Australian continent (Fichtner et al., 2009; Fishwick et al., 2008; Kennett et al., 2004; Simons et al., 1999). This provides insights into the lithospheric structure of the Mount Isa terrane and the Thomson Orogen.

In 1980 BMR employed magnetotelluric surveys that covered 12 sites along the Seismic Traverse n.1 in the Central Thomson Orogen (see Fig. 5.4 and Fig. 5.5 in chapter 5, section 5.3.2) (Spence and Finlayson, 1983). In 2006, magnetotelluric data were acquired and processed by Quantec Geoscience for Geoscience Australia and the Geological Survey of Queensland along the seismic line 07GA-IG1 (see Fig. 3.5 and Fig 3.7 in chapter 3, section 3.4). Magnetotelluric data provide information about the basin geometries and the structures of the underlying basement crust and upper mantle.

Constrained potential field analysis minimizes the ambiguity, provides scientific linkages between local scale observations and continental scale models and no other method provides such a high density data on a regional scale.

2.8 Forward modelling

Potential field forward modelling is a process in which a spatial model of a magnetisation or density distribution is tested to verify how the model fits the potential field data. Forward modelling technique provides a quantitative interpretation of magnetic and gravity datasets in 2–2.75 dimensions (Gunn et al., 1997) and allows geologic cross - sections to be constructed according to the geophysical response (McLean and Betts, 2003). Forward modelling along selected profiles was undertaken (chapters 5 and 6) to test the validity of the regional interpretation. Each block represents a geological unit and is assigned a density and a

susceptibility that do not vary across the block. This generates calculated magnetic and gravity profiles along the cross section which are compared to the observed geophysical responses. The parameters (the model architecture and the petrophysical properties of each block) are iteratively manipulated until the fit between the calculated and the observed data is satisfactory (Blakely, 1995). Geological and geophysical data, when available, can be successfully used to constrain the petrophysical properties of the geological units and/or to determine a-priori structuring of the region. Geological models have been built using *Geosoft's GM-SYSTM software*. The software provides integration of topographic, geologic, seismic, and well-log data.

Declaration for Thesis Chapter 3

Monash University

Declaration for Thesis Chapter 3

Declaration by candidate

In the case of Chapter 3, the nature and extent of my contribution to the work was the following:

Nature of contribution	Extent of contribution (%)
Processing and interpretation of gravity and aeromagnetic data; manuscript preparation	90

The following co-authors contributed to the work. If co-authors are students at Monash University, the extent of their contribution in percentage terms must be stated:

Name	Nature of contribution	Extent of contribution (%) for student co-authors only
Associate Professor Peter Betts	Supervisory role; interpretation	5
Dr. Laurent Ailleres	Supervisory role; interpretation	5

The undersigned hereby certify that the above declaration correctly reflects the nature and extent of the candidate's and co-authors' contributions to this work*.

**Candidate's
Signature**

Giovanni Pietro Tommaso Spampinato	Date
------------------------------------	-------------

**Main
Supervisor's
Signature**

Dr. Laurent Ailleres	Date
----------------------	-------------

Chapter 3: Structural architecture of the southern Mount Isa terrane in Queensland inferred from Magnetic and Gravity data

Giovanni P.T. Spampinato

PhD Candidate

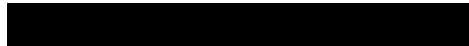
Monash University - School of Earth, Atmosphere and Environment

PO Box 84

Building 28, room 242

Clayton Campus, Wellington Road

Clayton, Vic 3800



Peter G. Betts

Associate Professor

Monash University - School of Earth, Atmosphere and Environment

PO Box 16

Building 28, room 239

Clayton Campus, Wellington Road

Clayton, Vic 3800



Laurent Ailleres

Senior Research Fellow

Monash University - School of Earth, Atmosphere and Environment

PO Box 28E

Building 28, room 144

Clayton Campus, Wellington Road

Clayton, Vic 3800



ABSTRACT

The basement rocks of the southern Mount Isa terrane are concealed under younger sedimentary units and its crustal architecture is understood using constrained regional potential field analysis. Combined deep seismic reflection data and geophysical interpretation indicate that the Mount Isa terrane comprises two broad tectonic domains. The Eastern Fold Belt accommodates thin-skinned, west-directed tectonic transport directions above the crystalline basement rocks. The Western Fold Belt is instead characterized by west-dipping structures that affect the basement crust during E-W-directed thick-skinned deformation.

The regional N-S- to NNW-trending geophysical anomalies of the Mount Isa terrane extend for ~250 km south of the exposed inlier and are abruptly interrupted by the Cork Fault. The southern Mount Isa Geophysical Domain is characterized by five juxtaposed tectonic sub-domains defined by long wavelength magnetic anomalies. Palaeoproterozoic basinal successions and major Palaeo- to Mesoproterozoic structures recorded in the Mount Isa Inlier continue southward under the Palaeozoic cover. The prominent regional magnetic and gravity anomalies are mostly attributed to shallowing of the Barramundi-aged basement and the distribution of metamorphosed sedimentary and volcanic rocks deposited during the formation of the ca. 1790 Ma to 1730 Ma Leichhardt Superbasin. Regional low magnetic and low gravity responses coincide with sedimentary successions deposited during the formation of the Calvert and Isa superbasins. Short wavelength magnetic anomalies that correlate with negative Bouguer gravity anomalies are interpreted to represent shallow and variously magnetized granitic intrusions.

The geophysical signature of the Mount Isa terrane is largely due to the fault architecture. In the southern parts of the Mount Isa terrane, Palaeoproterozoic sedimentary basins of the Western Fold Belt were controlled by half graben, within the NNW-trending Leichhardt River Fault Trough. To the east of the Pilgrim Fault, thick Palaeoproterozoic sedimentary and volcanic successions were deposited onto the crystalline basement and were controlled by major NNW-trending east-dipping normal faults. The Mesoproterozoic Isan Orogeny reactivated the existing extensional fault network and determined the current regional architecture, which is reflected by the prominent geophysical trend of the region. The wrenching phase of the Middle Isan Orogeny is represented by the activation of NW- and NE-oriented strike-slip faults overprinting the prominent N-S- to NNW-oriented structures. The emplacement of large NNW-

trending low density batholithic bodies may be coeval to the emplacement of the Williams Supersuite and may represent its southern extension. The southern Mount Isa terrane also appears to have been affected by post-Isan tectonics that resulted in sedimentary deposition and volcanic intrusions focused along the northern side of the Cork Fault.

Key Words: *Mount Isa terrane, Gravity, Magnetic, Proterozoic Australia, Basement architecture.*

3.1 Introduction

The Precambrian basement rocks of the Mount Isa terrane in northwest Queensland (Fig. 3.1) developed during a complex tectonic evolution that involved poly-cyclic tectonic events. These include intra-continental rift evolution, basin inversions, intra-plate igneous activity, regional high pressure - low temperature metamorphism, poly-phase orogenesis and extensive metasomatism (Betts et al., 2006; Edmiston et al., 2008; Eriksson et al., 1994; Geological_Survey_of_Queensland, 2010; Giles et al., 2006a; Giles et al., 2006b; O'Dea et al., 1997b; Wellman, 1992).

The exposed Mount Isa Inlier hosts world-class mineral deposits and has been extensively studied (Beardsmore et al., 1988; Betts et al., 2006; Bierlein and Betts, 2004; Bierlein et al., 2011; Blake, 1987; Blake and Stewart, 1992; Foster and Austin, 2008; MacCready, 2006b; O'Dea et al., 1997a; O'Dea et al., 1997b; Wellman, 1992). Regional potential field data show that unexposed parts of the Mount Isa terrane continue to the south, beneath the cover of younger sedimentary basins. The area of the concealed southern Mount Isa terrane is almost as extensive as the exposed inlier. It is nevertheless under-explored. As a result, the regional geology and crustal architecture of the southern unexposed Mount Isa terrane remains relatively poorly understood.

In this study, we undertake regional scale analysis through potential field data to map key features and resolve the crustal architecture of the concealed southern Mount Isa terrane. Regional potential field datasets are a valuable tool in the comprehension of regional geology of ancient tectonic systems with little or no geological exposure (Betts et al., 2003a; McLean and Betts, 2003) and can be used for plate tectonic reconstruction (Williams et al., 2010).

Interpretation of potential field data has non-unique solution, however the ambiguity can be significantly reduced by integrating geological data (Gunn et al., 1997).

The results of this study provide insights into the Proterozoic tectonic evolution of the Mount Isa terrane and have implications in understanding the distribution of economically significant depositional systems across the province.

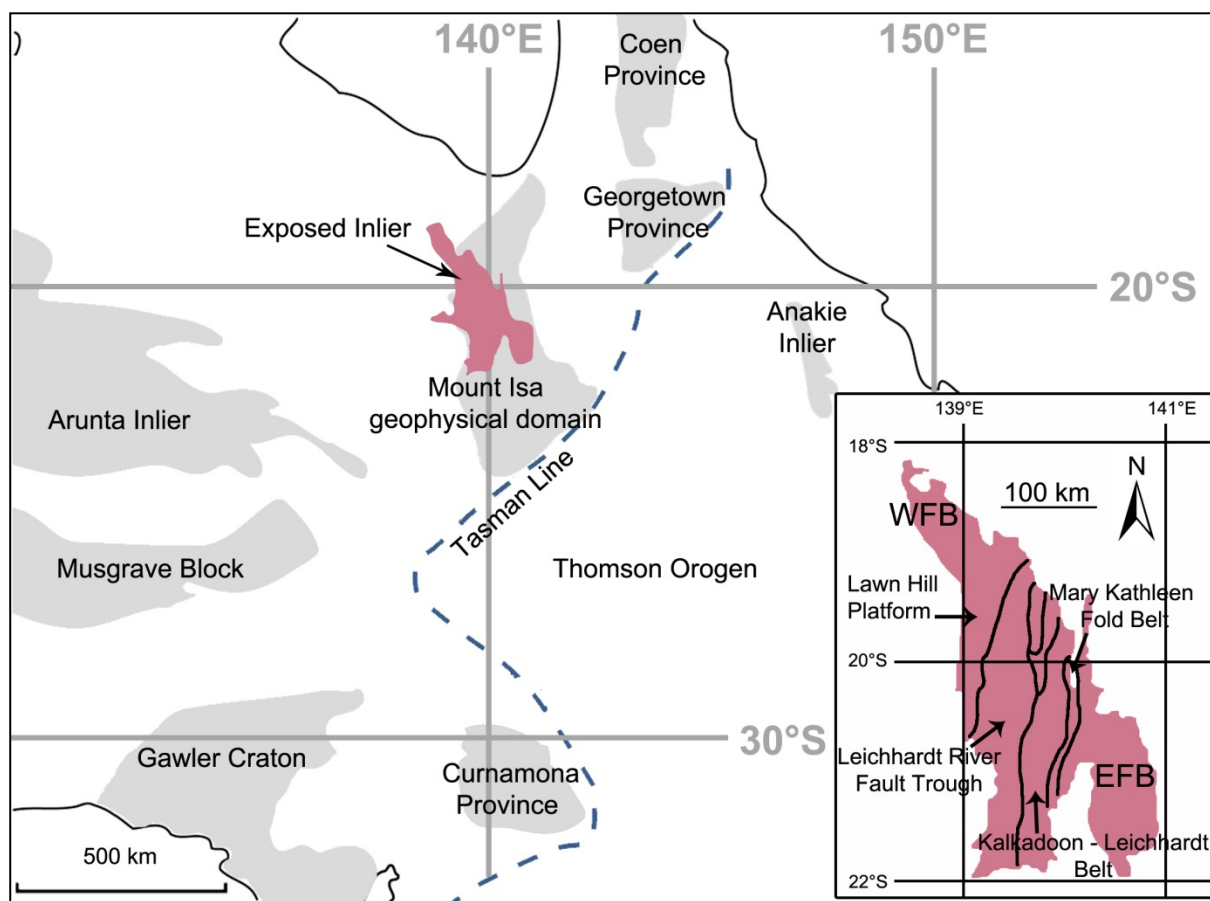


Fig. 3.1 Simplified tectonic map showing the exposed Mount Isa Inlier, the Mount Isa Geophysical Domain, as defined by Wellman (1992) and some of the surrounding geological provinces; modified from Betts et al. (2009). Bottom right inset shows the regional framework and tectonic subdivision of the Mount Isa Inlier; modified from Blake (1987) and O’Dea (1997b). WFB= Western Fold Belt; EFB= Eastern Fold Belt.

3.2 Regional geology

The Mount Isa terrane represents a continental crustal fragment that forms a major geological province of the eastern part of the North Australian Craton (Betts et al., in press; Betts et al., 2002). The region comprises mainly Palaeoproterozoic supra-crustal rocks (Betts et al., 2006; Bierlein and Betts, 2004; Giles et al., 2006a; MacCready, 2006a; Spikings et al., 2001) that overlie an interpreted Archaean basement (McDonald et al., 1997).

The exposed inlier (Figs. 3.1 and 3.2) preserves geological record that spans more than 350 million years between ca. 1870 and 1500 Ma (Betts et al., 2006). An early cycle of a ca. 1870 Ma orogenesis and ca. 1870 to 1850 Ma extensive batholith emplacement (Page and Williams, 1988) was succeeded by several cycles of superimposed basin formation and basin inversions (Giles et al., 2002; O'Dea et al., 1997b). This was followed by major period of Mesoproterozoic orogenesis, which has strongly influenced the structural and crustal architecture of the Mount Isa terrane (Betts et al., 2006; Drummond et al., 1998; Giles et al., 2006b).

The Kalkadoon-Leichhardt Domain forms a central belt (Blake, 1987). It contains Barramundi-aged basement rocks and separates the Western Fold Belt and the Eastern Fold Belt (Blake, 1987; Drummond et al., 1998; O'Dea et al., 1997a), which are characterized by different sedimentary depositional environments (O'Dea et al., 1997b) and deformation style (MacCready, 2006a).

3.2.1 Ca. 1900 – 1840 Ma crystalline basement

The basement rocks are formed by Palaeoproterozoic successions deformed and metamorphosed to amphibolite facies during the ca. 1900 - 1870 Ma Barramundi Orogeny (Betts et al., 2006; Blake, 1987; O'Dea et al., 1997b; Page and Williams, 1988). Exposures of the basement are found in the Kalkadoon-Leichhardt Domain and in the southern area of the Western Fold Belt (Fig. 3.2) (Betts et al., 2006). Ca. 1890 Ma mica schist, phyllite and gneiss of the Yaringa Metamorphics (Bierlein et al., 2008; Page and Williams, 1988) outcrop 30 km west of the city of Mount Isa (Fig. 3.2) (Wilson, 1987). The formation is intruded by the ca. 1800 Ma Big Toby Granite (Wyborn et al., 1987). Pre-basement lithologies, which have been recorded in the Kalkadoon-Leichhardt Domain (Fig. 3.2) (Bierlein and Betts, 2004; Bierlein et al., 2008; Foster and Austin, 2008), include the ca. 1875 - 1850 Ma granodioritic to monzogranitic intrusive rocks

of the Kalkadoon and Ewen batholiths and the ca. 1870 - 1840 Ma co-magmatic felsic Leichhardt Volcanics (Blake et al., 1990; Page and Sun, 1998). The ca. 1860 - 1850 Ma quartzofeldspathic gneiss of the Plum Mountain Gneiss (Blake, 1987; Blake et al., 1984) and the ca. 1860 Ma migmatitic, meta-sedimentary and meta-igneous rocks of the Kurbayia Migmatite (Bierlein et al., 2008; Page and Sun, 1998) are recorded east of the Mount Isa Fault (Fig. 3.2).

The ca. 1900 - 1870 Ma Barramundi Orogeny (Page and Williams, 1988) was a regional E-W to NE-SW shortening event (Blake, 1987; Blake and Stewart, 1992) and was characterized by an intense bedding - parallel gneissic foliation and N-S-trending upright folds (Betts et al., 2006; Blake, 1987; Etheridge et al., 1987). Emplacement of the Kalkadoon Batholith and the Leichhardt Volcanics are inferred to have occurred during the final stage of the Barramundi Orogeny (Page and Williams, 1988). The Kalkadoon Batholith shows arc-like affinities (Bierlein and Betts, 2004; McDonald et al., 1997) and may represent the remnant of a continental magmatic arc. However, Bierlein et al. (2011) indicated pre-1860 Ma emplacement of the Kalkadoon Batholith. They suggested that the Kalkadoon Batholith represents the remnant of a magmatic arc or transitional continental ribbon, inboard of the zone of active subduction, occurred between ca. 2200 and 1850 Ma, during the amalgamation of the North and West Australian cratons.

The Mount Isa Fault Zone (Fig. 3.2) has been interpreted as a Barramundi-aged suture (Shaw et al., 1996), although this interpretation has been questioned by Bierlein and Betts (2004) because of the similar isotopic character of pre-Barramundi-aged rocks on either side of the Mount Isa Fault. Bierlein et al. (2008) indicated that the Pilgrim Fault (Fig. 3.2) might represent the Early Proterozoic accretion of the Eastern Mount Isa terrane. The tectonic setting of the Barramundi Orogeny remains poorly understood because of poor preservation and strong overprinting due to the poly-cyclic Mesoproterozoic tectonics that affected the Mount Isa terrane (Betts et al., 2006). The orogeny may represent the final stage of growth of the North Australian Craton (Betts et al., 2002).

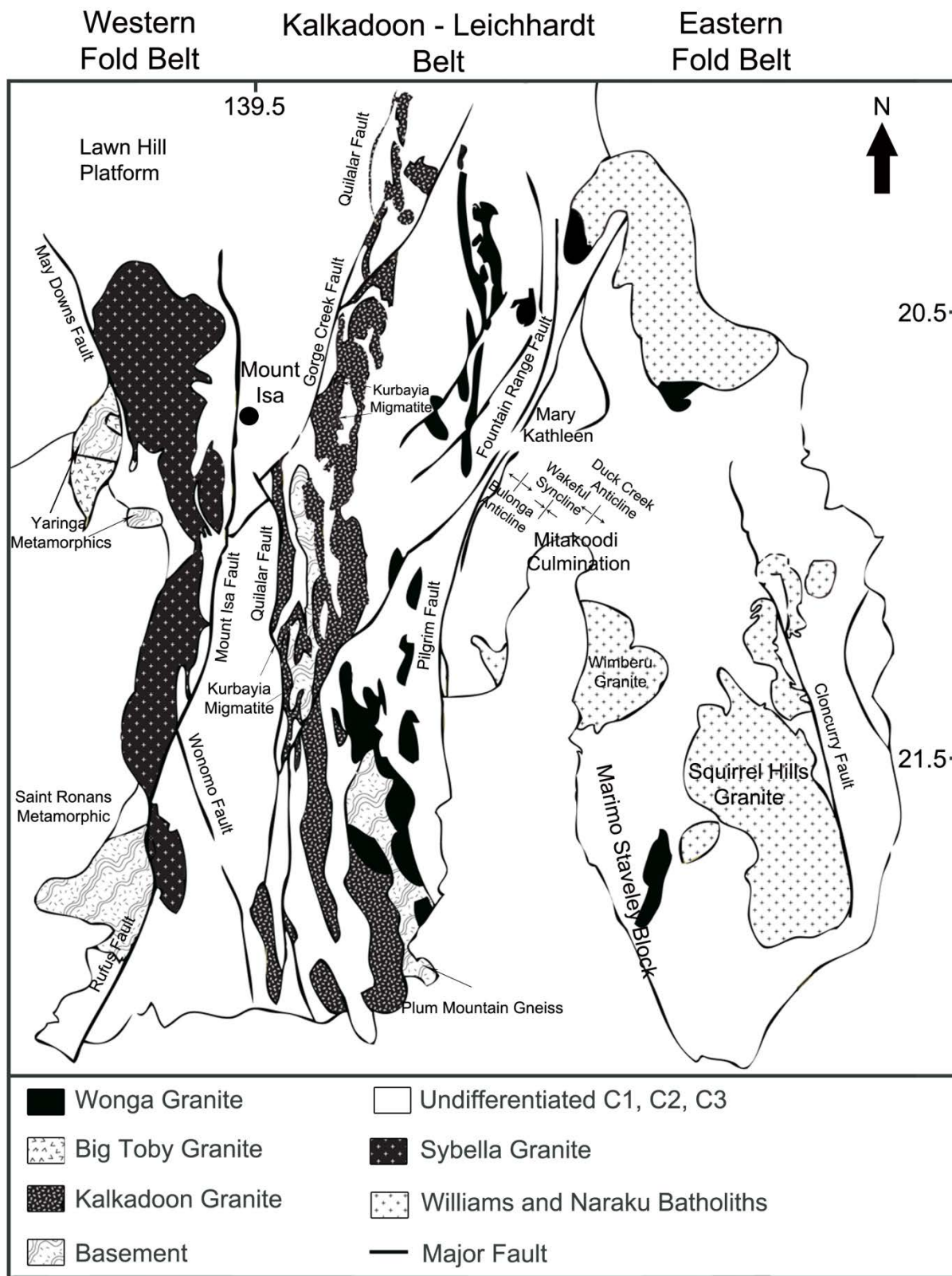


Fig. 3.2 Tectonic framework of the exposed Mount Isa Inlier; modified from Foster and Austin (2008) and O’Dea et al. (2006)

3.3 Pre - 1600 Ma Basinal Evolution

3.3.1 1790 - 1730 Ma *Leichhardt Superbasin*

Following the Barramundi Orogeny, the Mount Isa terrane records a protracted period of superimposed extensional basin formation in which several large Palaeoproterozoic superbasins evolved (Blake, 1987; Jackson et al., 2000; O'Dea et al., 1997b).

A ca. 1790 Ma E-W crustal extension resulted in the formation of the Leichhardt Superbasin. This phase of basin formation was characterized by the deposition of marine to fluvial sedimentation and voluminous continental tholeiitic basalts over a large area of the Mount Isa Inlier (Jackson et al., 2000; O'Dea et al., 1997b).

In the Western Fold Belt, sedimentation and volcanism were focussed into the elongate, N-S-trending Leichhardt Rift, which was defined by a series of half graben up to ~60 km wide (Betts et al., 2006; O'Dea et al., 1997b). The Quilalar, Mount Isa and the Gorge Creek faults (Fig. 3.2) bounded the margin of the rift and are considered to represent major structures that controlled the depositional sequences (O'Dea et al., 1997a; O'Dea et al., 1997b). Deposition of the ca. 1790 Ma Bottletree Formation (Page, 1983) and the ca. 1773 Ma Mount Guide Quartzite (Neumann et al., 2006b) reflects the transition from early deep marine sedimentation to fluvial and shallow-marine clastic facies in a rift-sag sequence (Blake, 1987; Derrick, 1982; Neumann and Fraser, 2007). The Mount Guide Quartzite is overlain by the basaltic Eastern Creek Volcanics (Jackson et al., 2000; O'Dea et al., 1997b). The Eastern Creek Volcanics has been associated with continental rifting (O'Dea et al., 1997b). Houseman and Hegarty (1987) suggested that the extrusion was driven to the rising of a mantle plume. Basaltic volcanism was followed by clastic sedimentation in coastal to shallow marine facies of the ca. 1775 Ma Myally Subgroup (Neumann and Fraser, 2007). The Myally Subgroup is inferred to have deposited in a predominantly syn-tectonic regime (Smith, 1969). E-W-trending rift faults bounding the N-S-trending half graben accommodated the deposition, inferred to have occurred during a N-S extension (O'Dea et al., 1997b).

In the Eastern Fold Belt, the Leichhardt Superbasin is represented by the ca. 1780 Ma Argylla Formation, a 1-5 km thick felsic volcanic formation interbedded with sandstones and siltstones (O'Dea et al., 1997b). The Argylla Formation is overlain by the ca. 1760 Ma mafic Marraba

Volcanics, which was erupted in a subaqueous to shallow marine environment (Foster and Austin, 2008; O'Dea et al., 1997b). The Pilgrim Fault (Fig. 3.2) has been interpreted as a prominent east-dipping normal fault that accommodated the basinal deposition during the development of the Leichhardt Superbasin (Blenkinsop et al., 2008; O'Dea et al., 1997b). To the immediate west of the Pilgrim Fault, the thinning of the Eastern Creek Volcanics and the Ballara Quartzite along with the lack of preservation of the Argylla Formation indicate that the Kalkadoon-Leichhardt Belt was a tectonic high at that time (MacCready, 2006b). Furthermore, Eriksson et al. (1994) indicated that the Bottletree Formation and the Mount Guide Quartzite successions were predominantly derived from the basement horst of the Kalkadoon-Leichhardt Domain further east.

The emplacement of an extensive granite body in the Mary Kathleen Domain (Fig. 3.2) has been interpreted to record an episode of a ca. 1760 - 1740 Ma mid-crustal N-S regional extension termed the Wonga Event (Holcombe et al., 1991). In the Eastern Fold Belt, deposition of the extensional-related ca. 1760 - 1750 Ma Ballara and Mitakoodi Quartzites (Foster and Austin, 2008; Potma and Betts, 2006) reflected near shore depositional environment and was coeval to the Wonga Event (Derrick et al., 1971; Holcombe et al., 1991; Jackson et al., 2000).

In the Western Fold Belt, a period of thermal subsidence between ca. 1750 and 1740 Ma is associated with the deposition on a continental shelf and shoreline facies of quartzite - carbonate package termed the Quilalar Formation (Foster and Austin, 2008; Jackson et al., 1990; O'Dea et al., 1997b). In the Eastern Fold Belt, carbonate - dominated successions of the ca. 1750 - 1745 Ma Doherty and Corella formations (Foster and Austin, 2008) overlie the Mitakoodi Quartzite and have been correlated with the Quilalar Formation (Derrick et al., 1980; Page and Sun, 1998).

In the Western Fold Belt, sedimentation associated with the Leichhardt Superbasin was terminated by a ca. 1735 - 1725 Ma basin inversion event which resulted in development of compressional structures and depositional hiatus (Betts et al., 1999; Derrick, 1982; Jackson et al., 2000). Basin inversion has not been recorded in the Eastern Fold Belt, where deposition of Doherty and Corella formations continued until ca. 1725 Ma (Betts et al., 2006).

3.3.2 1725 - 1690 Ma Calvert Superbasin

Renewed ca. 1725 - 1690 Ma NW-SE-directed extension marks the onset of the development of the Calvert Superbasin (Jackson et al., 2000; O'Dea et al., 1997b). The basal part of the Calvert

Superbasin includes the ca. 1725 Ma Peter Creek Volcanics (Jackson et al., 2000), which has been recorded northwest of the Mount Isa Inlier and is coeval to a rhyolite intruding the Doherty Formation in the Eastern Fold Belt (Foster and Austin, 2008). Early basin formation was accompanied by significant felsic magmatism and deposition of clastic-dominated sedimentary rocks into southeast-thickening half graben (Betts et al., 1999). These sediments were deposited between 1710 to 1690 Ma and are known only from the Western Fold Belt (Foster and Austin, 2008).

In the Western Fold Belt, clastic fluvial and shallow marine sedimentary rocks were deposited along the Leichhardt Rift (Derrick, 1982; O'Dea et al., 1997a; O'Dea et al., 1997b). The oldest sedimentary sequences include syn-rift conglomerates and sandstones of the Bigie Formation and the bimodal sub-aerial Fiery Creek Volcanics (Betts et al., 1999; Jackson et al., 2000; O'Dea et al., 1997b). The ca. 1709 Ma Fiery Creek Volcanics appear co-magmatic with the Weberra Granite (Foster and Austin, 2008; Neumann et al., 2006b). In the northern Sybella Domain and west to the Leichhardt River Domain, mid-Calvert Superbasin inversion is recorded by uplift and erosion of the Bigie Formation and Fiery Creek Volcanics (O'Dea et al., 1997b). Here, the lower packages of the Calvert Superbasin are missing from the stratigraphy (O'Dea et al., 1997b).

Renewed NNE- to SSW-directed extension (O'Dea et al., 1997b) resulted in deposition of the ca. 1700 to 1690 Ma Surprise Creek Formation, representing the upper part of the Calvert Superbasin (Derrick et al., 1980; Southgate et al., 2000a). The Surprise Creek Formation consists of conglomerates, sandstones and siltstones deposited in braided stream, alluvial fan to shallow marine environment (Blake et al., 1990) and locally unconformably overlies the Bigie Formation (Fig. 3.3) (O'Dea et al., 1997b). At this time, basin formation within the Leichhardt River Fault Trough occurred through mid-crustal shearing, which led to uplift and doming associated with magmatic intrusion, syn-extensional deformation and metamorphism at deeper levels (Gibson et al., 2008). To the west of the Mount Isa Fault Zone (Fig. 3.2), the ca. 1670 Ma syn-extensional Sybella Granite (Connors and Page, 1995) was emplaced and unroofed (Gibson et al., 2008). The Bigie Formation, Fiery Creek Volcanics and the Lower Surprise Creek Formation thicken towards the Quilalar and Gorge Creek Fault indicating that sedimentation and volcanism were controlled by half graben bounding normal faults (O'Dea et al., 1997a).

In the Eastern Fold Belt, the Llewellyn Creek Formation may have deposited with the Calvert Superbasin because, east of the Cloncurry Fault (Fig. 3.2), the formation has been intruded by a

tonalite dated at ca. 1686 Ma (U-Pb SHRIMP) (Rubenach et al., 2008). However, a maximum depositional age of $<1666 \pm 14$ Ma has been obtained from another sample from a unit mapped as Llewellyn Creek Volcanics as well (Foster and Austin, 2008; Giles and Nutman, 2002). This possibly suggests that this package needs to be readdressed.

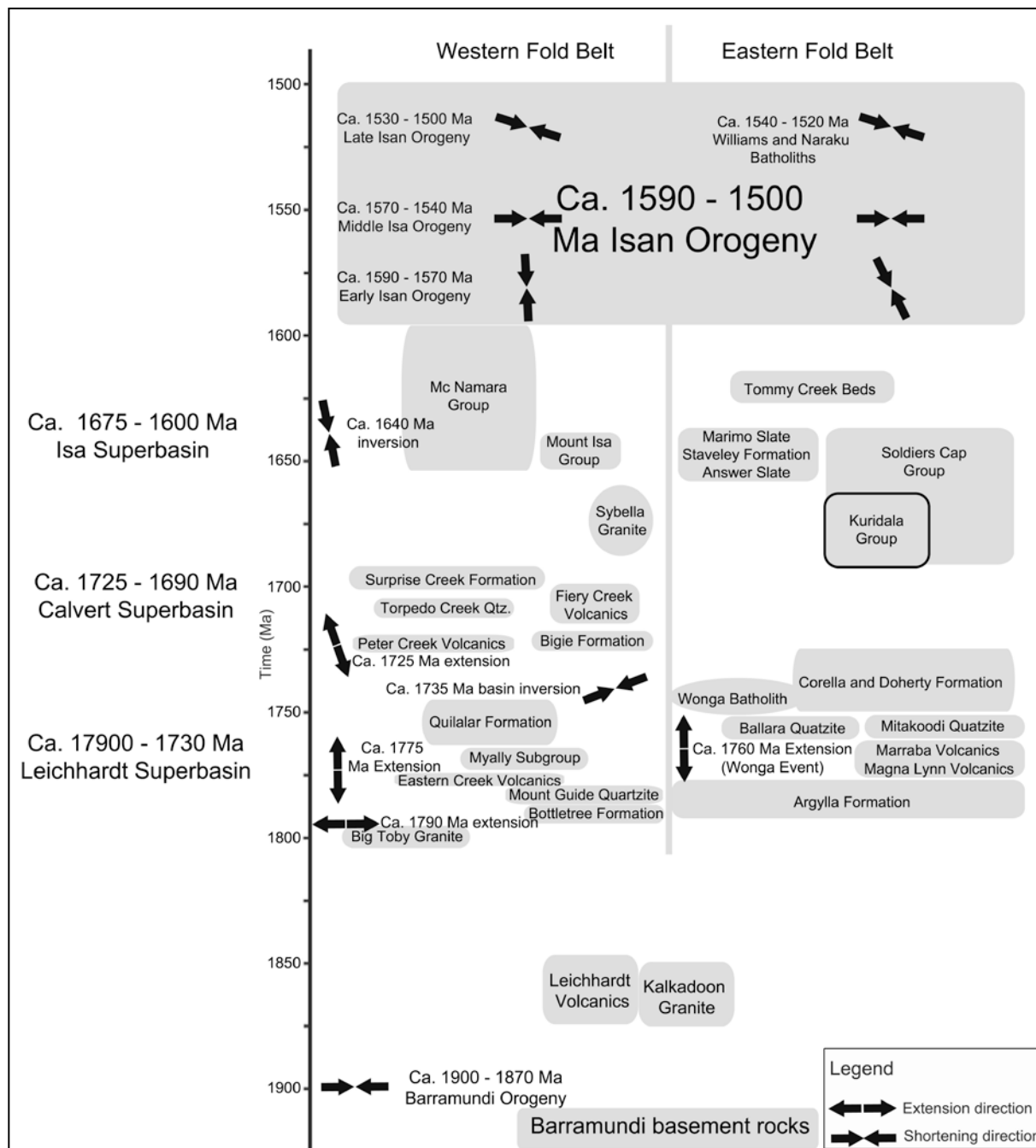


Fig. 3.3 Stratigraphic space - plot showing the timing of major depositional packages and major deformation and magmatic events; modified from Betts et al. (2006)

3.3.3 1675 – 1595 Ma Isa Superbasin

The development of the ca. 1675 - 1595 Ma Isa Superbasin marks the transition from extensional basin system to sag-phase sedimentation (Betts et al., 2006; Hutton et al., 2012). The Isa Superbasin is interpreted to reflect a period of thermal subsidence (Betts and Lister, 2001; Betts et al., 2001; Betts et al., 1999) accompanied by minor tectonic activity and fault reactivation (Andrews, 1998; Betts, 2001; Krassay et al., 2000; Scott et al., 1998), which could have controlled localized changes in basin geometry, igneous activity and the rate of sedimentation (Southgate et al., 2000a).

In the Eastern Fold Belt, the Isa Superbasin starts with the ca. 1676 to 1654 Ma (Foster and Austin, 2008) rift related succession of turbidite and quartzite, basalt and dolerite termed the Kuridala Formation, Upper Llewellyn Creek Formation (?) and Mount Norna Quartzite (Foster and Austin, 2008; Page and Sun, 1998). The upper part of the succession contains the ca. 1658 Ma Toole Creek Volcanics (Page, 1998). The Toole Creek Volcanics, Mount Norna Quartzite and Llewellyn Creek Formation were previously termed the Maronan Supergroup (Beardsmore et al., 1988). West of the Cloncurry Fault, deposition of the Marimo Slates, Answer Slates and Staveley Formation occurred (Betts et al., 2006; O'Dea et al., 1997b) and these are considered time equivalent (Foster and Austin, 2008).

In the Western Fold Belt, the development of the Isa Superbasin was preceded by the intrusion of the ca. 1670 - 1655 Ma Sybella Batholith (Fig. 3.2) (Connors and Page, 1995), which emplaced during (Gibson et al., 2008) or soon after (Connors and Page, 1995) extension and rift-related sedimentation of the Calvert Superbasin. Renewed sedimentation was dominated by carbonaceous shale, stromatolitic dolostone and turbiditic sandstones and siltstones of the McNamara Group on the Lawn Hill Platform and the equivalent ca. 1652 Ma (Page et al., 1994) Mount Isa Group (carbonates and siltstones hosting several Pb-Zn-Ag deposits) in the Leichhardt River Domain (Fig. 3.2) (Betts et al., 2006; O'Dea et al., 1997b).

Structural evidence and seismic data suggest that a ca. 1640 Ma N-S mild inversion occurred in the northern Lawn Hill Platform (McConachie and Dunster, 1998; Southgate et al., 2000b) and reversed pre-existing E-W-trending normal faults interrupting the Isa Superbasin deposition (Geological_Survey_of_Queensland, 2010). This inversion event occurred before the deposition of the ca. 1630 - 1595 Ma upper parts of the Isa Superbasin stratigraphy (O'Dea et al., 1997b).

The sedimentary hiatus recorded in the Western Fold Belt during this time has not been detected in the Eastern Fold Belt (Betts et al., 2006). Following the deposition of the Mount Isa Group, the Mount Isa terrane underwent a final N-S-directed extensional episode characterized by reactivation of pre-existing faults and formation of drag synclines in the hanging walls of south-dipping normal faults in the Western Fold Belt (O'Dea et al., 1997b).

Blenkinsop et al. (2008) indicated that the Pilgrim Fault controlled the deposition of the Calvert and Isa Superbasin successions. The Cloncurry Fault delineates the contact between the shallow water facies represented by the Doherty Formation to the west and the deep water rocks of the Soldiers Cap Group to the east (Gibson et al., 2006; Neumann et al., 2006a). This might indicate that the Cloncurry Fault Zone initiated as an extensional normal fault zone (Giles et al., 2006b) and formed the western margin of a rift basin (Austin and Blenkinsop, 2008).

3.3.4 The Isan Orogeny

The final architecture of the Mount Isa Inlier was imposed during the ca. 1590 - 1500 Ma Isan Orogeny (Bell, 1983; Blake, 1987; O'Dea et al., 1997b; Page and Bell, 1986), which strongly overprinted previous tectonic fabrics (Giles et al., 2006b). During the Isan Orogeny, the existing intra-plate rift system was shortened in a heterogeneous pattern (Blake and Stewart, 1992; O'Dea et al., 1997b). This event is characterized by the development of large felsic igneous provinces (Betts et al., 2007) and extensive high - temperature metamorphism (Giles et al., 2006b). At this time, deformation was superimposed upon a thinned and thermally weakened crust (Giles et al., 2006b). Although the crustal architecture produced during the Isan Orogeny shows an extraordinary geometrical variability and a complex deformation scheme (Giles et al., 2006b), areas with lower strain preserve their stratigraphic architecture and basinal structural features (O'Dea et al., 1997b).

In the Western Fold Belt, the early stages of the Isan Orogeny resulted in reverse thrust reactivation of E-W-oriented normal faults within the Leichhardt River Domain (Lister et al., 1999; O'Dea et al., 1997b). E-NE- to W-NW-trending faults initiated or were reactivated within the Century Domain and the Camooweal - Murphy Domain (Giles et al., 2006b).

In the Eastern Fold Belt, the early stage of the Isan Orogeny (ca. 1600 - 1580 Ma) occurred during N-S- to NW-directed thin-skinned deformation (Betts et al., 2006; Giles et al., 2006b; O'Dea et al., 2006). At this time, shallow inclined to recumbent folds and thrusts formed and

soled into a mid-crustal detachment (Giles et al., 2006b; O'Dea et al., 2006). Giles et al. (2006a) interpreted the early phase of the Isan Orogeny to involve reactivation of large faults systems (e.g., Overhang and Cloncurry overthrusts) and development of N- to NW-verging nappes (e.g., O'Dea et al., 2006; Betts et al., 2001).

The ca. 1570 - 1540 Ma Middle Isan Orogeny is characterized by a regional E-W crustal shortening event (Giles et al., 2006b; O'Dea et al., 1997b). At this time, deformation style switched from thin-skinned to thick-skinned. The change in deformation style is attributed to thickening and cooling of the orogenic belt (Giles et al., 2006b). Crustal-scale upright folds and N-S-trending reverse faults and thrusts developed at this time (Giles et al., 2006b; MacCready et al., 1998). In the Western Fold Belt, inversion of the Quilalar, Gorge Creek and Mount Isa faults (Fig. 3.2) occurred producing regional anticlines (Betts and Lister, 2001; Bierlein and Betts, 2004; MacCready et al., 1998; O'Dea et al., 1997a). In the Eastern Fold Belt, the west-vergent Mitakoodi Culmination may have developed in response to the displacement of E-W- to NW-trending thrusts and reverse faults, producing the Duck Creek Anticline, Wakeful Syncline and Bulonga Anticline (Fig. 3.2), although the deformation may have initiated during the early phase of the Isan Orogeny (O'Dea et al., 2006). Structures formed during E-W shortening are overprinted by faults interpreted to have formed during a late wrenching phase. These wrench faults display Riedel orientations and define a transition from ductile folding to brittle faulting as the primary mode of deformation (O'Dea et al., 1997b). The crustal shortening was accommodated by NW-striking sinistral and NE-striking dextral strike-slip faults (Lister et al., 1999; O'Dea et al., 1997b). Large-scale N-S-trending strike-slip faults including the Pilgrim and the Quilalar faults have been interpreted to post-date the folding and metamorphism of the Early to Middle Isan Orogeny (Blake, 1996). The ca. 1530 - 1500 Ma final stage of the Isan Orogeny occurred in an E-W- to ESE-WNW-directed shortening event. Coincident with this event was the extensive emplacement of A-type and I-type granites throughout the Eastern Fold Belt (Wyborn, 1998).

There is still poor understanding about the post-orogenic tectonics of the Mount Isa terrane (O'Dea et al., 1997b). However, $^{40}\text{Ar}/^{39}\text{Ar}$ data from Palaeo- to Mesoproterozoic rocks from the Mount Isa Inlier show that the region experienced periods of cooling between 1490-1410 Ma, 1280-1050 Ma, 750-650 Ma and 600-500 Ma. These events might correlate to the assembly and break-up of post 1500 Ma super-continent (Spikings et al., 2001, 2002). The Cambrian to Early

Ordovician sediments of the Georgina Basin, the Permian to Triassic Galilee Basin and the Late Jurassic to Early Cretaceous successions of the Carpentaria and Eromanga basins unconformably overlie the Palaeo- to Mesoproterozoic rocks of the Mount Isa terrane (Spikings et al., 2001). The depositional sequences are generally flat except along major fault zones where Neoproterozoic and Phanerozoic episodes of crustal displacement and exhumation have been inferred (Spikings et al., 2001).

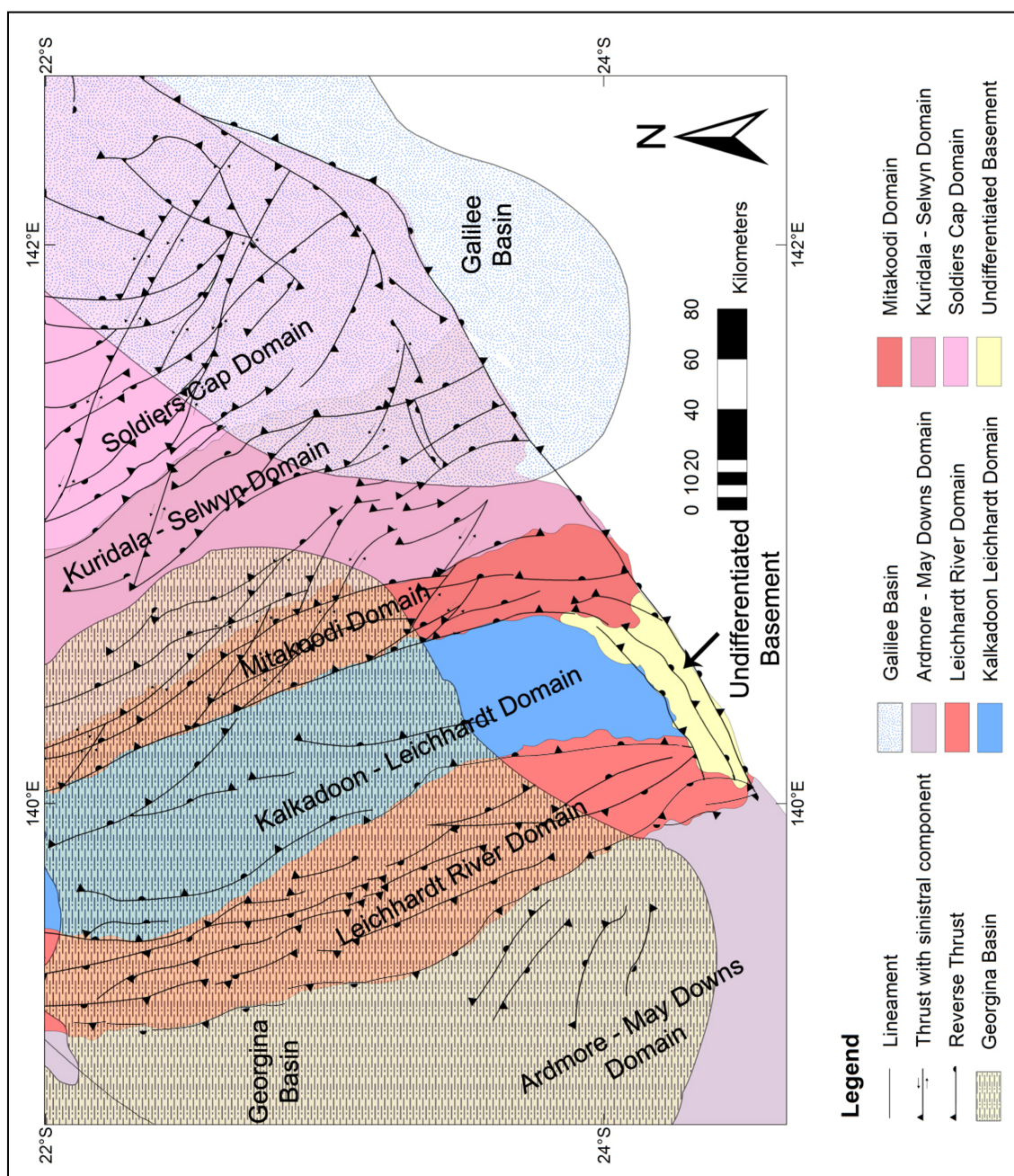


Fig. 3.4 Map of the geological domains and major structural features of the southern Mount Isa terrane

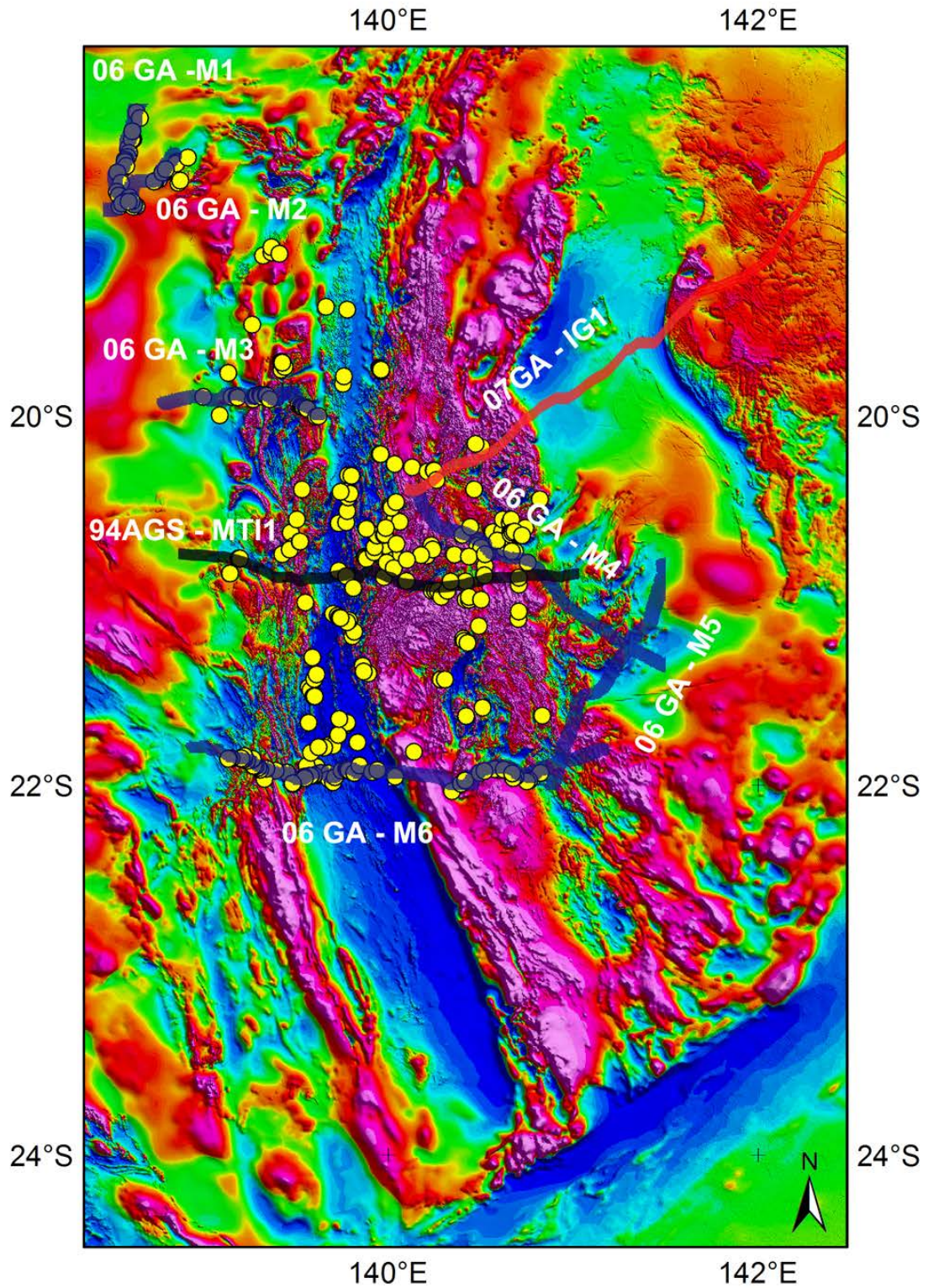
3.4 Previous geophysical surveys

In 2006 and 2007 deep seismic reflection surveys have been conducted across North Queensland in a joint operation program that involved Geoscience Australia and the Geological Survey of Queensland (Fig. 3.5). A total of 2,287 km of seismic reflection data were collected to 20s two way travel time equating to about 60 km in depth. The seismic data provided new insights to determine the geodynamic framework of the North Queensland and to understand the tectonic style of major depositional systems (Murray, 2007). Two Mount Isa deep seismic lines shot by Australian Geological Survey Organisation in 1994 were reprocessed as well using the same standard methodology in order to present uniform data (Fig. 3.5). Seismic Transects 06GA-M5 and 06GA-M6 cross the central Mount Isa terrane and provided new information about the crustal architecture of the region (Fig. 3.5). Regionally the Mount Isa terrane shows a weakly reflective and seismically homogeneous thick crust that extends to ~55 km depth (Fig. 3.6) (Korsch et al., 2012; MacCready, 2006a).

Fig. 3.5 (next page) Location of the 2006 Deep Seismic Transects across the Mount Isa terrane and rock magnetic property data from hand samples and drillholes over a TMI map. On the top right context map; modified from Korsch et al. (2009)

The 2006 seismic survey has been undertaken by Geoscience Australia in collaboration with the Queensland Geological Survey, the Predictive Mineral Discovery Cooperative Research Centre and Zinifex Pty Ltd. Processing has been undertaken at Geoscience Australia. 2007 seismic survey reflection data cover a total linear distance of 1,387 km and link with the 2006 seismic surveys to the northeast of Cloncurry. The survey was carried out in a joint collaboration program between the Australian Government's Onshore Energy security Program, the Queensland Government's smart mining and Smart Exploration initiatives and Auscope. The data were acquired by the National Research Facility for Earth Sounding and processed by Geoscience Australia.

The compilation of rock magnetic property data was released by Geosciences Australia. Dataset author: Meixner, A.J. Copyright Commonwealth of Australia 2009 and Geoscience Australia.



In the Western Fold Belt, the seismic reflection profiles show predominantly west-dipping structures that affect and deform the crystalline basement (Fig. 3.6) (MacCready, 2006a). In the

Eastern Fold Belt, a major feature termed the Tewinga Detachment, is imaged at a depth of 3-9 km (MacCready, 2006a). The detachment occurs at the top of the crystalline basement and accommodates high strain west-directed deformations in rocks that overlie the detachment (MacCready, 2006a). In turns, the Tewinga Detachment is displaced by a set of predominantly east-dipping faults that penetrate into the basement rocks (Fig. 3.6) (MacCready, 2006a).

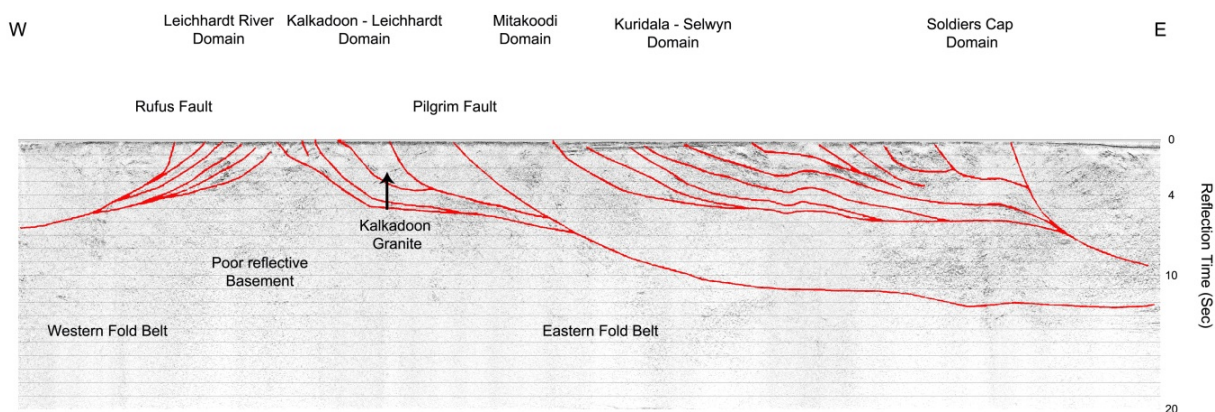


Fig. 3.6 Deep Seismic Transects N. 06GA-M6 crossing the central part of the Mount Isa terrane; modified from Korsch (2008)

Regional seismic reflection profile 07GA-IG1 (Fig. 3.5) imaged the presence of a low reflective zone showing a planar geometry and dipping to the west (Fig. 3.7) (Korsch et al., 2012). This zone can be traced from the surface to the Moho and defines the boundary between the non-reflective and thick Mount Isa terrane from thinner and two-layered crust of the Numil Seismic Province further east (Fig. 3.7) (Korsch et al., 2012). Magnetotelluric data were acquired and processed by Quantec Geoscience for Geoscience Australia and the Geological Survey of Queensland along the seismic line 07GA-IG1. These data show that the major crustal feature imaged in the seismic data juxtaposes the highly resistive Mount Isa terrane to the west against the highly conductive Numil Seismic Province to the east (Korsch et al., 2012). The discontinuity has been interpreted to represent a major suture since it divides two terranes showing different geophysical characters and has been termed the Gidyea Suture (Korsch et al., 2012). The Gidyea Suture underlies ca. 1660 - 1600 Ma supracrustal successions (Foster and Austin, 2008) and is interpreted to represent the juxtaposition of the Mount Isa and Numil provinces which occurred between 1850 and 1800 Ma (Betts et al., in press).

The west-dipping Gidyea Suture Zone has a prominent linear gravity response with a strike-length of several hundred km and it is interpreted to represent mafic and ultramafic oceanic lithosphere (Betts et al., in press).

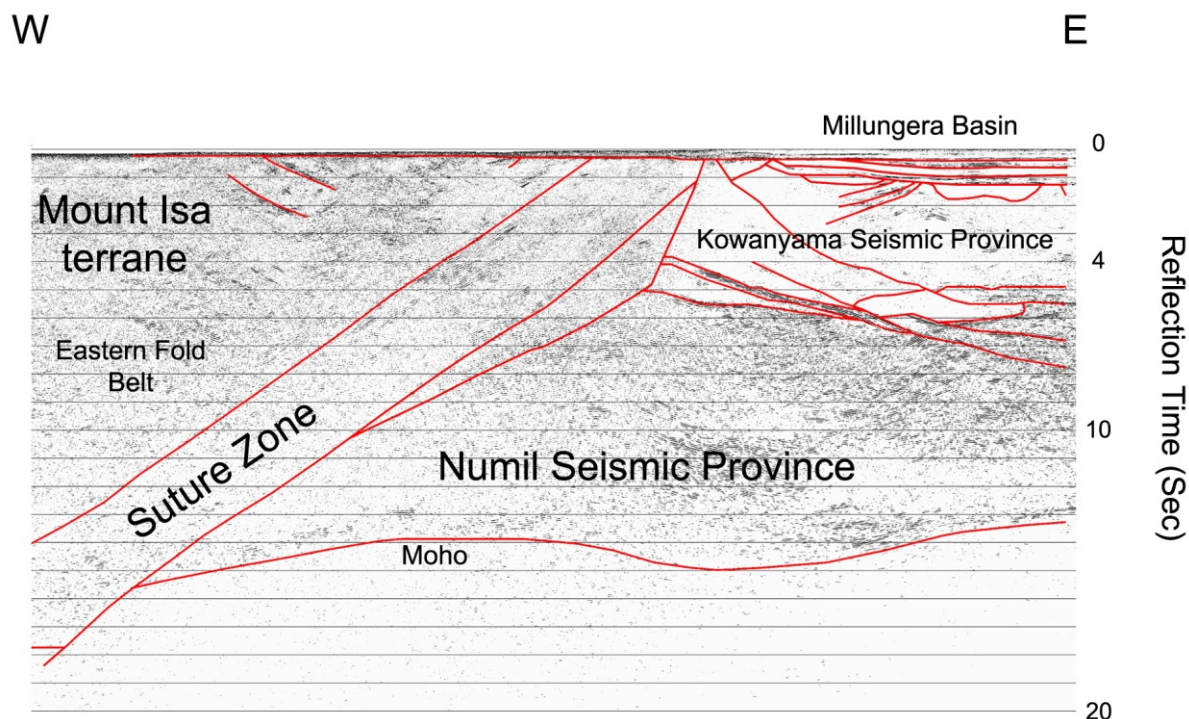


Fig. 3.7 Southwest end of the Deep Seismic Profile 07GA-IG1 crossing the eastern Mount Isa terrane and the Numil Seismic Province; modified from Korsch et al. (2012)

Seismic line 07GA-IG1 imaged also a previously unknown basin overlying the Kowanyama and the Numil Seismic provinces (Fig. 3.7). The basin shows flat lying succession extending for ~2.8 - 3.5 km depth thickening towards the northeast and has been termed the Millungera Basin (Korsch et al., 2012). SHRIMP detrital zircons derived from drillholes that penetrated into the Millungera Basin about 150 km south of the Deep Seismic Transect 07GA-IG1 gave maximum depositional age of 1560 to 1593 Ma (Neumann and Kositsin, 2011) and post-date the deposition of the Isa Superbasin. Short intersections of the western part of the basin were also imaged in the 2006 seismic lines 06GA-M4 and 06GA-M5 (Gibson et al., 2010; Hutton and Korsch, 2008). The southwest margin of the Millungera Basin appears to be faulted by SW-dipping structures while the northeast margin is truncated by NE-dipping thrust faults (Korsch et al., 2012). The Millungera Basin is underlain by a non-reflective zone up to 1.5 km thick which has been interpreted to be pervasively intruded by granitic intrusions (Korsch et al., 2012; Korsch et al.,

2011). Magnetotelluric data along the seismic profile 07GA-IG1 indicate that the Millungera Basin is a conductive region and coincides with regional low gravity anomalies (Chopping and Henson, 2009; Korsch et al., 2009).

3.5 Methods

Geophysical interpretation outlines the distribution and geometries of source bodies with contrasting petrophysical properties. The method provides insights into structural architecture and kinematics in regions with little or no geological exposure (Aitken and Betts, 2009; Stewart and Betts, 2010b). The aeromagnetic response of different rock types mostly reflects their magnetite content and oxidation state (Whiting, 1986). The distribution of magnetite is reflected in the texture of aeromagnetic images. Sedimentary and meta-sedimentary rocks are characterized by homogeneous distribution of magnetite resulting in a smooth magnetic texture. Initial composition and heterogeneous crystallisation temperature in igneous rocks instead (Haggerty, 1979) results in a ‘stippled’ or ‘mottled’ magnetic response (Betts et al., 2003b).

Since 2006, the Geological Survey of Queensland increased the acquisition of both gravity and airborne geophysics data in the Mount Isa terrane and surrounding areas. Gravity data were collected in 36,643 stations with a spacing of 4 km x 4 km over an area of ~440,000 km². Modern airborne geophysical surveys were carried out at a line spacing of 400 m and a ground clearance of 80 m which cover an area of ~405,000 km² (Chopping and Henson, 2009).

Filtering and image enhancement of the acquired geophysical grids were undertaken in order to improve the geophysical signal and to resolve source bodies at different crustal levels. The total magnetic intensity grid was reduced to the pole to bring anomalies over their source bodies and to remove asymmetries in the magnetic anomalies caused by the Earth’s inclined field (Arkani-Hamed, 1988; Blakely and Simpson, 1986; Ervin, 1976). The vertical derivative filter calculates the vertical rate of change in the magnetic signal and sharpens the geophysical anomalies (Hood et al., 1982; Miller and Singh, 1994; Roest et al., 1992). This filter was applied to locate more accurately source bodies and to highlight the regional architecture of the area. The tilt derivative filter calculates the ratio of the vertical gradient and the total horizontal gradient and it was applied to better define the boundaries between the source bodies (Miller and Singh, 1994). The tilt derivative filter processes the signal irrespectively of the amplitude of the magnetic field thus enhancing the geophysical signal of weak anomalies. A low pass filter was applied in order to cut

the noise generated by the derivative filters and to locate source bodies a mid- to low crustal level.

3.5.1 Rock Properties

Gravity and magnetic data do not have unique solution (Betts et al., 2003b; Stewart and Betts, 2010b). As many different geological settings could give the same geophysical response, constraining the interpretation with existing geological and geophysical data can reduce significantly the ambiguity.

Mapping and correlation in this study are largely based on the data released in the ‘Rock property data of the Mount Isa region’ report (Meixner, 2009) and the ‘Density and susceptibility characterization of major rock units and rock types of Mount Isa Inlier’ report (Barlow, 2004). The compilation of rock magnetic property data (Fig. 3.8) consists of 442 samples from the Mount Isa region from hand samples, drill cores and rock outcrops released by Geosciences Australia. Approximately 200 samples were collected along the deep seismic lines 06GA-M1, 06GA-M2, 06GA-M3 and 06GA-M6 in the Mount Isa/Cloncurry area (Fig. 3.5) and measured by the Economic Geology Research Unit, School of Earth and Environmental Sciences, James Cook University and the Queensland Department of Mines and Energy, Geological Survey of Queensland (Blenkinsop et al., in prep.). Approximately 200 samples consist of density and magnetic susceptibility measurements sourced from Hone et al. (1987); Approximately 75 density and some magnetic susceptibility measurements were provided by Sampath and Ogilvy (1974) and Mutton and Almond (1979). The dataset was integrated with the density and magnetic susceptibility measurement database over the Mount Isa Inlier released by Xstrata (2004) which partly reproduces BMR database.

Magnetic susceptibility measurements have been also undertaken by Austin and Blenkinsop (2008) from 277 stations along the Cloncurry fault zone in the Eastern Fold Belt. Although the lithology coverage is not uniform, the combined datasets provide insights for petrophysical characterisation of the basement rocks and depositional package of the Mount Isa terrane.

Basalt	Density (saturated) N/M/SD (g/cc)			Density (grain) N/M/SD (g/cc)			Magnetic Susceptibility N/M/SD (SI*10 ⁵)		
Cromwell	3	2.96	0.10	3	3.01	0.10	5	5750	4643
Pickwick	4	2.98	0.02	3	3.02	0.05	4	2900	2843
ECV - Undiff	14	2.81	0.12	2	2.75	0.07	81	2412	2429
Toole Creek	9	2.99	0.16	1	3.10	-	8	157	172
Marraba	2	2.77	0.09	1	2.79	-	2	2725	3500
Generic Dyke	12	2.91	0.14	9	2.97	0.10	12	3145	3208
Granite	Density (saturated) N/M/SD (g/cc)			Density (grain) N/M/SD (g/cc)			Magnetic Susceptibility N/M/SD (SI*10 ⁵)		
Big Toby	5	2.67	0.05	5	2.68	0.05	5	150	282
Mount Dore	1	2.64	-	1	2.66	-	1	138	-
Kalkadoon	22	2.68	0.05	22	2.70	0.05	22	193	666
Wonga	11	2.65	0.06	11	2.68	0.06	12	226	570
Naraku	11	2.66	0.04	9	2.68	0.04	11	3647	3892
Sybella	7	2.63	0.05	-	-	-	8	110	170
Weberra	5	2.56	0.02	5	2.59	0.02	5	7	11
Wimberu; Mt Margaret	5; 4	2.62; 2.67	.02; .05	5	2.66	0.03	5; 5	977; 4936	1772; 2093
Quartzite	Density (saturated) N/M/SD (g/cc)			Density (grain) N/M/SD (g/cc)			Magnetic Susceptibility N/M/SD (SI*10 ⁵)		
Ballara	1	2.82		1	2.93		1	12690	
Mitakoodi	4	2.77	0.09	2	2.82	0.04	3	3138	1716
Mt Guide	2	2.65	0.04				3	42	72
Mt Norna	18	2.84	0.33				18	2182	6060
Volcanics	Density (saturated) N/M/SD (g/cc)			Density (grain) N/M/SD (g/cc)			Magnetic Susceptibility N/M/SD (SI*10 ⁵)		
Fiery Creek	1	2.53		1	2.54		1	13	
Argylla	11	2.69	0.09	7	2.73	0.11	8	47310	128145
Tewinga(Leichardt?)	1	2.68							
Bottletree	4	2.65	0.01	2	2.68	0.01	4	2513	2902
Leichardt	9	2.71	0.09	5	2.66	0.03	9	290	525
Non- Volc. Sequences	Density (saturated) N/M/SD (g/cc)			Density (grain) N/M/SD (g/cc)			Magnetic Susceptibility N/M/SD (SI*10 ⁵)		
Surprise Ck	5	2.57	0.13				9	20	40
Corella Fm	66	2.78	0.18	38	2.85	0.26	113	1581	3757
Marimo	11	2.45	0.27	11	2.77	0.24	1	2	
Overhang	10	2.84	0.29	10	2.92	0.22	11	2676	6038
Soldiers Cap	5d	2.76	0.14	2	2.97	0.19	5	3793	8416
Myally Sub	2	2.60					43	15	63
Gneiss	Density (saturated) N/M/SD (g/cc)			Density (grain) N/M/SD (g/cc)			Magnetic Susceptibility N/M/SD (SI*10 ⁵)		
Tewinga Un	9	2.66	0.06	9	2.68	0.07	9	1106	2284
Tewinga – May Downs	2	2.84	0.28				2	63	90
Rock	Density (saturated) N/M/SD (g/cc)			Density (grain) N/M/SD (g/cc)			Magnetic Susceptibility N/M/SD (SI*10 ⁵)		
Quartzite	28	2.79	0.28	7	2.77	0.01	31	1989	5110
Felsic Volcanic	34	2.81	0.16	10	2.72	0.15	101	2027	2363
Granite	94	2.66	0.06	80	2.68	0.06	101	858	2041
Sedimentary	172	2.74	0.18	99	2.81	0.21	275	2279	2212
Basalt	22	2.94	0.12	17	2.99	0.09	101	1511	2487
Gneissic	11	2.69	0.13	9	2.68	0.07	11	917	2086

Fig. 3.8 Major Rock type densities and susceptibilities of the Mount Isa region; modified from Barlow (2004)

3.6 Observations and results

The geophysical domain of the Mount Isa terrane extends for ~200 km north and ~250 km south of the exposed inlier (Fig. 3.9) (Wellman, 1992). The Mount Isa terrane is characterized by regional arcuate N-S- to NNW-trending anomalies and shows the highest geophysical amplitude signature when compared to the surrounding regions. To the south of the exposed inlier, the Bouguer gravity map shows NNW-trending long wavelength positive gravity anomalies with several areas beyond $250 \mu\text{m} \cdot \text{s}^{-2}$ (Fig. 3.11), onto which short wavelength (5 - 15 km) anomalies

are superimposed. The magnetic grid is characterized by positive magnetic responses and a broad magnetic low located to the centre of the Mount Isa terrane (Fig. 3.10). Major trends and anomalies in the Bouguer gravity map correlate with regional magnetic anomalies (Fig. 3.9) (Wellman, 1992).

3.6.1 Geophysical boundaries

To the west, the Mount Isa Geophysical Domain, following the definition by Wellman (1992), terminates against the proto-North Australian Craton (NAC, Fig. 3.9) (Betts et al., in press). The boundary is well defined along the Rufus Fault (Fig. 3.9), which shows a distinctive geophysical response and separate the N-S-trending geophysical anomalies of the Mount Isa terrane from the WNW- to SE-trending features of the Tennant Creek Province (Korsch et al., 2009).

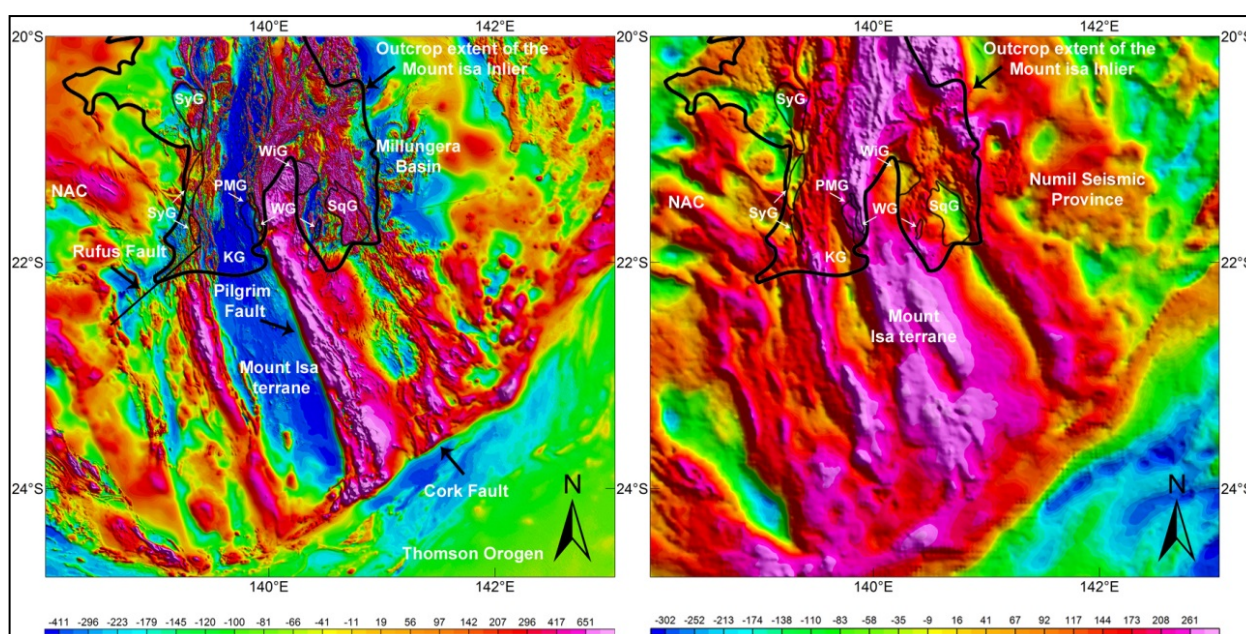


Fig. 3.9 Context map showing the geological provinces surrounding the Mount Isa Geophysical Domain and major structures within the area of study over a a) RTP map and b) Bouguer Gravity map. Values in the scale bar are in nT (a) and $\mu\text{m}^2\text{s}^{-2}$ (b). NAC= North Australian Craton; KG= Kalkadoon Batholith; SyG= Sybella Granite; PMG= Plum Mountain Gneiss; WG= Wonga Granite; WiG= Wimberru Granite; SqG= Squirrel Hill Granite

The eastern boundary between the Mount Isa terrane with the Numil Seismic Province is best imaged in the Bouguer gravity map (Fig. 3.9) and corresponds to N-S- to NNW-trending positive gravity anomalies which define a discrete belt of rocks (Korsch et al., 2012). The abrupt termination that defines the southern boundary of the Mount Isa terrane at the Cork Fault is well defined both in the magnetic and Bouguer gravity maps (Figs. 3.9, 3.10 and 3.11). Here, the

positive NNW-trending anomalies of Mount Isa Geophysical Domain (Wellman, 1992) terminate against SE-oriented low gravity and low magnetic anomalies of the Thomson Orogen. The steep NW-oriented geophysical gradients (~ 150 nT/km and $\sim 50 \mu\text{m}^2/\text{s}^2/\text{km}$) decreasing towards the southeast represent the geophysical expression of the Cork Fault that extends for more than 500 km (Spampinato et al., Unpublished results-a). The southern Mount Isa terrane is characterized by a series of distinctive juxtaposed tectonic sub-domains (Figs. 3.10 and 3.11) that broadly correlate with long wavelength anomalies, which we describe below.

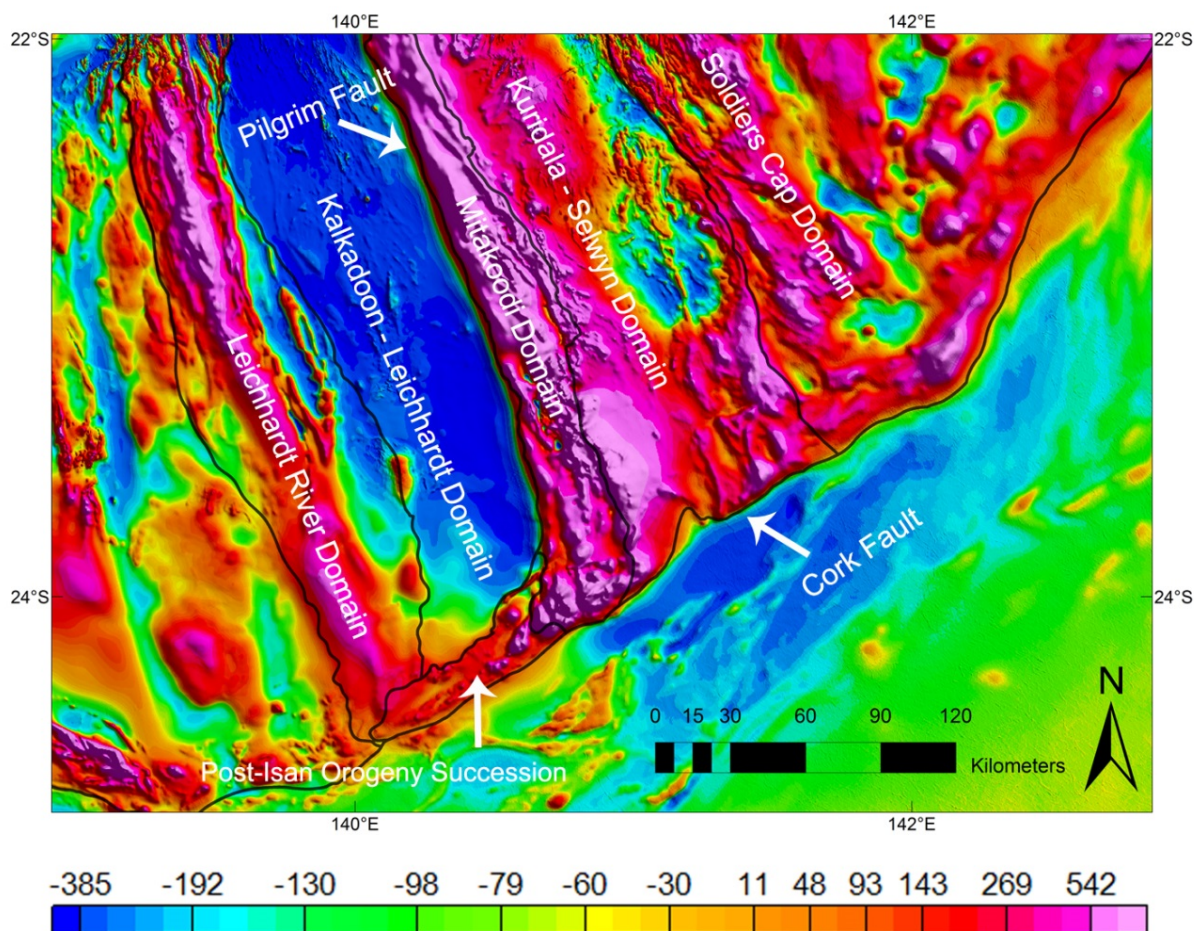


Fig. 3.10 RTP magnetic map of the southern Mount Isa terrane along with its geophysical sub-domains. Values in the scale bar are in nT.

3.6.2 Leichhardt River Domain

The western and central parts of the Leichhardt River Domain (Figs. 3.12 and 3.13) show positive NNW-trending long wavelength magnetic (~ 20 - 35 km) and Bouguer gravity (~ 20 km up to ~ 50 km) responses with magnetic amplitude values ranging between -150 to 1400 nT and

Bouguer gravity values between 0 to $350 \mu\text{m}^*\text{s}^{-2}$ (Figs. 3.10 and 3.11). The Leichhardt River Domain is divided in a north-western part (Fig. 3.12) characterized by higher magnetic anomalies with amplitude values up to 1500 nT and stippled texture and a south-western part (Fig. 3.12), which shows lower regional magnetic amplitudes (below 600 nT) and is characterized by a smoother magnetic texture (Fig. 3.10).

The eastern part of the central Leichhardt River Domain (Fig. 3.12) is characterized by a relatively broad NNW-oriented magnetic low (below 0 nT) punctuated by NNW-trending linear magnetic horizons having amplitude values between 0 and 200 nT and wavelength of ~5-10 km (Fig. 3.10). The low magnetic region correlates with regional positive gravity anomalies with amplitude values comprised between 100 and $350 \mu\text{m}^*\text{s}^{-2}$ and a wavelength of more than 45 km (Fig. 3.11).

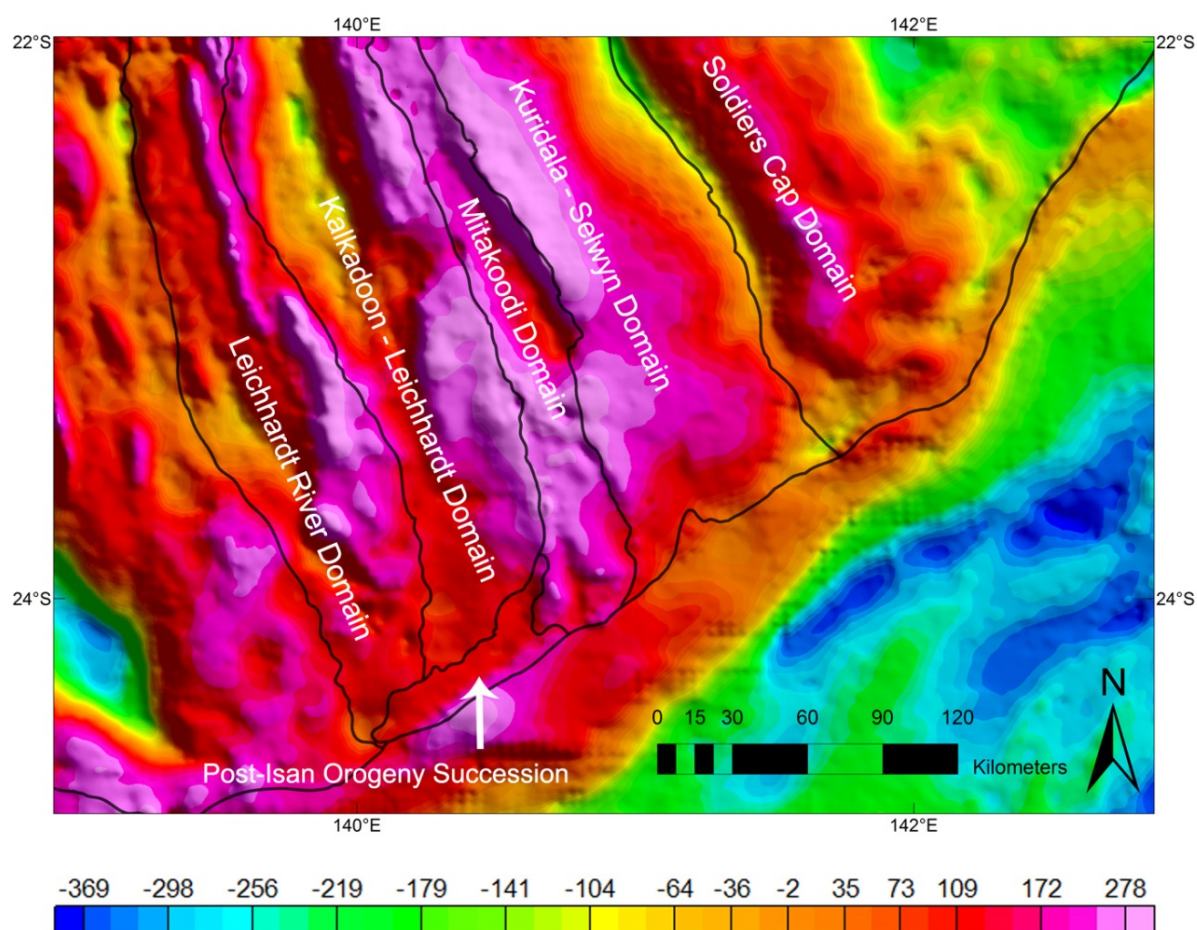


Fig. 3.11 Bouguer gravity map of the southern Mount Isa terrane along with its geophysical sub-domains. Values in the scale bar are in $\mu\text{m}^*\text{s}^{-2}$

A NNW-trending low density source body (Fig 3.11) lies in the western central part of the Leichhardt River Domain (Fig. 3.13) and correlate with low magnetic anomalies (Fig. 3.10). The extent of this anomaly is ~50 km long and ~15 km wide. The Bouguer gravity map shows the source body with an asymmetric response with the lowest amplitude values towards the east that terminate against NNW-oriented positive gravity anomalies (Figs. 3.11 and 3.13). In the southern part of the Leichhardt River Domain, several positive sub-circular magnetic anomalies overprint the NNW regional trend. These anomalies correlate with either relative low or high Bouguer gravity anomalies.

The prominent NNW-trending anomalies appear to be displaced by NE- and NW-trending structures. NW-trending structures are predominantly located in the southern part of the domain and the magnetic markers show apparent displacements of ~3 - 6 km. NE-trending structures are more apparent in the northern part of the region and the displacement rate of the NNW-trending magnetic anomalies is similar.

3.6.3 Kalkadoon-Leichhardt Domain

The Kalkadoon-Leichhardt Domain is characterized by a broad magnetic low ~65 km wide and smooth texture (Fig. 3.10). The regional magnetic anomalies show amplitude values between -300 and -500 nT. The Bouguer gravity map is characterized by NNW-trending regional Bouguer anomalies with amplitudes between -150 and 360 $\mu\text{m}^*\text{s}^{-2}$, which regionally decrease towards the west (Fig. 3.11). The Bouguer gravity regional response ranges in wavelength from 20 - 25 km to ~50 km. Short wavelength (10 km) Bouguer gravity anomalies are superimposed onto the regional signal and are most evident in the south-eastern part of the domain (Fig. 3.13). Overall the RTP magnetic and the Bouguer gravity grids show poor correlation within the domain.

An elongated low gravity anomaly that has a strike length of more than 180 km long characterizes the eastern and central part of the Kalkadoon-Leichhardt Domain (Figs. 3.12 and 3.13). The source body shows gravity amplitudes between 100 and -140 $\mu\text{m}^*\text{s}^{-2}$ and poor magnetic expression (-350 to -450 nT, Figs. 3.10 and 3.11). To the west, the body source is bounded by positive gravity anomalies that are interpreted to define the limit between the Leichhardt River Domain and the Kalkadoon-Leichhardt Domain. However, the boundary is less well defined in the RTP magnetic grid. The regional magnetic anomalies do not show significant variation across the boundary between the Leichhardt River Domain and the Kalkadoon-

Leichhardt Domain (Fig. 3.10). Instead, prominent magnetic gradients of ~ 140 nT/km decreasing towards the east occur 10 - 25 km west of the inferred limit. Both the magnetic and gravity gradients appear relatively steep in the northern part of the grid and shallow in the southern part of the grid.

In the northern Kalkadoon-Leichhardt Domain (Fig. 3.13), regional gravity gradients comprised between 15 and $25 \mu\text{m}^*\text{s}^{-2}/\text{km}$ define the boundary between the low density source body and eastern N-S- to NNW-trending high gravity anomalies having a regional wavelength of ~ 50 km (Fig. 3.11). In this part of the domain, the geophysical signature is characterized by positive Bouguer gravity anomalies between 200 and $350 \mu\text{m}^*\text{s}^{-2}$ and low magnetic anomalies ranging between -250 and -350 nT. Similarly, the southern part of the Kalkadoon-Leichhardt Domain may be divided in a narrow western block showing low to moderate (~ 100 to $200 \mu\text{m}^*\text{s}^{-2}$) NNW-trending gravity anomalies and an eastern region characterized by positive (~ 200 to $350 \mu\text{m}^*\text{s}^{-2}$) N-S- to NNW-trending gravity anomalies and negative (below -200 nT) magnetic anomalies (Figs. 3.12 and 3.13). The low density and positive gravity regions are defined by E-W gravity gradients decreasing towards the west. However, in the southern part of the domain, the Bouguer gravity gradients are more gentle (7 to $10 \mu\text{m}^*\text{s}^{-2}/\text{km}$) if compared to the northern part of the domain. The southern part of the Kalkadoon-Leichhardt Domain is also punctuated by elongated positive magnetic anomalies ~ 15 km long and $5 - 10$ km wide, showing low to moderate gravity signature.

The southernmost part of the Kalkadoon-Leichhardt Domain is characterized by elongated NE-trending high wavelength ($\sim 2 - 4$ km) high magnetic and low gravity anomalies that are focused along the northern side of the Cork Fault. To the east, the low magnetic Kalkadoon-Leichhardt Domain terminates against the NNW-trending Pilgrim Fault, which is defined by significant positive magnetic anomalies with gradients between 100 and 150 nT/km (Fig. 3.10).

3.6.4 Mitakoodi Domain

The Mitakoodi Domain is characterized by regional NNW- to N-S-trending anomalies. Positive to moderate regional Bouguer gravity anomalies show wavelength of $\sim 30 - 40$ km and amplitude values between 80 and $360 \mu\text{m}^*\text{s}^{-2}$ (Fig. 3.11). The region shows positive magnetic anomalies with wavelengths of $\sim 35 - 40$ km and amplitudes values more than 400 nT. However, shorter

wavelength magnetic anomalies of ~10 km are superimposed onto the regional signal and show peak amplitudes up to 2250 nT (Figs. 3.10 and 3.12).

On the Bouguer gravity map, the Mitakoodi Domain is sub-divided in northern, central and southern parts (Fig. 3.13). The northern part is characterized by NNW-trending gravity anomalies with amplitude values comprised between 200 and 350 $\mu\text{m}^*\text{s}^{-2}$. On the Bouguer gravity grid, the peak anomaly amplitudes coincide with the boundary between the Mitakoodi Domain and the adjacent Kuridala - Selwyn Domain to the east, whereas the lowest amplitude values occur to the west and are delimited by the positive NNW-trending Bouguer gravity anomalies of the eastern Kalkadoon-Leichhardt Domain (Fig. 3.11). On the RTP magnetic map, this part of the domain show positive NNW-trending anomalies punctuated by short wavelength sub-circular anomalies. Here, the amplitudes range from 500 to 1500 nT (Fig. 3.10).

In the central part of the Mitakoodi Domain, a 70 km wide body source is defined by NNW-trending, relative low amplitude Bouguer gravity anomalies with amplitude values ranging between 200 $\mu\text{m}^*\text{s}^{-2}$ and 75 $\mu\text{m}^*\text{s}^{-2}$. The body source is best imaged in the tilt derivative grids (Figs. 3.12 and 3.13). Stippled NNW-trending magnetic anomalies above 500 nT with peak amplitude exceeding 2000 nT characterize this part of the domain (Fig 3.10). In the central part of the Mitakoodi Domain, NW-trending magnetic lineaments appear to overprint and displace the prominent NNW-trending geophysically defined structural grain.

The southern part of the domain is characterized by positive Bouguer gravity anomalies comprised between 150 $\mu\text{m}^*\text{s}^{-2}$ and 350 $\mu\text{m}^*\text{s}^{-2}$. The NNW regional trend is less well defined as several short wavelength (~6 - 10 km) circular to elongated anomalies overprint the NNW-trending anomalies. The Pilgrim Fault, which marks the boundary between the Kalkadoon-Leichhardt Domain and the Mitakoodi Domain (Fig. 3.10), is well defined in the RTP magnetic data because of the steep gradient that decreases towards the west but is poorly defined in the Bouguer gravity map. In the southern part of the Mitakoodi Domain, the prominent NNW- to N-S-trending magnetic anomalies are displaced (~5 km) by NE- and NW-trending linear magnetic anomalies (Fig. 3.12).

At the southern termination of the Mitakoodi Domain, the regional NNW- to N-S-trending geophysical anomalies are overprinted by NE-trending high magnetic and low gravity anomalies, which appear to be focused along the northern side of the Cork Fault.

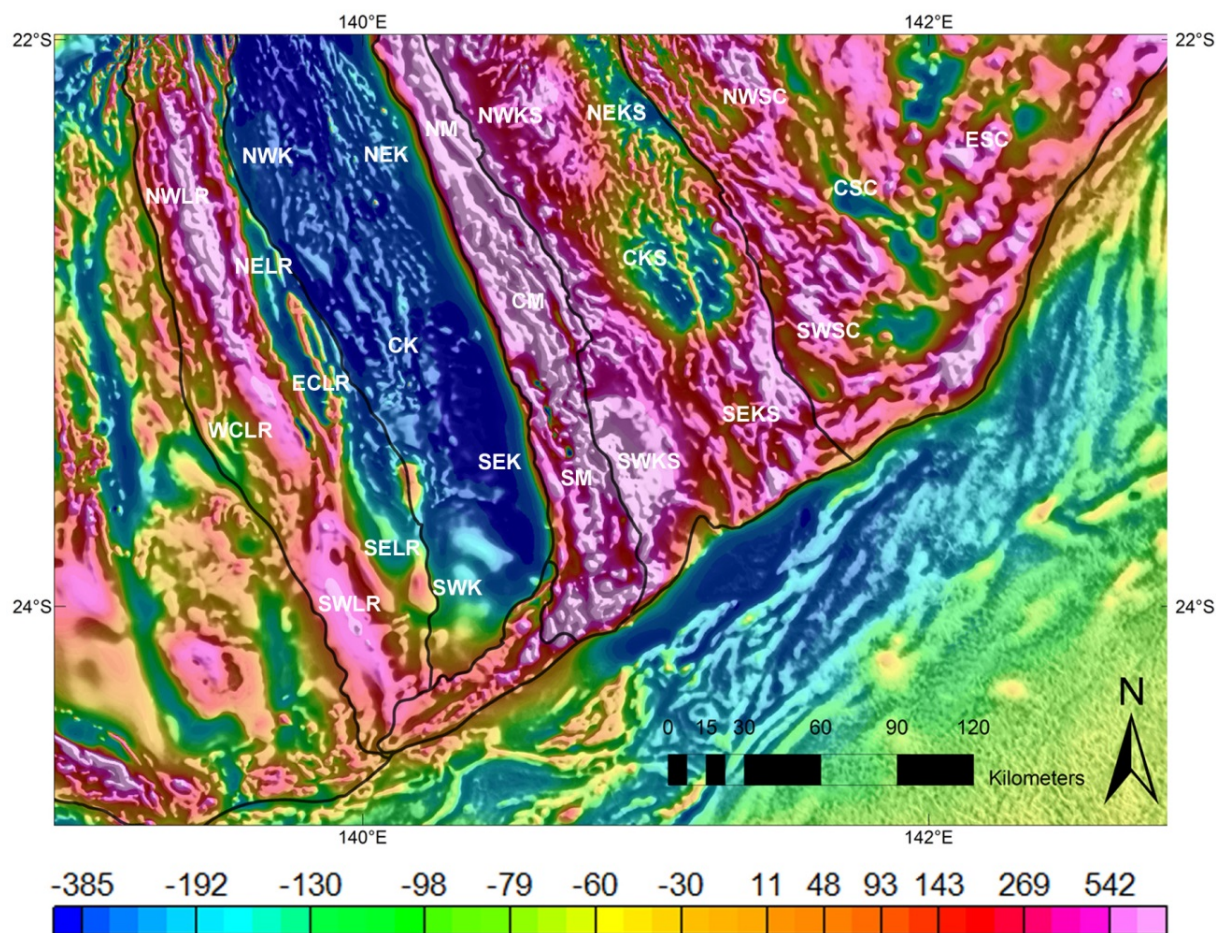


Fig. 3.12 composite RTP and tilt derivative magnetic map of the southern Mount Isa terrane along with its geophysical subdomains. Values in the scale bar are in nT.

NWLR= north-western Leichhardt River Domain; *NELR*= north-eastern Leichhardt River Domain; *WCLR*= western central Leichhardt River Domain; *ECLR*= eastern central Leichhardt River Domain; *SWLR*= south-western Leichhardt River Domain; *SELR*= south-eastern Leichhardt River Domain; *NWK*= north-western Kalkadoon-Leichhardt Domain; *NEK*= north-eastern Kalkadoon-Leichhardt Domain; *CK*= central Kalkadoon-Leichhardt Domain; *SWK*= south-western Kalkadoon-Leichhardt Domain; *SEK*= south-eastern Kalkadoon-Leichhardt Domain; *NM*= northern Mitakoodi Domain; *CM*= central Mitakoodi Domain; *SM*= southern Mitakoodi Domain; *NWKS*= north-western Kuridala - Selwyn Domain; *NEKS*= north-eastern Kuridala - Selwyn Domain; *CKS*= central Kuridala - Selwyn Domain; *SWKS*= south-western Kuridala - Selwyn Domain; *SEKS*= south-eastern Kuridala - Selwyn Domain; *NWSC*= north-western Soldiers Cap Domain; *SWSC*= south-western Soldiers Cap Domain; *CSC*= central Soldiers Cap Domain; *ESC*= eastern Soldiers Cap Domain.

3.6.5 Kuridala - Selwyn Domain

The Kuridala - Selwyn Domain contains positive regional gravity anomalies decreasing towards the ENE (Fig. 3.11). The magnetic response in this domain is heterogeneous (Fig. 3.10). The north-western part of the domain is characterized by elongated NNW-trending positive gravity anomalies having wavelength more than 30 km long and amplitude values up to $400 \mu\text{m}^*\text{s}^{-2}$ that

correlate with moderate to high magnetic anomalies (200 - 600 nT). The magnetic anomalies show a NNW trend. However in the northernmost part of the region, NE-trending anomalies form the main geophysical response. The north-eastern part of the domain (Figs. 3.12 and 3.13) shows regional gravity anomalies having a wavelength of ~90 km that decrease towards the Soldiers Cap Domain. The boundary between the two domains coincides with a broad magnetic low.

High gravity anomalies (~ 150 to $200 \mu\text{m}^*\text{s}^{-2}$) in the central part of the domain are associated with a low magnetized (~ -200 to -300 nT) NNW-trending elongated anomaly that is ~60 km long and ~35 km wide (Figs. 3.10 and 3.11). The magnetically low region is cross-cut by NNW-trending elongated high wavelength and high magnetic anomalies.

To the southwest, a network of NE- and NW-trending anomalies with amplitude values between 200 and $300 \mu\text{m}^*\text{s}^{-2}$ are evident in the tilt derivative Bouguer gravity map. On the RTP magnetic map, this part of the domain is characterized by arcuate N-S-trending positive magnetic anomalies with amplitude greater than 400 nT. These anomalies deflect towards the NNW-trending anomalies of the southern Mitakoodi Domain. The south-westernmost part of the Kuridala - Selwyn Domain (Figs. 3.12 and 3.13) is almost featureless. The NNW trend is not apparent and the domain is mostly characterized by NE-trending linear magnetic anomalies and several highly magnetized sub-circular anomalies. To the southeast, NNW-trending high magnetic anomalies with amplitude values that vary between 200 and 800 nT are offset by NE-trending linear magnetic anomalies with apparent dextral strike-slip offset. This part of the domain is characterized by a broad gravity high ($\sim 200 \mu\text{m}^*\text{s}^{-2}$), which decreases in amplitude towards the southeast (Fig. 3.11).

At its southern termination, the Kuridala - Selwyn Domain shows NE-oriented high magnetic and low gravity anomalies which appear to overprint the regional NNW-trending geophysical anomalies, and are preferentially located along the northern side of the Cork Fault.

3.6.6 Soldiers Cap Domain

The Soldiers Cap Domain is associated with regions showing lower magnetic responses. The boundary between the Kuridala - Selwyn Domain and the Soldiers Cap Domain is characterized by elongated NNW-trending low Bouguer gravity anomalies with amplitude values below $0 \mu\text{m}^*\text{s}^{-2}$ that are associated with positive magnetic responses with amplitudes that vary between 0

and 550 nT (Fig. 3.10). To the immediate east of the boundary, the Soldiers Cap Domain shows NNW-trending positive Bouguer gravity and magnetic anomalies with regional amplitudes greater than $100 \mu\text{m}^2\text{s}^{-2}$ and 200 nT respectively and stippled texture in the magnetic data. These anomalies define a discrete belt of rock which lies adjacent to the Kuridala - Selwyn Domain (Figs. 3.10 and 3.11). Regionally, the positive NNW-trending gravity anomalies of the Soldiers Cap Domain decrease towards the east with a wavelength of $\sim 70 - 100$ km and terminate against NE-trending gravity anomalies.

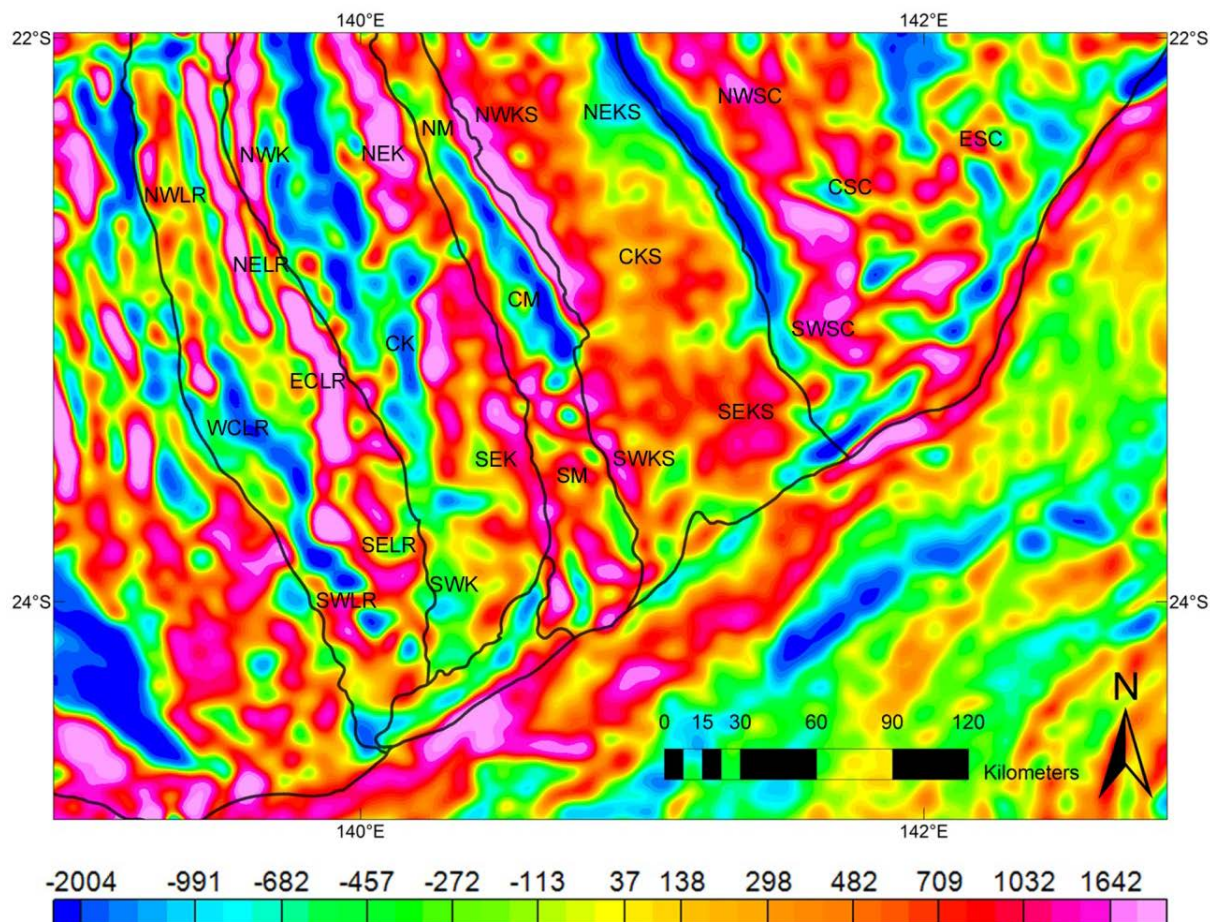


Fig. 3.13 Tilt derivative Bouguer map of the southern Mount Isa terrane along with its geophysical sub-domains. Values in the scale bar are in $\mu\text{m}^2\text{s}^{-2}/\text{m}$

NWLR= north-western Leichhardt River Domain; *NELR*= north-eastern Leichhardt River domain; *WCLR*= western central Leichhardt River Domain; *ECLR*= eastern central Leichhardt River Domain; *SWLR*= south-western Leichhardt River Domain; *SELR*= south-eastern Leichhardt River Domain; *NWK*= north-western Kalkadoon-Leichhardt Domain; *NEK*= north-eastern Kalkadoon-Leichhardt Domain; *CK*= central Kalkadoon-Leichhardt Domain; *SWK*= south-western Kalkadoon-Leichhardt Domain; *SEK*= south-eastern Kalkadoon-Leichhardt Domain; *NM*= northern Mitakoodi Domain; *CM*= central Mitakoodi Domain; *SM*= southern Mitakoodi Domain; *NWKS*= north-western Kuridala - Selwyn Domain; *NEKS*= north-eastern Kuridala - Selwyn Domain; *CKS*= central Kuridala - Selwyn Domain; *SWKS*= south-western Kuridala - Selwyn Domain; *SEKS*= south-eastern Kuridala - Selwyn Domain; *NWSC*= north-western Soldiers Cap Domain; *SWSC*= south-western Soldiers Cap Domain; *CSC*= central Soldiers Cap Domain; *ESC*= eastern Soldiers Cap Domain.

On the magnetic map, the central part of the domain is characterized by an elongated magnetic low having amplitudes below 0 nT. The region appears to be overprinted by short wavelength sub-circular positive magnetic anomalies. The northeastern part of the domain (Fig. 3.12 and 3.13) is characterized by N-S- to NNW-trending high magnetic anomalies having smooth texture associated with positive Bouguer gravity signature, with amplitudes between -100 and 100 $\mu\text{m}\cdot\text{s}^{-2}$. The southern and eastern parts of the domain (Figs. 3.12 and 3.13) differ from the structural grain of the Mount Isa terrane and are characterized by prominent NE-trending gravity and magnetic anomalies.

3.7 Discussion

Geophysical data allows tracing exposures of rocks and structures under cover providing information about the fault architecture and the associated kinematics. Geological data from the exposed Mount Isa Inlier (Figs. 3.2 and 3.9) and the Deep Seismic Transects (Figs. 3.5, 3.6 and 3.7) provided constraints for our interpretation (Figs. 3.14 and 3.20). Where no constraining data were available, gradients and offset in the gravity and magnetic data have been used to assist in understanding the geometries and architecture of the faults. Fault kinematics is interpreted through overprinting relationships and the apparent offset of geophysical markers. Basin formation and subsequent deformation have been heterogeneous across the five sub-domains, which we describe below.

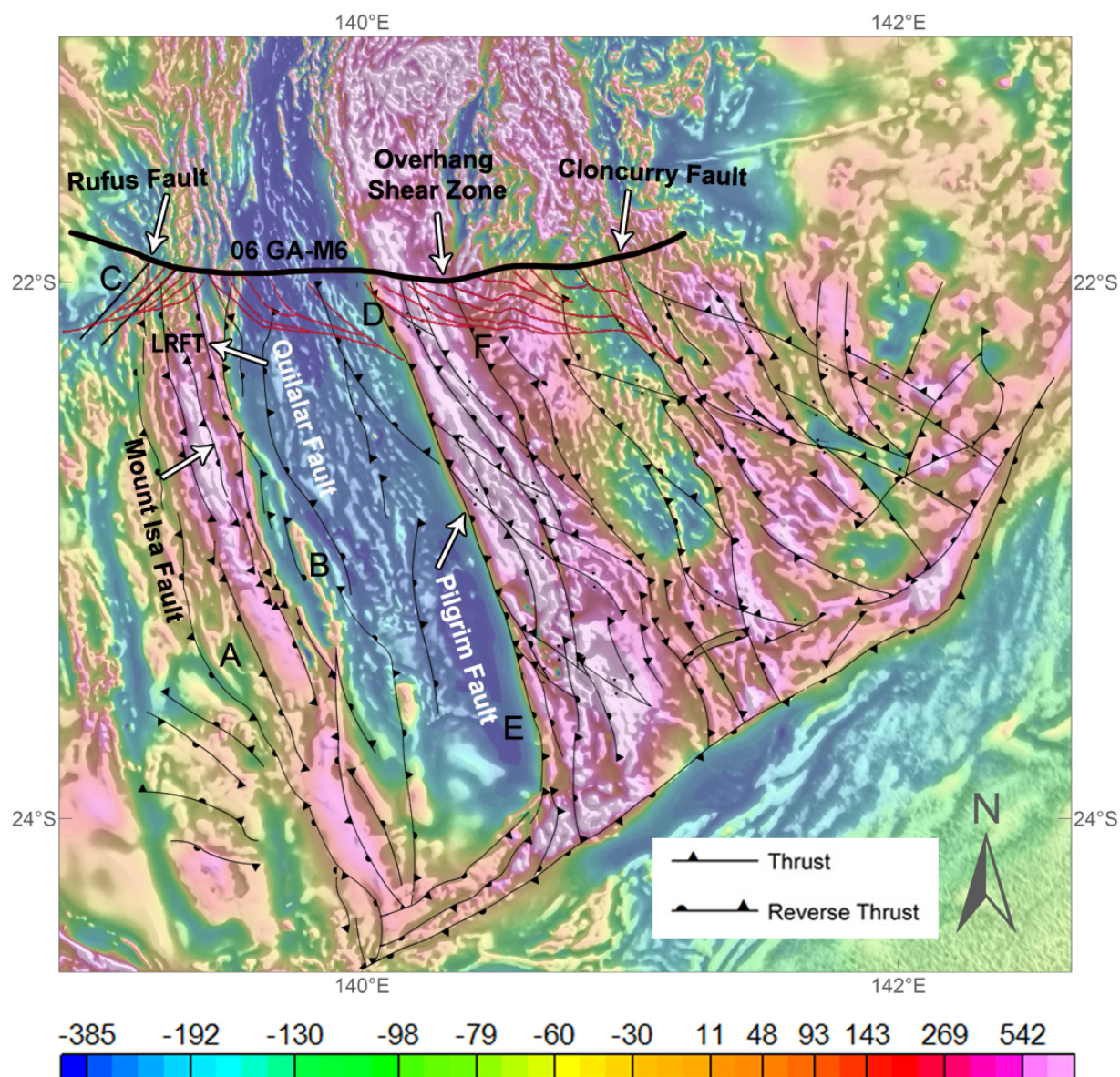


Fig. 3.14 Fault architecture of the southern Mount Isa Geophysical Domain constrained by the Deep Seismic Transect 06GA-M6 over a RTP and tilt derivative magnetic map.

3.8 Interpretation of the geophysical signature of the southern Mount Isa terrane

3.8.1 Leichhardt River Domain

The N-S-trending Leichhardt Rift is estimated to have been up to 60 km wide (O'Dea et al., 1997b) and is now preserved in the Leichhardt River Fault Trough (Derrick, 1982). In the

exposed parts of the Leichhardt River Fault Trough, the extensional fault architecture during the development of the Leichhardt Superbasin consisted in NNW- to N-S-trending normal faults and E-W-trending normal faults (O'Dea et al., 1997b). The NNW-trending, west-dipping faults controlled the deposition of the Mount Guide Quartzite and the Eastern Creek Volcanics, which show evidence of stratal growth towards major structures, including the Mount Isa Fault and the Quilalar Fault (O'Dea et al., 1997a). In the exposed inlier, the west-dipping (O'Dea et al., 1997a) Quilalar/Gorge Creek Fault Zone represents the boundary between the western meta-sedimentary package preserved in the Leichhardt River Domain and the eastern crystalline basement of the Kalkadoon-Leichhardt Domain (Figs. 3.2 and 3.14) (Blake, 1987; Blake and Stewart, 1992). Further west, the west-dipping (MacCready et al., 1998) Mount Isa Fault (Figs. 3.2 and 3.14) is associated with a distinctive N-S-trending magnetic lineament. These faults formed part of the main architecture of the Leichhardt River Fault Trough and underwent several episodes of reactivation as normal faults during the ca. 1800 - 1600 Ma basinal deposition and as reverse thrusts during basin inversions and during the Isan Orogeny (O'Dea et al., 1997b). West of the Mount Isa Fault, the emplacement of the Sybella Granite (Figs. 3.2 and 3.9) is reflected by low Bouguer gravity signature (Fig. 3.9). N-S-trending gravity and magnetic highs are associated with the Eastern Creek Volcanics which outcrop near the Mount Isa Fault (Drummond et al., 1998) and is preserved into the Leichhardt River Fault Trough (Derrick, 1982; Wellman, 1992). Deposition of the Myally Subgroup was controlled by E-W-striking syn-sedimentary normal faults, which are present down the axis of the Leichhardt Rift and accommodated northward stratal growth (O'Dea et al., 1997b).

On the geophysical grids, the Quilalar Fault Zone corresponds to the juxtaposition of a western positive magnetic block against an eastern poorly magnetized region (Fig. 3.14) (Wellman, 1992). The ENE gradients associated with the Quilalar Fault Zone can be mapped further south for at least 100 km (Fig. 3.14), supporting the interpretation that this fault zone is a major NNW-trending structural boundary (Wellman, 1992) which separates blocks of different petrophysical properties. The Quilalar Fault appears to define the western extent of the prominent geophysical anomalies associated with the Eastern Creek Volcanics (Fig. 3.14) and is therefore interpreted to have controlled the deposition of the formation.

To the immediate south of the Mount Isa Inlier, the Mount Isa Fault appears to be terminated by the NE-trending, west-dipping Rufus Fault Zone (Figs. 3.2 and 3.14, locality C) (Blake et al.,

1984; Korsch et al., 2008). However, a prominent N-S- to NNW-trending magnetic lineament can be traced to the immediate south of the Rufus Fault (Fig. 3.14). The magnetic lineament runs parallel to the NNW-trending Quilalar Fault Zone and may represent the geophysical expression of an NNW-trending structure tectonically linked to the Mount Isa Fault. The Bouguer gravity anomalies that characterize both the Mount Isa and Quilalar Fault zones do not show significant asymmetries and are characterized by steep gradients in correspondence to the faults. This suggests that the Mount Isa and Quilalar faults are steep dipping structures displacing the crystalline basement and the basinal sequences.

The positive magnetic and gravity anomalies associated with the distribution of the Eastern Creek Volcanics extend undercover in a NNW strike. On the Bouguer gravity grid, short wavelength (10 km) anomalies are superimposed onto the regional signal and are bounded to the east by the Quilalar Fault (Fig. 3.13). This is interpreted to reflect a combination of the shallowing of the crystalline basement and the overlying Eastern Creek Volcanics.

Short wavelength positive magnetic and gravity anomalies that increase in amplitude towards the Mount Isa Fault are interpreted to reflect the thickening of the Eastern Creek Volcanics or buttressing. Buttressing may occur when relatively incompetent rocks in the hanging wall (i.e. the Eastern Creek Volcanics) are juxtaposed against relatively competent rocks in the footwall (i.e. the crystalline basement), which results in the formation of folds adjacent to fault segments (Betts et al., 2004). The more severe the buttressing of magnetic unit, the more intense is the magnetic response (Betts et al., 2004).

The positive magnetic anomalies decrease towards the southern part of the Leichhardt River Domain and this may be due to the thinning of the Eastern Creek Volcanics, although the smoother texture also suggests its burying under younger meta-sedimentary rocks.

Similar to the exposed Mount Isa Inlier, the highest geophysical anomalies associated with the thickening of the Eastern Creek Volcanics are interrupted by an elongated low density region located west of the Mount Isa Fault, which is best imaged in the tilt derivative Bouguer gravity map (Fig. 3.13). The low NNW-trending gravity anomalies are interpreted to reflect granitic intrusions, which appear to link with the exposed Sybella Granite (Fig. 3.9) (Blake, 1987; Blake et al., 1984) and may represent its continuation undercover (Fig. 3.20).

Elongated low magnetic and high gravity signature that characterizes the western part of the Leichhardt River Domain (Figs. 3.12 and 3.13) is interpreted to represent the geophysical response of the Mount Guide Quartzite (Fig. 3.20) which outcrop in the inlier to the immediate east of the Eastern Creek Volcanics (MacCready, 2006a). In the central western part of the Leichhardt River Domain (Fig. 3.14, locality A), elongate N-S-trending low gravity and magnetic anomalies are interpreted to indicate thick accumulations of low density and poorly magnetized sedimentary successions of the Calvert and Isa superbasin, although it may also be representative of the relatively low dense Quilalar Formation. The lower Bouguer gravity signature and the steep gradients towards NNW-trending anomalies suggest that deposition might have occurred in a half graben setting and was controlled by the NNW-trending, west-dipping normal faults (Fig. 3.16).

The E-W-trending faults prevalent in the northern parts of the Mount Isa Inlier are not apparent in the southern Mount Isa terrane. This suggests that E-W faults were focussed to the northern inlier. An implication of this interpretation is that during deposition of the upper parts of the Myally Subgroup the basin depocentre was focussed in the north and the Myally Subgroup is less well represented in the south.

In the central eastern part of the Leichhardt River Domain (Fig. 3.14, locality B), short wavelength positive magnetic anomalies are interpreted to represent highly magnetized mafic sills intruded into meta-sedimentary packages. These sills have been folded about first generation folds (F1) with NNW-trending axial traces. The magnetic horizons define fold hinges. The gradients of the magnetic anomalies in the hinge zone indicate they are north-plunging folds.

Regionally, NNW-trending positive structures displacing the basement and the basinal sequences along with the NNW-trending axial traces of major folds in the Leichhardt River Domain, may indicate ENE-directed crustal shortening event and might be coeval with the development of crustal-scale upright folds and N-S-trending reverse faults and thrusts (Giles et al., 2006b; MacCready et al., 1998) that developed during the Middle Isan Orogeny (Fig. 3.18) (Giles et al., 2006b; O'Dea et al., 1997b).

NW-trending linear magnetic anomalies overprint the prominent NNW-oriented magnetic trend with an apparent sinistral strike-slip offset (Fig. 3.19) and are thus interpreted to be younger structures. They can be consistently assigned to the NW-striking sinistral and NE-striking dextral

strike-slip fault network that accommodated crustal shortening during the wrenching phase of the Isan Orogeny (Lister et al., 1999; O'Dea et al., 1997b).

It is thus interpreted that the Leichhardt Rift was at least a 300 km long structure formed by prominent N-S- to NNW-trending faults bounding west-dipping (O'Dea et al., 1997a; O'Dea et al., 1997b) half graben. The main fault architecture preserved in the Leichhardt River Fault Trough extends into the concealed southern Mount Isa terrane.

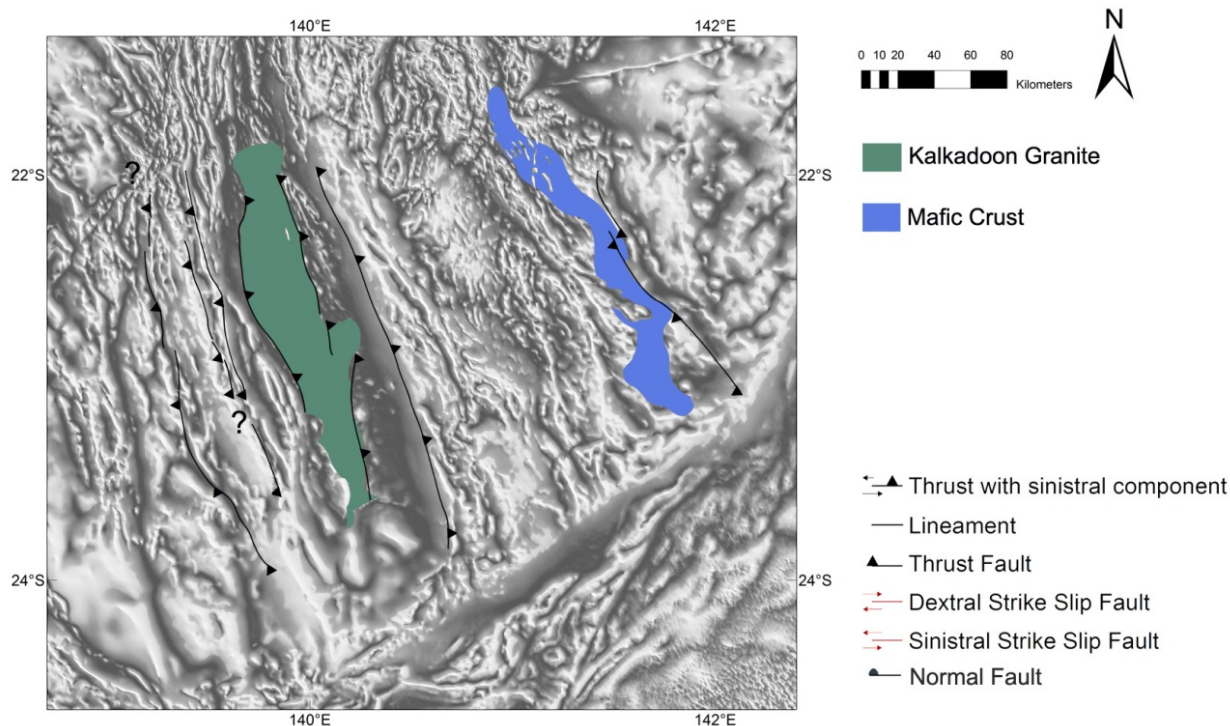


Fig. 3.15 Map showing some structure active during the ca. 1870–1850 Ma Barramundi Orogeny. The Pilgrim Fault form a prominent geophysical feature can be traced until the southern termination of the Mount Isa Geophysical Domain. N-S- to NNW-oriented structures including the Mount Isa Fault Zone, the Rufus Fault and the Pilgrim Fault were active structures during the Barramundi Orogeny.

3.8.2 Kalkadoon-Leichhardt Domain

In the Kalkadoon-Leichhardt Domain, the Palaeoproterozoic deposition appears to have been controlled by NNW-trending, east-dipping normal faults which have subsequently been reactivated as reverse thrusts during the Isan Orogeny (Korsch et al., 2008; MacCready, 2006a; MacCready et al., 1998). In the exposed inlier, the basal sequences of the Mount Guide Quartzite lie unconformably on the western extent of the Kalkadoon-Leichhardt Domain basement rocks

(MacCready, 2006a). In the eastern part of the Kalkadoon-Leichhardt Domain, the tectonic contact between the Kalkadoon Batholith and the successions of the Leichhardt and Calvert superbasins is defined by NNW-trending, low angle thrusts that appear to connect into a shallow east-dipping detachment above the crystalline basement (Figs. 3.6 and 3.14) (Korsch et al., 2008; MacCready et al., 1998).

In the study area, the broad magnetic and gravity low that characterizes the Kalkadoon-Leichhardt Domain is interpreted to reflect the emplacement of the low magnetic Kalkadoon Batholith, which continues undercover to the south of the exposed inlier (Fig. 3.9) and forms a major belt defined by NNW-trending anomalies (Fig. 3.20). However, into the central and western part of the domain, the ca. 1750 - 1720 Ma Wonga Batholith intrusion (Figs. 3.2 and 3.9) (Blake, 1987) may be indistinguishable from the Kalkadoon Batholith as they may have similar geophysical responses.

To the west of the low density Kalkadoon Batholith, the Kalkadoon-Leichhardt Domain is characterized by N-S- to NNW-trending high gravity anomalies. These anomalies show steep gradients towards the west and shallow gradients towards the east. The asymmetric gravity profile may reflect east-dipping faults and link to the east-dipping faults east of the Quilalar Fault imaged in the Deep Seismic Profile 06GA-M6 (Figs. 3.6 and 3.14) (Korsch et al., 2008). The positive Bouguer gravity anomalies are associated with low magnetic responses and are ascribed to NNW-trending structures defining the southern distribution of the low magnetic Mount Guide Quartzite or the underlying (O'Dea et al., 1997b) Bottletree Formation. The basement rocks of the Plum Mountain Gneiss outcrop in the western part of the exposed Kalkadoon-Leichhardt Domain (Fig. 3.2), therefore shallowing of the crystalline basement is interpreted as well.

In the eastern Kalkadoon-Leichhardt Domain, positive gravity anomalies show asymmetric gravity profile. Steep gradients decreasing towards the west can be traced all along the domain and link to an east-dipping structure imaged in the Deep Seismic Profile 06GA-M6 (Fig. 3.14). The positive gravity anomalies are interpreted to represent the southern continuation of the poorly magnetic carbonate and quartz-rich successions of the Corella Formation, which has been extensively mapped in the exposed inlier (MacCready, 2006a; O'Dea et al., 1997b). Further to the west, the high gravity and low magnetic anomalies associated with the Corella Formation appear to be terminated by the NNW-trending Pilgrim Fault (Fig. 3.14, see next paragraph), which represents also the eastern limit of the Kalkadoon-Leichhardt Domain. Weakly magnetic

horizons are contained in the mapped Corella Formation (Fig. 14, locality D) and may be attributed to the underlying (MacCready, 2006a; O'Dea et al., 1997b) Leichardt Volcanics, although the formation shows relatively little magnetization. The preferred interpretation has the magnetic anomalies representing the distribution of the felsic volcanic rocks of the Argylla Formation, which is characterized by higher magnetic responses. The magnetic horizons associated with the Argylla Formation appear to have been folded about F1 folds with NNW-trending axial traces. The magnetic horizons that define the closure of the anticline suggest the folds are north-plunging anticlines. In the south-eastern Kalkadoon-Leichhardt Domain, NNW-trending short wavelength (10 km) positive Bouguer gravity anomalies are superimposed onto the long wavelength positive anomalies (Figs. 3.11 and 3.14, locality E) and are best imaged in the Bouguer vertical derivative map (Fig. 3.13). The Bouguer gravity signature may represent N-S-trending anticlines and synclines folding the mapped Corella Formation. As an alternative, a decollement style tectonics may be inferred, in which a network of NNW-trending faults are reflected in the short wavelength anomalies. In this context, they may connect to a detachment above a relatively shallow crystalline basement which is reflected by the positive regional anomalies. In this scenario, the fault architecture observed in the exposed inlier and imaged in the deep seismic surveys (Fig. 3.6) (Korsch et al., 2008; MacCready, 2006a) continues southward undercover.

The inferred thrusting and folding in a N-S to NNW direction might reflect E-W- to ENE-directed shortening and deformation that affected the crystalline basement and the sedimentary package. This shortening event can be consistently associated with the Middle Isan Orogeny (Fig. 3.18).

3.8.3 Mitakoodi Domain

In the Mitakoodi Domain, the prominent N-S- to NNW-trending, east-dipping Pilgrim Fault (Blenkinsop et al., 2008) appears to have controlled the deposition in an apparent ENE-directed extension (Foster and Austin, 2008; O'Dea et al., 1997b; Potma and Betts, 2006) and was subsequently inverted during the Isan Orogeny (Blenkinsop et al., 2008; O'Dea et al., 1997b). West of the Pilgrim Fault, the ca. 1780 to 1755 Ma Leichardt Superbasin successions are less well represented, suggesting that the fault separated a tectonic high to the west (Foster and Austin, 2008) from a major depocenter to the east (Blenkinsop et al., 2008). The subsequent ca.

1590 to 1500 Ma shortening event related to the Isan Orogeny is well preserved and documented in the Mitakoodi Culmination. The Mitakoodi Culmination is a regional anticlinorium which is cored by the Argylla Formation and the Bulonga and Marraba Volcanics (MacCready, 2006a; O'Dea et al., 2006; Potma and Betts, 2006). Seismic reflection sections show decollement style tectonics with a detachment above the crystalline basement overprinted by basement cutting reverse faults (Figs. 3.6 and 3.14) (Korsch et al., 2008; MacCready et al., 1998). The Pilgrim Fault forms part of a network of east-dipping shallow structures that connects to the detachment surface (Korsch et al., 2008). In the exposed inlier, doubling and shallowing of the magnetized Argylla Formation and Bulonga Volcanics across the Mitakoodi Culmination (Fig. 3.2) is reflected in the magnetic grid as positive regional anomalies.

The magnetic anomalies associated with the NNW-trending Pilgrim Fault form the most prominent geophysical signature of the southern Mount Isa terrane. The fault is defined by prominent steep gradients coincident with the boundary between the low magnetic Kalkadoon-Leichardt Domain and the highly magnetized rocks of the Mitakoodi Domain that can be traced from the Mount Isa Inlier (MacCready, 2006a; O'Dea et al., 1997b) all the way to the southern Mount Isa Geophysical Domain (Fig. 3.14). The block to the immediate west of the Pilgrim Fault (eastern Kalkadoon-Leichardt Domain) shows higher regional gravity signature, if compared to the Mitakoodi Domain (Fig. 3.11). This suggests that the crystalline basement may be shallower west of the Pilgrim Fault and deeper to the east.

The high magnetic signature of the Mitakoodi Domain persists towards the south and is inferred to represent the distribution of the highly magnetized Marraba, Bulonga and Argylla Volcanics (Fig. 3.20). These magnetic anomalies are coincident with short wavelength (10 km) positive Bouguer gravity anomalies and might represent regional-scale anticlinoria in which the Bulonga and Marraba volcanics are thicker and shallower.

An elongated NNW-trending low density source body in the central part of the Mitakoodi Domain (Fig. 3.13) is interpreted as granitic rocks (Fig. 3.20). The geophysical anomalies associated with the intrusion are located to the immediate south and link to the low density Wimberru Granite (Figs. 3.2 and 3.9). They form a N-S- to NNW-trending low density belt and may represent the extension of the ca. 1540 - 1520 Ma Williams Supersuite (Blake, 1987) undercover. NNW-trending low magnetic and low gravity anomalies within the domain are inferred to represent NNW-trending synclines terminating against the major NNW-trending

structures and containing remnants of the less dense and non-magnetic Calvert and Isa superbasin equivalent rocks.

The geophysical interpretation implies that the Pilgrim Fault initially formed an east-dipping, continental-scale structure controlling the basinal deposition (Fig. 3.16) (Blenkinsop et al., 2008), which is predominantly reflected in the geophysical anomalies associated with the Leichhardt Superbasin rock package (Fig. 3.20). Later deformation (MacCready, 2006a; O'Dea et al., 2006) and reactivation of the Pilgrim Fault (Fig. 3.18) (Blenkinsop et al., 2008) might have resulted in buttressing and uplifts of the basinal sequences, which is now evident in the prominent positive magnetic and gravity signature of the domain. The regional NNW-trending gravity anomalies suggest that, although the Pilgrim Fault was reactivated as a reverse fault or thrust (Blenkinsop et al., 2008; O'Dea et al., 1997b), a component of normal offset of the basement persisted and is reflected by the lower regional Bouguer gravity anomalies if compared to the block west of the fault.

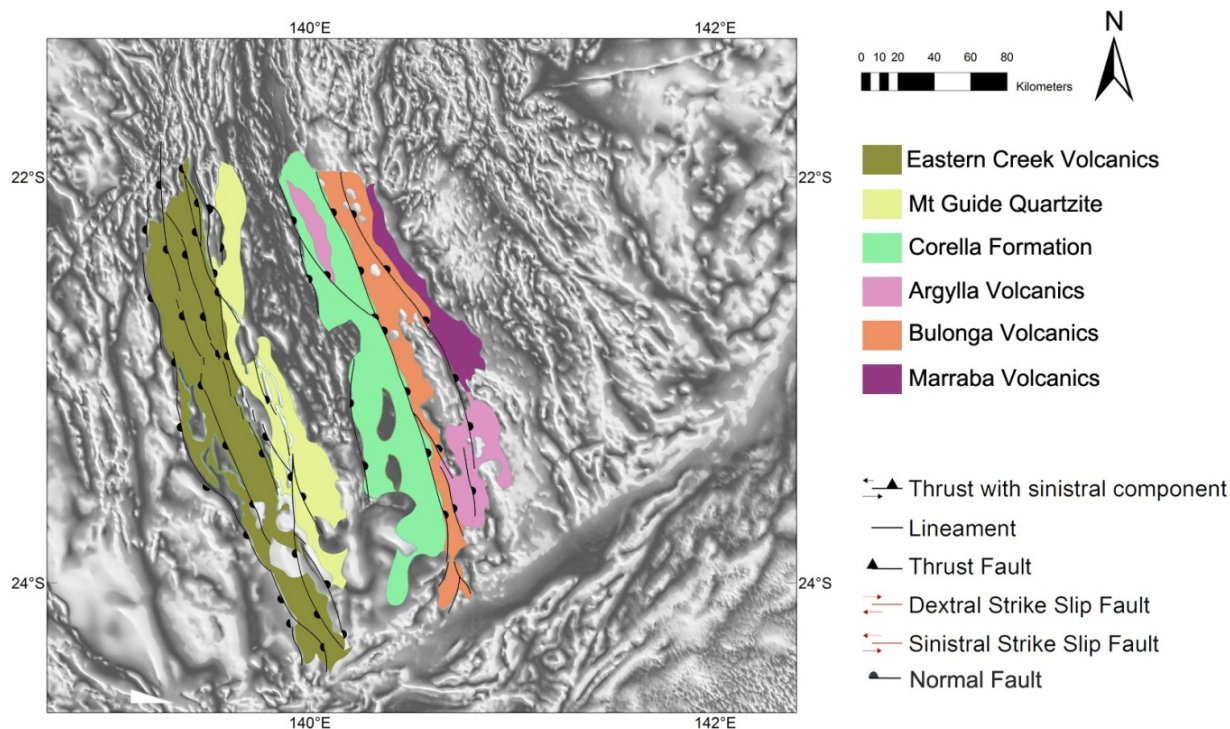


Fig. 3.16 Map showing major structures that accommodated the ca. 1800 – 1740 Ma Leichhardt Superbasin sedimentation

In the Mount Isa Inlier, the 1550 and 1540 Ma wrenching phase (Lister et al., 1999; O'Dea et al., 1997b) is represented by NW-striking sinistral and NE-striking dextral strike-slip fault network offsetting the N-S- to NNW-oriented major structures. In the southern Mitakoodi Domain, the prominent NNW regional magnetic trend is overprinted by NE-trending magnetic anomalies with an apparent dextral strike-slip offset and NW-oriented linear magnetic anomalies with an apparent sinistral strike-slip offset with apparent displacements that vary between 3 and 6 km (Fig. 3.19). These linear magnetic anomalies may reflect a subsequent tectonic event that can be consistently correlated with the wrenching phase of the Isan Orogeny (Fig. 3.19).

3.8.4 Kuridala - Selwyn Domain

In the Mount Isa Inlier, the Kuridala - Selwyn Domain is characterized by NE-trending structures which partly overlap the northernmost part of the study area (Fig. 3.12, locality NWKS). Within this domain, the basinal deposition has been accommodated by SE-dipping (Betts et al., 2006; Giles et al., 2006b; O'Dea et al., 2006) and east-dipping (MacCready, 2006a; MacCready et al., 1998) normal faults, which were reactivated as reverse thrusts during the Isan Orogeny (Betts et al., 2006; O'Dea et al., 2006). The NE-trending structures have been described by Potma and Betts (2006), Giles et al. (2006a) and O'Dea et al. (2006) as shallow SE-dipping reverse thrusts, which were reactivated in the Early Isan Orogeny, although the timing of earlier extensional movement along these structures is poorly constrained. The Overhang Shear Zone represents the eastern bounding fault of the Mitakoodi Culmination and has been interpreted as an east-dipping extensional detachment prior to the Isan Orogeny (O'Dea et al., 2006). The Overhang Shear Zone has been reactivated as reverse thrust during the Isan Orogeny (Blenkinsop et al., 2008; MacCready, 2006a). Along this fault, rocks of the Leichhardt Superbasin are juxtaposed against the Isa Superbasin successions (O'Dea et al., 2006). In the exposed Mount Isa Inlier, the Kuridala Formation lies to the southeast of the Marimo-Steveley Block (Blake, 1987; O'Dea et al., 2006) and is characterized by regional low magnetic and gravity amplitude values. Within the domain, the Toole Creek Volcanics is interpreted to be exposed in the cores of synformal closure east of the Marimo Steveley Block (Giles et al., 2006b).

The architecture of the central and southern parts of the domain in the study area (Figs. 3.12 and 3.13) is predominantly formed by NNW-trending structures, although the NNW trend is less well defined if compared to the Mitakoodi Domain. On the Bouguer gravity grid, the steep western

and shallow eastern gradients (Fig. 3.11) indicate that the NNW-trending structures dip towards the east (Fig. 3.14). The NE-trending faults in the eastern Fold Belt are not apparent in the central and southern Kuridala - Selwyn Domain, which might indicate that the early stage of the Isan Orogeny did not importantly affect the southern Mount Isa terrane or deformations were inconsistent across the region.

The geophysical expression of the Overhang Shear Zone can be traced further south for ~170 km in a NNW strike and is coincident with the boundary between the Mitakoodi Domain and the Marimo - Staveley Block / Kuridala - Selwyn Domain (Fig. 3.14). It also corresponds to major linear magnetic anomalies that separate two distinctly geophysical regions (Fig. 3.14, location F). Along this structure, the western high magnetic rock packages of the inferred Marraba and Bulonga Volcanics are juxtaposed against a lower magnetic region that is interpreted to reflect the distribution of the Marimo Slate, Answer Slate, and Staveley Formation (Young Australia Group, (Foster and Austin, 2008) to the immediate east of the Overhang Shear Zone.

The NNW-trending low amplitude geophysical anomalies associated with the Kuridala Formation extend to the south, beneath younger sedimentary cover (Fig. 3.20). Relative high gravity and low magnetic areas may represent either the distribution of the Mount Norna Quartzite, which outcrops east of the Marimo - Staveley Block (Giles et al., 2006b) or shallowing of the underlying (MacCready et al., 1998) Mount Doherty Formation/Corella Formation. The smooth positive magnetic anomalies are associated with the distribution of the Toole Creek Volcanics (Fig 3.20). In this context, the Overhang Shear Zone formed an east-dipping extensional detachment more than 120 km long that was active during the Mesoproterozoic basinal development (O'Dea et al., 2006). The region east of the Overhang Shear Zone formed a major depocenter.

Long wavelength NNW-trending positive gravity anomalies between the eastern Mitakoodi Domain and the western Kuridala - Selwyn Domain suggest that the Barramundi-aged basement might be shallower across the boundary and dislocation of the basement may be controlled by NNW-trending east-dipping structures. To the centre of the Kuridala-Selwyn Domain, bands of highly magnetized sills intrude the sedimentary pile and provide petrophysical contrast (Betts et al., 2001), which is evident in the geophysical data as magnetic horizons defining the closure of high gravity NNW-trending north-plunging folds. Shallowing of the basement along NNW-trending structures and regional-scale folding of magnetic marker horizons with NNW-trending

axial traces (F1) suggest that inversion and deformation occurred after the deposition of the Isa Superbasin basinal sequences. Deformation and basement shallowing in the central and southern part of the Kuridala - Selwyn Domain are consistent with ENE-directed crustal shortening event and they are interpreted to reflect the Middle Isan Orogeny (Fig. 3.18) (Giles et al., 2006b; O'Dea et al., 1997b). The NNW-oriented prominent trend of geophysical anomalies appears to be overprinted by high wavelength circular positive gravity and magnetic anomalies attributed to mafic igneous rocks that are emplaced into and post-date the Kuridala Formation. These mafic rocks are interpreted to be related to the late tectonic Williams Supersuite (Blake, 1987).

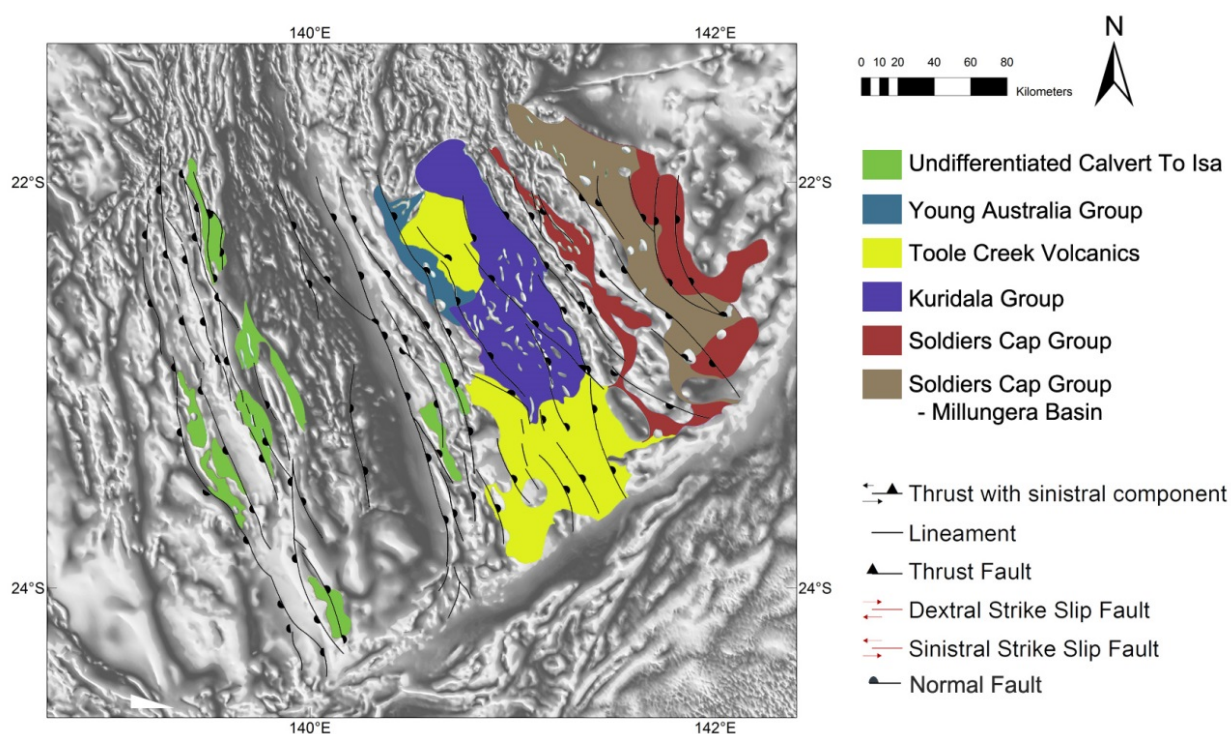


Fig. 3.17 Map showing major structures active during the ca. 1720 – 1600 Ma Calvert to Isa Superbasin extension

3.8.5 Soldiers Cap Domain

In the exposed inlier, the steeply-dipping, east-dipping Cloncurry Fault Zone (Fig. 3.2) juxtaposes the western Corella - Doherty formations against the eastern Soldiers Cap Group (Austin and Blenkinsop, 2008; O'Dea et al., 1997b). The Cloncurry Fault has been interpreted as a major basin bounding normal fault, which formed during the development of the Isa Superbasin (Austin and Blenkinsop, 2010; Blenkinsop et al., 2008), and was inverted as reverse

thrust during the Isan Orogeny (Austin and Blenkinsop, 2010; Blenkinsop et al., 2008; MacCready, 2006a). In the eastern margin of the Mount Isa terrane, the ca. 1850 Ma Gidyea Suture Zone represents the eastern boundary of the Mount Isa terrane and is interpreted to reflect the remnants of a west-dipping subduction zone (Fig. 3.7) (Korsch et al., 2012) recording the collision of the Mount Isa terrane and the Numil Seismic Province (Korsch et al., 2012). The Gidyea Suture Zone coincides with prominent N-S-trending positive magnetic and gravity anomalies. To the east of the suture, the deep seismic transects have imaged sedimentary rocks of the low density Millungera Basin (Figs. 3.7 and 3.9), which overlies the Kowanyama and the Numil seismic provinces that in turn are intruded by several granitic bodies (Korsch et al., 2012).

The geophysical expression of the Cloncurry Fault Zone corresponds to a prominent magnetic and gravity lineament that can be identified for at least 160 km south of the exposed inlier along a north-northwest strike (Figs. 3.2 and 3.14). In the study area, this structure divides a narrow NNW-trending high magnetic and low density region to the west from denser and variously magnetized rocks to the east. The positive magnetic and low gravity anomalies are interpreted to represent an elongated granitic body, which is located to the immediate south of the low density Squirrel Hills Granite (Figs. 3.2 and 3.9) (Beardsmore et al., 1988; Blake, 1987). Similar to the Squirrel Hills Granite, the source body shows N-S to NNW trend and is bounded by the Cloncurry Fault Zone. By inference, we interpret that the granitic intrusion may represent the southern continuation of the Williams Supersuite (Beardsmore et al., 1988; Blake, 1987). Rocks to the immediate east of the Cloncurry Fault Zone have been mapped as Soldiers Cap Group. The Soldiers Cap Group is characterized by a variety of magnetic responses. Regions showing higher magnetic anomalies are interpreted to represent the distribution of the Toole Creek Volcanics. Lower magnetized areas may correspond to the thickening of the Mount Norna Quartzite or other meta-sedimentary successions of the Soldiers Cap Group. In this context, the Cloncurry Fault (Austin and Blenkinsop, 2010; Blenkinsop et al., 2008) acted as a continental-scale (up to 200 km long) extensional detachment and formed the boundary between the shallow water facies of the Kuridala Formation to the west and the deep water rocks of the lower Soldiers Cap Group to the east. It is therefore inferred that the Cloncurry Fault Zone represented the western margin of a rift (Austin and Blenkinsop, 2010; Blenkinsop et al., 2008) that extended all along the southern Mount Isa terrane.

In the central part of the Soldiers Cap Domain, regional high gravity anomalies (Fig. 3.11) define a discrete belt of relatively high density rocks. The arcuate N-S-trending belt of rocks can be traced along the entire Mount Isa Geophysical Domain (Wellman, 1992) and corresponds to the inferred west-dipping 30 km wide suture which records the collision between the Mount Isa terrane and the Numil Seismic Province (Korsch et al., 2012). This prominent high gravity anomaly is inferred to represent the southern continuation of the suturing between the Mount Isa terrane and the Numil Seismic Province (Fig. 3.20) (Betts et al., in press; this study). Along the inferred suture, the amplitudes of the Bouguer gravity anomalies show initial regional decreases (Betts et al., in press), followed by increasing amplitude values in the southernmost part of the Soldier Cap Domain. This may suggest that the suture deepens to the immediate southeast of the Mount Isa inlier, being concealed under the Palaeoproterozoic to Phanerozoic basins (Betts et al., in press), but is shallower in the southernmost part of the Mount Isa terrane.

To the east of the suture, low Bouguer gravity anomalies may reflect the southern continuation of the Millungera basinal sequences (Fig. 3.20). Long wavelength Bouguer anomalies decrease towards the east (Fig. 3.11) and may reflect the thickening of the Millungera Basin. Low Bouguer gravity anomalies and steep gradients towards NNW-oriented anomalies suggest that deposition of the Millungera basinal sequences might have occurred in a half graben, in which the sedimentary packages thicken towards the southeast and are controlled by east-dipping normal faults. Circular high magnetic and high gravity source bodies have been mapped as mafic intrusions while short wavelength high magnetic and low gravity anomalies might represent shallow granitic bodies. Because of the short wavelength character, these granites are interpreted to intrude the underlying Soldiers Cap Group and represent the southern continuation of the suite of granitoids intruding the crust beneath the Millungera Basin (Korsch et al., 2012). By inference they are inferred to be coeval to the Williams Supersuite.

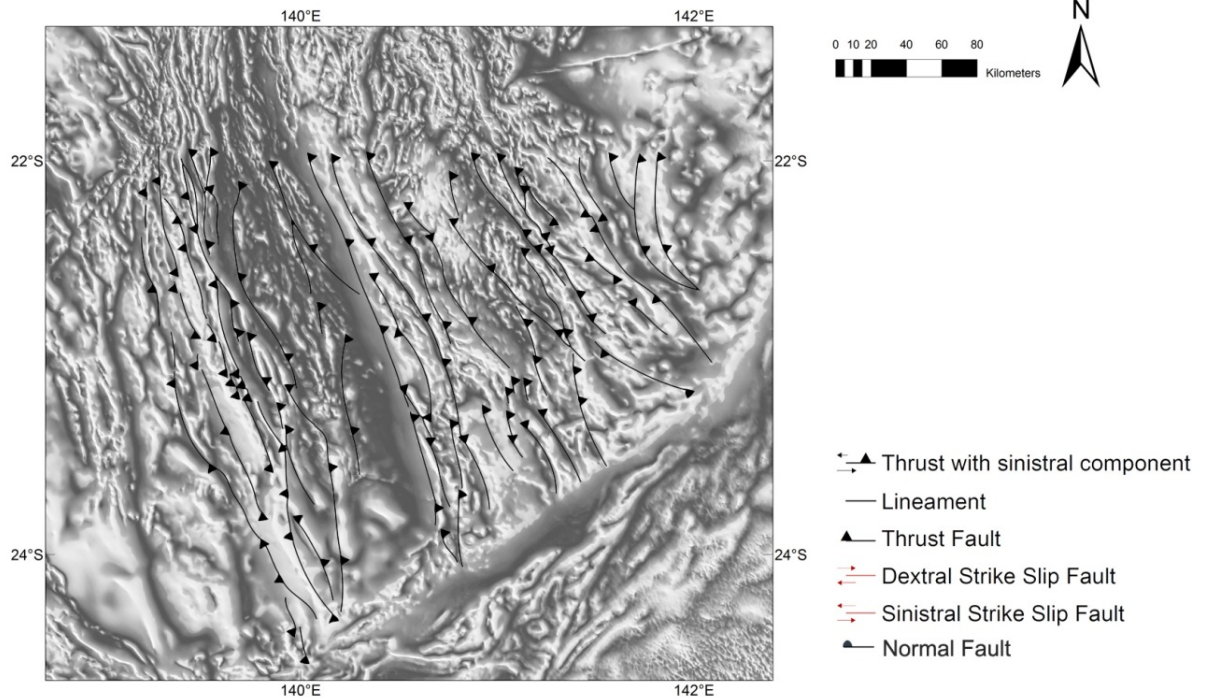


Fig. 3.18 Map showing major structures active during the ca. 1570 – 1550 Ma Middle Isan Orogeny. It is assumed that pre-existing fault network and weakened surfaces, being in a favourable orientation, might be repeatedly reactivated under a regional stress field (Giles et al., 2006b).

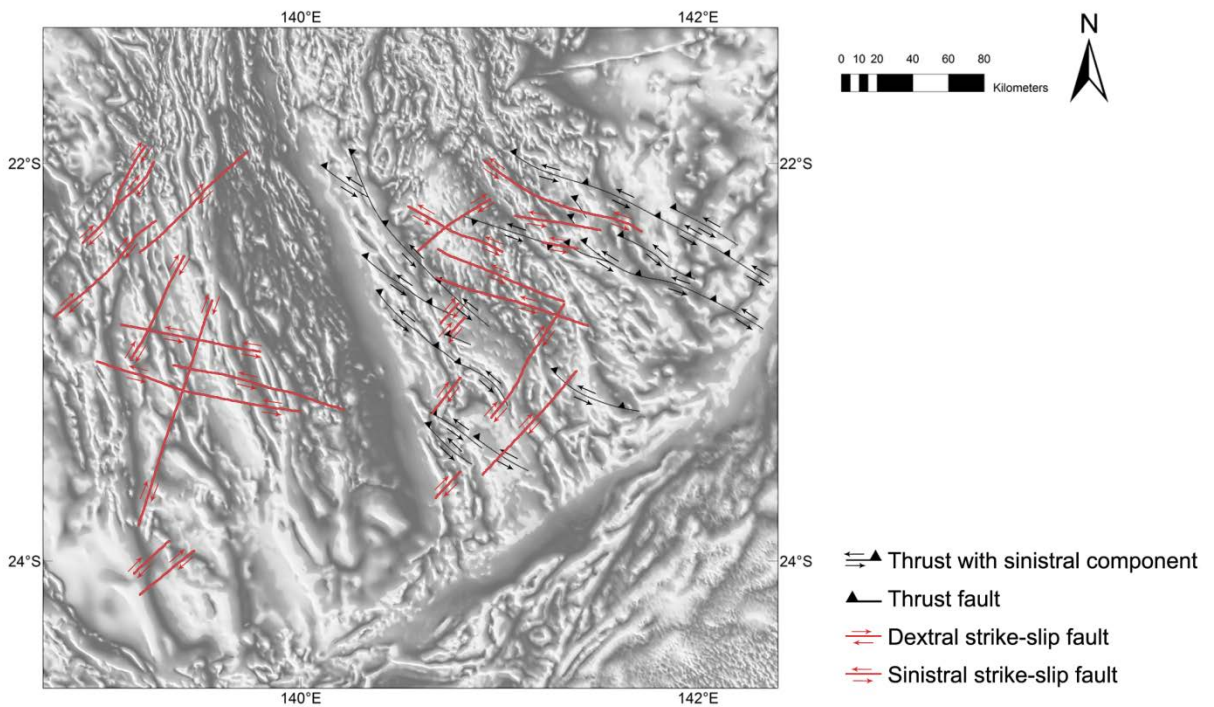


Fig. 3.19 Map showing some structures active during the ca. 1550 – 1540 Ma wrenching phase of the Isan Orogeny

3.8.6 *Cork Fault Zone*

In the southernmost part of the study area, the N-S- to NNW-trending geophysical anomalies associated with the Mount Isa terrane are abruptly terminated by the prominent Cork Fault (Wellman, 1992) which does not outcrop. Geophysical interpretation suggests that the Cork Fault is a major NE-trending, south-dipping structure (Spampinato et al., Unpublished results-a; Wellman, 1992). Time of initiation of the Cork Fault post-dates the Isan Orogeny and may be Late Mesoproterozoic (Spampinato et al., Unpublished results-a), with several episodes of reactivations during the Neoproterozoic (Harrington, 1974; Spampinato et al., Unpublished results-a), Late Carboniferous and Permian (Esso_Australia_Limited, 1984; Hawkins and Harrison, 1978). In the southeastern Soldiers Cap Domain, K-Ar analyses on granitic rocks in drill hole CPC Ooroonoo 1 yielded a Precambrian age (ca. 858 Ma) (Murray and Kirkegaard, 1978) further indicating that post-Isan tectonics affected the southernmost part of the Mount Isa terrane. NE-trending, short wavelength magnetized source bodies punctuate the southernmost parts of the Mount Isa terrane and are interpreted to represent shallow positive gravity mafic intrusions and low density granitic rocks. They are focused along the northern flank of the Cork Fault and form a continuous NE-trending belt that overprints the NNW-trending architecture of the Mount Isa terrane. In the southernmost parts of the Leichhardt River, Kalkadoon-Leichhardt and Soldiers Cap domains, elongated ENE- to NE-trending low gravity and low magnetic anomalies are interpreted to represent meta-sedimentary rock packages bounding the NE-trending granitic intrusions. In the eastern part of the Soldiers Cap Domain, the northeast trend is superimposed onto the NNW regional anomalies which are less well defined. Instead the Bouguer gravity grid shows a network of NE-trending and NW- to N-S-trending anomalies. We interpret that the orthogonal faults and fold interference patterns result in a series of low density troughs and high gravity highs. The asymmetric gravity anomalies with the lowest amplitude values towards positive NW- and NE-trending anomalies indicate stratal thickening towards NW- and NE-trending structures. The overprinting relationships indicate that deposition might result from post-Isan Orogeny tectonics and may be associated with Late Mesoproterozoic to Phanerozoic extensional events that affected the southernmost part of the Mount Isa region. In this scenario, associated granitic bodies intruded the crust of the Mount Isa terrane during the time of initiation or reactivation of the Cork Fault and associated structures, which formed the locus for magmatism and controlled the sedimentary deposition.

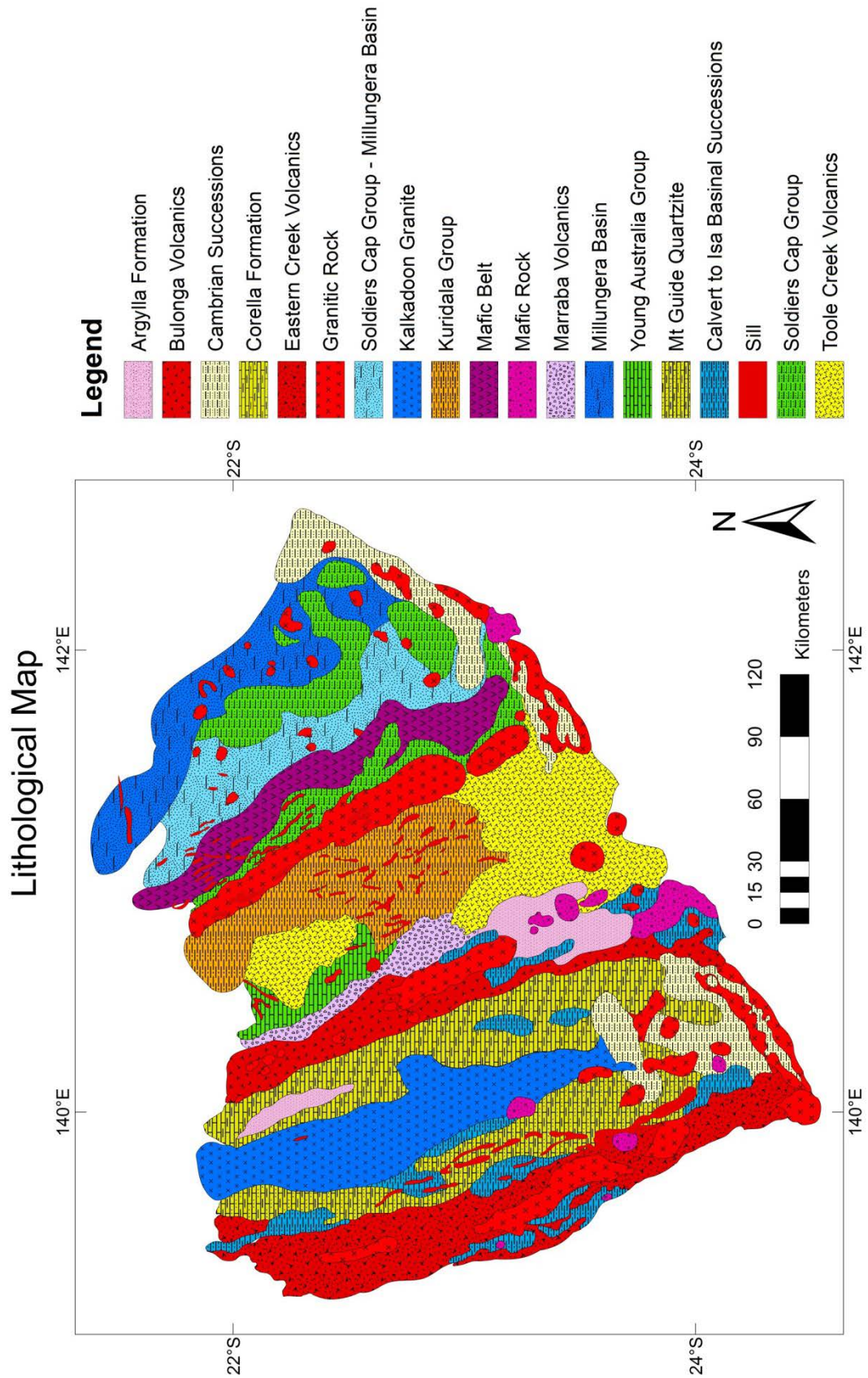


Fig. 3.20 Lithological interpretation map of the southern Mount Isa terrane

3.9 Conclusions

The depositional sequences and the bipartite regional architecture of the exposed Mount Isa Inlier are interpreted to continue southward under the Palaeozoic cover. In the Western Fold Belt, the Leichhardt River Fault Trough is interpreted to form a structure up to 300 km long defined by N-S- to NNW-trending west-dipping faults. In the Eastern Fold Belt, the east-dipping Pilgrim, Overhang, and Cloncurry fault zones extend undercover and represent major geological boundaries. The geophysical grids highlight a prominent gravity and magnetic feature that continues undercover and might represent the southern continuation of the suturing between the Mount Isa terrane and the Numil Seismic Province.

Late Palaeoproterozoic basinal sequences were deposited onto a Palaeoproterozoic basement, resulting in complex superimposed and stacked basins prior to intense basin inversion associated with a protracted deformation event. The prominent magnetic and gravity signature of the area are mostly determined by the distribution of the Eastern Creek Volcanics in the Leichhardt River Domain, the Kalkadoon Batholith, the Mount Guide Quartzite and the Corella Formation in the Kalkadoon-Leichhardt Domain, the Bulonga, Marraba and Argylla Volcanics in the Mitakoodi Domain, the Kuridala Group in the Kuridala - Selwyn Domain, the Soldiers Cap Group and the Numil Seismic Province sedimentary sequences in the Soldiers Cap Domain. NNW-trending low magnetic and low density features showing smoother texture are inferred to represent areas of thicker sedimentation of the Calvert and Isa Superbasin equivalent rocks. The 1800 - 1600 Ma basinal deposition was controlled by prominent NNW-trending normal faults and occurred in half graben setting.

Deformations during the Early Isan Orogeny might have been confined to the northern part of the Mount Isa terrane. The Middle Isan Orogeny recorded the inversion of major rift faults in a favourable orientation and resulted in regional scale culminations. This event determined the current regional architecture which is reflected by the prominent NNW-oriented geophysical signature of the area. The wrenching phase of the Isan Orogeny is represented by strike-slip faults offsetting N-S- to NNW-oriented structures. Emplacement of large NNW-trending granitic intrusions occurred during the Isan Orogeny and they might correlate with the Williams Supersuite.

The geophysical anomalies at the southern termination of the Mount Isa terrane reflect the deposition of rock packages and emplacement of volcanic intrusions that overprint the prominent NNW trend and resulted from post-Isan tectonics.

Overall the southern part of the Mount Isa terrane is characterized by a series of tectonic domains juxtaposed as a result of a complex and protracted tectonic evolution. Steep gradients reveal major fault zones that controlled the architecture of the area during rifting, sedimentation, inversion or collision of the constituting blocks.

Acknowledgement

We gratefully acknowledge Geoscience Australia, Queensland Geological Survey, pmd*CRC and Zinifex Ltd for access to the Mount Isa and the Isa - Georgetown Deep Crustal Seismic Surveys (copyright Commonwealth of Australia – Geoscience Australia 2009). Rock property data (densities and magnetic susceptibilities) of the Mount Isa region were sourced from Geoscience Australia (copyright Commonwealth of Australia – Geoscience Australia 2009). Potential field datasets were acquired by the Queensland Geological Survey and are gratefully sourced from Geoscience Australia.

Declaration for Thesis Chapter 4

Monash University

Declaration for Thesis Chapter 4

Declaration by candidate

In the case of Chapter 4, the nature and extent of my contribution to the work was the following:

Nature of contribution	Extent of contribution (%)
Processing and interpretation of gravity and aeromagnetic data; manuscript preparation	90

The following co-authors contributed to the work. If co-authors are students at Monash University, the extent of their contribution in percentage terms must be stated:

Name	Nature of contribution	Extent of contribution (%) for student co-authors only
Dr. Laurent Ailleres	Supervisory role; interpretation	5
Associate Professor Peter Betts	Supervisory role; interpretation	5

The undersigned hereby certify that the above declaration correctly reflects the nature and extent of the candidate's and co-authors' contributions to this work*.

**Candidate's
Signature**

Giovanni Pietro Tommaso Spampinato

Date

**Main
Supervisor's
Signature**

Dr. Laurent Ailleres

Date

Chapter 4: Early tectonic evolution of the Thomson Orogen in Queensland inferred from constrained magnetic and gravity data

Giovanni P.T. Spampinato

PhD Candidate

Monash University - School of Earth, Atmosphere and Environment

PO Box 84

Building 28, room 242

Clayton Campus, Wellington Road

Clayton, Vic 3800



Peter G. Betts

Associate Professor

Monash University - School of Earth, Atmosphere and Environment

PO Box 16

Building 28, room 239

Clayton Campus, Wellington Road

Clayton, Vic 3800



Laurent Ailleres

Senior Research Fellow

Monash University - School of Earth, Atmosphere and Environment

PO Box 28E

Building 28, room 144

Clayton Campus, Wellington Road

Clayton, Vic 3800



ABSTRACT

The crustal architecture as well as the kinematic evolution of the Thomson Orogen in Queensland is poorly resolved because the region is concealed under thick Phanerozoic sedimentary basins and the basement geology is known from limited drill holes.

Deep seismic reflection data show the presence of high angle thrust faults which are the main crust-scale structural elements in the mid- to lower crust. In contrast, the structure of the upper basement is not as clearly defined because of the lack of seismic reflectors. Seismic data are used to constrain regional gravity and magnetic datasets which provide an effective tool to resolve the 3D crustal architecture of the Thomson Orogen.

Combined potential field and seismic interpretation indicates that the Thomson Orogen is characterized by prominent regional NE- and NW-trending structural grain defined by long wavelength and low amplitude geophysical anomalies. The ‘smooth’ magnetic signature is interpreted to reflect deeply buried source bodies at mid- to low crustal level. Short wavelength positive magnetic features that correlate with negative gravity anomalies are interpreted to represent shallower granitic intrusions. They appear to be focused along major fault zones that might have controlled the locus for magmatism.

Gravity data indicate that the eastern and western parts of the Thomson Orogen have a different crustal architecture. The eastern Thomson Orogen is characterized by a prominent NE structural grain and orthogonal faults and fold interference patterns resulting in a series of troughs and highs. The negative gravity anomalies reflect mostly the distribution of the basinal sequences inferred from drill holes and deep seismic surveys. The western part appears as a series of NW-trending structures interpreted to reflect reverse thrust faults.

Sedimentation and basin development are interpreted to have initiated during the Neoproterozoic to Early Cambrian during an E-W- to ENE-directed extension, possibly related to the Rodinia break-up. This extensional event was followed by Late Cambrian shortening recorded in the Maneroo Platform area, possibly correlated with the Delamerian Orogeny. Renewed deposition and volcanism occurred during the Ordovician and may have continued until Late Silurian, resulting in thinned Proterozoic basement crust and extensive basin systems that formed in a distal continental back-arc environment. This period of crustal extension correlates with extensional basins that formed in the Lachlan Orogen.

The Devonian extensional Adavale Basin formed in a continental setting. At this time the extension was controlled by the existing NE- and NW-trending fault architecture.

Our interpretation places the Thomson Orogen to the west of the Neoproterozoic passive margin that occurred in the Anakie Inlier. The region is likely to represent the interior extensional architecture during the Rodinia break-up that has been subsequently extensively modified by multiple extensional basin forming events and transient episodes of crustal shortening and basin inversions.

The Early Palaeozoic tectonic evolution of the continental crust of the Thomson Orogen differs from that of the oceanic crust of the Lachlan Orogen to the south and amalgamation of the two geological terranes might have occurred during Middle Palaeozoic.

Key Words: Thomson Orogen, Tasmanides, Gravity, Magnetic, Phanerozoic Australia, Basement Setting

4.1 Introduction

The Thomson Orogen is the largest tectonic domain of the eastern Australian Tasmanides (Glen, 2005; Glen et al., 2006) and represents approximately one-eighth of the Australian continent. The region records a protracted tectonic evolution that spans the Neoproterozoic to Triassic and is coincident with one of the largest periods of continental growth of the Australian continent (Glen, 2005).

The basement rocks of the Thomson Orogen are concealed under thick sedimentary basins, which has made it difficult to unravel the crustal architecture and tectonic evolution of the region (Draper, 2006; Finlayson et al., 1988; Glen et al., 2010; Murray and Kirkegaard, 1978). In this study, we use high resolution regional potential field datasets to interpret the crustal architecture of the Thomson Orogen. The data has been demonstrated to be effective in determining the crustal architecture (Stewart and Betts, 2010b), structural setting (Betts et al., 2003b; McLean and Betts, 2003), and associated kinematics (Betts et al., 2007) in regions with little or poor geological exposure. Interpretation of potential field data is ambiguous by its nature but the ambiguity can be reduced via the incorporation of geological constraints and other geophysical datasets (Gunn et al., 1997). Nevertheless, the method is very effective at constraining crustal architecture over large areas, and is the only tool that allows 3D mapping of the architecture of

geological provinces such as the Thomson Orogen, where there is limited outcrop and drill holes intersecting the basement rocks.

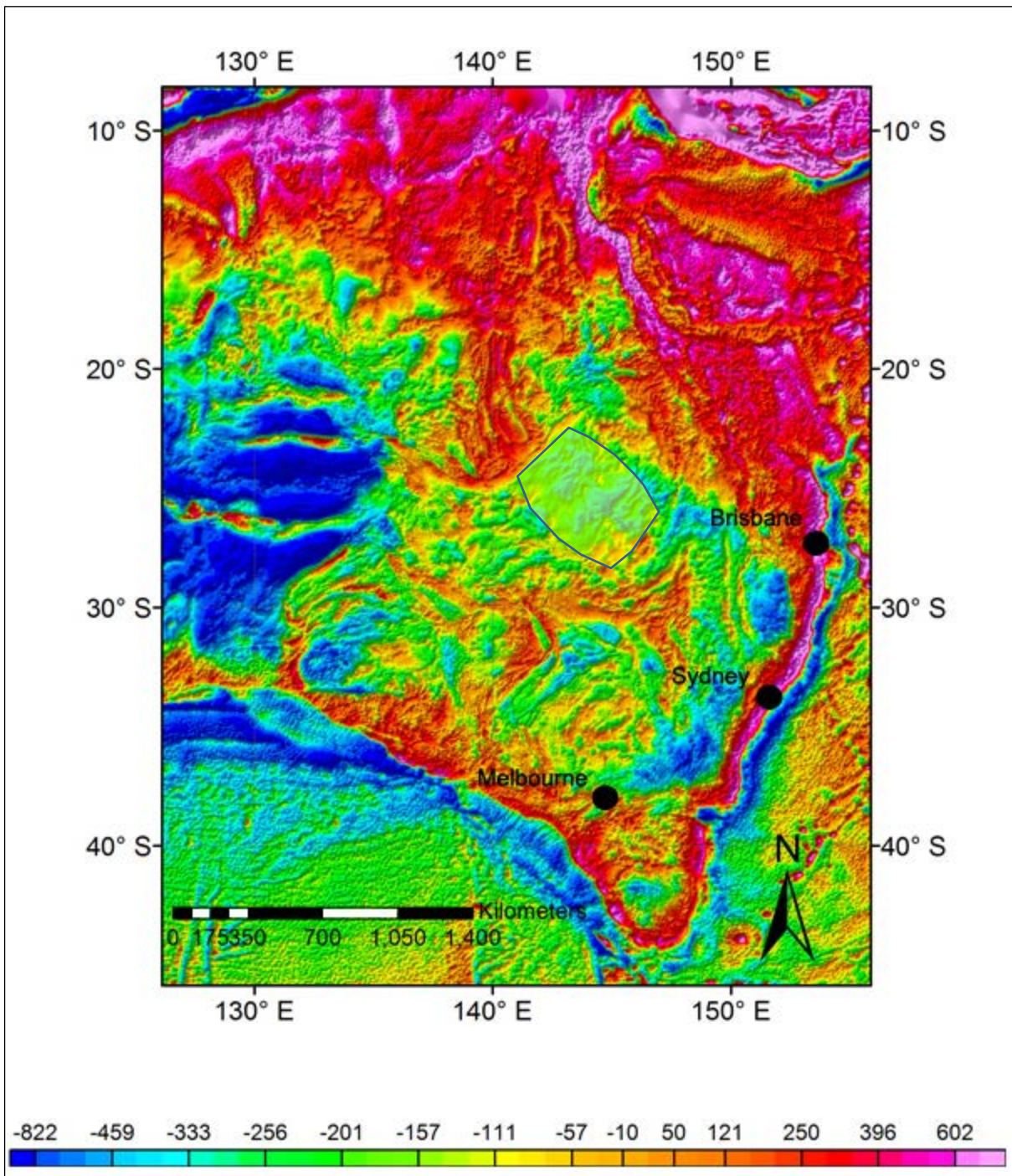


Fig. 4.1 Area of study over a Bouguer gravity map of the Australian continent. The Thomson Orogen is juxtaposed to the southern edge of the Proterozoic Mount Isa terrane and forms part of the Tasmanides of eastern Australia (Glen, 2005). Values in the legend bar are in $\mu\text{m}\cdot\text{s}^{-2}$

The results of this study provide insights into the timing and kinematics of major tectonic events in the Thomson Orogen. Understanding the crustal architecture of the region has implications for reconstructing the evolution of the eastern Australian continent during the transition from the Neoproterozoic break-up of Rodinia and the subsequent Phanerozoic evolution of east Gondwana. Then we compare our results and evolution model with the extensively studied Lachlan Orogen in the southern Tasmanides.

4.2 Geological setting

The northern extent of the Thomson Orogen is defined by the prominent Cork Fault (Figs. 4.3 and 4.5), which separates the Thomson Orogen from the Mount Isa terrane (Wellman, 1990). The southern boundary is mostly defined by the Nebine Ridge (Finlayson and Collins, 1987; Finlayson et al., 1990b), although in the western part of the region the Olepoloko Fault Zone is interpreted to mark the transition from the Thomson Orogen to the Lachlan Orogen (Fig. 4.2) (Glen et al., 2013). The eastern Thomson Orogen incorporates the Anakie Inlier and Charters Towers Province (Fergusson and Henderson, 2013; Fergusson et al., 2009; Kirkegaard, 1974; Withnall et al., 1995). The western boundary between the Warburton Basin and the Thomson Orogen is less well defined because it is buried beneath deep sedimentary basins (Murray and Kirkegaard, 1978).

The basement rocks of the Thomson Orogen lie beneath three stacked Middle Palaeozoic to Mesozoic sedimentary systems (Murray and Kirkegaard, 1978), which include, from top to bottom, the Early Jurassic to Late Cretaceous Eromanga Basin (Moss and Wake-Dyster, 1983), the Permian to Triassic Cooper and Galilee basins (Finlayson et al., 1988) and the Devonian Adavale Basin (Fig. 4.3) (Finlayson et al., 1988).

Terrestrial to shallow marine sedimentary rocks of the intra-cratonic Eromanga Basin (Wake-Dyster et al., 1983) define the upper stratigraphic unit in the area of study. The widespread Eromanga Basin extends over an area of approximately 1,200,000 km² (Finlayson et al., 1988; Mathur, 1983; Spence and Finlayson, 1983). This basin is unconformably underlain by the Cooper and Galilee basins (Figs. 4.3 and 4.4) (Finlayson et al., 1988).

The Cooper Basin (Fig. 4.3) forms a NE-trending structural depression extending for ~130,000 km² between South Australia and Queensland. It contains glacial, fluvial and lacustrine sediments (Thornton, 1979). The basin architecture has been controlled by NE-trending and NW-

trending pre-Permian basement structures (Apak et al., 1997; Sun, 1997). The Cooper Basin overlies also the Cambrian – Devonian Warburton Basin to the east and Carboniferous and igneous rocks to the west (Battersby, 1976; Gatehouse, 1986). The Eromanga and Cooper basins have undergone inversion associated with minor Cenozoic compressive events which mostly reactivated existing faults (Leven et al., 1990; Moss and Wake-Dyster, 1983).

The Galilee Basin (Fig. 4.3) is a large intra-cratonic basin which is predominantly filled by fluvial sediments (Hawkins and Harrison, 1978; Jackson et al., 1981; Van Heeswijck, 2010). It overlies the Devonian Adavale Basin to the south, the Late Devonian to Early Carboniferous Drummond Basin to the east (Fig. 4.2) and Proterozoic to Early Palaeozoic basement rocks to the north (Van Heeswijck, 2010). The upper succession of the Galilee Basin can be correlated with the adjacent Cooper Basin in the Thomson Orogen and Bowen Basin (Van Heeswijck, 2010). The Galilee Basin formed inboard of the New England Orogen (Fig. 4.2) which developed along eastern Gondwana in the Late Palaeozoic to Early Mesozoic (Van Heeswijck, 2010).

The underlying Adavale Basin (Figs. 4.3 and 4.4) (Finlayson et al., 1988) is interpreted by Evans et al. (1992) as a rift-sag basin developed during an Early Devonian intra-continental transtensional event (McKillop et al., 2007). Felsic intrusive magmatism accompanied the crustal extension event throughout the broader Thomson Orogen (Murray, 1994). Deposition was initially dominated by fluvial sedimentation followed by a marine incursion that resulted in a mixed carbonate - siliciclastic deposition (McKillop et al., 2007). The Middle and Late Devonian sedimentary successions define a restricted marine and fluvio - lacustrine environment (McKillop et al., 2007) prior to an Early to Middle Carboniferous deformation (Finlayson, 1993). The Adavale Basin is interpreted to have formed in response to continent-dipping subduction to the east in the New England Orogen (McKillop et al., 2007; Murray, 1990) and thus represents a continental back-arc basin. The Adavale Basin was inverted during the Kanimblan Orogeny and local uplift and erosion of upper sedimentary packages occurred (Finlayson, 1993; Leven et al., 1990). The remnant synclinal structures within the deeper synclinal keel of the Adavale Basin are imaged in deep seismic data and include - *from west to east* - the Warrabin, Barcoo, Quilpie, Cooladdi and Westgate troughs (Figs. 4.6, 4.8 and 4.10) (Mathur, 1983; Pinchin and Senior, 1982).

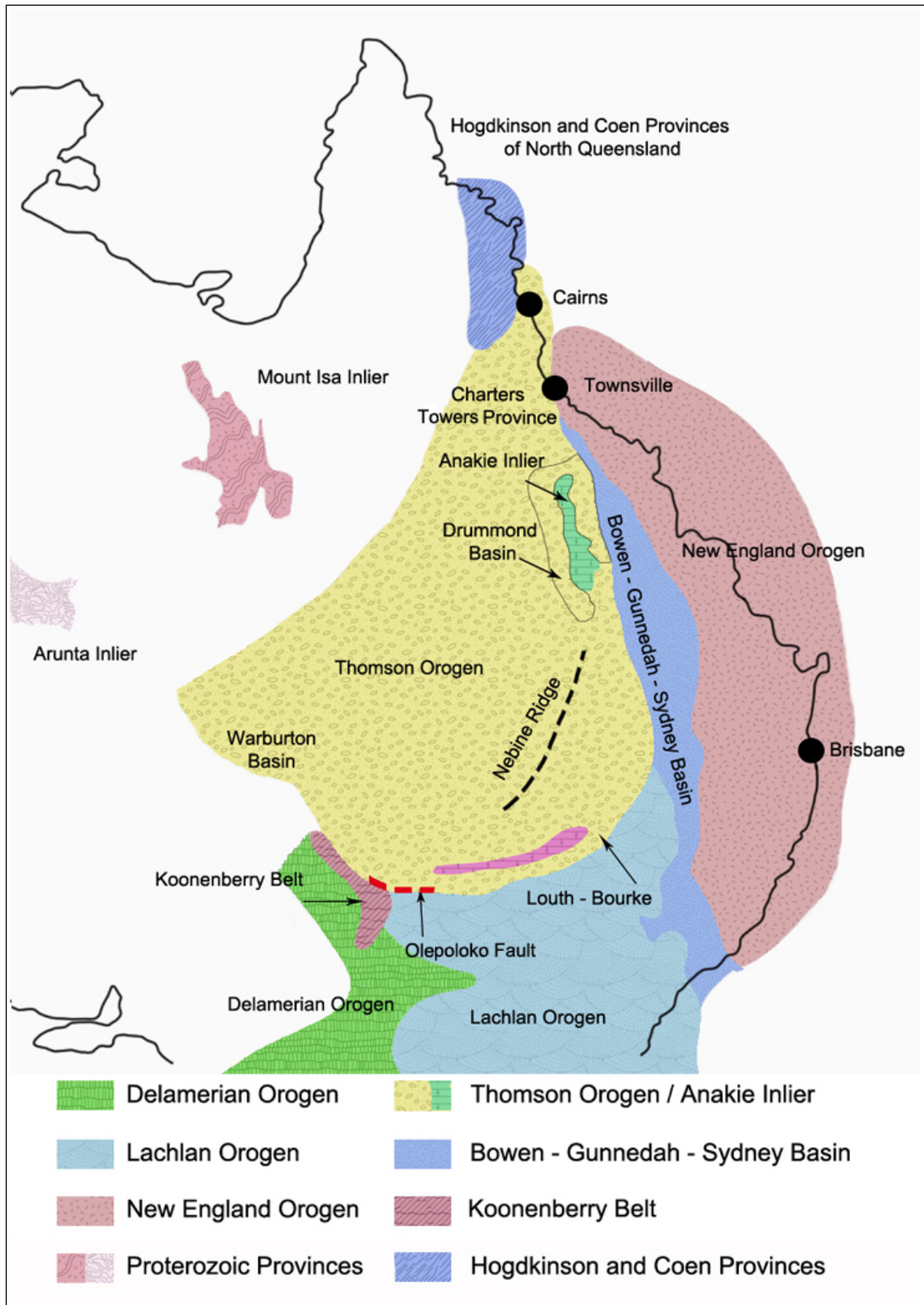


Fig. 4.2 Sketch showing the distribution of major geological features and the extension of the geological provinces surrounding the Thomson Orogen; modified from Kositsin et al. (2009).

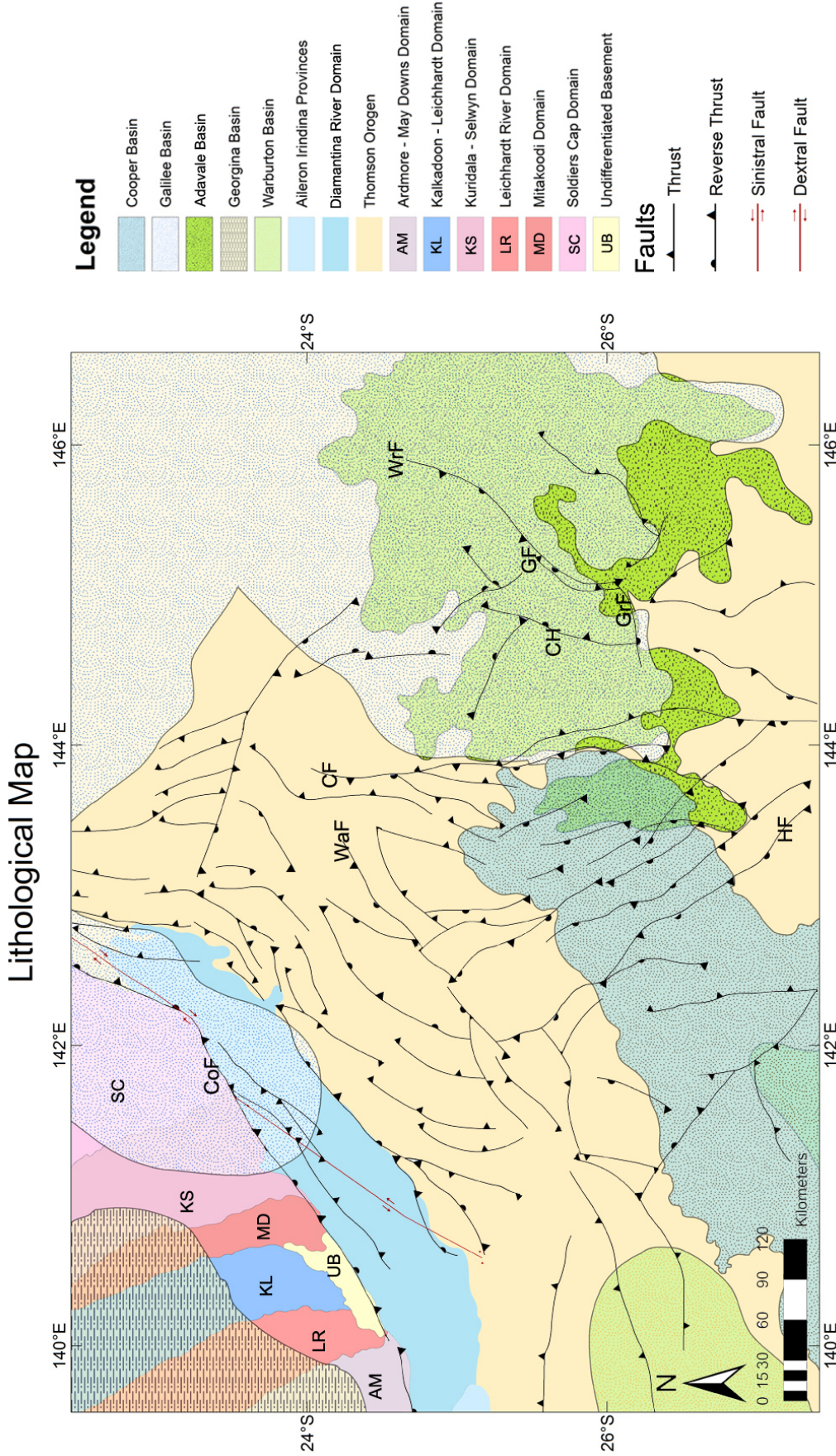


Fig. 4.3 Map of the geological domains and major structures of the Central Thomson Orogen; CoF= Cork Fault; CF= Canaway Fault; WaF= Warreccan Fault; HF= Harkaway Fault; CH= Cothalow Arch; GrF= Grenfield Fault; GF=Gumbardo Fault; WwF= Warrego Fault

Meta-sedimentary basement rocks underlie the un-metamorphosed Phanerozoic sedimentary sequences (Murray and Kirkegaard, 1978). Several drill holes penetrated mostly phyllitic, quartzitic and schistose basement rocks which are inferred to largely represent the Thomson Orogen (Murray, 1994). The basement rocks of the Thomson Orogen show remarkable similarities with the marine meta-sedimentary rocks of the Anakie Inlier (Fig. 4.2) and the two provinces might correlate (Fig. 4.4) (Fergusson et al., 2007a; Withnall et al., 1995). With few exceptions, all the rocks within the Thomson Orogen have deposited in a deep water environment (Murray, 1994).

In the Maneroo Platform and surrounding areas, Early to late Cambrian (K-Ar and Rb-Sr analyses in drill cores from AAP Fermoy 1) schistose and phyllitic basement rocks have been encountered by several drill holes (e.g. AAP Mayneside 1, AAO Penrith 1 and AAO Beryl 1, Fig. 4.5) (Murray, 1994; Murray and Kirkegaard, 1978). An unconformity is observed at the basal Early Ordovician volcanic rocks in GSQ Maneroo 1 drill hole (Draper, 2006). Murray and Kirkegaard (1978) and Murray (1994) suggested that the Thomson Orogen was affected by a Middle to Late Cambrian tectonic event coeval with the Delamerian Orogeny (Cayley et al., 2011; Fergusson et al., 2001; Foden et al., 2006; Glen, 2005; Withnall et al., 1995; Withnall et al., 1996).

Early Ordovician black graptolitic shales overlie Cambrian carbonate successions in the Warburton Basin area (Murray and Kirkegaard, 1978). Early to Middle Ordovician (Draper, 2006; McKillop et al., 2007) rhyolite and brecciated crystal tuff have been intersected beneath the northern part of the Thomson Orogen (GSQ Maneroo 1, AMX Toobrac 1), in the Drummond Basin (BEA Coreena 1) and Adavale Basin (PPC Carlow 1 and PPC Gumbardo 1, Fig. 4.5) (Kositcin et al., 2009). McKillop et al. (2007) reported volcanic rocks beneath the Devonian Adavale Basin in PPC Cothalow 1 drill hole (Fig. 4.5) and interpreted them as the same age as the basal volcanic rocks in PPC Gumbardo 1 drill hole. Fergusson et al. (2007a) and Fergusson et al. (2007b) indicated that Early to Middle Ordovician volcanic and sedimentary successions in north-eastern Australia occurred in a back-arc setting reflecting an overall extensional setting associated with a convergent margin located further to the east.

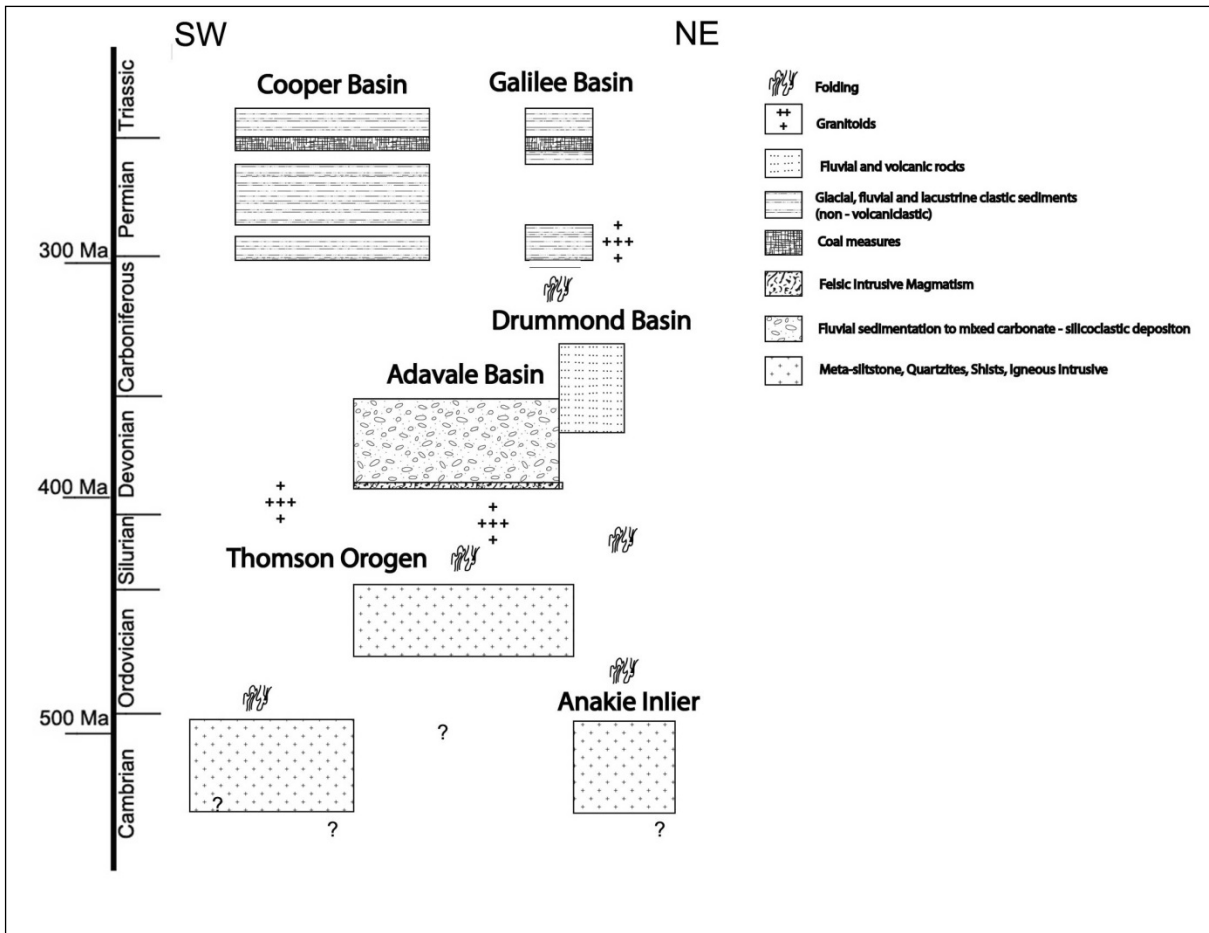


Fig. 4.4 Time – space diagram illustrating the major depositional units of the Thomson Orogen; modified from Murray (1990). The Cambrian basement rocks in the Anakie Inlier might correlate with the meta-sedimentary rocks of the Maneroo Platform and Nebine Ridge of the Thomson Orogen (Withnall et al., 1995; Withnall et al., 1996).

Late Ordovician to Early Silurian deformation has been recorded in the Anakie Inlier, Greenvale Province and Charters Towers Province (Fig. 4.2) and has been associated with the widespread Benambran Orogeny (Fergusson et al., 2005; Fergusson et al., 2007b; Withnall et al., 1995). In the Thomson Orogen, this event may be reflected in the sedimentary record by uplift and transition to shallow marine and continental deposition environment (Finlayson, 1993) or positive relief and a lack of repositories for sediment (Fergusson and Henderson, 2013). Although the Benambran Orogeny may have been recorded in the southernmost part of the Thomson Orogen in New South Wales (Burton, 2010), Draper (2006) indicated that Early Ordovician volcanic rocks underlying the Adavale Basin are undeformed, suggesting that deformation associated with the Benambran Orogeny did not importantly affect the interior of the Thomson Orogen (Fergusson and Henderson, 2013). Post-orogenic (?) Middle Silurian (ca.

428 Ma) felsic magmatic rocks have been intersected in the BMR Longreach 1 drill hole on the Maneroo Platform, the PPC Etonvale 1 and AOP Balfour 1 drill holes in the Adavale Basin, and the DIO Ella 1 and TEA Roseneath 1 drill holes in the Cooper Basin (Draper, 2006).

Murray and Kirkegaard (1978) indicated that the prominent NE-trending structural grain in the Thomson Orogen might be related to pre-Permian structures based on the observation that most fold axes within the Permian and Mesozoic cover trend northeast and appear to be controlled by the underlying basement structures.

4.3 Previous geophysical surveys

In the early 1980s the Australian Bureau of Mineral Resources (BMR) started extensive deep seismic survey across the Central Eromanga Basin (Fig. 4.5). The main objective was to investigate basement structures and provide insights into the geological history of the area. The survey covers a total linear distance of 1,400 km. The information is integrated with 5,000 km of older data with 2,300 km being reprocessed and digitized (Moss and Wake-Dyster, 1983; Wake-Dyster et al., 1983). Among the seismic profiles, traverses 1 and 10 were recorded to investigate the geology of the Devonian Warrabin Trough and Quilpie Trough. Traverse 6 is located to cross the Barcoo Trough while traverses 6 and 8 cross the Canaway Ridge (Fig. 4.5).

The top reflective zone has been interpreted to correlate with the sedimentary successions of the Eromanga, Cooper and Adavale basins (Pinchin and Senior, 1982). The Devonian sedimentary successions generally thicken towards the southeast in the study region (Finlayson et al., 1988) increasing from 1,600 m in the Barcoo Trough to 3,000 m in the Quilpie and Warrabin troughs, and up to 9,500 m within the Adavale Basin (Passmore and Sexton, 1984). A zone of no reflection between 2.5 and 8 seconds might reflect a seismically homogeneous upper basement (Finlayson et al., 1988). The non-reflective seismic character has been attributed to severe deformations which do not provide continuous sub-horizontal reflectors (Finlayson et al., 1984; Lock et al., 1986; Mathur, 1983; Spence and Finlayson, 1983), although strong reflectors associated with Permian coals may have also hindered seismic penetration (Wake-Dyster et al., 1983). Mathur (1983), Lock et al. (1986) and Spence and Finlayson (1983) have interpreted this zone to represent the basement rocks of the Thomson Orogen. The zone between 7-8 and 13-14 seconds is characterized by short reflection segments having alternating high and low velocities which may represent a thick layer in the lower crustal level changing gradually in its bulk composition (Mathur, 1983). This zone has been interpreted to correspond to the lower crust

(Finlayson et al., 1989; Finlayson et al., 1990b; Finlayson et al., 1990c; Mathur, 1983). The alternating reflections may represent horizontal shearing of contrasting lithologies or sills of basaltic melt intruded from the asthenosphere during a crustal extension (Finlayson et al., 1989; Finlayson et al., 1990b; Finlayson et al., 1990c). The underlying zone with no reflection is interpreted to represent the upper mantle (Mathur, 1983).

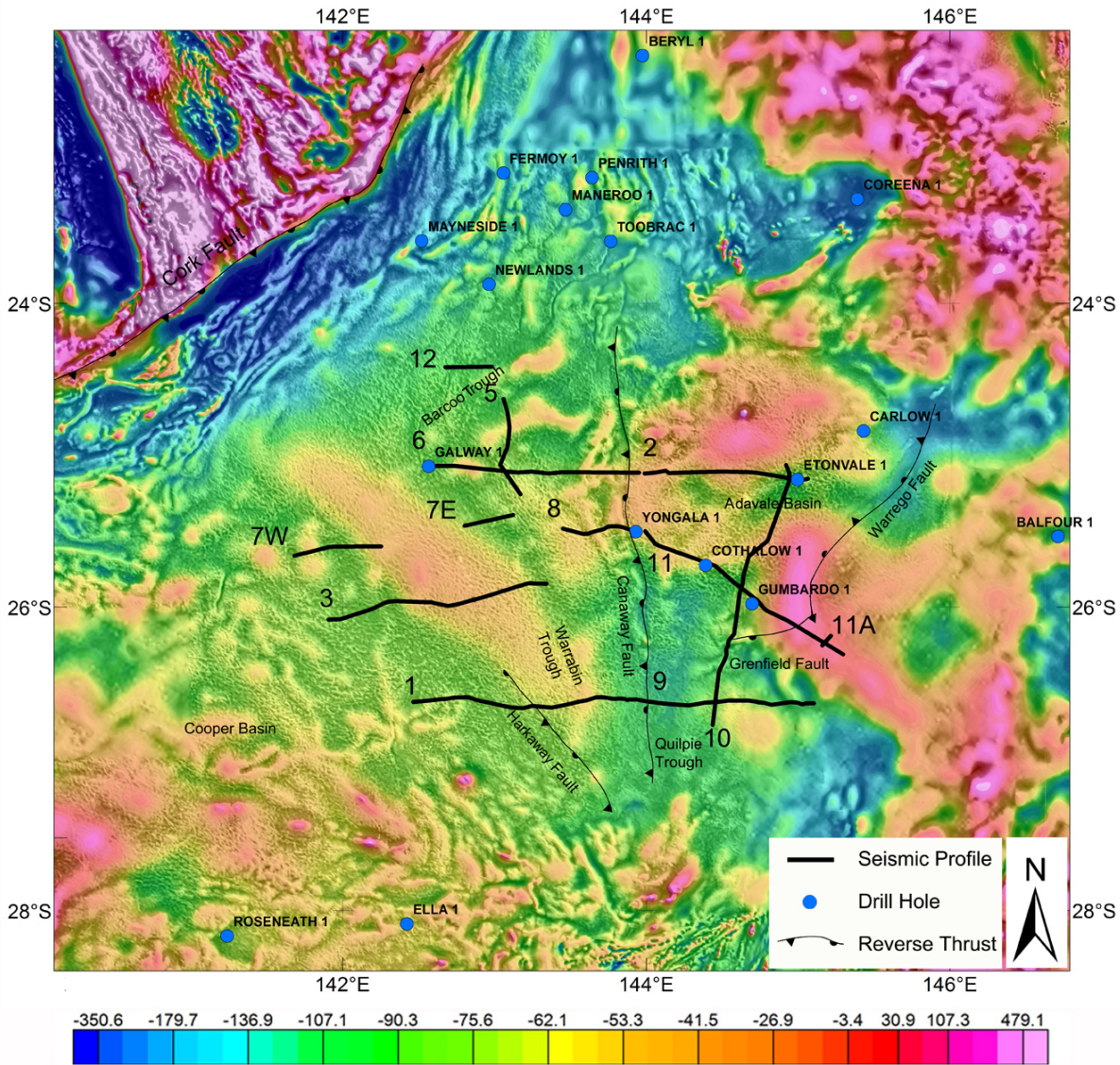


Fig. 4.5 Location of the BMR deep seismic profiles and drill holes along with major known structures over a composite RTP and tilt derivative magnetic map of the Central Eromanga Basin. Amplitude values in the legend bar are in nT.

Seismic data indicate that high angle reverse faults form the main deformation style (Finlayson et al., 1988). However, structures penetrating the basement are rarely evident on seismic sections (Finlayson et al., 1988; Finlayson et al., 1990c; Mathur, 1983, 1984).

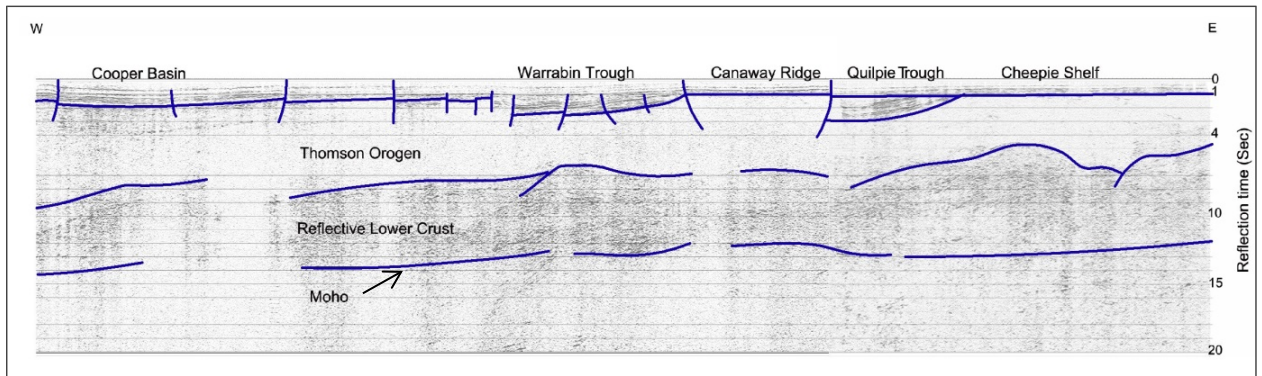


Fig. 4.6 Interpreted seismic zones along the traverses 1 and 9 of the BMR seismic sections; modified from Finlayson et al. (1990b).

Early to Middle Devonian reflective rocks in the Adavale Basin, as well as in the margins of the Warrabin Trough are imaged in half graben and graben (Hoffmann, 1988, 1989). Murray (1994) indicated that within the Adavale Basin the fault blocks are rotated from east, northeast and southeast towards the Canaway Ridge in an overall westerly direction. The Early Devonian sequence onlaps the Canaway Ridge from both the Adavale Basin and the Warrabin Trough (Evans et al., 1992). This implies that the Canaway Ridge was a basement high during the Devonian (Hoffmann, 1989). The N-S-trending Warrabin Trough includes also faults down-thrown to the east during the deposition of the Devonian sequence (Figs. 4.6 and 4.8) (Evans et al., 1992).

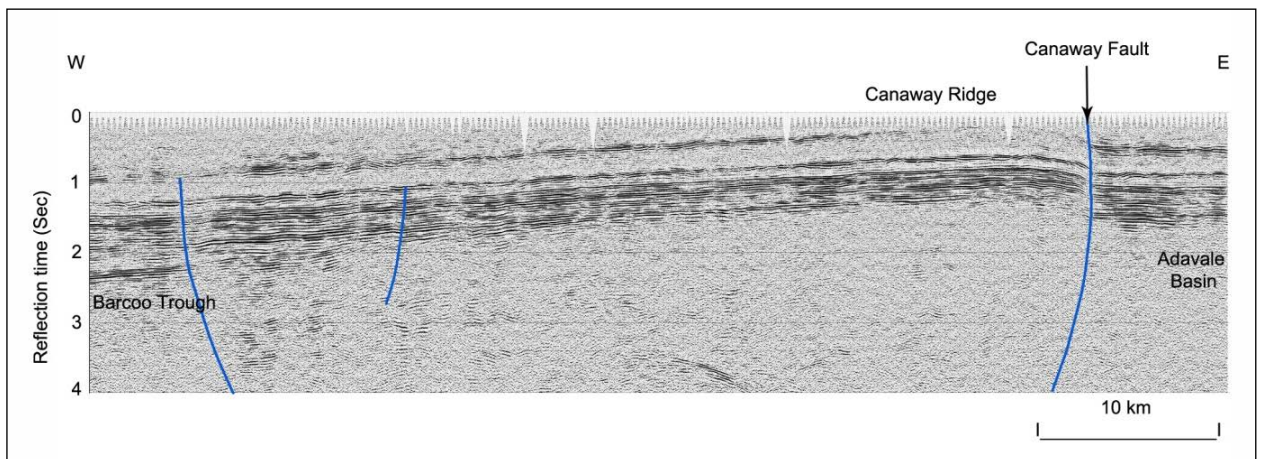


Fig. 4.7 Fault architecture along the Deep Seismic section n. 6. The Canaway Ridge separates the Devonian sedimentary units of the Adavale Basin and the Barcoo Trough; modified from Wake-Dyster et al. (1983).

Leven and Finlayson (1986) suggested that the Devonian sedimentary sequences were affected by two deformation events. An Early Carboniferous N-S shortening event was reflected by E-W-

striking thrusts and associated N-S tear faults. A subsequent Late Carboniferous tectonic event resulted in the formation of N-S-striking thrust faults. Early Carboniferous thrusts were reactivated as tear faults. The tectonic style of this composite orthogonal network of faults suggests that the upper and lower crusts of the Thomson Orogen were mechanically decoupled (Finlayson et al., 1988; Leven and Finlayson, 1986; Leven et al., 1990).

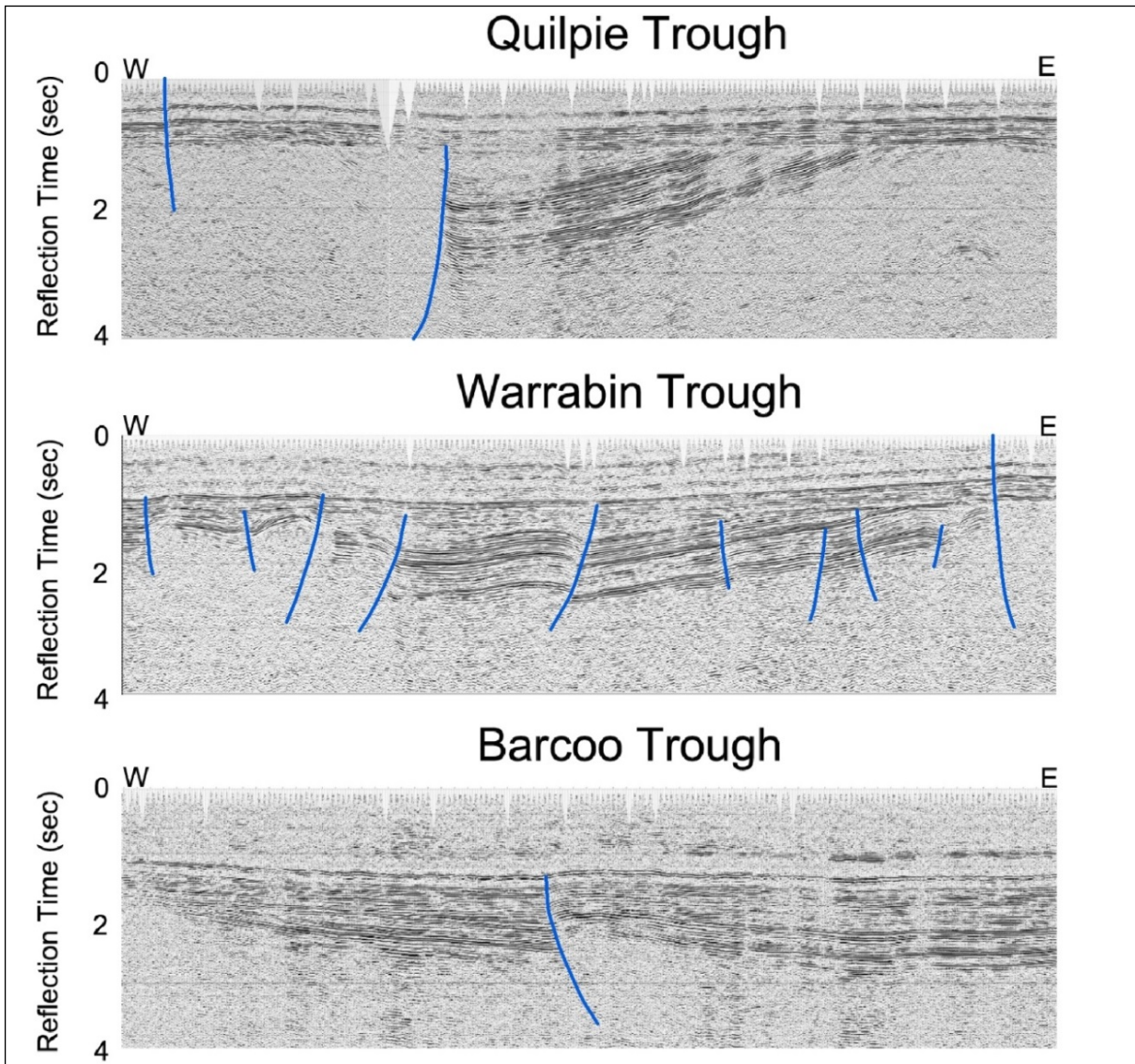


Fig. 4.8 Seismic reflection sections showing the structural setting of the Quilpie (section n. 9, fig. 4.5), Warrabin (section n. 1, fig. 4.5) and Barcoo troughs (section n. 6, fig. 4.5); modified from Wake-Dyster et al. (1983). The folded Devonian basinal successions of the Quilpie Trough underlie the Eromanga sediments which are characterized by lower amplitude deformations (Leven et al., 1990). The Warrabin Trough is preserved to the west of the Canaway Ridge. It contains up to 3000 m of Devonian sedimentary rocks which are displaced by high angle reverse faults (Pinchin and Senior, 1982). The Warrabin Trough appears extensively faulted when compared to the Quilpie and the Barcoo Troughs (Leven et al., 1990; Pinchin and Senior, 1982).

4.4 Methods

Analysis of gravity and magnetic data is effective at extrapolating sparse and relatively small-scale geological information into a regional context (Aitken and Betts, 2009; Betts et al., 2003b; Stewart and Betts, 2010b). Gravity and magnetic data allow discriminating rocks with different densities and magnetic susceptibilities, although the method is limited because it does not diagnose rock types (Clark, 1981; Clark and Schmidt, 1982). Nevertheless, the ambiguity inherent in gravity and magnetic data can be significantly reduced where geological or geophysical constraints such as seismic data, drill holes or geochemical data are available. Since 2006 the Geological Survey of Queensland has acquired high resolution regional gravity and airborne geophysical data throughout Queensland. Over 50% of the state has been covered by gravity data collected using station spacing between 2 and 4 km (Chopping and Henson, 2009). Aeromagnetic data have been collected with a line spacing of 400 m and an 80 m ground clearance (Chopping and Henson, 2009).

Grid processing and image enhancement of aeromagnetic and Bouguer gravity grids were undertaken to glean the geophysical texture and to obtain information at different crustal levels. Firstly, the total magnetic intensity grid was reduced to the pole to remove the effects of the inclined magnetic field on the anomaly shapes and to center anomalies over their source bodies. Then combinations of filters were applied to the RTP magnetic and Bouguer gravity grids to assist in the geological interpretation.

The vertical derivative filter calculates the vertical rate of change in the magnetic signal sharpening the geophysical anomalies and was applied in order to highlight shallow magnetic sources as well as geometries and boundaries between the source bodies. The tilt derivative filter was used to better detect vertical contacts from the grids. This filter enhances weak magnetic anomalies calculating the ratio of the vertical gradient to the total horizontal gradient, irrespective of the amplitude or wavelength of the magnetic field. As a result, it can be successfully applied to improve the geophysical response of weak anomalies and highlight structural trends. The low pass filter removes the shortest wavelengths from the spectrum retaining the long wavelengths and was applied to preserve deeper source responses. Processed images provided great contrast between anomalies and gradients and allowed improving the geophysical signal of buried source bodies (Figs. 4.9, 4.10, 4.11 and 4.12).

<i>Filter</i>	<i>Description</i>	<i>Used for</i>
Reduction to the pole	Magnetic data are recalculated as if the inducing magnetic field was vertical	Centering the anomalies over their source bodies
Band-pass	Retains or reject a range of wavenumber from the spectrum	Preserving the geophysical signal at different crustal levels
Low-pass	Retains long wavelengths, low frequencies	Enhancing the signal of deeply buried source bodies
Hi-pass	Retains short wavelength, high frequencies	Enhancing the signal of shallow source bodies
Butterworth	Retains or reject a range of wavenumber from the spectrum	Preserving the signal at different crustal levels; by controlling the degree of roll-off ringing (Gibb's phenomena) can be avoided.
Downward Continuation	Brings the plane of measurement closer to the source	Enhancing the response from shallow source bodies. Use of high pass filter is recommended in order to avoid noise.
Upward Continuation	Brings the plane of measurement farther to the source	Minimising the geophysical response of shallower source bodies
Vertical Derivative	Calculates the vertical rate of change in the magnetic signal	Enhancing shallow anomalies, enhancing the shape of source bodies.
Tilt Derivative	Calculates the ratio of the vertical gradient and the total horizontal gradient irrespective of the amplitude or wavelength of the geophysical anomalies	Improving vertical contacts between the source bodies; improving the geophysical response of weak anomalies.

Table 1 Major filters used in geophysical processing and their effect on the filtered grid

4.5 Observations and results

The overall magnetic signature of the Thomson Orogen is characterized by smooth textures and anomalies amplitude between -650 and 150 nT (Fig. 4.9). The Bouguer gravity map shows prominent northeast regional trends having moderate (-200 to $-150 \mu\text{m}^*\text{s}^{-2}$) amplitude values (Fig. 4.10). This NE-oriented structural grain is less well defined to the west and gives way to NW-oriented gravity anomalies that progressively abuts the Warburton Basin area. The Thomson Orogen is separated into several major regions and features, which we describe below.

4.5.1 Cork Fault

The northern extent of the Thomson Orogen is defined by the geophysical expression of the Cork Fault, which separates the regional positive NNW-trending structural grain of the Mount Isa terrane (Wellman, 1990) from the NE-trending low geophysical anomalies of the Diamantina River Domain of the Thomson Orogen (Figs. 4.9 and 4.10). The Cork Fault zone forms a prominent feature in both the magnetic and gravity grids and is characterized by steep NW-

oriented gradients (~ 150 nT/km and $\sim 50 \mu\text{m}^*\text{s}^{-2}$ /km) decreasing towards the south that extend for more than 500 km (Figs. 4.9, 4.10, 4.11 and 4.12).

4.5.2 Diamantina River Domain

The NE-trending Diamantina River Domain lies to the immediate south of the Cork Fault. This domain is characterized by long wavelength magnetic anomalies between -650 nT and -150 nT (Fig. 4.9), that are the lowest regional magnetic amplitudes within the area of study. The region is punctuated by NE-trending short wavelength positive magnetic anomalies that are best imaged in the RTP grid (Fig. 4.9). They show a circular shape to the west and elongated shape to the centre of the domain. NNE-trending linear magnetic anomalies cross the central part of the Diamantina River Domain and offset ENE- to NE-trending magnetic features (Fig. 4.9). This prominent magnetic lineament can be traced for at least 300 km towards both the Central Thomson Orogen and the Mount Isa terrane (Figs. 4.9 and 4.11).

The eastern part of the Diamantina River Domain is characterized by a series of sub-parallel NNE-trending low to moderate magnetic anomalies with amplitudes between -300 and -100 nT. At their terminations these structures deflect towards NE-trending faults defined by prominent linear magnetic anomalies (Fig. 4.13).

Bouguer gravity data shows that the Diamantina River Domain is characterized by arcuate NE-trending positive anomalies with regional amplitudes between -100 and 200 $\mu\text{m}^*\text{s}^{-2}$ and little magnetic expression. These anomalies define a discrete belt of rock which lies immediately adjacent to the Cork Fault at the southern termination of the Mount Isa terrane (Fig. 4.10).

4.5.3 Maneroo Platform

The Maneroo Platform is characterized by moderate Bouguer gravity responses ($\sim -200 \mu\text{m}^*\text{s}^{-2}$) and low to moderate magnetic signature having regional amplitude values of ~ -60 nT (Figs. 4.9 and 4.10). Alternating N-S-trending, short wavelength high and low Bouguer gravity responses between $-300 \mu\text{m}^*\text{s}^{-2}$ and $-120 \mu\text{m}^*\text{s}^{-2}$ terminate to the south against a NW-trending fault, informally referred to as the Maneroo Lineament (Fig. 4.9). This lineament extends at least for 400 km (Figs. 4.11 and 4.12) and is defined by relatively steep gradients of $\sim 8.5 \mu\text{m}^*\text{s}^{-2}$ /km decreasing towards the southwest. N-S-trending magnetic anomalies of the Maneroo Platform correlate well with gravity anomalies. The Maneroo Lineament instead is poorly defined in aeromagnetic data. However, to the south of the Maneroo Lineament, the magnetic texture appears smoother (Fig. 4.9) and the gravity grid shows a broad low amplitude domain (Figs. 4.10

and 4.12) suggesting that this structure bounds regions of different geophysical character or there is a greater depth to the source rocks.

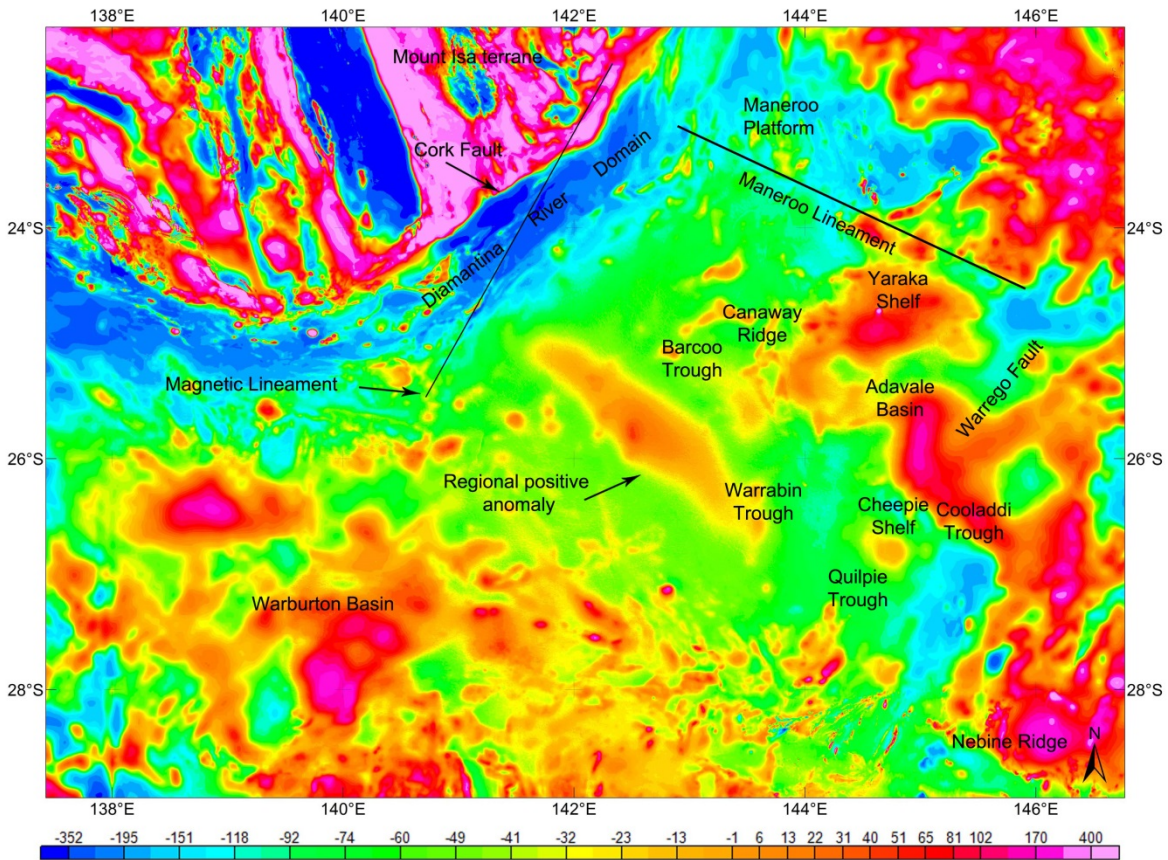


Fig 4.9 Map of the regional RTP magnetic anomalies of the Thomson Orogen and surrounding regions. Values in the legend bar are in nT.

4.5.4 Southeast Thomson Orogen

The south-eastern part of the Thomson Orogen is characterized by a regional gravity low, delimited by prominent NE-trending positive gravity structures including the Warbreccan Dome - Newlands Trend, the Yaraka Shelf, the Warrego Fault and the Nebine Ridge (Figs. 4.10 and 4.12). NE-trending magnetic anomalies are imaged at the south-western termination of the Adavale Basin and along the Nebine Ridge region (Figs. 4.9 and 4.12). However, the northeast structural grain is less well defined in the aeromagnetic data.

4.5.5 Canaway Ridge

The Canaway Ridge is characterized by N-S-trending gravity anomalies that can be traced from the Quilpie and Warrabin troughs region to the Maneroo Platform further to the north (Fig. 4.10).

The positive Bouguer gravity anomalies (more than $-200 \mu\text{m}^*\text{s}^{-2}$) of the Canaway Ridge separate the low density domains of the Adavale, Quilpie and the Cooladdi troughs to the east from the Warrabin and the Barcoo troughs to the west (Fig. 4.10). The Canaway Ridge shows steeper gravity gradients in its eastern edge with values comprised between 8 and $20 \mu\text{m}^*\text{s}^{-2}/\text{km}$ while the western limit shows more gentle gradients comprised between 4 and $9 \mu\text{m}^*\text{s}^{-2}/\text{km}$. The Canaway Fault (Fig. 4.3) represents the eastern edge of the Canaway Ridge and is defined by N-S-trending linear magnetic anomalies that are best imaged in the vertical derivative grids (Figs. 4.11 and 4.12) and can be traced for at least 300 km. The Canaway Ridge is characterized by a relatively high gravity signature but has no clear magnetic expression. This ridge is punctuated by short wavelength circular to elongated NW- to NE-trending positive magnetic anomalies (Figs. 4.9 and 4.11).

4.5.6 Adavale Basin

The Adavale Basin (Fig. 4.10) is characterized by low gravity amplitudes (up to $-500 \mu\text{m}^*\text{s}^{-2}$). The negative amplitude anomalies associated with the Adavale Basin extend for $\sim 19,400 \text{ km}^2$ and show an overall northeast trend. The lowest amplitude values are located along its south-eastern margin, where the basin terminates against positive gravity anomalies associated with the NE-trending Warrego Fault and the ENE-trending Grenfield Fault (Figs. 4.3 and 4.12). These faults are defined by significant gravity gradients between 15 and $20 \mu\text{m}^*\text{s}^{-2}/\text{km}$. The regional gravity anomalies of the Adavale Basin appear to gradually decrease in amplitude towards the northwest where the basin terminates against the Canaway Ridge to the east and the Yaraka Shelf to the north.

Within the Adavale Basin, the gravity map shows relative high amplitude anomalies ($\sim -330 \mu\text{m}^*\text{s}^{-2}$) along the Cothalow Arch (Fig. 4.5, location Cothalow 1). The north-western flank of the Warrego Fault is bounded by a N-S- to NE-trending positive magnetic source body that has an associated anomaly approximately 25 km wide and extends for approximately 90 km along strike of the anomaly (Figs. 4.9 and 4.12).

4.5.7 Nebine Ridge

The low gravity anomalies that characterize the southeast Thomson Orogen are terminated to the south by the positive gravity Nebine Ridge (Fig. 4.10). The Nebine Ridge trends parallel to the NE-trending Warrego Fault, Warbreccan Dome - Newlands Trend and the Cork Fault further to

the north (Figs. 4.10 and 4.12). The Nebine Ridge is characterized by Bouguer gravity anomalies with amplitudes between -250 and $-100 \mu\text{m}^*\text{s}^{-2}$ in its north-eastern part and -50 to $100 \mu\text{m}^*\text{s}^{-2}$ in the south-western part. NW-trending gravity anomalies separate the two geophysically distinguished regions.

The trend in the magnetic data correlates with the Bouguer gravity data and is characterized by regional high amplitude responses in the southwest (0 to 250 nT) and low magnetic signature in the northeast (-150 to 50 nT). The Nebine Ridge is punctuated by high magnetic and low density circular geophysical anomalies.

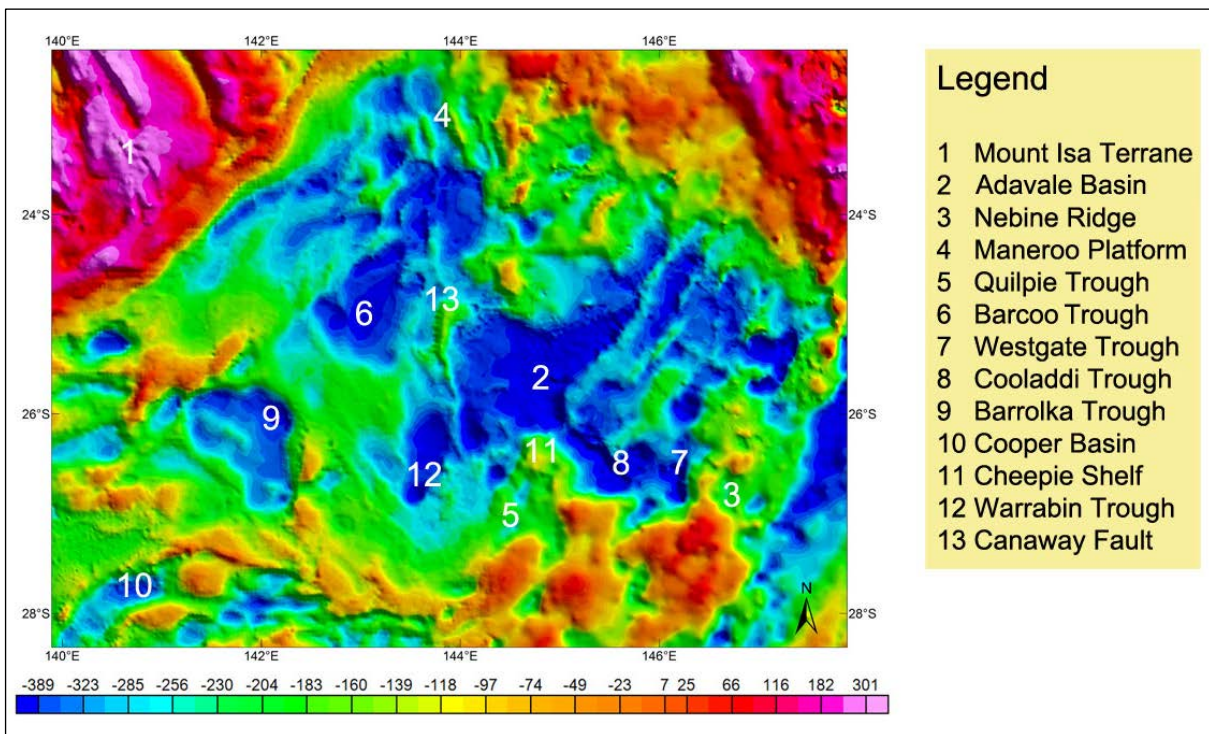


Fig. 4.10 Map of the regional Bouguer gravity anomalies in the Central Thomson Orogen. Values in the legend bar are in $\mu\text{m}^*\text{s}^{-2}$

4.5.8 Westgate Trough

The Westgate Trough (Fig. 4.10) forms a N-S-trending structure that is defined by Bouguer gravity anomalies with amplitudes below $-350 \mu\text{m}^*\text{s}^{-2}$. These anomalies are symmetric and terminate against the Pleasant Creek Arch to the northwest and the Nebine Ridge to the northeast. To the west, the Westgate Trough is separated from the Cooladdi Trough by N-S-trending relative high gravity anomalies (Fig. 4.10). The Westgate Trough is characterized by relative N-S-trending high amplitude magnetic responses of ~ 40 nT that increases to ~ 100 nT

towards its eastern boundary. The trough extends for $\sim 1,100 \text{ km}^2$, however an adjacent N-S-trending low density region extending for $\sim 1,450 \text{ km}^2$ might represent the northern continuation of the trough. The two regions are separated by E-W-trending relative high amplitude gravity anomalies of $\sim -300 \mu\text{m}^*\text{s}^{-2}$.

4.5.9 Cooladdi Trough

The NW-trending Cooladdi Trough (Fig. 4.10) shows the lowest gravity signature of the study area with amplitude values up to $\sim -540 \mu\text{m}^*\text{s}^{-2}$ in its south-eastern part. The Cooladdi Trough has no clear magnetic expression as NE-trending magnetic anomalies increase from -150 nT in the western part to 50 nT in the eastern part. The trough is separated from the Adavale Basin by NE-trending relative positive Bouguer gravity anomalies ($\sim -350 \mu\text{m}^*\text{s}^{-2}$) associated with the Grenfield Fault (Fig. 4.12). The Cooladdi Trough is delimited by the positive Bouguer gravity anomalies of the Cheepie Shelf to the west and the Pleasant Creek Arch to the east. The low gravity anomalies that define the Cooladdi Trough form an 'L' like shape that extends for $\sim 3,000 \text{ km}^2$.

4.5.10 Cheepie Shelf

The Cheepie Shelf (Fig. 4.10) is characterized by Bouguer gravity anomalies with amplitudes greater than $-250 \mu\text{m}^*\text{s}^{-2}$ that regionally trend in a northeast direction. The Cheepie Shelf separates the Cooladdi Trough from the Quilpie Trough and is overprinted by an orthogonal set of N-S- and E-W-trending structures that are defined by short wavelength positive Bouguer gravity anomalies. These structures are oblique and are superimposed to the regional northeast trend. The Cheepie Shelf has a very little magnetic expression.

4.5.11 Quilpie Trough

The N-S- to NE-trending Quilpie Trough (Fig. 4.10) is characterized by Bouguer gravity anomalies with amplitudes exceeding $-280 \mu\text{m}^*\text{s}^{-2}$. These anomalies extend for $\sim 2,200 \text{ km}^2$. The trough is bounded by the positive gravity anomalies of the Cheepie Shelf to the east and the Canaway Ridge to the west. The Quilpie Trough is characterized by asymmetric gravity anomalies with the lowest amplitude values towards the west against the Canaway Fault. The Quilpie Trough is characterized by moderate magnetic signature and contains a smooth circular positive aeromagnetic anomaly located in its northern part (Fig. 4.9).

4.5.12 Warrabin Trough

The N-S- to NNE-trending Warrabin Trough (Fig. 4.10) is characterized by regional Bouguer gravity anomalies with amplitudes up to $-430 \mu\text{m}^2\text{s}^{-2}$. The central portion of the trough is characterized by NW-trending high Bouguer gravity anomalies of up to $\sim -370 \mu\text{m}^2\text{s}^{-2}$ that divide the trough in two low density sub-domains. The Warrabin Trough is slightly asymmetric with the lowest gravity amplitudes located in its western flank. The Warrabin Trough is characterized by moderate magnetic anomalies ($\sim -40 \text{ nT}$) with smooth texture, punctuated by short wavelength circular positive magnetic anomalies with amplitudes of $\sim -10 \text{ nT}$ (Fig. 4.9). The low gravity anomalies associated with the Warrabin trough extend for $\sim 3,600 \text{ km}^2$.

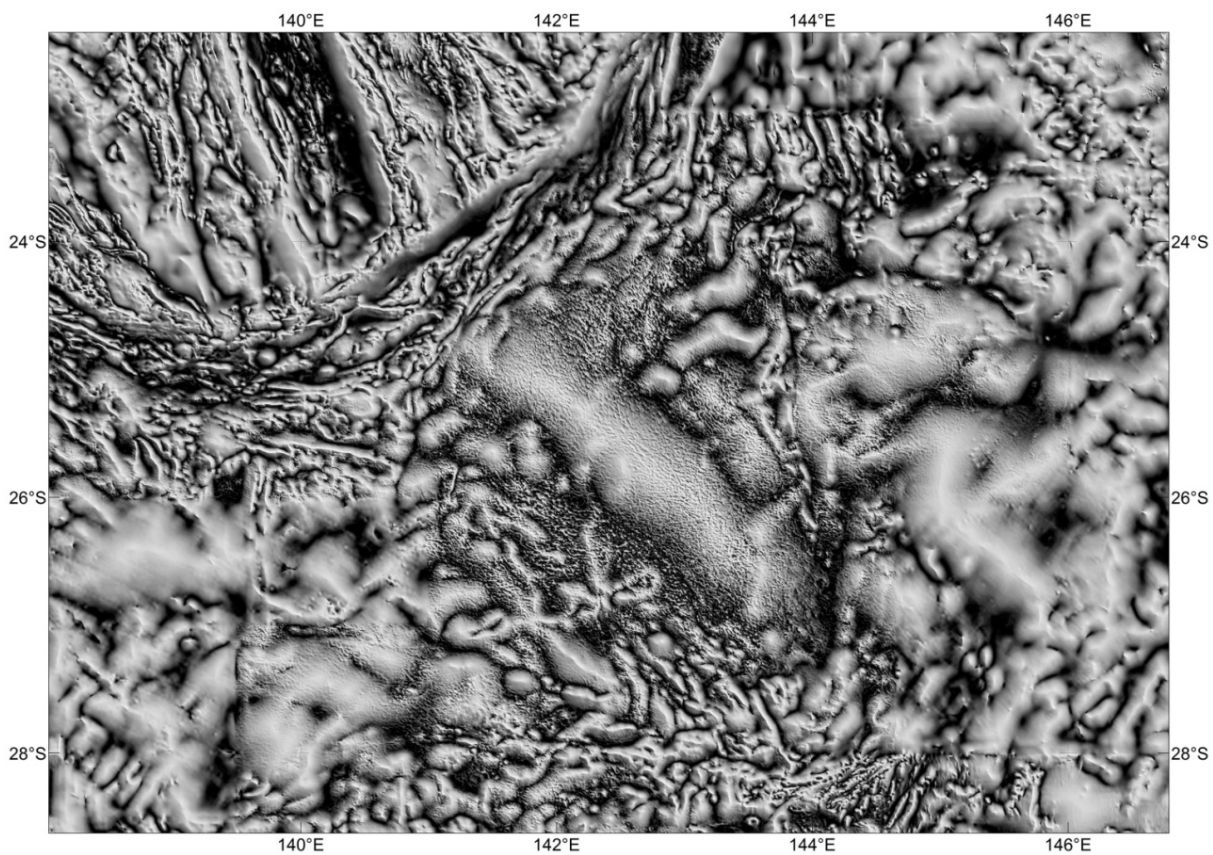


Fig. 4.11 Greyscale tilt derivative map of the Thomson Orogen and surrounding regions

4.5.13 Barcoo Trough

The Barcoo Trough (Fig. 4.10) is $\sim 5,600 \text{ km}^2$ in dimension. An extension of the Barcoo Trough may be indicated by low Bouguer gravity anomalies between the Canaway Ridge and the Maneroo Platform further northeast (Fig. 4.10), which together would increase the size of the

trough to 14,300 km². The trough is characterized by approximately NE-trending low Bouguer gravity anomalies with amplitudes between -350 and -430 $\mu\text{m}^*\text{s}^{-2}$. The regional amplitudes of the gravity anomalies appear to decrease towards the northwest, where the trough terminates against the NE-trending Warbreccan Structure. The Warbreccan Structure is defined by positive Bouguer gravity anomalies and a regional gradient of $\sim 8 \mu\text{m}^*\text{s}^{-2}/\text{km}$. To the west, the edges of the Barcoo Trough are defined by NW-oriented high gravity anomalies and, to the southeast, by the N-S-trending positive anomalies of the Canaway Ridge. The Barcoo Trough shows moderate aeromagnetic responses with amplitude values of ~ -50 nT. The trough is characterized by high wavelength circular to elongated NE- and NW-trending positive aeromagnetic anomalies.

4.5.14 Western Thomson Orogen

The geophysical signature of the western part of the Thomson Orogen corresponds to the distribution of the sediment packages of the Eromanga and the underlying Cooper and Barrolka basins (Fig. 4.10). The geophysical signature is characterized by heterogeneous geophysical trends and shows a significantly different gravity pattern if compared to the eastern part of the Thomson Orogen.

A NW-trending long wavelength positive aeromagnetic anomaly lies to the immediate west of the Canaway Ridge and has a strike length of approximately 140 km (Fig. 4.9). The aeromagnetic anomaly represents an enigmatic geophysical feature of the Central Thomson Orogen. The Bouguer gravity map shows that this zone of magnetisation is coincident with positive regional Bouguer gravity anomalies with an amplitude of $\sim -200 \mu\text{m}^*\text{s}^{-2}$. Shorter wavelength anomalies having high magnetic (between -270 and -100 nT) and low gravity (between -250 and -350 $\mu\text{m}^*\text{s}^{-2}$) signature are superimposed on the longer wavelength regional geophysical signal of the area.

4.5.15 Barrolka Trough and Cooper Basin

The Barrolka Trough is characterized by negative Bouguer gravity anomalies with amplitudes up to -400 $\mu\text{m}^*\text{s}^{-2}$, which extend over an area of $\sim 3,900$ km². The highest value amplitudes are located on the western edge of the trough and decrease towards the northeast. The Barrolka Trough terminates against NW-trending high gravity anomalies associated with the Harkaway Fault zone (Fig. 4.5). The termination is defined by a gradient of $\sim 12 \mu\text{m}^*\text{s}^{-2}/\text{km}$. In contrast, the regional Bouguer gravity anomalies associated with the overlying Cooper Basin are almost orthogonal and trend northeast (Fig. 4.10). The Cooper Basin shows Bouguer gravity amplitude

comprised between 0 and $-200 \mu\text{m}^*\text{s}^{-2}$ except in its western part where the amplitudes exceed $-350 \mu\text{m}^*\text{s}^{-2}$ and are associated with regional synclines.

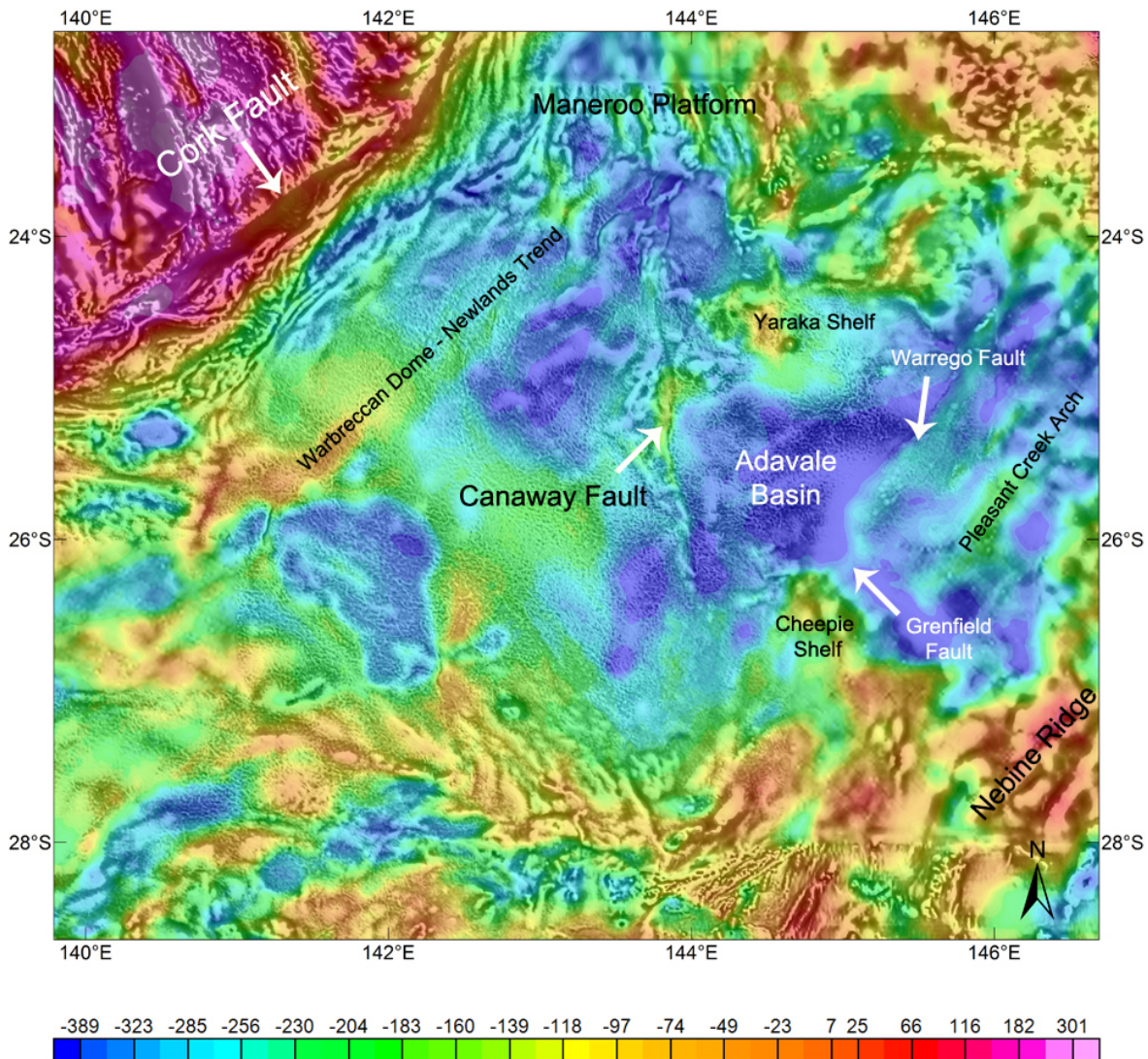


Fig. 4.12 Composite map of the regional Bouguer gravity anomalies, tilt derivative and vertical derivative magnetic anomalies of the southern Mount Isa terrane and the Thomson Orogen. Values in the legend bar are in $\mu\text{m}^*\text{s}^{-2}$

4.6 Interpretation

4.6.1 Cork Fault

The prominent NE-trending anomalies that characterize the Cork Fault define one of the major geophysical structures on the Australian continent that separates the Thomson Orogen to the south from the Mount Isa terrane (North Australian Craton) to the north. The nature of this

boundary has been subject to significant debate (Direen and Crawford, 2003) and has been interpreted as a fundamental structure associated with the break-up of the supercontinent Rodinia (Murray and Kirkegaard, 1978; Powell et al., 1994; Veevers, 2000a; Veevers and Powell, 1984; Wellman, 1990). In this context, the variation in the magnetic response, with highly magnetized basement rocks of the Mount Isa terrane to the north and considerably less magnetic crust of the Thomson Orogen to the south, could be interpreted to represent a fundamental crustal boundary in which rock packages on either side of the fault are different. In this scenario, the Cork Fault would represent a terrane boundary. Alternatively, the prominent gradient associated with the Cork Fault and decreasing towards the southeast may represent the thinning and burying at depth of a magnetic crust with Precambrian affinities which lies under the Thomson Orogen. In this model the Cork Fault would be a major SE-dipping normal fault.

4.6.2 Diamantina River Domain

To the immediate south of the N-S- to NNW-trending geophysical anomalies associated with the Mount Isa terrane, the persistent low magnetic signature and the NE-trending structural grain suggests a different crustal structure. A regional high gravity anomaly defines a discrete belt of relatively high density rocks bounding the southern termination of the Mount Isa terrane. This belt trends in an arcuate northeast direction and extends for approximately 350 km. The positive gravity signature may represent a horst of basement rocks or a package of denser rocks. The overall low magnetic signature of the belt suggests that the basement rocks have a significantly lower magnetic susceptibility than the magnetic crust of the adjacent Mount Isa terrane. The geophysical response is interpreted to represent shallow meta-sedimentary basement rocks. The interpretation is constrained by drill holes that encountered the shallow basement rocks of the Thomson Orogen across the area (e.g. AAP Fermoy 1, AAP Mayneside 1 and GSQ Maneroo 1) which are Late Neoproterozoic to Ordovician in age (Brown et al., 2014; Carr et al., 2014; Draper, 2006; Murray, 1994; Murray and Kirkegaard, 1978).

Short wavelength magnetic anomalies in the Central Diamantina River Domain are interpreted to represent magnetic horizons with meta-sedimentary packages that have been refolded about first generation folds (F1) with NE-trending axial traces and second generation folds (F2) which have NW-trending axial traces (Figs. 4.12 and 4.13, locality A). Deflections of the NNE-trending magnetic anomalies against NE-trending lineaments associated with shear bands result in large scale equivalent of drag folds and sigmoidal foliation of the supracrustal unit. The tectonic

pattern in the eastern Diamantina River Domain is inferred to represent a shear zone (Figs. 4.12 and 4.13) and might represent a large scale equivalent of S and C surface development in a dextral ductile shear zone. The fold interference pattern is consistent with a first episode of NW-directed shortening, which may also have been responsible for the development of NE-trending thrusts. Folds refolded along NW-trending axial traces and the reactivation of the existing NE-trending structures as dextral faults may reflect a subsequent NE-directed shortening episode.

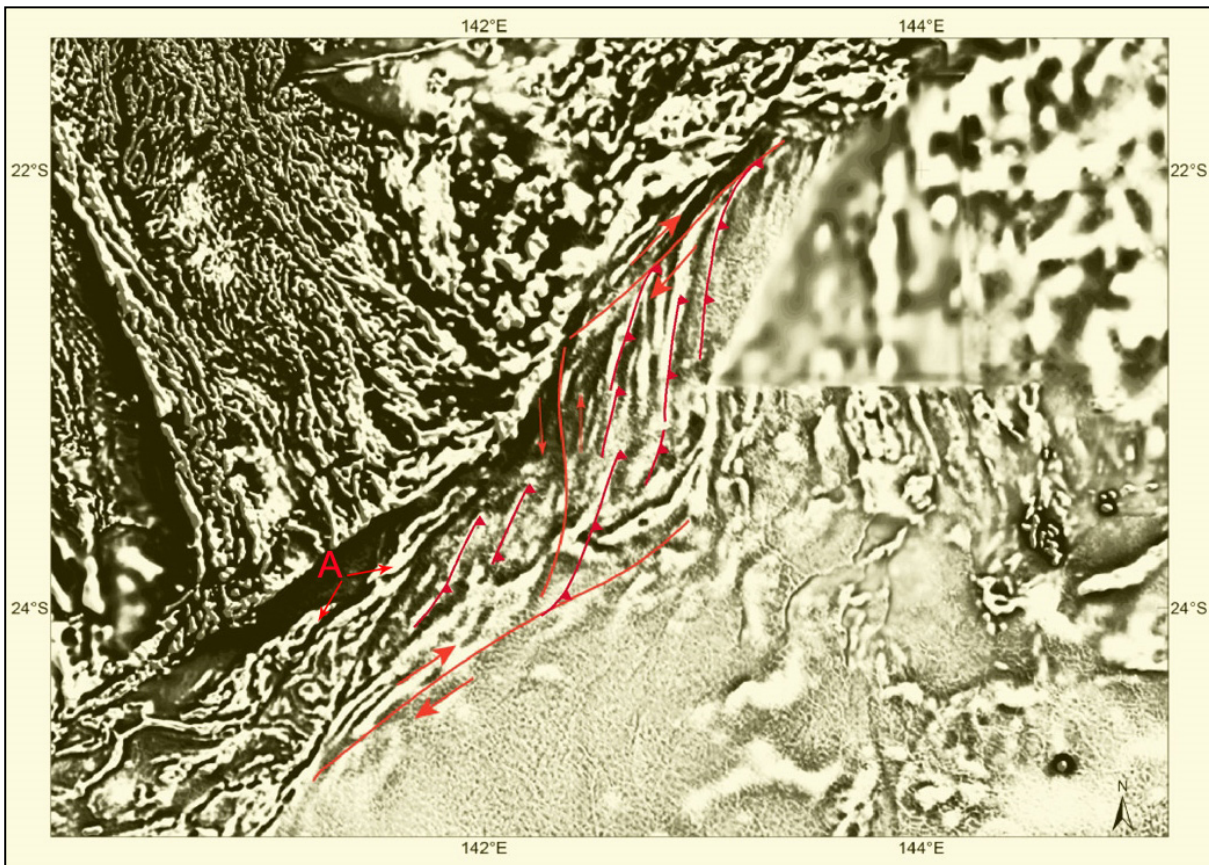


Fig. 4.13 Interpreted shear zone in the eastern part of the Diamantina River Domain on a tilt derivative and vertical derivative magnetic grid. NNE-trending thrusts terminate as large scale drag folds. Major NE-trending dextral faults accommodate the deformation.

The shear zone indicates apparent dextral kinematics and is overprinted by a late N-S-trending fault which offsets the magnetic anomalies up to 10 km with an apparent sinistral strike-slip offset (Fig. 4.13) and is therefore associated with a younger tectonic event.

NE-trending short wavelength high magnetic and low gravity anomalies are interpreted to be sourced from elongated and shallow granitic intrusions that are focused along major fault structures (Figs. 4.13 and 4.14). Linear high magnetic belts having positive gravity responses are associated with mafic bodies (Fig. 4.14). The orientation of the magmatic intrusions appears

mostly parallel to deformation structures suggesting that they might be controlled by the architecture of the area or they are sills intruded parallel to the stratigraphy.

4.6.3 Maneroo Platform

Alternating N-S-trending bands of short wavelength magnetic anomalies in the Maneroo Platform are interpreted to reflect shallow source bodies and might represent either a moderate magnetic upper basement within horst and graben structures or a series of shallow granitic intrusions. In the latter case, the preferential orientation of the geophysical anomalies suggests that the architecture of the area seems to control the distribution of the intrusions.

Drill holes AAP Fermoy 1 intersected shallow meta-sedimentary basement rocks of Cambrian age. The basement rocks in drill holes AAP Mayneside 1 and GSQ Maneroo 1 appear to correlate with the basement rocks intersected by drill hole AAP Fermoy 1 (Australian_Aquitaine_Petroleum_PTY, 1965). The drill holes are located over a high gravity belt having roughly northeast orientation associated with the Warbreccan Dome - Newlands Trend (Figs. 4.5 and 4.14). The latter, along with the relative regional positive Bouguer gravity responses that define the Maneroo Platform, has been mapped as Cambrian basement rocks (Fig.4.14).

4.6.4 Canaway Ridge

The positive Bouguer gravity responses under the Canaway Ridge might reflect shallower meta-sedimentary basement rocks of the Thomson Orogen as confirmed by seismic data and several drill holes (Figs. 4.6 and 4.7). The Canaway Fault delimits negative gravity anomalies associated with thick Devonian sedimentary rock packages. This is consistent with interpretations that suggest that the Canaway Ridge was a structural high at the time of deposition of the Devonian basinal successions (Evans et al., 1992; Murray, 1994) and continued to be a basement high during the post-Devonian depositional phases (Hoffmann, 1989). The low magnetic signature and the smooth texture of the Canaway Ridge suggest that the shallow basement rocks of the Thomson Orogen are weakly or non-magnetic. The Canaway Ridge divides the Thomson Orogen in two separate gravity domains. To the east, the region is characterized by orthogonal faults and folds that produce a series of troughs and highs. To the west is a domain characterized by NW-trending structural grain (Figs. 4.3 and 4.14). Circular and elliptical short wavelength high

magnetic anomalies that are coincident with low gravity anomalies have been mapped as granitic intrusions (Fig. 4.14).

4.6.5 Eastern Thomson Orogen

In the eastern Thomson Orogen, the shallower parts of the basement rocks are defined by positive gravity anomalies (Fig. 4.14). Sparse drill holes have intersected Late Cambrian to Silurian meta-volcanic and meta-sedimentary rocks (Brown et al., 2014; Carr et al., 2014; Draper, 2006; Murray and Kirkegaard, 1978), which are interpreted to largely represent the basement rocks of the Thomson Orogen.

Large structures such as the Gumbardo Fault and the Cothalow Arch (Fig. 4.3) are prominent in gravity data but do not show a significant magnetic expression (see also Chapter 5). Finlayson et al. (1988) and Finlayson and Leven (1987) indicated that these structures seem to affect only the upper basement crust. This might indicate that the upper basement of the eastern Thomson Orogen is weakly or non-magnetic. Instead long wavelength magnetic and gravity anomalies occur under prominent structures including the Warrego and Warbreccan faults. These structures are considered major lithospheric features and may penetrate the entire crust (Finlayson and Leven, 1987; Passmore and Sexton, 1984), possibly indicating that the regional magnetic signature of the Thomson Orogen could be sourced from the lower basement.

4.6.6 Devonian sedimentary basins

To the east of the Canaway Fault, the regional negative gravity anomalies that characterize the Thomson Orogen reflect mostly regional synclines, basinal sequences and granitic bodies (Fig. 4.14) inferred from drill holes and deep seismic surveys (Pinchin and Senior, 1982). The lowest Bouguer gravity anomalies (below $-300 \mu\text{m} \cdot \text{s}^{-2}$) correspond to the distribution of the Early Devonian sedimentary succession (Figs. 4.3 and 4.14) (Moss and Wake-Dyster, 1983; Pinchin and Senior, 1982).

The Devonian Adavale Basin and associated troughs are characterized by asymmetric gravity lows, reflecting tilted block units. Within the Adavale Basin, the gravity anomalies decrease towards the northwest and, discounting the effect of inferred low density intrusions (Fig. 4.14), this might indicate that the Devonian sedimentary succession regionally thickens towards the southeast. Major shallowing of the Devonian strata occurs along the positive gravity Cothalow Arch in the southern Adavale Basin (Fig. 4.14) (Finlayson et al., 1988). Similarly, the low

gravity anomalies that characterize the Warrabin, Barcoo, Westgate, Quilpie and Colladdi troughs (Figs. 4.10 and 4.14) correlate with the increase in thickness of Devonian sedimentary rocks inferred from drill holes and seismic data (Collins and Lock, 1983; Finlayson et al., 1988; Finlayson et al., 1990b; Pinchin and Senior, 1982). The Cooladdi Trough shows regional thickening towards the Warbreccan Fault which might indicate that the Devonian deposition was accommodated along the Warbreccan Fault within half graben. The asymmetry of the Quilpie Trough defined in gravity and seismic reflection data (Figs. 4.6 and 4.8) (Leven et al., 1990) indicate asymmetric dips of the eastern and western limbs. Leven et al. (1990) suggested that the Quilpie Trough might have formed as a ramp syncline formed above a mid-crustal detachment recognized in seismic reflection data.

4.6.7 Western Thomson Orogen

The broad NW-trending regional magnetic anomaly identified to the west of the Canaway Fault may be attributed to a source body buried at depth or alternatively a change in the basement rock types of the Central Thomson Orogen. However, there are no supporting data suggesting a major change in the crustal composition in the Central Thomson Orogen (Finlayson et al., 1989; Fishwick et al., 2008; Murray and Kirkegaard, 1978; Spence and Finlayson, 1983). Therefore, we interpret that the regional positive magnetic and gravity anomalies and the smooth texture may reflect the morphology of the lower basement or magnetized source bodies at mid- to low crustal level.

The low gravity signature under the Barrolka Trough is inferred to reflect a considerable thick sequence of Devonian (?) sediments beneath the Permian to Triassic Cooper Basin. The steep gradients in its eastern margin suggest that the trough is asymmetric and may have formed as a half graben with sediments thickening to the east.

4.6.8 Regional interpretation

Overall the positive anomalies associated with the Maneroo Platform, Warbreccan Dome - Newlands Trend Yaraka Shelf, Cheepie Shelf and Warrego - Grenfield Structure correlate with the shallower parts of the basement and delimit the regional distribution of the Devonian sedimentary rocks which regionally thickens against NE- and NW-trending structures in a half graben setting.

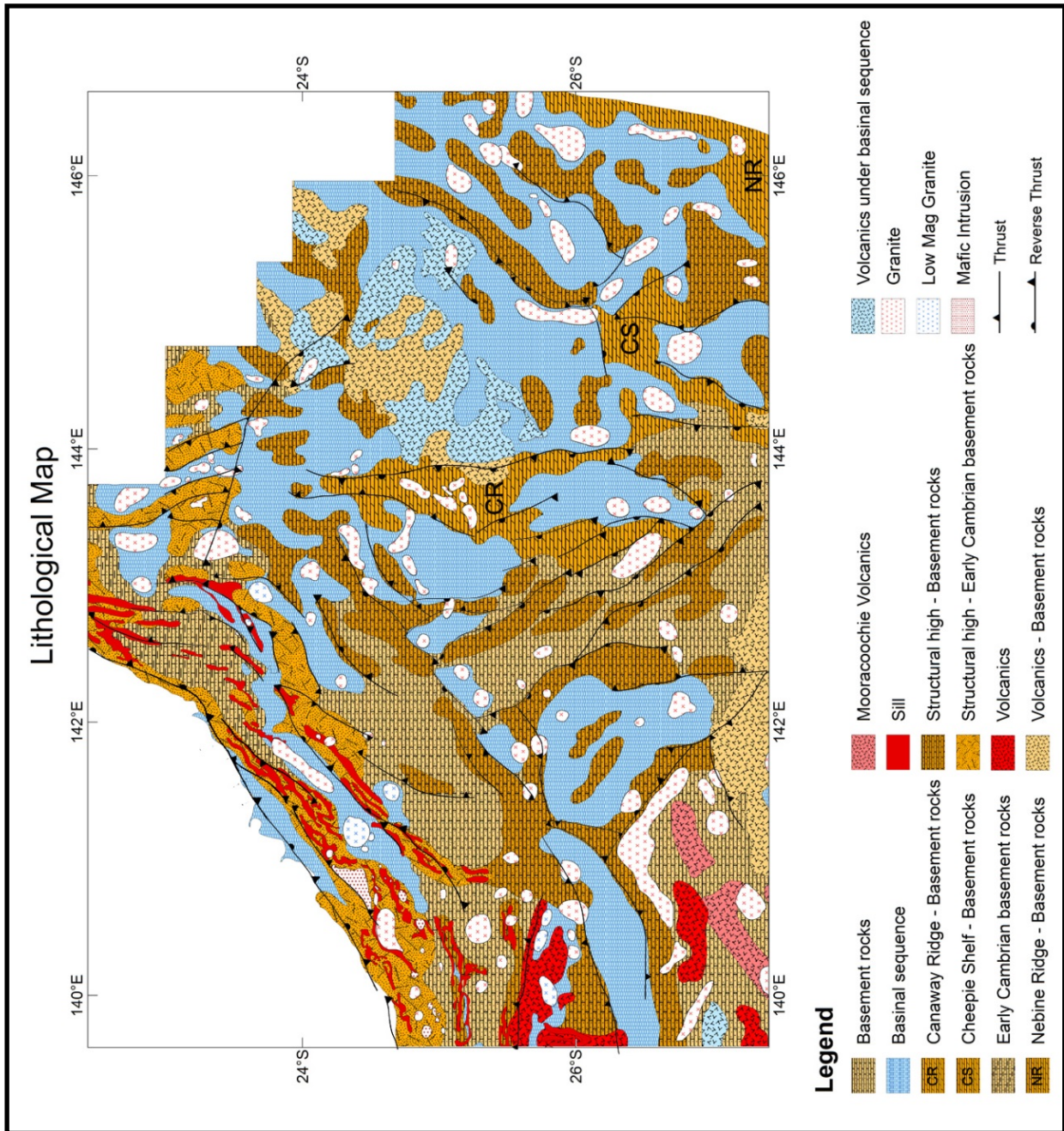


Fig. 4.14 Lithological interpretation map of the Thomson Orogen

The overall magnetic signature of the Thomson Orogen is characterized by smooth textures and anomalies amplitude between -400 and 400 nT, which is interpreted to reflect significant depths to magnetic sources beneath the non-magnetic Eromanga, Cooper, and Adavale basins. We interpret the regional magnetic low across the Diamantina River Domain to represent the burying at depth of a magnetic crust with Precambrian affinities. This is outlined in more detail in Spampinato et al. (Unpublished results-a).

4.7 Late Proterozoic to Middle Palaeozoic tectonic evolution of the Thomson Orogen

4.7.1 *The Rodinia break-up*

The timing of the break-up of the supercontinent Rodinia occurred during several episodes of crustal extension, which is now preserved along the eastern edge of the Proterozoic provinces of Australia. The initial stages of break-up are recorded by the emplacement of the NW-trending Gairdner Dykes at ca. 827 Ma (Wingate et al., 1998) followed by discrete extensional events at ca. 780 Ma (Powell et al., 1994; Preiss, 2000) and ca. 580 Ma (Crawford et al., 1997; Direen and Crawford, 2003; Glen, 2005). The geological record of this protracted period of crustal extension and supercontinent dispersal is best preserved within the Adelaide Fold Belt (Preiss, 2000; Williams et al., 2002). The rock record of this break-up extends as far north as the Anakie Inlier, along the eastern edge of the Thomson Orogen, where a ca. 600 Ma magma-poor passive margin setting has been interpreted (Fergusson et al., 2009). However, Fergusson et al. (2009) suggested that the ca. 600 Ma rifting to form the eastern margin of the Neoproterozoic Australia may have occurred after the initial break-up of Rodinia and was associated with rifting of a micro-continent.

Fergusson et al. (2001) and Fergusson et al. (2007a) suggested that the rocks of the Anakie Metamorphic Group, which reflect a magma-poor passive margin setting, correlate with volcanic passive margin successions in the Koonenberry Belt and the Adelaide Fold Belt in south Australia. If that is the case, an equivalent large scale event occurred synchronously in the eastern Australian continent, including the Thomson Orogen, which is located between the Anakie Inlier and the Koonenberry Belt (Fergusson et al., 2001; Fergusson et al., 2007a; Fergusson et al., 2009).

We observe that a number of major geophysical lineaments including the Warbreccan Dome - Newlands Trend, the Warrego-Grenfield Fault and the Nebine Ridge are parallel to the orientation of the NE-trending Cork Fault. Finlayson et al. (1988) suggested that these structures originated during a Late Neoproterozoic NW-directed rifting event. In this scenario a segment of the volcanic-poor passive margin of Fergusson et al. (2009) extended through the Central Thomson Orogen. Major NE-trending structures including the Cork, Warbreccan and Warrego faults might have controlled tilted blocks of the passive margin.

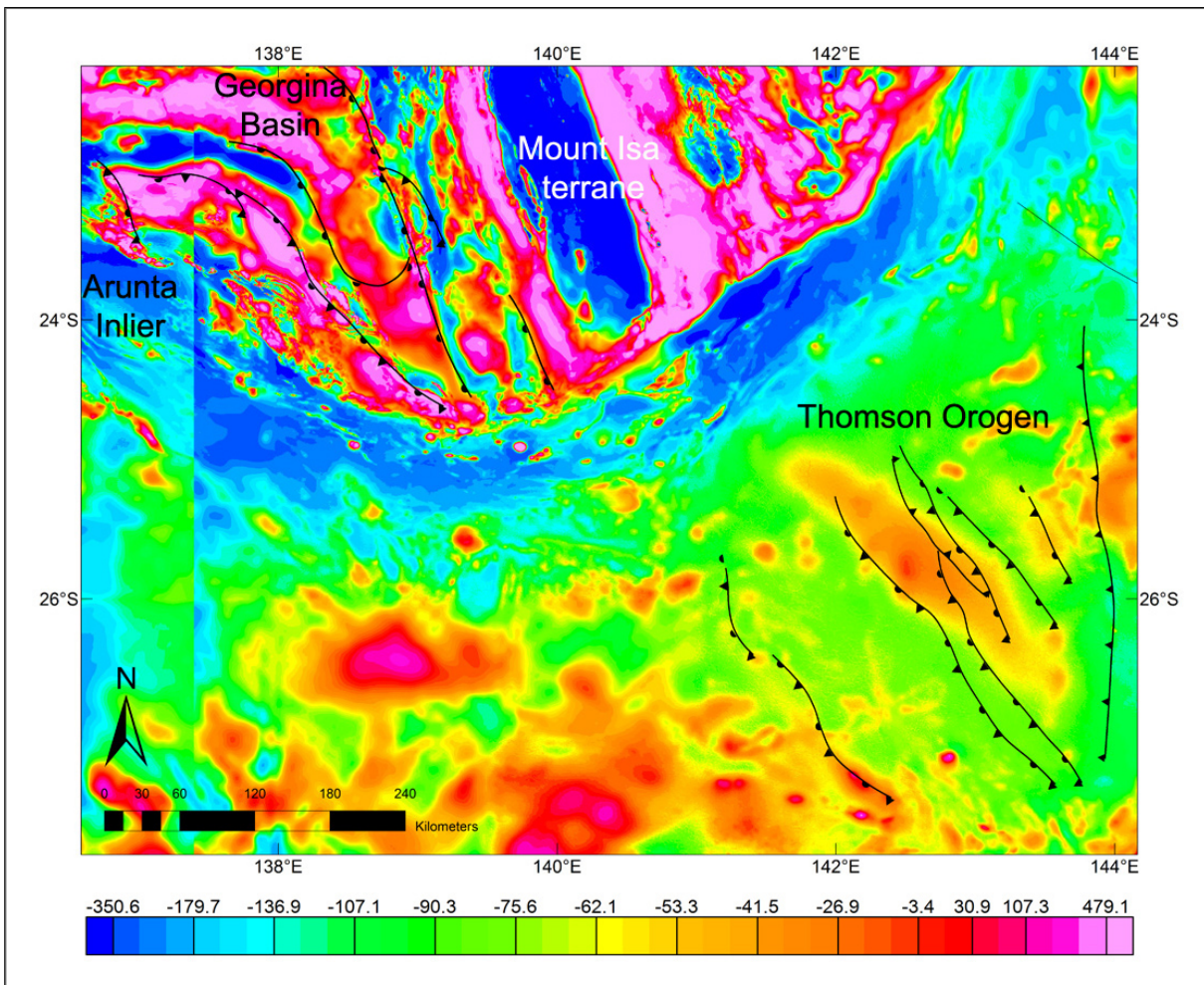


Fig. 4.15 Major structures from Greene (2010) and this study on a RTP magnetic map of the Thomson Orogen, Mount Isa terrane and eastern Arunta Province. Neoproterozoic NNW- to NW-striking high angle reverse faults detected by Greene (2010) may correlate with NW-trending major structures within the Thomson Orogen.

Geological and geophysical interpretations of major Neoproterozoic faults to the immediate north of the Cork Fault (Fig. 4.16) (Dunster et al., 2003; Greene, 2010) may provide indirect constraints for the understanding of the Neoproterozoic evolution of the adjacent Thomson Orogen. In the Georgina Basin, sedimentation associated with the break-up of Rodinia (Champion et al., 2009) occurred along a NW- to NNW-trending rift system (Dunster et al., 2003) which might have initiated during a ca. 700 Ma to 600 Ma NE-directed extension (Greene, 2010). Major NW-striking faults evident in seismic reflection (Finlayson et al., 1988) and potential field data in the western Thomson Orogen highlight similar architecture to that documented by Greene (2010) and might represent the southern continuation of his interpreted extensional fault architecture. The two fault systems trend to the northwest and dip to the west. They are both imaged in seismic data as high angle reverse faults having a listric form at depth.

Both of these faults extend to the Moho and appear to have controlled the architecture of the north-eastern Arunta Inlier and the Thomson Orogen respectively.

In this context, a Neoproterozoic rifting initiated during a NE-directed extensional event and determined major NW- to NNW-trending structures in the Thomson Orogen and southern Georgina Basin. NW- to NNW-striking segments evolved into a rift basin. NE-striking segments including the Cork Fault might have acted as lateral or sidewall faults. This model implies that the Thomson Orogen records the interior extensional architecture during the Rodinia break-up, which occurred further east, along the Anakie Inlier (Fergusson et al., 2001; Fergusson et al., 2007a; Fergusson et al., 2009). This also implies that the Cork Fault was active during the Neoproterozoic as a strike-slip fault system.

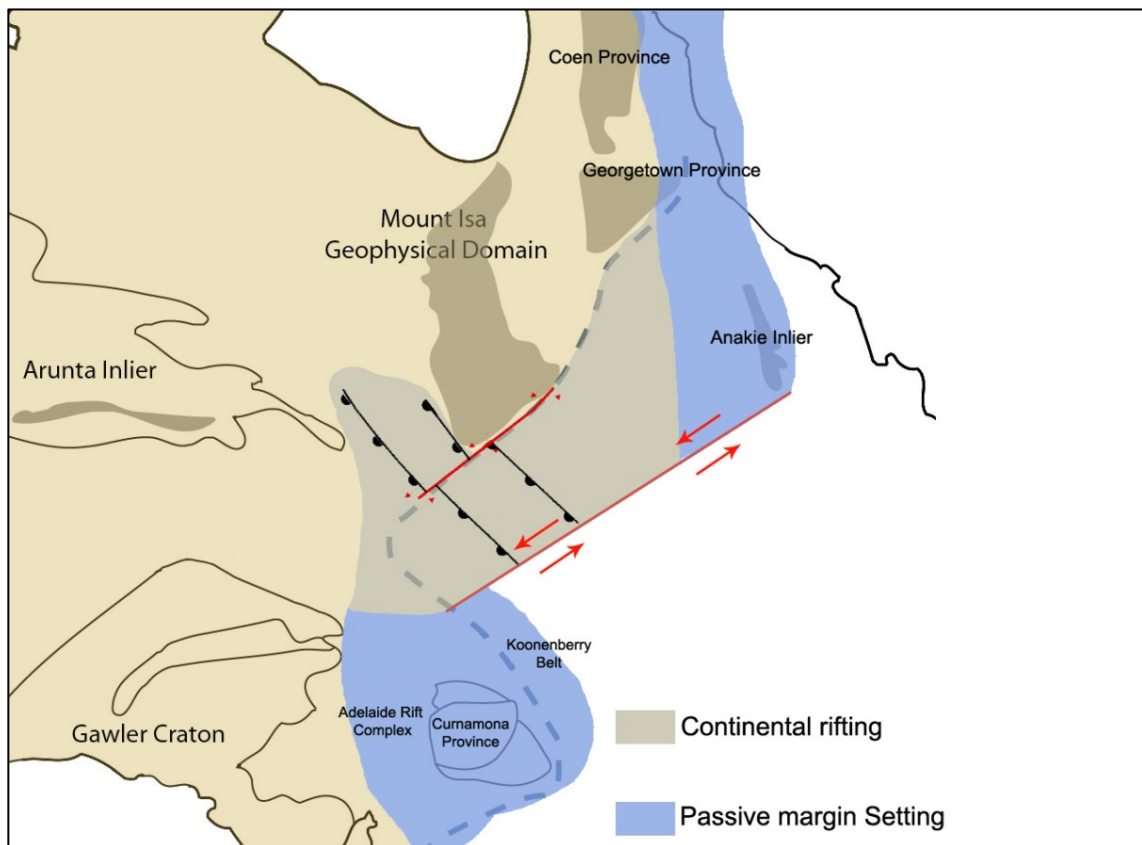


Fig. 4.16 Tectonic setting of the Thomson Orogen during the Neoproterozoic Rodinia Break-up. The coastline is for location purpose only.

Recent geological data gained from the Warraweena area to the south of the Thomson Orogen (Fig. 4.2) may provide an alternative model to the passive margin setting. A number of drill holes

have intercepted andesites and basalts about 35 km ENE of Bourke region (Fig. 4.17) (Burton et al., 2008). Drill holes ACDWE008 and ACDWE009 show that andesites display a calc-alkaline to shoshonitic affinities whereas the basalts from ACDWE010 display an intra-plate affinity (Burton et al., 2008). On the gravity and magnetic grids, these rocks correlate with NE-trending positive gravity and magnetic anomalies that can be traced for several kilometers (Fig. 4.17). They have been informally named *Warraweena Volcanics* (Burton, 2010; Glen et al., 2010). Burton et al. (2008) suggested that the andesites represent a magmatic arc that formed in the overriding plate of a northward-dipping subduction zone.

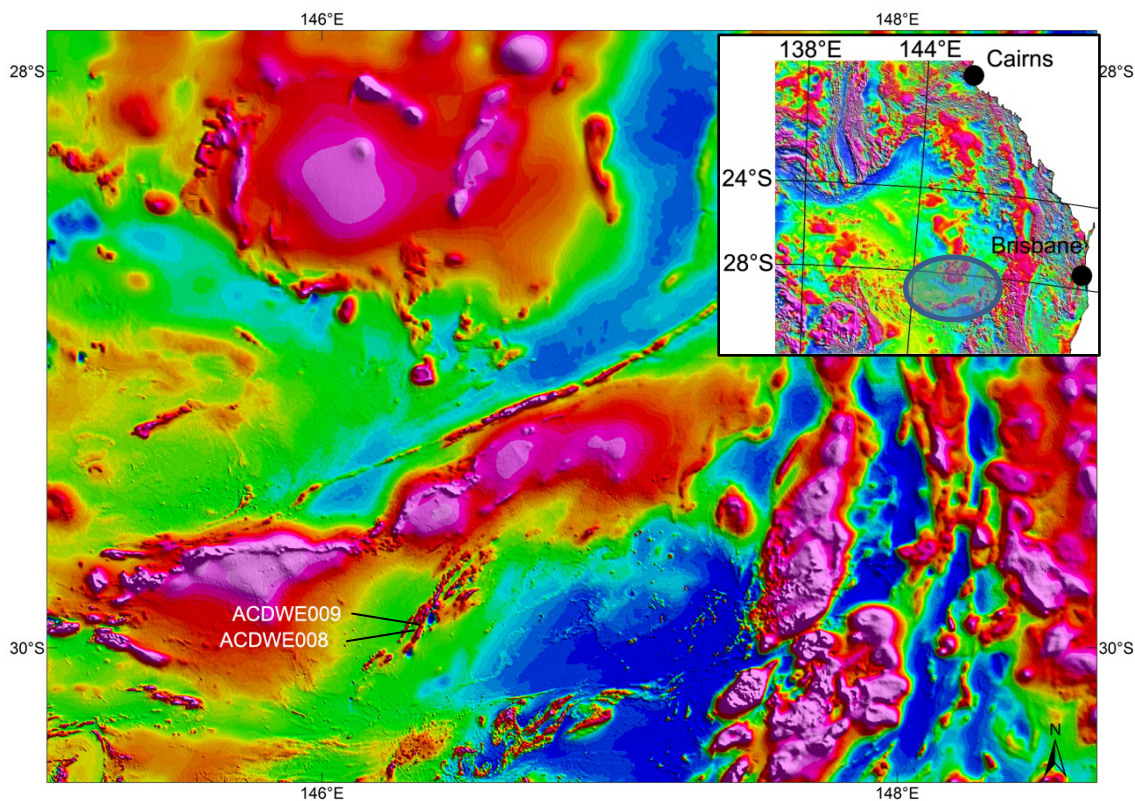


Fig. 4.17 RTP magnetic map of the Bourke – Brewarrina area with location of the drill holes ACDWE008 and ACDWE009

Zircon analyses on drill hole ACDWE009 reveal a population at ca. 630 - 550 Ma with a peak at 582 Ma and a secondary population between ca. 517 and 500 Ma with a peak at ca. 504 Ma (Glen et al., 2010). Glen et al. (2013) pointed out that negative eHf values of the ca. 577 Ma zircons in the calc-alkaline andesites might indicate that the melt was extracted from underlying older continental crust, possibly indicating that the Warraweena Volcanics represents a continental volcanic arc. If this interpretation is correct, then the Thomson Orogen may have transitioned from a passive margin setting to a continental back-arc setting at ca. 580 Ma.

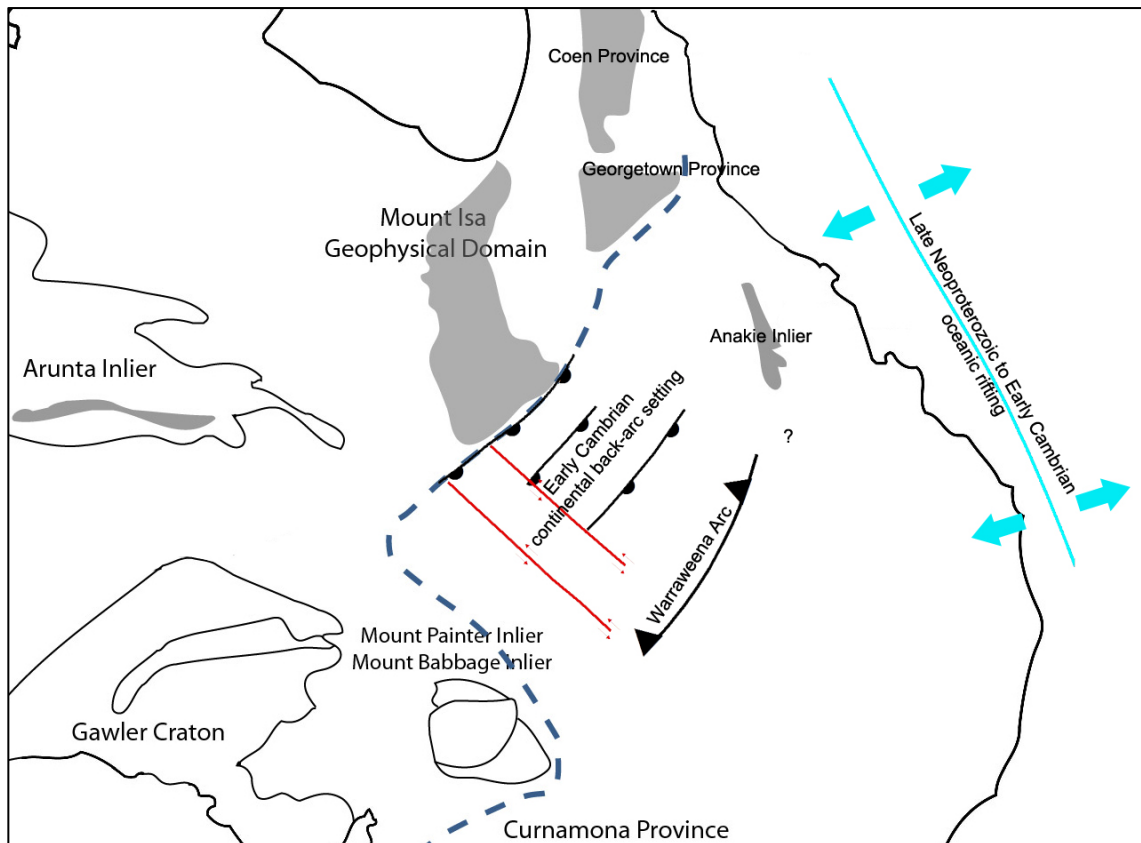


Fig. 4.18 Inferred tectonic setting of the Thomson Orogen during the Late Neoproterozoic to Early Cambrian. The coastline is for location purpose only.

4.7.2 Middle Cambrian to Late Silurian

The Delamerian Orogeny appears to have affected the interior of the Thomson Orogen at least to the Maneroo Platform and Warbreccan Dome - Newlands Trend area. The age of the imposition of the inferred shear zone in the Diamantina River Domain is poorly constrained. However Rb-Sr analyses on schistose basement rocks intersected by the Drill hole AAP Fermoy 1, located at the south-eastern edge of the shear zone, gave Late to Early Cambrian age which is coeval with the Delamerian Orogeny (Murray and Kirkegaard, 1978). The Delamerian Orogeny in northern Thomson Orogen might have resulted in development or reactivation of NE-trending structures. In the eastern Diamantina River Domain, the kinematics of the shear zone indicates an overall E-W-directed shortening and involved reactivation of NE-trending structures as strike-slip faults. The shear zone might have initiated during the Delamerian Orogeny but might have a protracted tectonic history. Final reactivation and refolding is likely to have occurred during the composite Kanimblan Orogeny (Leven and Finlayson, 1986). The sparse geological data do not allow determining the effects of the Delamerian Orogeny in the rest of the Thomson Orogen.

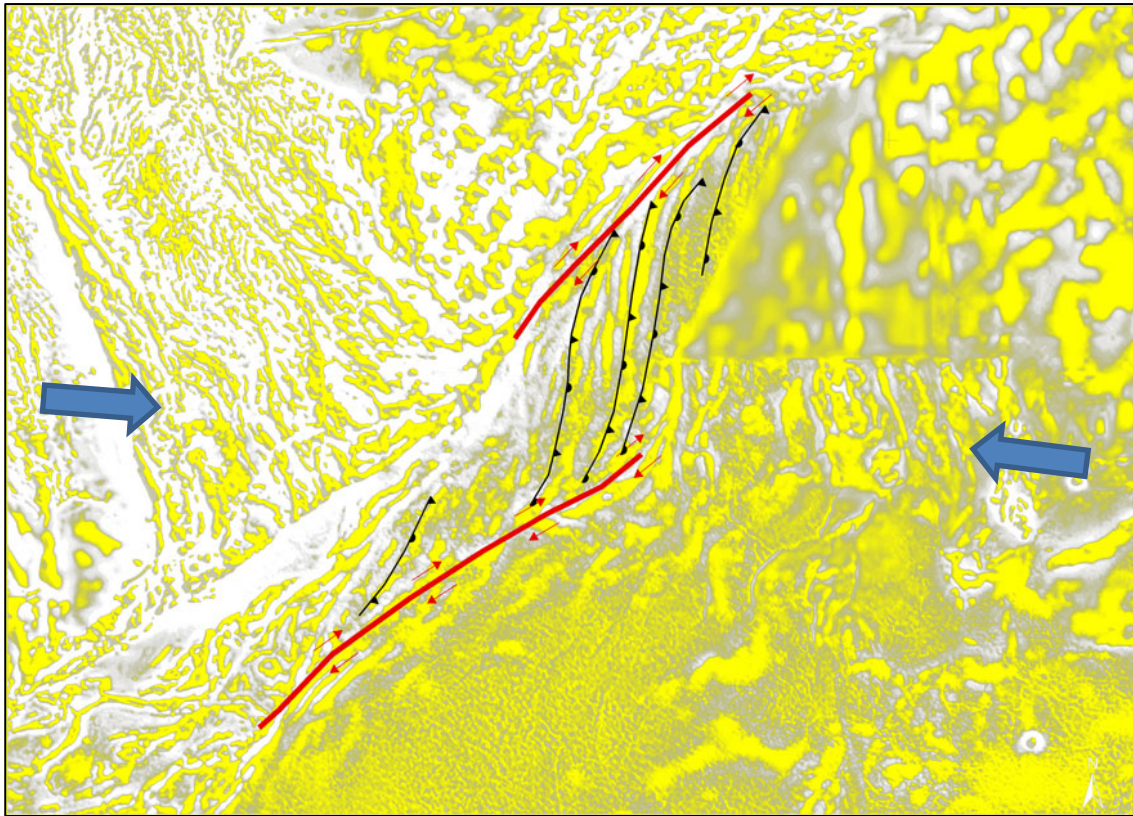


Fig. 4.19 Inferred Delamerian shortening which might have reactivated Neoproterozoic faulting zones

SHRIMP analyses from rhyolite in GSQ Maneroo 1 and BEA Coreena 1, granite in AMX Toobrac 1 and rhyolitic ignimbrite and brecciated crystal tuff in PPC Carlow 1 yielded Early to Middle Ordovician dates (Draper, 2006). They are likely to represent the post-Delamerian extensional phase along with Early Ordovician Quartzose turbiditic sequences and graptolitic shales in the Warburton area (Murray and Kirkegaard, 1978). However, the nature of the post-Delamerian extensional phase in the Thomson Orogen is mostly unresolved.

Middle Silurian felsic intrusives drilled in the Thomson Orogen may represent the contractional phase of the late Benambran Orogeny which has been documented further east in the Anakie Inlier, Charters Towers Province and Greenvale Province (Fergusson et al., 2005; Fergusson et al., 2007b; Withnall et al., 1995). However, undeformed Early Ordovician volcanics underlying the Adavale Basin (Draper, 2006) and underformed Cambrian to Ordovician sequences in the Warburton Basin (Meixner, 1999) suggest that deformation associated with the Benambran Orogeny did not importantly affect the interior of the Thomson Orogen (Fergusson and Henderson, 2013) or was inconsistent across the region. However, the eastern Thomson Orogen was importantly affected by post-Devonian tectonics (Finlayson, 1990; Finlayson and Leven,

1987; Finlayson et al., 1988; Leven and Finlayson, 1986) and deformations might simply not be apparent in the drill holes.

Clues to the Silurian evolution of the Thomson Orogen might be provided by a modern reconstruction of the Tasmanide accretionary event (Moresi et al., 2014). To the south of the Thomson Orogen, the Lachlan Orocline is defined by arcuate belts of Ordovician turbidites and Silurian volcanic rocks formed in an arc and back-arc tectonic setting (Glen, 2005; VandenBerg et al., 2000).

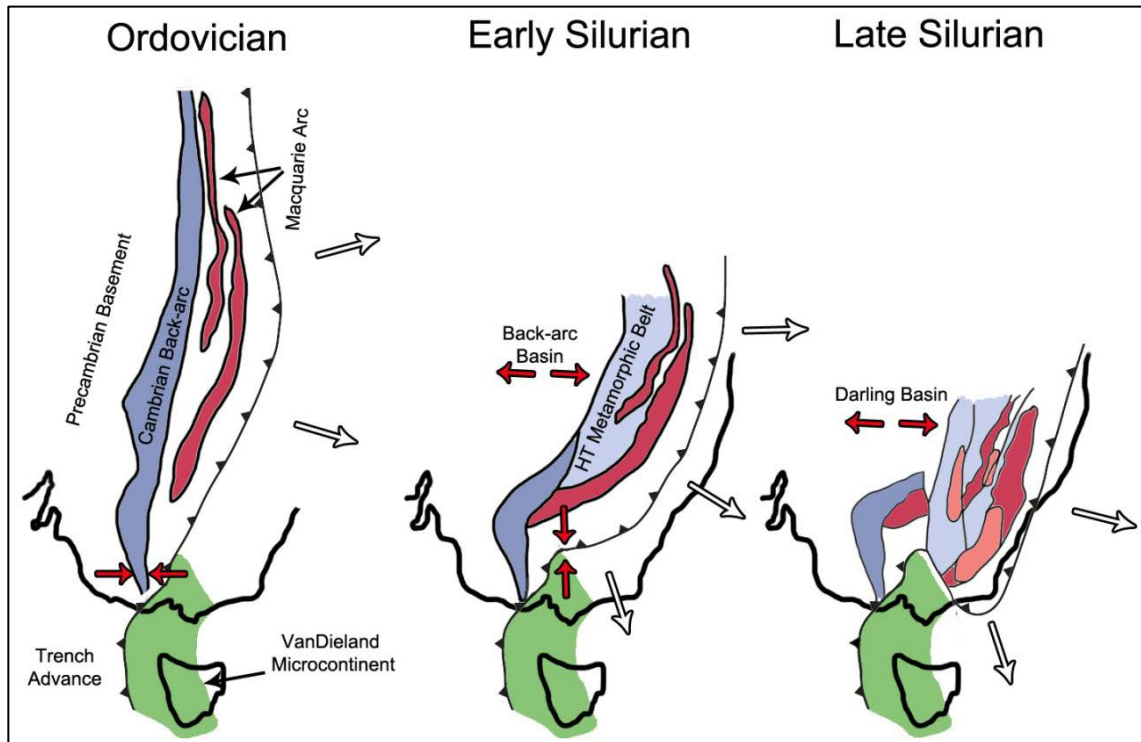


Fig. 4.20 Reconstruction of the Tasmanides accretionary event; modified from Moresi et al. (2014).

The northern Macquarie Arc and accretion of the micro-continent VanDieland to the south represented a N-S-trending Ordovician stable convergent margin (Moresi et al., 2014). Moresi et al. (2014) indicated that shortly after the accretion of VanDieland micro-continent, a Silurian transitional phase of the margin was represented by rollback of the slab to the north of the micro-continent. This resulted in shortening along the length of the trench that is anchored to the micro-continent, and extension where the subduction was retreating, forming a tightly arcuate trench (Fig. 4.20). In the northern Lachlan Orogen, the northern retreating slab resulted in the development of the Darling and Newell basins which were in a back-arc setting. In this context, the Thomson Orogen might have undergone Early to Late Silurian extension because of the

retreat of the transitional plate margin, which resulted in emplacement of granitic bodies. This occurred before the re-establishment of a linear convergent margin during the Early Devonian (Moresi et al., 2014).

4.7.3 Devonian extension

Increasing low gravity anomalies and prominent gradients against NE- and NW-trending major structures - including the Warbreccan and Warrego-Grenfield faults to the east, the Harkaway Fault (Fig. 4.3) to the west and the Maneroo Lineament to the east - indicate that these structures controlled the Devonian sedimentation during back-arc basin formation. The sedimentary sequences in the Adavale Basin onlap towards the Canaway Ridge (Murray, 1994) and the Yaraka Shelf (Finlayson et al., 1988) suggesting that they must have been structural highs at that time. The Devonian rocks also thicken towards the Warrego Fault. The increasing gravity gradients towards the south along the Canaway Fault - which represents the eastern limit of the Adavale Basin - are consistent with southeast tilting. Along the prominent Maneroo Lineament, seismic line EAL-Y81A-1006 (ESSO Australia Ltd., 1985) shows a series of Devonian half graben (Hoffmann, 1989) rotated towards the Canaway Fault. Murray (1994) suggested that the fault blocks within the Devonian Adavale Basin are rotated from east, northeast and southeast towards the Canaway Ridge in an overall westerly direction, resulting in half graben. Geophysical evidence indicate that the sedimentary successions in the Cooladdi Trough onlap towards the Canaway Ridge and thickens towards the Warbreccan Fault.

The gravity grid and supporting seismic data also indicate that the sedimentary deposition in the Warrabin Trough shows an overall thickening towards the west and the block is regionally rotated towards the Canaway Ridge, although a number of NNW-trending faults have been down-thrown to the east during the deposition of the Devonian sequence (Evans et al., 1992).

Evans et al. (1992) and Finlayson (1990) interpreted that the Adavale Basin architecture reflects NE- to SE-directed extension. Hoffmann (1989) postulated that the extensional terrane mapped in the Adavale Basin would require a detachment fault dipping to the west to accommodate the sense of movement on the extensional blocks. We adapt the models proposed by Evans et al. (1992), Finlayson (1990) and Hoffmann (1989) suggesting that an overall ENE-directed extension, possibly associated with subduction roll-back at the Gondwanan margin, reactivated existing orthogonal features. A set of NE- and NW-trending faults accommodated the Devonian depositional sequences. The change of trend in the structures controlling the Devonian deposition

reflects the reactivation of existing structures rather than indicating the stress regime that occurred at that time (Fig. 4.21).

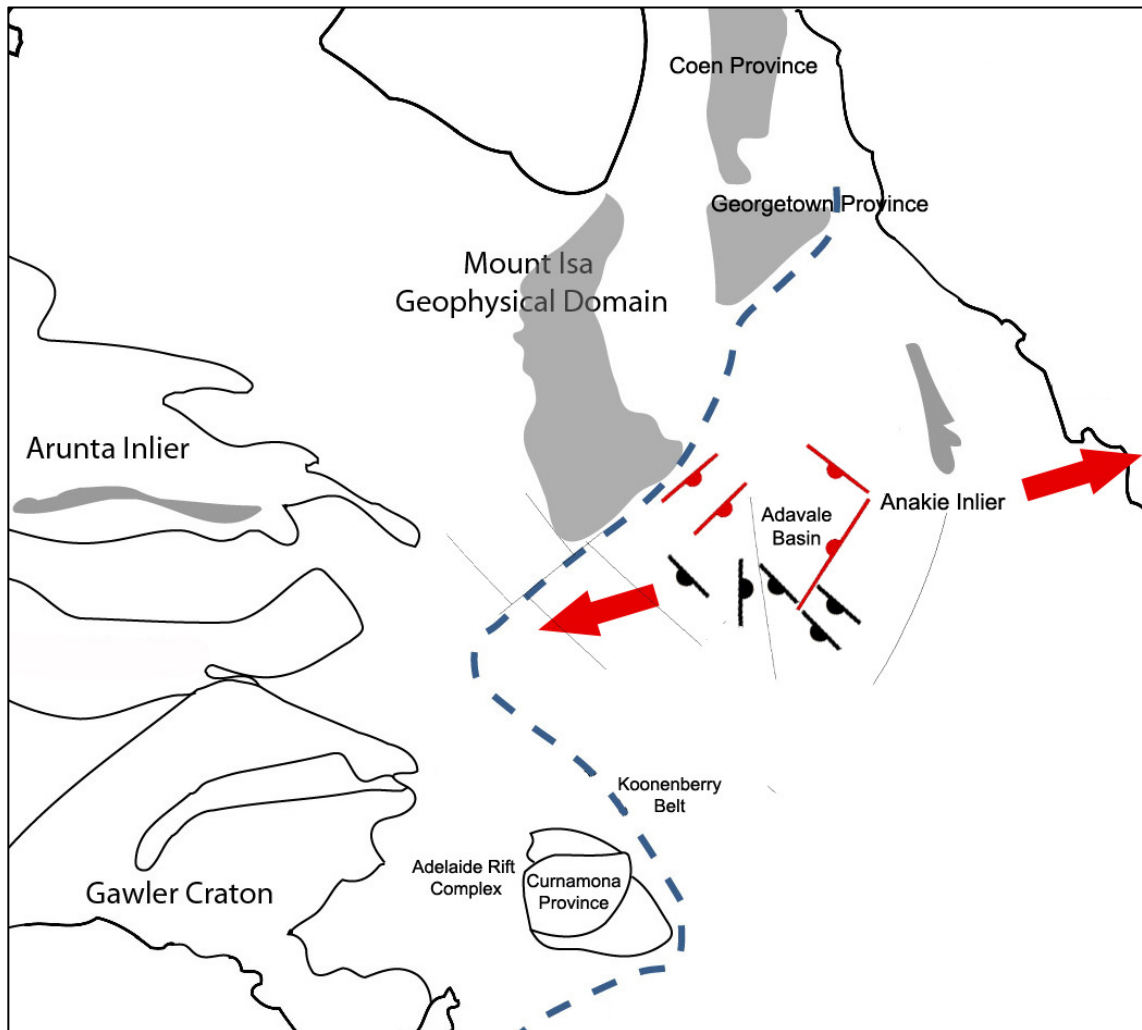


Fig. 4.21 Interpreted Devonian tectonic evolution of the Thomson Orogen. The coastline is for location purpose only.

Several elongated granitic intrusions appear to border the faults that accommodated the Devonian deposition. Volcanic rocks beneath the Galilee Basin, the Drummond Basin and the Anakie Inlier have been dated as Early Middle Devonian (Draper, 2006; McKillop et al., 2007; Withnall et al., 1995). Granitic rocks in PPC Etonvale 1 and AOP Balfour 1 drill holes indicate Late Silurian and Early Devonian intrusive activity (Murray and Kirkegaard, 1978). The mapped granitic intrusions bound major structures. It is inferred that major fault zones controlled the locus for magmatism. If this is the case, the emplacement of Silurian to Devonian granitic intrusions in the Thomson Orogen is associated with multiple reactivation episodes of major fault zone.

4.8 A global perspective

Little consensus has been reached regarding the relative positions of Rodinia's fragments (Cawood et al., 2013; Greene, 2010; Li et al., 2014; Wingate et al., 2002). Also, there has been much debate whether the Rodinia break-up in the Australian continent developed as NE-oriented rift segments offset by NW-trending transform faults or NW-oriented rift segments offset by NE-oriented transform faults (Fig. 4.22) (Greene, 2010; Shaw et al., 1991; Veevers, 2000b). Our interpreted Neoproterozoic structural architecture contributes to the debate and has implications for how Rodinia broke up along the eastern margin of Australia.

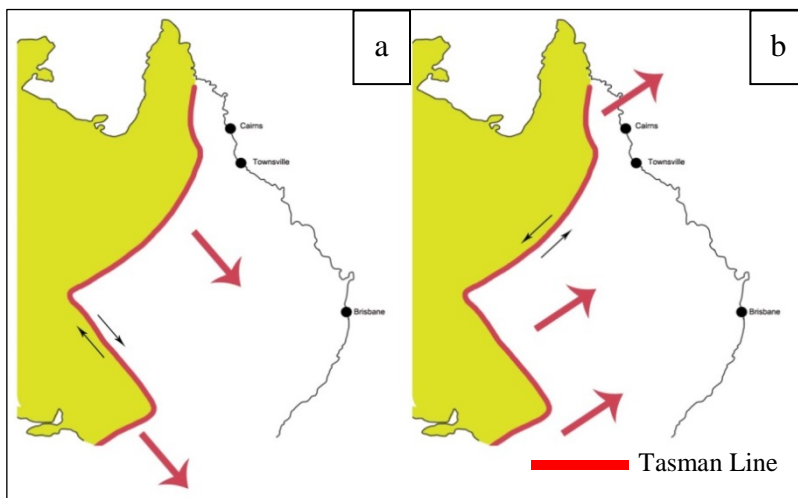


Fig. 4.22 Alternative interpretations of extension direction postulated during the Neoproterozoic Rodinia break-up.

a) SW extension during the Rodinia break-up (Shaw et al., 1991; Veevers, 2000b)

b) NE extension during the Rodinia break-up (Greene, 2010)

Geophysical (Finlayson et al., 1989) and geochemical data (Fergusson et al., 2001) are consistent with the Thomson Orogen being floored by Precambrian continental crust. Tomographic data also indicate that the continental break-up should be placed further east of any inferred Tasman Lines (Fishwick et al., 2008; Kennett et al., 2004). Our results suggest that the interpreted continental rift in the southern Georgina Basin of Greene (2010) might extend southward in the Thomson Orogen. Thus, the Thomson Orogen might record the interior extensional architecture during the Rodinia break-up that occurred further east and south to the area of study. In this scenario, the Cork Fault does not define the zone of break-up as it has been previously proposed (Fig. 4.23a), nor it is required to represent the boundary between the Proterozoic crust and the Phanerozoic crust of the Australian continent.

Rocks in the Anakie Inlier, Charters Towers and Greenvale provinces were deformed during the Delamerian Orogeny (Fergusson et al., 2001; Fergusson et al., 2007a; Fergusson et al., 2007b; Withnall et al., 1995; Withnall et al., 1996). This orogeny also appears to have affected the

northern interior of the Thomson Orogen. However, the sedimentary succession in the Warburton Basin to the west is conformable to the Early Cambrian to Middle Ordovician (Meixner, 1999) and the orogeny resulted in minor uplift and an unconformity in the Georgina Basin (Ambrose et al., 2001) suggesting that Delamerian deformations decreased towards the west and might have been negligible into the western interior of the Thomson Orogen.

Widespread magmatism between 485 - 460 Ma and Early Ordovician marine sedimentary rocks recorded back-arc sedimentation in North Queensland (Fergusson et al., 2007b; Henderson, 1986; Withnall et al., 1997). The Early to Middle Ordovician rocks of the Thomson Orogen may be correlated to the metamorphosed Cape River Metamorphics and mica schist of the Anakie Metamorphics in the Anakie Inlier (Fig. 4.2) and may suggest that an Early to Mid-Ordovician extensional tectonics affected an extensive area in the central and northern Queensland.

The following Benambran deformation event have been documented in the Lachlan Orogen (Foster and Gray, 2000; Glen et al., 2009; Glen et al., 2007b; VandenBerg et al., 2000), the Koonenberry belt (Gilmore et al., 2008), the Anakie Inlier, Greenvale Province and Charters Towers Province (Fergusson et al., 2005; Fergusson et al., 2007b). Benambran deformation in the interior of the Thomson Orogen might have been negligible. Instead the development of the Darling Basin in a back-arc setting in the northern Lachlan Orogen and intrusion of granitic bodies in the Thomson Orogen might have occurred during the retreating of an Early to Late Silurian transitional plate margin.

Early and Middle Devonian extensional basins developed throughout the Charters Towers Province (Korsch et al., 2012), the Lachlan Orogen (Fergusson, 2010; Glen et al., 2013; Gray and Gregory, 2003; Neef, 2004; VandenBerg et al., 2000), the Koonenberry Belt (Neef and Bottrill, 1991) and the Thomson Orogen (McKillop et al., 2007). Devonian sedimentary rocks might have deposited also within the Hodgkinson Province (Arnold and Fawckner, 1980) and the Drummond Basin (Olgers, 1969). They all formed in the overriding plate of a west-dipping subduction zone at the edge of Gondwana and therefore have been interpreted as continental back-arc basins (Vos et al., 2006).

4.9 Conclusions

The Thomson Orogen is characterized by a regional prominent northeast structural trend with increasing deformation grade eastward. The Canaway Ridge seems to divide the region in an eastern and western domains having different structural grain.

While the eastern part is characterized by a prominent NE structural trend and a grid of orthogonal faults and folds resulting in a series of troughs and highs, the western part of the orogen is characterized by major NW-trending structures. The regional negative gravity anomalies that characterize the Thomson Orogen mostly reflect regional synclines, and basal sequences inferred from drill holes and deep seismic surveys. The smooth magnetic signature of the Thomson Orogen is interpreted to represent features at mid- to lower crustal level. High frequency magnetic anomalies are attributed either to widely distributed intrusive bodies.

Neoproterozoic extension in the Thomson Orogen may have been controlled by NW-oriented rift segments and occurred in a continental setting as a distal response to the NE-directed Rodinia break-up, which occurred further east. By the Late Neoproterozoic to Middle Cambrian the Thomson Orogen may have switched to a continental back-arc setting driven by the roll-back of a NW-dipping subduction zone. The Delamerian Orogeny affected the Thomson Orogen to the northern interior and might have resulted in a dextral shear zone to the immediate south of the Cork Fault. Protracted post-Delamerian extension accommodated a second phase of deposition and emplacement of volcanic rocks until the Benambran Orogeny. The Benambran shortening event did not importantly affect the Thomson Orogen. By Mid-Silurian, the Thomson Orogen might have been in an extensional tectonic setting driven by the roll-back of a west-dipping to north-dipping subduction zone. The Devonian Adavale Basin initiated as an extensional basin. At this time, the existing fault architecture controlled the deposition and the depositional rate might have resulted from the interaction of major pre-existing NW- and NE-oriented structures that accommodated the sedimentary sequence. The Adavale basin is interpreted to record a distal back-arc basin in the interior of the Australian continent.

In our reconstruction, the Thomson Orogen represents the interior extensional architecture during the Rodinia break-up which occurred further east and south to the area of study and continental break-up did not occur along the Cork Fault as many interpretations of the Tasman Line have proposed.

Acknowledgement

The Central Eromanga Basin Seismic Surveys (copyright Commonwealth of Australia – Geoscience Australia) were conducted by the Bureau of Mineral Resources and are gratefully sourced from Geoscience Australia. TMI magnetic and Bouguer gravity grids (copyright Commonwealth of Australia – Geoscience Australia 2009) were obtained from Geoscience Australia. Teagan Blakie is thanked for proofreading the manuscript. Constructive comments by Robin Armit significantly improved the manuscript. Chris Fergusson is thanked for helpful discussions around this work.

Declaration for Thesis Chapter 5

Monash University

Declaration for Thesis Chapter 5

Declaration by candidate

In the case of Chapter 5, the nature and extent of my contribution to the work was the following:

Nature of contribution	Extent of contribution (%)
Interpretation of gravity and magnetic data; 2D forward modelling; manuscript preparation	90

The following co-authors contributed to the work. If co-authors are students at Monash University, the extent of their contribution in percentage terms must be stated:

Name	Nature of contribution	Extent of contribution (%) for student co-authors only
Associate Professor Peter Betts	Supervisory role; interpretation	5
Dr. Laurent Ailleres	Supervisory role; assistance with 2D forward modelling	5

The undersigned hereby certify that the above declaration correctly reflects the nature and extent of the candidate's and co-authors' contributions to this work*.

Candidate's Signature	Giovanni Pietro Tommaso Spampinato	Date
------------------------------	------------------------------------	-------------

Main Supervisor's Signature	Dr. Laurent Ailleres	Date
------------------------------------	----------------------	-------------

Chapter 5: Crustal architecture of the Thomson Orogen in Queensland inferred from forward modelling technique

Giovanni P.T. Spampinato

PhD Candidate

Monash University - School of Earth, Atmosphere and Environment

PO Box 84

Building 28, room 242

Clayton Campus, Wellington Road

Clayton, Vic 3800



Laurent Ailleres

Senior Research Fellow

Monash University - School of Earth, Atmosphere and Environment

PO Box 28E

Building 28, room 144

Clayton Campus, Wellington Road

Clayton, Vic 3800



Peter G. Betts

Associate Professor

Monash University - School of Earth, Atmosphere and Environment

PO Box 16

Building 28, room 239

Clayton Campus, Wellington Road

Clayton, Vic 3800



ABSTRACT

The basement rocks of the Thomson Orogen are concealed by mid-Palaeozoic to Triassic intra-continental basins and direct information about the orogen is gleaned from sparse geological data. As a result, the basement geology of the region is still poorly resolved. Constrained forward modelling interpretation technique has been undertaken to highlight key features and to resolve deeply sourced anomalies within the Thomson Orogen. Deep seismic reflection data indicate that the region can be distinctly divided in an upper non-reflective basement underlying the sedimentary sequences and a lower seismically reflective basement.

The Thomson Orogen is characterized by long wavelength and low amplitude geophysical anomalies if compared to the northern and eastern Precambrian terranes of the Australian continent. The magnetic grid shows smooth texture punctuated by short wavelength positive anomalies which indicate magnetic contribution at different crustal levels. It is interpreted that meta-sedimentary basement rocks of the Thomson Orogen encountered in several drill holes represent the upper non-magnetic to weakly magnetic basement. Short wavelength magnetized source bodies characterized by negative gravity signature are interpreted to represent shallow granitic intrusions. Long wavelength magnetic anomalies are inferred to reflect the topography of the magnetic lower basement.

Forward modelling indicates that the Thomson Orogen might be a single terrane. We interpret that the lower basement consists of attenuated Precambrian and mafic enriched continental crust which differs from the Lachlan Orogen further south.

Key Words: Thomson Orogen, Lachlan Orogen, Gravity, Magnetics, Crustal architecture, Phanerozoic Australia, Basement Setting, Forward modeling

5.1 Introduction

The Thomson Orogen is a key feature of the Tasmanides that record the Neoproterozoic Rodinia break-up followed by the growth of Phanerozoic orogenic belts along the eastern margin of Gondwana (Fig. 5.1) (Glen, 2005; Glen et al., 2006). Although the Thomson Orogen extends over most of central Queensland and northern New South Wales (Glen, 2005; Glen et al., 2006; Glen et al., 2013; Murray and Kirkegaard, 1978), the basement rocks are totally concealed by

thick sedimentary sequences (Finlayson, 1993; Finlayson et al., 1984; Murray and Kirkegaard, 1978). Deep seismic reflections imaged major tectonic features and provided great contribution to the understanding of the intra-basinal setting (Finlayson, 1990, 1993; Finlayson and Collins, 1987; Finlayson et al., 1988; Finlayson et al., 1989; Finlayson et al., 1990b; Finlayson et al., 1990c; Leven and Finlayson, 1987; Leven et al., 1990; Spence and Finlayson, 1983). However, the architecture of the underlying basement has not been fully clarified because of the lack of reflections. It remains unclear whether the Thomson Orogen was built either on extended continental crust or on oceanic crust (Finlayson et al., 1989; Glen, 2005; Harrington, 1974; Murray, 1990) or both (Glen et al., 2013; Musgrave, 2013). Understanding the nature of the deep crust of the Thomson Orogen has broader implications for determining the connections with the surrounding geological provinces as well as reconstructing the evolution of the Tasmanides.

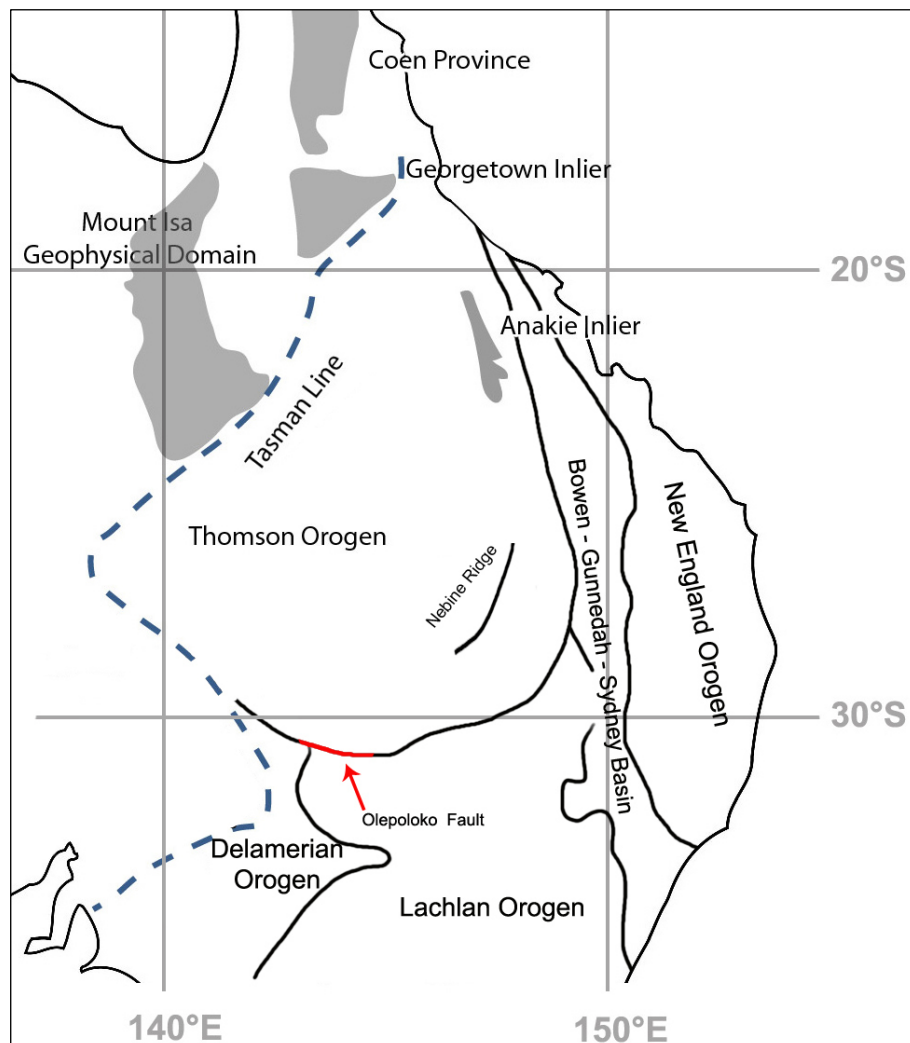


Fig. 5.1 Location map showing the distribution of some of the eastern Australian orogens; modified from Glen (2005).

In this study we use constrained magnetic and gravity data to determine the source to the regional geophysical anomalies that characterize the Thomson Orogen. Potential field method is effective at imaging magnetic basement under sedimentary basins because of their large petrophysical contrast and provides details of crustal architecture in regions where rocks are poorly exposed (Gunn et al., 1997; McLean and Betts, 2003; McLean et al., 2009). Forward modelling of magnetic and gravity data has been undertaken to investigate the nature of the basement crust of the Thomson Orogen. The outcome provides insights to better understand the geodynamic evolution of the region and the relationship and time of interaction with the Phanerozoic Lachlan Orogen.

5.2 Geological background

Neoproterozoic to Ordovician basement rocks of the Thomson Orogen (Figs. 5.1 and 5.2) (Brown et al., 2014; Carr et al., 2014; Draper, 2006; Murray, 1994; Murray and Kirkegaard, 1978; Withnall et al., 1995) form the basement of Middle Palaeozoic to Triassic basinal sequences (Apak et al., 1997; Hoffmann, 1988; McKillop et al., 2007; Murray and Kirkegaard, 1978; Pinchin and Senior, 1982; Senior, 1978). Steeply dipping slate, phyllite, schists and quartzite intersected in several wells within the area (e.g. AAP Fermoy 1, AAP Mayneside 1, AAO Beryl 1, AAO Penrith 1, FPC Galway 1, AOD Yongala 1, Fig. 5.4) are inferred to be representative of the basement rocks of the Thomson Orogen (Murray, 1994; Murray and Kirkegaard, 1978). With few exceptions, the basement rocks of the Thomson Orogen were deposited in deep water environment (Murray, 1994).

Following the Rodinia break-up, the Thomson Orogen was affected by major tectonic events until the Carboniferous (Murray and Kirkegaard, 1978). Initial deposition is likely to have occurred during the Neoproterozoic to Early Cambrian (Draper, 2006; Murray, 1994; Murray and Kirkegaard, 1978) and might correlate to the break-up of Rodinia which is recorded in the adjacent Anakie Inlier, Charters Towers and Greenvale provinces and in North Queensland (Direen and Crawford, 2003; Fergusson et al., 2001; Fergusson et al., 2007a; Fergusson et al., 2009). Middle to Late Cambrian deformation event coeval with the Delamerian Orogeny deformed the rocks of the Thomson Orogen (Harding, 1969; Murray and Kirkegaard, 1978). This event is recorded in Early to Late Cambrian schistose and phyllitic basement rocks that have been drilled by drill holes AAP Fermoy 1, AAP Mayneside 1, AAO Penrith 1 and AAO Beryl 1 in the Maneroo Platform and eastern Diamantina River Domain of the Thomson Orogen (Fig.

5.4) (Draper, 2006; Murray, 1994; Murray and Kirkegaard, 1978). However, because of the sparse geological data the nature of the Delamerian shortening event in the Thomson Orogen is still poorly resolved.

Renewed Ordovician extension was widespread across the Tasmanides (Fergusson et al., 2007b; Glen, 2005; Henderson, 1986) and central Australia (Li and Powell, 2001). Volcanism and deposition are inferred from several drill holes (i.e. PPC Gumbardo 1, AMX Toobrac 1, GSQ Maneroo 1, BEA Coreena 1 and PPC Carlow 1, Fig. 5.4) which encountered Early to Middle Ordovician meta-sedimentary and meta-volcanic rocks (Draper, 2006; Murray, 1994; Murray and Kirkegaard, 1978). Fergusson et al. (2007b) indicated that during the Early to Middle Ordovician, the volcanic and sedimentary successions of north-eastern Australia occurred in a back-arc setting associated with a convergent margin further east.

Late Ordovician to Early Silurian Benambran Orogeny has been recorded in the surrounding Greenvale Province, Anakie Inlier and Charters Towers Province further east (Fergusson et al., 2005; Fergusson et al., 2007b) and the Koonenberry Belt (Greenfield et al., 2010) and the Lachlan Orogen (Burton, 2010; Cayley, 2011; Cayley et al., 2011; Foster and Gray, 2000) to the south of the Thomson Orogen. Middle Silurian (ca. 428 Ma) felsic magmatism occurred in the Maneroo Platform (BMR Longreach 1), in south-western Thomson Orogen (PPC Etonvale 1, AOP Balfour 1), and eastern Thomson Orogen (DIO Ella 1, TEA Roseneath 1) (Draper, 2006). The pervasive granitic intrusions have been interpreted to reflect Late Benambran contractional deformation (Draper, 2006) although the areal extent of the deformation is not resolved (Champion et al., 2009). However, it appears that deformation associated with the Benambran Orogeny were mild or not apparent towards the interior of the Central Thomson Orogen (Fergusson and Henderson, 2013; Meixner, 1999). Middle Silurian felsic magmatism in the Central Thomson Orogen may also reflect extensional tectonics driven by the roll-back of a west-dipping to north-dipping subduction zone to the southeast (Moresi et al., 2014; Spampinato et al., Unpublished results-b).

Early Devonian intra-continental transtension resulted in the formation of the Adavale Basin (Fig. 5.3) (Evans et al., 1992; McKillop et al., 2007). The ca. 410 Ma Gumbardo Formation (Draper, 2006) forms the basal package of the basin (McKillop et al., 2007), constraining the time of initiation of the Adavale Basin. The Adavale Basin is interpreted to have been triggered by a subduction to the east in the New England Orogen (Fig. 4.1) (McKillop et al., 2007;

Murray, 1990) and was part of a larger continental back-arc system that formed in the overriding plate of a west-dipping subduction zone at the edge of Gondwana (Vos et al., 2006). The Adavale Basin correlates with Early to Middle Devonian extensional basins that developed throughout the Charters Towers Province (Korsch et al., 2012) and the Lachlan Orogen (Fergusson, 2010; Glen et al., 2013; Gray and Gregory, 2003; Neef, 2004; VandenBerg et al., 2000).

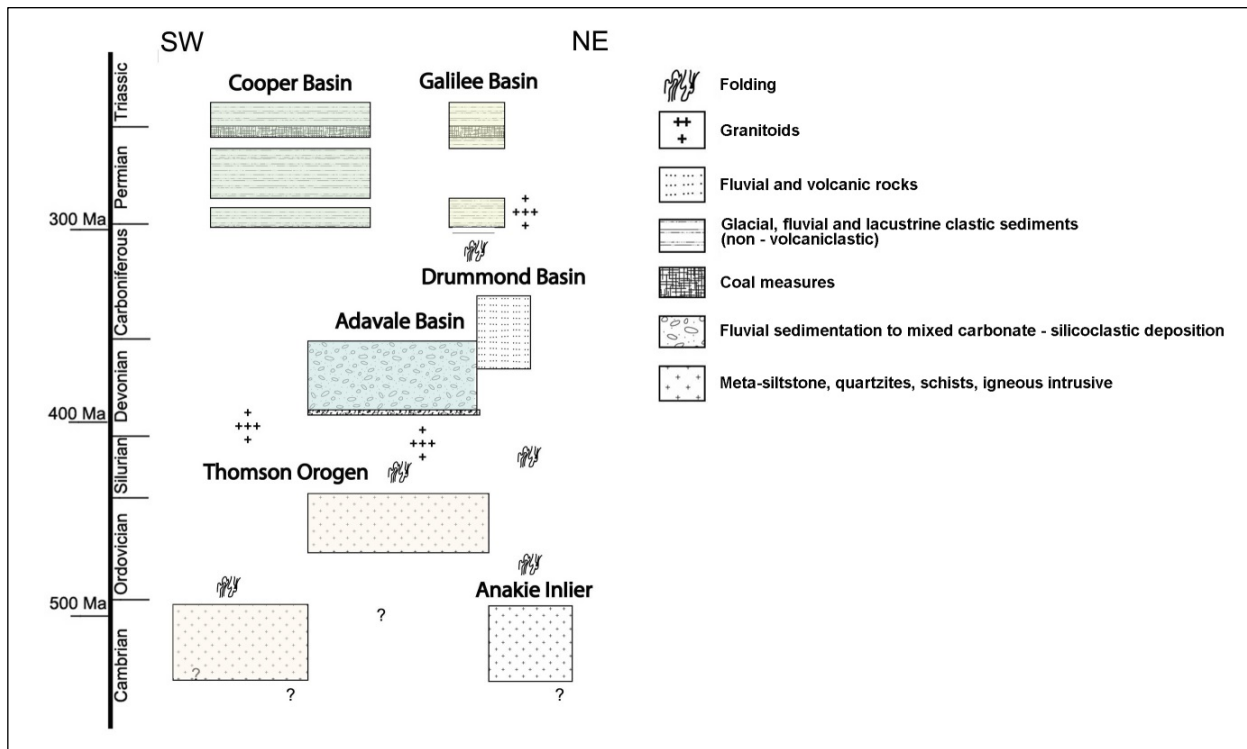


Fig. 5.2 Time - space diagram illustrating the major depositional sequences along the Thomson Orogen and the Anakie Inlier during the Palaeozoic; modified from Murray (1990).

A subsequent Carboniferous deformation event deformed the Adavale Basin and exhumation took place (Finlayson et al., 1990c). Leven and Finlayson (1986) indicated that the deformation event occurred in two distinct phases: an Early Carboniferous N-S shortening episode activated E-W-striking thrusts and associated N-S tear faults. A later E-W shortening is reflected by N-S-striking thrust faults. Early Carboniferous thrusts were reactivated as tear faults (Leven and Finlayson, 1987). This composite tectonic event resulted in regional-scale folds and widespread erosion (McKillop et al., 2007). The remnant synclinal structures reflecting the deeper portions of the Adavale Basin and recorded in deep seismic surveys are termed - from west to east - the Warrabin, Quilpie, Cooladdi and Westgate troughs (Figs. 5.8 and 5.9) (Mathur, 1983; Pinchin and Senior, 1982).

Although the Thomson Orogen has been repeatedly affected by post-Carboniferous tectonics that resulted in the development of the Permian – Triassic sequences of the Cooper and Galilee basins (Fig. 4.3) and the Early Jurassic to Late Cretaceous Eromanga Basin (Finlayson et al., 1988; Mathur, 1983; Spence and Finlayson, 1983), the basement architecture has not changed and the area might be considered cratonised after the Carboniferous (Murray and Kirkegaard, 1978).

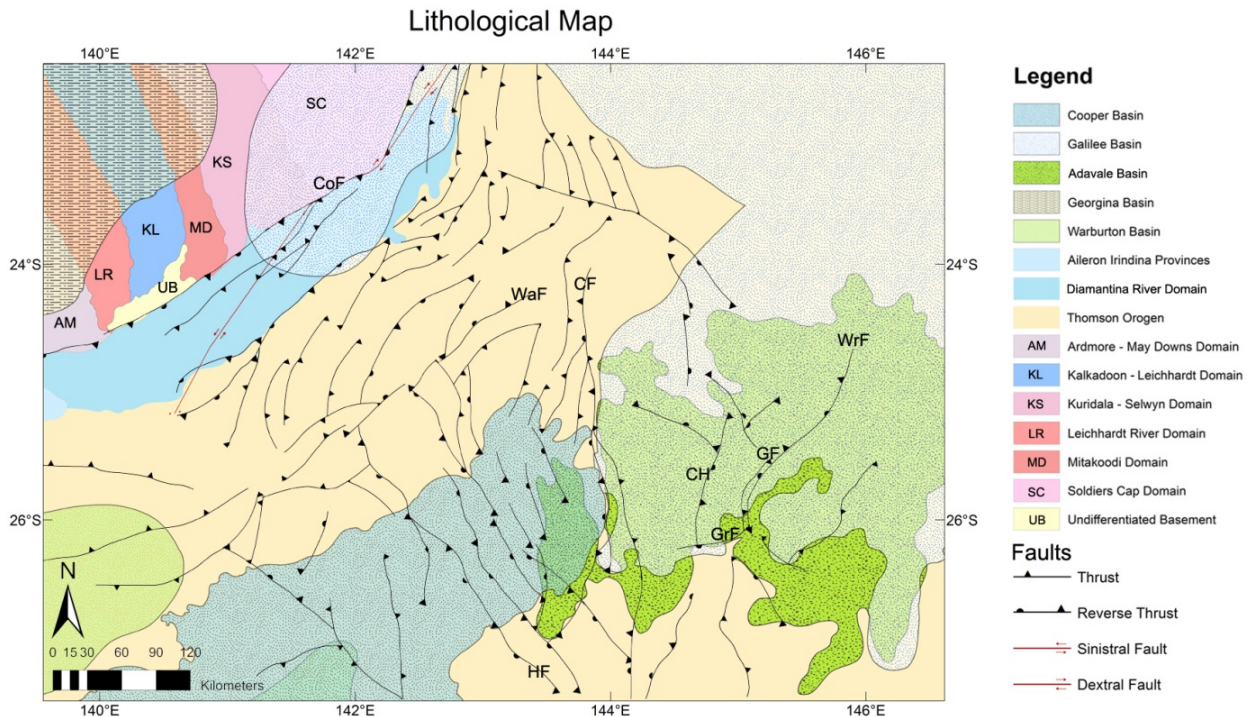


Fig. 5.3 Map of the geological domains and major structural features of the Central Thomson Orogen; CoF= Cork Fault; CF= Canaway Fault; WaF= Warbreccan Fault; HF= Harkaway Fault; CH= Cothalow Arch; GrF= Grenfield Fault; GF=Gumbardo Fault; WrF= Warrego Fault.

5.3 Previous geophysical surveys

From 1980 the Australian Bureau of Mineral Resources (BMR) undertook extensive deep seismic surveys that provided insights into the crustal architecture and the distribution of the sedimentary sequences in the Central Eromanga Basin (Moss and Wake-Dyster, 1983; Wake-Dyster et al., 1983). Regional seismic traverses cover a total linear distance of 1,400 km (Fig. 5.4) that join 5,000 km of older data, 2,300 km of which was reprocessed and digitalized (Moss and Wake-Dyster, 1983; Wake-Dyster et al., 1983).

Seismic data indicate that high angle thrust faults form the dominant deformation style (Finlayson et al., 1988). However, the upper basement is not clearly defined either because of the similar acoustic impedance between the basement rocks and the overlying sediments (Wake-

Dyster et al., 1983) or the effect of severe deformations which do not provide continuous sub-horizontal reflectors (Finlayson et al., 1984; Lock et al., 1986; Mathur, 1983; Spence and Finlayson, 1983).

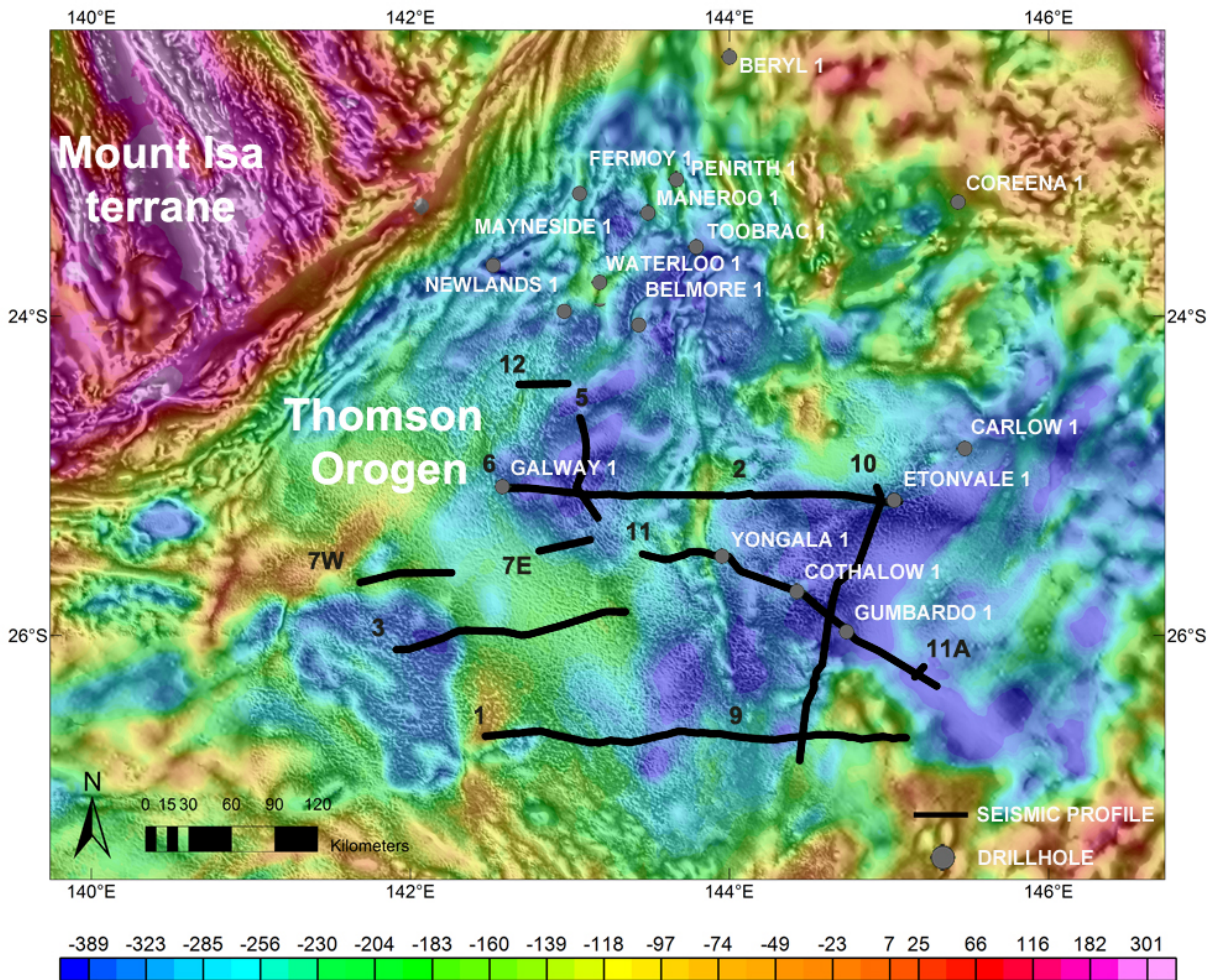


Fig. 5.4 Location of the BMR Central Eromanga Deep Seismic Transects and drill holes intersecting the basement in the Central Eromanga Basin over a composite Bouguer and tilt derivative magnetic map. Values in the legend bar are in $\mu\text{m}^*\text{s}^{-2}$

The top reflective zone is inferred to correlate with the sedimentary successions of the Eromanga, Cooper - Galilee and Adavale basins (Figs. 5.3, 5.5, and 5.6) (Pinchin and Senior, 1982).

A zone of no reflection between 2.5 and 8 seconds having a velocity range between 5.6 and 6.3 km/s suggests a seismically homogeneous upper basement (Figs. 5.5 and 5.6) (Finlayson et al., 1990a; Finlayson et al., 1988; Mathur, 1983, 1987). Mathur (1983), Lock et al. (1986) and

Spence and Finlayson (1983) indicated that this zone could represent the meta-sedimentary and meta-volcanic basement rocks of the Thomson Orogen.

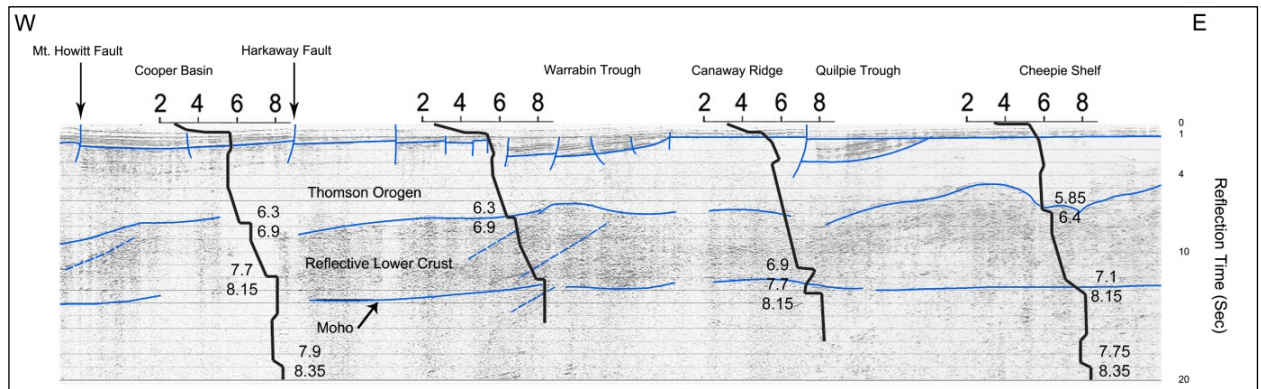


Fig. 5.5 Traverses 1 and 9 of the BMR seismic sections along with the main structures; modified from Finlayson et al. (1990b). Velocities are in km/s.

The zone between 8 and 12.5 seconds shows a prominent velocity increase to 6.6 – 7.5 km/s and sub-horizontal short reflection segments (Figs. 5.5 and 5.6) (Finlayson et al., 1990a; Mathur, 1983, 1987). The boundary between the non-reflective and the reflective zones shows undulating profile (Figs. 5.5 and 5.6). Mathur (1983) suggested that the long reflection features (~3 km) in the lower crust may represent sills of basaltic melt intruded from the asthenosphere during crustal extension in the early tectonic evolution of the area. Finlayson et al. (1989) and Finlayson et al. (1990b) suggested that the stretched Precambrian crust is now represented by the layered lower crust. The lower crustal reflections might be a product of poly-phase layering from the extensional events (Finlayson et al., 1990b) and might be due either to intrusion of sill-like mafic bodies or horizontal shearing of contrasting lithologies (Finlayson et al., 1989; Finlayson et al., 1990b; Finlayson et al., 1990c). The bottom of the seismically reflective crust at ~38 - 42 km depth displays a regional flat geometry and is interpreted to represent the Moho (Finlayson et al., 1990b; Leven and Finlayson, 1987; Mathur, 1983, 1987). Regional shallowing of the Moho occurs under the Canaway Ridge (~35 km depth, Fig 5.5 and 5.6) (Finlayson and Collins, 1987; Finlayson et al., 1990b). The underlying zone with no reflection and refraction velocities of 8.2 km/s represents the seismically homogeneous upper mantle (Leven and Finlayson, 1987; Mathur, 1983, 1987).

In the Thomson Orogen, the seismic data consistently indicate that the P-Wave velocities show a prominent increase at mid-crustal level (20 - 24 km depth) and the step in velocity increase corresponds to the top of the reflecting lower crust (Finlayson et al., 1984). However, below the

Canaway Ridge there is no evidence of the outstanding mid-crustal P-wave velocity increase (Finlayson and Collins, 1987; Finlayson et al., 1984).

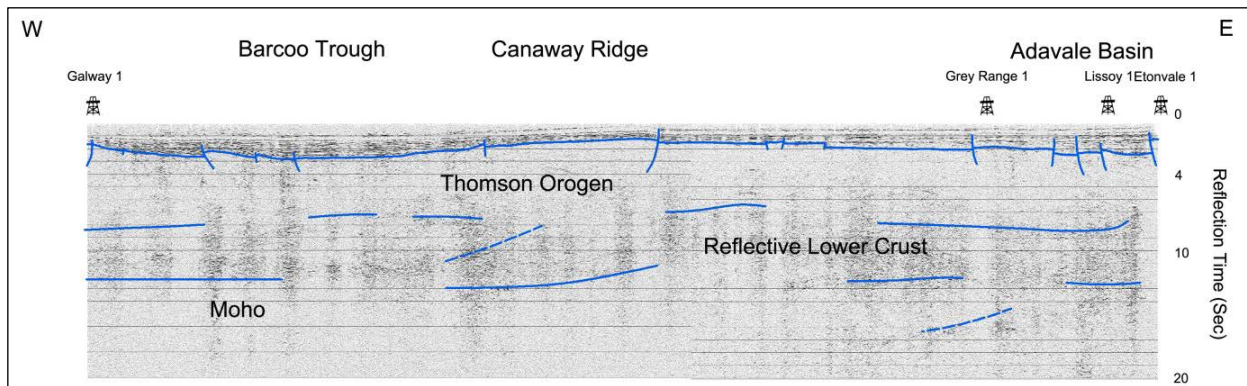


Fig. 5.6 Traverses 6 and 2 of the BMR seismic sections along with the main structures; modified from Finlayson et al. (1990b)

5.3.1 Nebine Ridge

The Nebine Ridge (Fig. 5.8) is interpreted to represent the southern termination of the Thomson Orogen (Murray and Kirkegaard, 1978) and shows a different seismic fabric when compared to the Central Thomson Orogen (Finlayson and Collins, 1987; Finlayson et al., 1990b). The minimum thickness of the non-reflective upper crust is about 6 km, whereas it is much thicker (minimum of about 15 km) in the Central Thomson Orogen (Finlayson et al., 1990b). Such as in the Canaway Ridge, in the Nebine Ridge there is no clearly subdivision of the velocity structure and the mid-crustal velocity pattern is not detectable (Finlayson and Collins, 1987). The basement topography shows remarkable gaps and the average velocities of the upper crust are lower than those interpreted under the rest of the central Eromanga region (Finlayson and Collins, 1987).

5.3.2 Magnetotelluric survey

In 1980, BMR employed magnetotelluric survey in the Thomson Orogen. The aim was to determine the basin geometries and the structures of the underlying basement crust and upper mantle. The survey covered 12 sites along the Seismic Traverse n.1 (Fig. 5.4). The MT data indicate a very resistive layer exceeding 500 ohm x m, with values comprised predominantly between 900 and 2000 ohm x m, underlying the relative low resistive basin sedimentary successions (Spence and Finlayson, 1983). The resistive layer is inferred to represent the basement rocks of the Thomson Orogen (Spence and Finlayson, 1983). The magnetotelluric

studies indicate that the basement of the Thomson Orogen is generally isotropic and one dimensional resistivity models are appropriate for the region (Spence and Finlayson, 1983).

5.3.3 Tomographic data

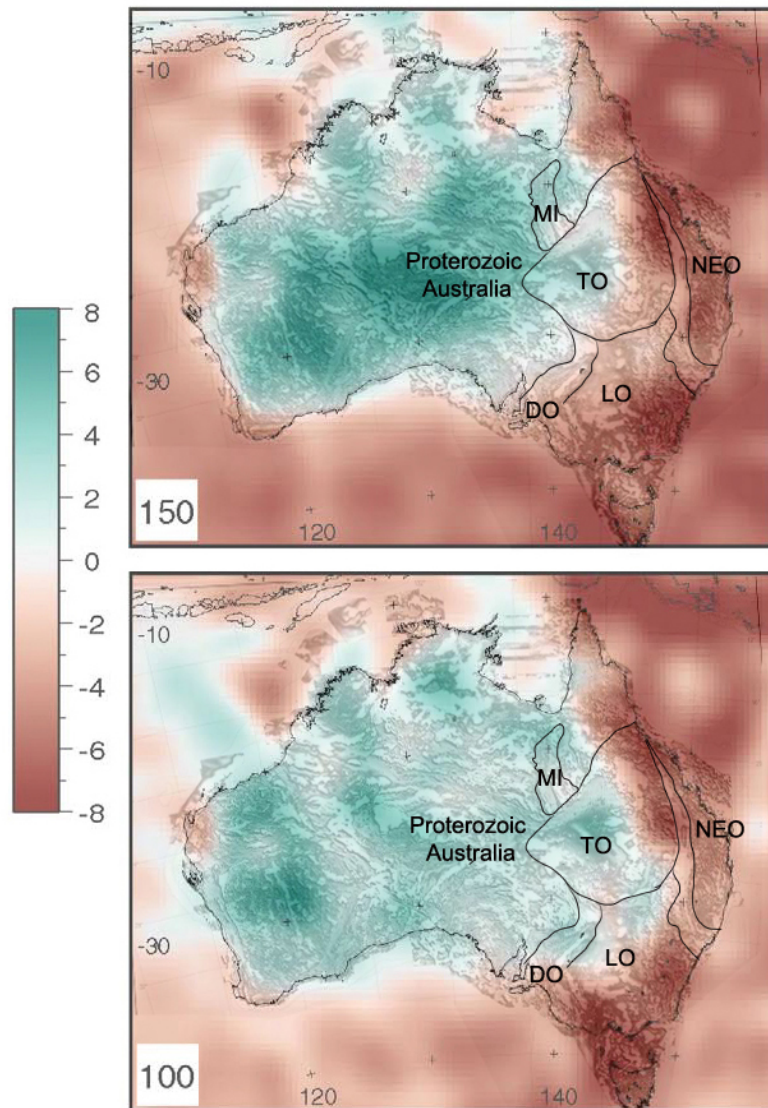


Fig. 5.7 Images of the tomographic S-wave velocity models at 100 and 150 km depth over a map of the geological provinces of the Australian continent. MI= Mount Isa terrane; TO= Thomson Orogen; DO= Delamerian Orogen; LO= Lachlan Orogen; NEO= New England Orogen; modified from Fishwick et al., (2005).

Modern surface wave tomography imaging (Fichtner et al., 2009; Fishwick et al., 2008; Kennett et al., 2004; Simons et al., 1999) indicates that within 250 km depth, wave propagation appears to be slow in the Phanerozoic eastern Australia while the central Proterozoic and the western Archean domains show high wave speeds. The Thomson Orogen is characterized by relative high wave speed lithosphere that differs to the low wave speed lithosphere under the eastern Australian continent including the Lachlan Orogen (Fig. 5.7) (Fishwick et al., 2008; Kennett et al., 2004).

5.4 Evolutionary models

The geodynamic evolution of the Thomson Orogen remains a matter of debate. Several authors tentatively proposed different tectonic models for the region. Harrington (1974) suggested rifting of the Nebine Volcanic Arc represented by the NE-trending Nebine Ridge (Fig. 5.1) from the Proterozoic Craton. In his view, the Nebine Volcanic Arc

bounded an epi-continental shallow sea in a back-arc setting lying to the northwest termed the Barcoo Marginal Sea (Fig. 5.14). The Barcoo Marginal Sea was subsequently inverted during the Delamerian Orogeny (Harrington, 1974). Finlayson et al. (1984) indicated that the seismic fabric beneath the Eromanga Basin is consistent with higher mafic content and metamorphic grade if compared to the shallower basement crust. They suggested that the crustal structure is consistent with a peri-cratonic or back-arc basin that was subsequently cratonised after a convergent tectonic episode in the Early Palaeozoic. Kirkegaard (1974) suggested that the Thomson Orogen was in a Precambrian passive margin setting which transitioned to an oceanic crust at its eastern limit. The Precambrian passive margin model was also favoured by Fergusson et al. (2009) and Fergusson et al. (2007a), for which the easternmost part of the Thomson Orogen was interpreted as a ca. 600 Ma magma poor rifted margin setting. Henderson (1980) envisaged that a Precambrian basement floors the Thomson Orogen and suggested that the Precambrian North Australian Craton represents, at least in part, the basement of the Thomson Orogen. Mathur (1983) pointed out that the reflection characteristics of the deep crust beneath the Drummond Basin and the Nebine Ridge are similar to those beneath the Georgina Basin and differ from the rest of the Central Eromanga Basin. He suggested that the crust under the Thomson Orogen formed by extensional attenuation of continental crust which has been intruded by sills of basaltic melt. In this interpretation, the Nebine Arc represented an isolated Precambrian micro-continental terrane that had drifted from the Australian continent. The model favoured by Murray (1990) implies that the Thomson Orogen is mostly floored by stretched Precambrian crust represented by the layered lower basement evident in the deep seismic profiles. In his view, the layering may be due to mafic intrusion or horizontal shearing of contrasting lithologies.

5.5 Method

Gravity and magnetic data are successfully used in order to understand the geometries of concealed crystalline basements (Aitken and Betts, 2009; Stewart and Betts, 2010a; Williams et al., 2009). In this study, we constrain the architecture of the Thomson Orogen by 2D forward modelling gravity and magnetic data using seismic data. The forward modelling technique provides a quantitative interpretation of magnetic and gravity datasets (Gunn et al., 1997) and allows geologic cross-sections to be constructed based on geophysical response (McLean and Betts, 2003). Each geological unit is assigned petrophysical properties which are assumed to be homogeneous across the layer (McLean et al., 2008). The calculated geophysical response

associated with the initial model is compared to the observed data. The parameters are adjusted iteratively until the calculated and observed geophysical profiles correlate satisfactorily (Blakely, 1995). Potential field method has non-unique solutions (Betts et al., 2003b; Stewart and Betts, 2010b). However, the rock properties and the geometries of source bodies can be constrained by surface observations, well data and other integrating geophysical data (Jessell, 2001; McLean and Betts, 2003). There is currently no constraining rock property data in the Thomson Orogen, however the structuring of the basement is defined by the drill holes and seismic data and these constraints are used to determine a-priori structuring of the region.

Total magnetic and Bouguer gravity data have been extracted along the Central Eromanga Deep Seismic Transects n. 1-9, n. 3, n. 6-2 and n. 11. The forward models cover a total line distance of ~815 km and have been modelled to 50 km depth using GM-SYS[®] Profile Modelling. The software provides integration of topographic, geologic, seismic, and well-log data. Forward models provided insights into the geometries and physical properties of major structures and source bodies at different crustal levels.

5.6 Observation and results

5.6.1 Regional geophysical signature of the Thomson Orogen

Regions east of the positive gravity Canaway Ridge (Fig. 5.8) display low gravity signature with amplitude values comprised between $-250 \mu\text{m}^*\text{s}^{-2}$ and $-550 \mu\text{m}^*\text{s}^{-2}$ and a prominent northeast regional trend. Negative gravity amplitudes below $-300 \mu\text{m}^*\text{s}^{-2}$ define the distribution of the Devonian sedimentary rocks of the Adavale Basin and the Colladi, Quilpie, Warrabin and Barcoo troughs. The Devonian sequences are bounded by positive gravity anomalies that define NE-trending structures associated with the Maneroo Platform, Warbreccan Dome - Newlands Trend, the Yaraka Shelf, the Warrego Fault and the Nebine Ridge (Fig. 5.8).

Regions to the west of the Canaway Ridge are characterized by NW-trending positive regional Bouguer gravity anomalies with amplitudes exceeding $-240 \mu\text{m}^*\text{s}^{-2}$ (Fig. 5.8). The Canaway Ridge shows positive N-S-trending gravity anomalies above $-250 \mu\text{m}^*\text{s}^{-2}$ that extend for ~300 km from the southern termination of the Maneroo Platform to the northern limit of the Cheepie Shelf. The positive gravity anomalies associated with the Canaway Ridge separates the low density Adavale Basin, the Quilpie Trough and the Colladi Trough to the east from the low density Warrabin Trough and Barcoo Trough to the west (Fig. 5.8). A detailed description of the

geophysical anomalies of the Thomson Orogen is contained in Spampinato et al. (Unpublished results-b) which indicated that the regional gravity signature well represent the topography of the shallow Late Neoproterozoic to Ordovician basement rocks. In their view, the prominent northeast and northwest trends represent major reverse thrusts originated in the Late Proterozoic to Early Palaeozoic that controlled the architecture of the region during the Phanerozoic.

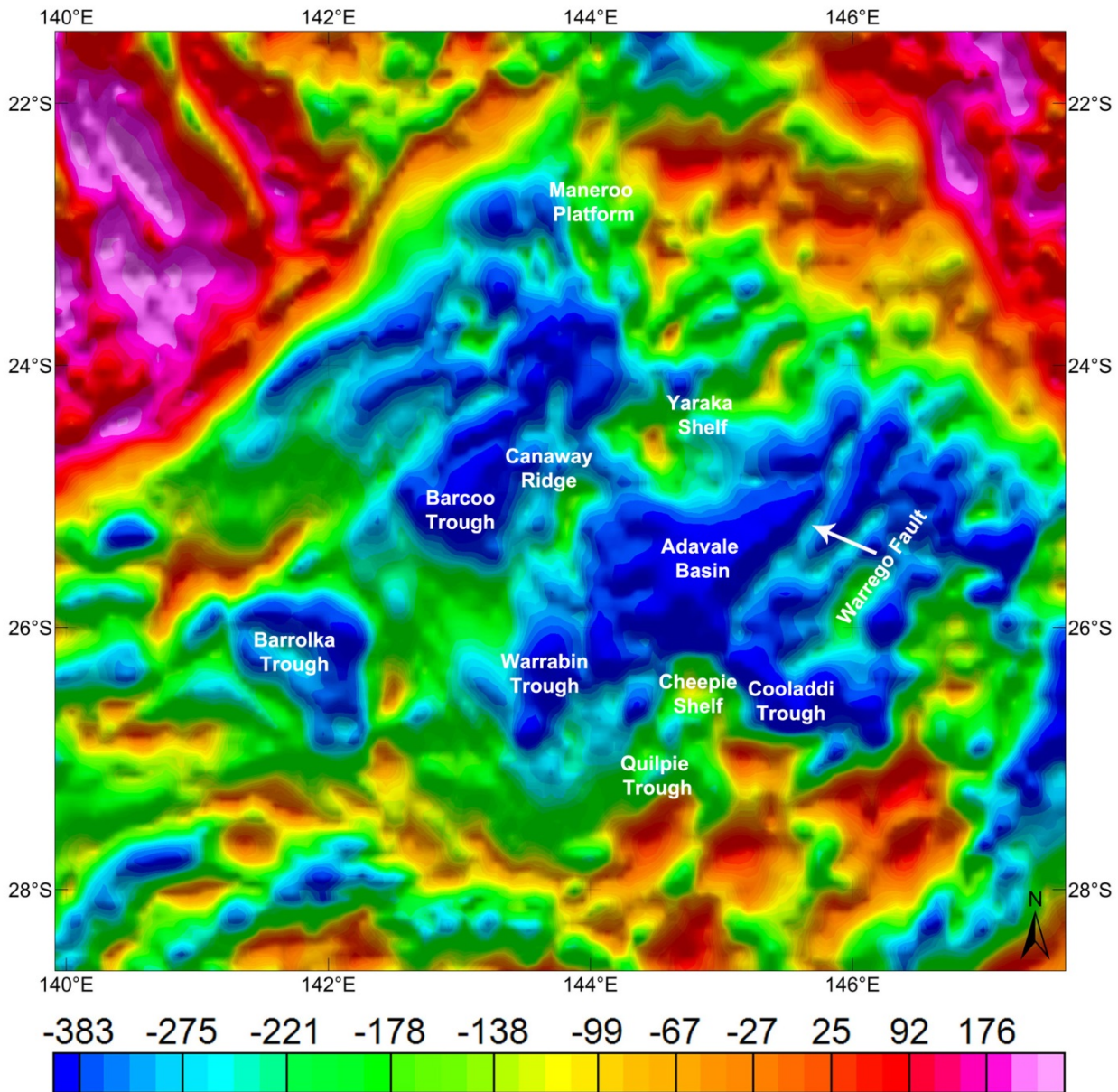


Fig. 5.8 Bouguer gravity map of the Thomson Orogen and surrounding provinces. Values in the legend bar are in $\mu\text{m}\cdot\text{s}^{-2}$

On the magnetic grid, the Thomson Orogen is characterized by long wavelength and low amplitude anomalies between -60 and 150 nT (Fig. 5.9). The grid is characterized by widespread

short wavelength positive magnetic anomalies that punctuate the region and correlate with low gravity anomalies. There is a poor correlation between the distribution of the sedimentary sequence and the magnetic signature of the region. The Adavale Basin and the associated troughs are not well defined in the magnetic grid (Fig. 5.9).

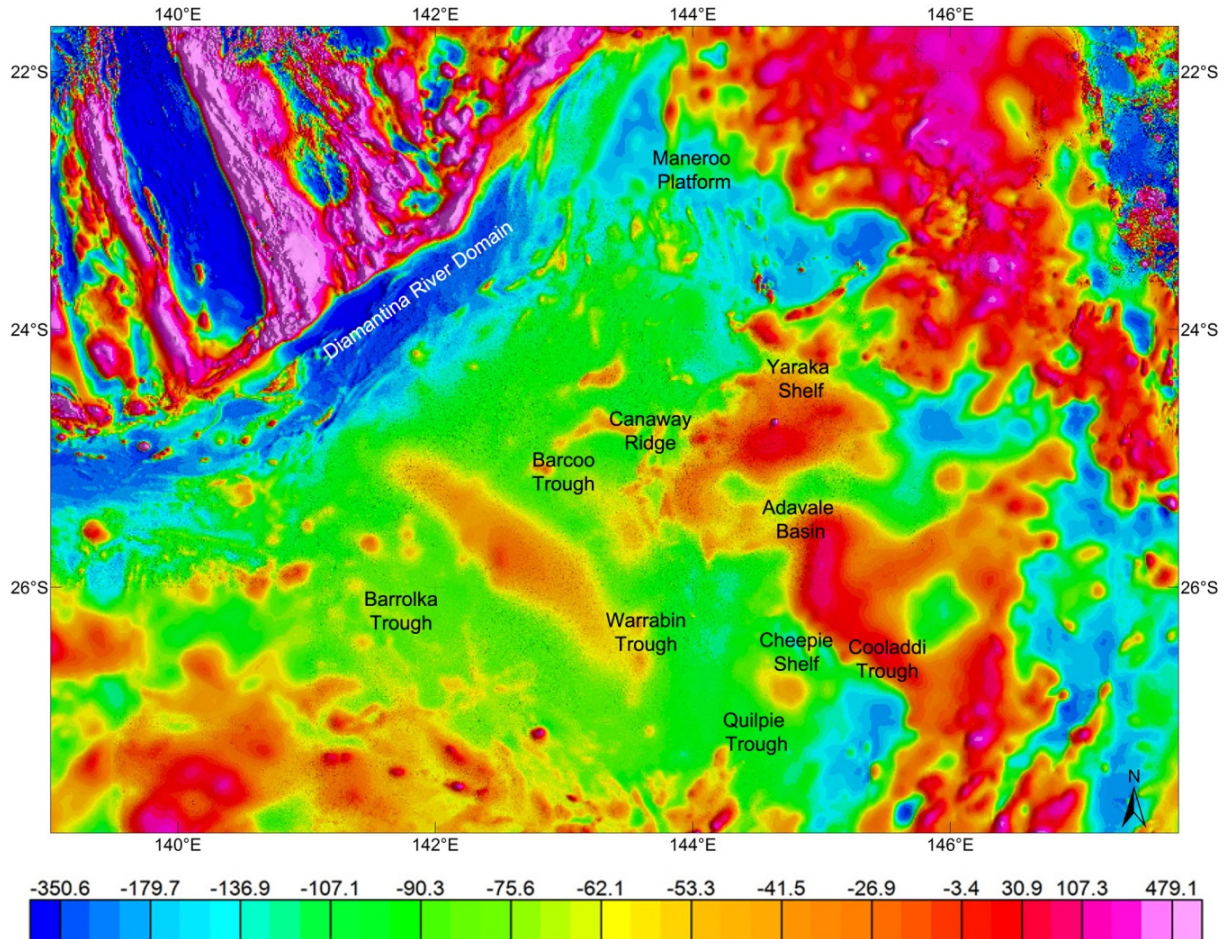


Fig. 5.9 RTP magnetic map of the Thomson Orogen and surrounding provinces. Values in the legend bar are in nT

Spampinato et al. (Unpublished results-b) suggested that the smooth magnetic texture of the Thomson Orogen reflects deeply buried source bodies. Spampinato et al. (Unpublished results-a) indicated that the prominent gradient associated with the Cork Fault and the persistent low magnetic signature of the Diamantina River Domain may represent the thinning and burying at depth of a magnetic crust with Precambrian affinities under the Thomson Orogen.

Several short wavelength positive magnetic features correlate with low gravity anomalies and have been associated with shallow granitic intrusions. These intrusions appear to be focused

along major structures (i.e. the Canaway Ridge and the Warrego Fault, Fig. 5.9), suggesting that these faults may have controlled their emplacement.

5.7 Forward models

The crust and the upper mantle are forward modelled as four discrete layers. The top geological unit is represented by the highly reflective Devonian to Triassic sedimentary sequences of the Adavale, Cooper and Eromanga basins. The underlying non-reflective layer having a velocity range between 5.6 and 6.3 km/s represents the shallow basement rocks of the Thomson Orogen, which has been modelled from 1 - 7 km to 17 - 22 km depth. The transition to the reflective lower crust is defined by an increase of seismic velocities to 6.6 - 7.5 km/s and has been imaged to 38 - 42 km depth. The underlying upper mantle is represented by a non-reflective zone and increased seismic velocities (~8.2 km/s). This zone represents the bottom layer in the forward models. To honour the constraining seismic data, the Moho has been modelled being relatively flat at ~38 - 42 km depth, however the latter appears to be shallower beneath the Canaway Ridge and has been modelled at ~35 km depth.

5.7.1 Forward model n. 1

Profile n.1 is ~265 km long and it is oriented east - west along the Deep Seismic Transects n. 1 and 9 to intersect the Mt Howitt Fault, the Harkaway Fault, the Warrabin Trough and the Quilpie Trough (Fig. 5.10). Drill holes DIO Mt Howitt 1, LEA Kenmore 1, GSQ Eromanga 1 and GSQ Quilpie 1 provide structural control and constrain the depth of the sedimentary sequences and the shallower basement rocks (Fig. 5.10).

Negative regional gravity anomalies correspond to increase in thickness of the sedimentary sequences. The lowest gravity anomalies (less than -30 mgal in fig. 5.10 equating to $-300 \mu\text{m}^*\text{s}^{-2}$) represent the distribution of the Devonian basinal succession of the Quilpie and Warrabin troughs. The highest amplitude gravity anomalies up to -6 mgal ($-60 \mu\text{m}^*\text{s}^{-2}$) reflect shallower basement rocks of the Thomson Orogen and are associated - from west to east - with the Mt Howitt Anticline, the Canaway Ridge and the Cheepie Shelf. Basement shallowing is interpreted to occur within the Cooper Basin due to a positive flower structure which is reflected by relative positive gravity anomalies of ~ -21 mgal ($-210 \mu\text{m}^*\text{s}^{-2}$).

The regional magnetic trend is characterized by long wavelength anomalies that range in amplitude between -10 and -130 nT. Best fit reconstruction suggests that the smooth magnetic

texture reflects the topography of a magnetized lower crust above the Curie depth. The positive gravity Mt Howitt Anticline, the Cheepie Shelf and the Canaway Ridge show poor magnetic expression. The little correlation between the topography of the upper basement and the magnetic trend indicates that the shallow crust is poorly magnetized along the profile.

In our best fit reconstruction, the non-magnetic basinal sequence shows an average density of 2.55 g/cm^3 and thickens significantly under the Devonian troughs being up to ~ 4 km depth. The underlying non-magnetic layer, which represents the Thomson Orogen basement rocks, has been assigned a density of $2.74 - 2.85 \text{ g/cm}^3$ and has been modelled to $18 - 28$ km with an average thickness of ~ 21 km. The reflective lower crust has been assigned a magnetic susceptibility of 0.025 SI and a density of 2.95 g/cm^3 extending to $38 - 42$ km and having an average thickness of ~ 17 km. Short wavelength positive magnetic and negative gravity anomalies have been modelled as elongated shallow granitic intrusions emplaced within the upper basement at $\sim 7 - 9$ km depth. They have been assigned a density of 2.67 g/cm^3 and their susceptibility ranges from 0.044 to 0.063 SI. The Moho is imaged relatively flat at $\sim 38 - 42$ km and regionally deepens towards the east. The upper mantle appears shallower beneath the Canaway Ridge (~ 38 km depth). The underlying mantle ($D= 3.25 \text{ g/cm}^3$) does not affect the regional magnetic signature of the Thomson Orogen being well under the Curie depth.

East-dipping and west-dipping high angle faults connect into major east-dipping detachment surfaces which appear to control the architecture of the area. The Mt Howitt, Harkaway and Canaway faults are imaged as high angle west-dipping faults having listric form at depth. In the eastern part of the Warrabin Trough, steep shallow east-dipping faults are rotated towards the Canaway Ridge. Early to Middle Devonian reflective rocks of the Warrabin Trough onlap the Canaway Ridge which implies that the latter was a horst at the time of deposition. The lower crust is significantly offset by the Harkaway Fault (~ 4 km). The Harkaway Fault deforms also the basinal sequences of the Eromanga Basin, Cooper Basin and thin Devonian strata. However, deformation decreases towards the upper basement and the Devonian strata (up to $1 - 2$ km), suggesting that the fault had a protracted evolution and that major offsets may pre-date the Devonian. The Eromanga Basin is only weakly deformed which might indicate that the existing basement faults have been repeatedly reactivated as reverse thrusts.

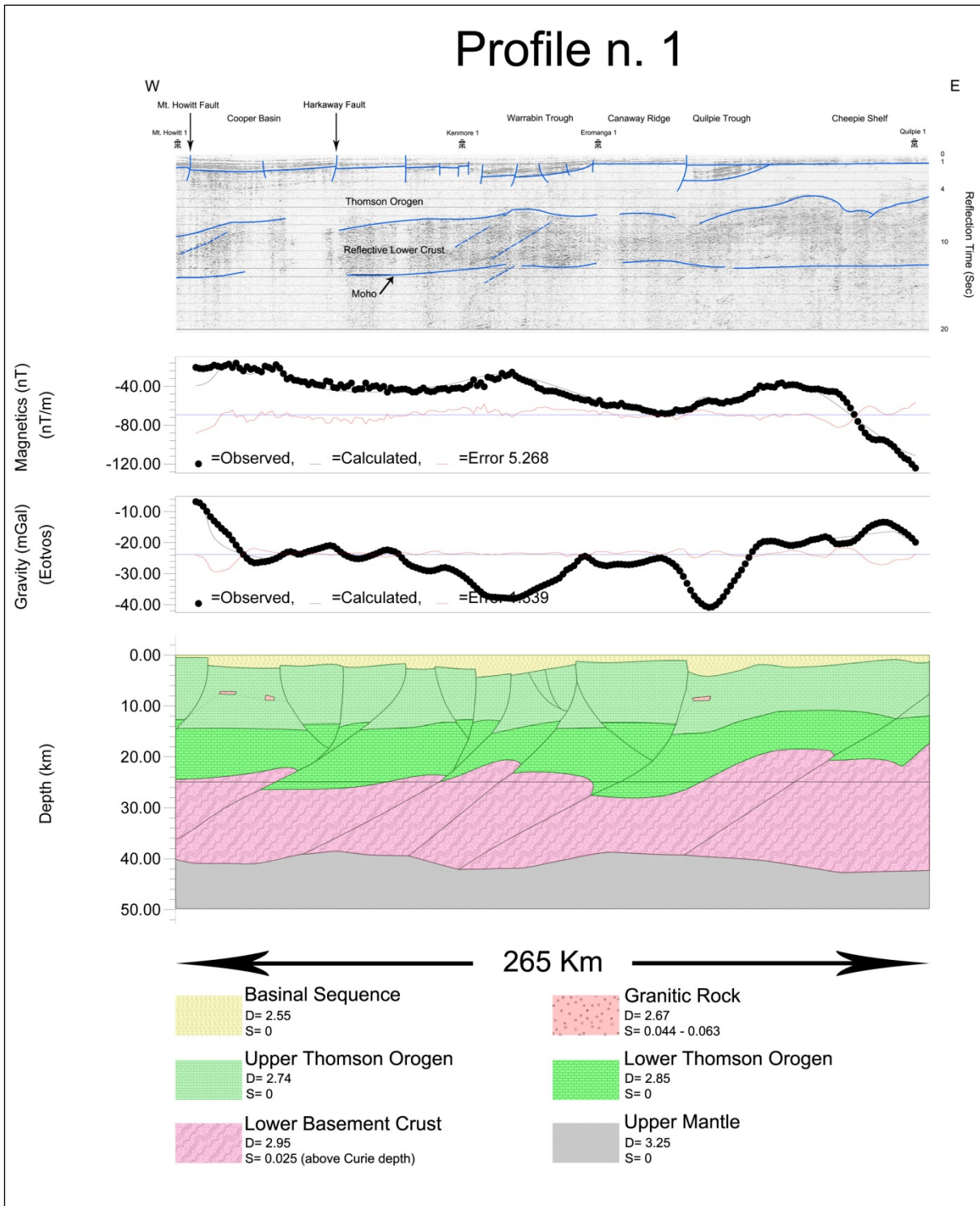


Fig 5.10 Forward model n.1 along the Deep Seismic Transects n. 1 and 9

5.7.2 Forward model n. 2

Profile n.2 is ~145 km long and it is oriented northeast along the Deep Seismic Transect n. 3. This profile incorporates the Barrolka Trough, the Harkaway Fault and the Chandos Anticline which represents the southeastern edge of the Barcoo Trough (Fig. 5.11). Drill holes AAP Tanbar 1 and AOD Chandos 1 intersected the basement and provide additional constraints.

In the western part of the profile, thickening of the non-magnetic sedimentary sequence occurs within the Barrolka Trough ($D= 2.55 \text{ g/cm}^3$) which may contain a sedimentary rock package up to 4 km thick and corresponds to a broad gravity low exceeding -30 mgal ($-300 \mu\text{m}^*\text{s}^{-2}$). In the eastern part of the profile, shallowing of the upper basement ($D= 2.74 - 2.85 \text{ g/cm}^3$) to ~1 - 2 km depth is associated with positive gravity signature (-20 mgal, equating to $-200 \mu\text{m}^*\text{s}^{-2}$) but show little magnetic expression. Thus, the upper crust has been assigned no magnetization and has been modelled to ~18 - 23 km depth. The magnetic profile is characterized by long wavelength (~80 - 90 km) anomalies that range in amplitude values between -60 and 0 nT (Fig. 5.11). The smooth texture and gentle gradients of ~1.5 nT/km extending for ~40 km east and west of a positive magnetic peak located in the eastern part of the profile are consistent with a deep source body. Beneath the peak magnetic response, the lower crust is imaged as being shallower (~18 - 20 km depth). Best fit reconstruction shows that a magnetized lower crust has a density of 2.92 g/cm^3 and magnetic susceptibility of 0.025 SI increasing to 0.075 SI eastward, which accounts for the smooth magnetic response and the regional gravity trend along the profile. A positive magnetic anomaly having wavelength of ~7 km correlates with low gravity responses and is inferred to be due to a shallow granitic intrusion ($D= 2.67 \text{ g/cm}^3$; Susc. 0.0069 SI). The source body is ~2 km wide and ~7 km long and has been modelled to intrude the upper basement rocks at ~5 km depth. The Moho is ~43 - 44 km depth and shows an undulating profile, therefore the upper mantle ($D= 3.25 \text{ g/cm}^3$) has no magnetization being under the Curie depth.

The low gravity signature under the Barrolka Trough is inferred to reflect Devonian (?) sedimentary sequences beneath the Cooper Basin. The steep gradients in its eastern margin suggest that the trough is asymmetric and may have formed as a half graben with sedimentary packages thickening towards the east. The Barrolka Trough terminates against a positive flower structure associated with gravity gradients of $\sim 12 \mu\text{m}^*\text{s}^{-2}/\text{km}$. The western edge of the flower structure is defined by the east-dipping Cunnavalla Fault, which has been modelled to connect into the west-dipping Harkaway Fault (Fig. 5.11). The Harkaway, Monkey - Coolah and

Tallyabra faults are modelled as high angle west-dipping faults and penetrate the entire crust. The displacing of the lower crust results in regional variation of the magnetic signature along the profile.

West-dipping detachments appear to control the architecture of the area, similar to the model n. 1. The lower crust shows displacement comprised between 1 and 3 km. The faults show variation in amplitude of seismic horizon displacement. The displacement rate decreases towards the middle and upper crust, possibly suggesting a protracted evolution involving multiple reactivations of basement faults.

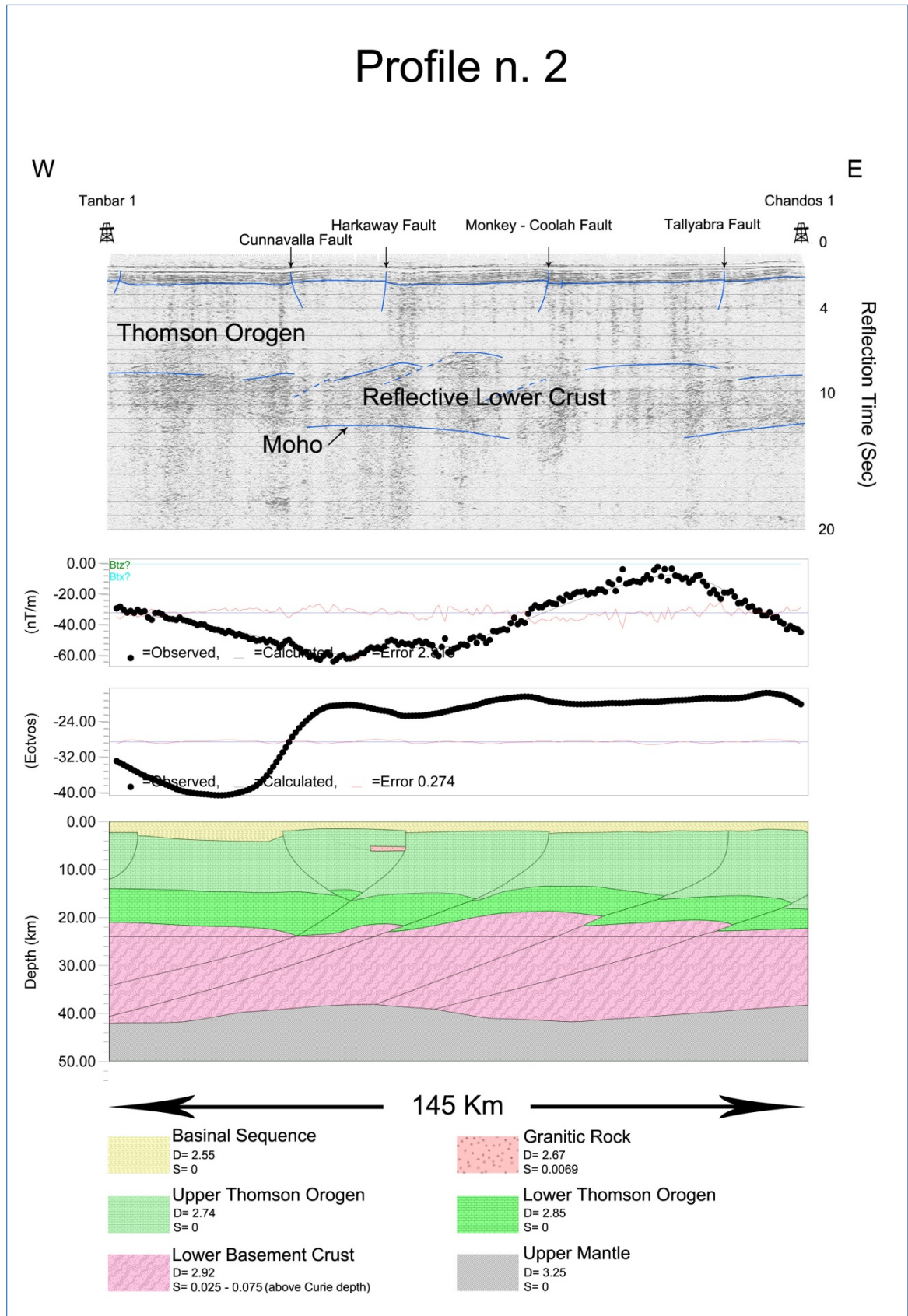


Fig. 5.11 Forward model n.2 along the Deep Seismic Transect n. 3

5.7.3 Forward model n. 3

Profile n. 3 is ~250 km long and it is oriented east - west along the Deep Seismic Transects n. 6 and 2 to intersect the Barcoo Trough, the Canaway Ridge and the Adavale Basin (Fig. 5.12). Drill holes FPC Galway 1, HEP Grey Range 1, PPC Lissoy 1 and PPC Etonvale 1 intersected the basinal sequence and the upper basement along the profile.

The positive gravity anomalies associated with the Canaway Ridge (up to -15 mgal equating to -150 $\mu\text{m}\cdot\text{s}^{-2}$) appear to divide two regions having distinctly low gravity responses and characterized by anomaly amplitudes below -27 mgal (-270 $\mu\text{m}\cdot\text{s}^{-2}$), which are associated with thick sedimentary rock packages of the western Barcoo Trough and the eastern Adavale Basin ($D= 2.55 \text{ g/cm}^3$). The sedimentary sequence varies from 1 km under the Canaway Ridge to 3 - 4 km under the Adavale Basin and the Barcoo Trough. Relative positive gravity anomalies represent shallower basement rocks under the Devonian sedimentary sequences and are associated with the Thomson Anticline in the Barcoo Trough and the Grey Range Fault in the Adavale Basin. The topography of the upper crust ($D= 2.74 - 2.85 \text{ g/cm}^3$), which has been modelled from 1 - 4 km to 15 - 19 km, shows little correlation with the regional magnetic signature indicating that the shallow basement rocks are poorly magnetized.

The regional magnetic trend is characterized by long wavelength anomalies. The western side of the profile shows high magnetic anomalies with amplitude values of ~ -25 nT. A prominent gradient of ~3nT/km determines a low magnetic region which dominates the eastern side of the profile. The gradient is located over a west-dipping structure inferred from the seismic transects which appears to be a blind thrust because it seem to have no expression at shallow level. The decreasing in the regional magnetic signature correlates with regional deepening of the lower crust ($D= 2.92 \text{ g/cm}^3$) from ~15.5 km depth to ~18 km depth. The forward model indicates that a magnetized lower crust having a susceptibility of 0.088 SI above the Curie depth is appropriate for the model. Positive magnetic anomalies (up to 15 nT) that range in wavelength amplitude between 5 and 9 km indicate rock property contrast at shallow depth and are associated with the intrusion of low density granitic bodies. They are modelled to be emplaced within the upper basement at ~4 - 8 km depth. They have been assigned a density of 2.67 g/cm^3 and their susceptibility range from 0.023 to 0.074 SI.

The Moho is imaged relatively flat at ~37 - 39 km depth. However the latter appears to be shallower beneath the Canaway Ridge and has been modelled at ~35 km depth. The underlying

upper mantle ($D= 3.25 \text{ g/cm}^3$) does not affect the regional magnetic signature of the Thomson Orogen being well under the Curie depth.

High angle west-dipping listric faults penetrating the lower crust form the major crustal structures along the profile. The displacement rate in the lower crust (~3 km) is greater than the displacement in the upper crust (up to 1.5 km). Deformation also decreases within the sedimentary unit and the sedimentary rocks within the Eromanga basin are gently folded.

The blind thrust seems to offset the Moho (~3.5 km) but not to have expression through the shallowest units, suggesting that movement pre-dates basin formation. The displacement of the Moho and the lower crust beneath the Canaway Ridge causes the higher regional gravity anomalies in this area. The east-dipping Thomson and Grey Range faults are interpreted as shallow structures and they are only modelled in the upper crust because they are represented by short wavelength high gravity anomalies.

The Barcoo and the Adavale basins onlap the basement in the footwall of the Canaway Fault which is likely to have been a basement high during the deposition of the Devonian sedimentary successions. The shallow structures of the Thomson and Grey Range faults are inferred to be post-Devonian structures since there is no significant variation of the Devonian thickness across these faults (Hoffmann, 1989).

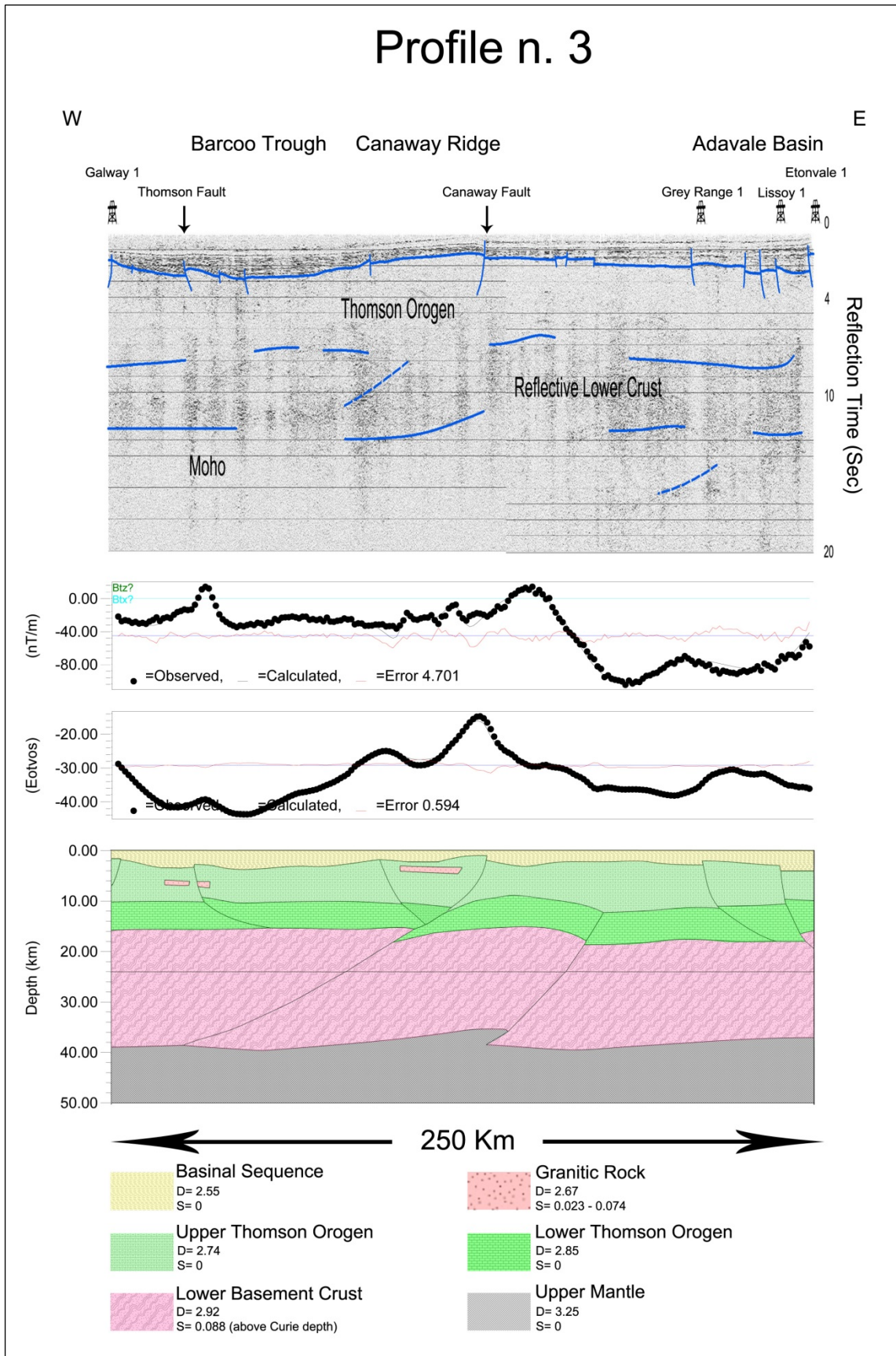


Fig. 5.12 Forward model n. 3 along the Deep Seismic Transects n. 6 and 2

5.7.4 Forward model n. 4

Profile n.4 is ~155 km long and it is oriented northwest-southeast to intersect the Cothalow Arch, the Gumbardo Fault and the Grenfield Fault (Fig. 5.13). The deep seismic profile n. 11 has been used as a constraint (Fig. 5.13).

The regional low gravity signature shows anomaly amplitudes comprised between -30 and -48 mgal (-300 and $-480 \mu\text{m}^*\text{s}^{-2}$) and decreases towards the southeast. The low gravity response well reflects the thickening of the Adavale basin ($D= 2.55 \text{ g/cm}^3$) until ~5 km depth in the south-eastern part of the profile. The basement rocks beneath the Cothalow Arch and the Gumbardo Fault are relatively shallower at ~2.5 - 3 km and this is reflected by higher gravity amplitude values (greater than -38 mgal equating to $-380 \mu\text{m}^*\text{s}^{-2}$). However, the positive gravity anomalies associated with the shallowest part of the basement rocks ($D= 2.74 \text{ g/cm}^3$) consistently show poor magnetic expression. This may suggest that the upper basement of the Thomson Orogen is non-magnetic or poorly magnetic if compared to the lower crust.

The magnetic signature is characterized by amplitudes between -100 and 0 nT. The regional magnetic anomalies generally increase towards the south-eastern part of the profile, where the amplitude values are greater than -70 nT. The increase of the magnetic anomalies correlates with the shallowing of the lower crust ($D= 2.92 \text{ g/cm}^3$), which has been modelled at ~17 - 20 km depth. The lower crust has been assigned a magnetic susceptibility of 0.082 SI to account for the regional magnetic anomalies. In the western part of the profile, the lower crust is deeper and is imaged at ~21 - 23 km depth. Positive magnetic anomalies with wavelengths of ~11 - 13 km have been imaged as elongated granitic intrusions at ~12 - 15 km depth because of their low gravity response. They have been assigned a density of 2.67 g/cm^3 and a susceptibility of 0.069 SI.

The Moho is imaged relatively flat at ~40 - 42 km depth and regionally deepens towards the southern part of the profile. The underlying mantle has been modelled with a density of $D= 3.25 \text{ g/cm}^3$.

SE- and NW-dipping faults form the main tectonic pattern along the profile. Positive gravity anomalies with amplitude values of ~ -33 mgal ($-330 \mu\text{m}^*\text{s}^{-2}$) reflect the relative shallow basement rocks beneath the Cothalow Arch. The latter has been modelled to form a shallow positive flower structure that lies into the upper crust. This structure is poorly represented in the seismic profile. However it may be possible that the NW-dipping fault that represents the

southern edge of the Cothalow Arch continues through the lower crust because the latter appears to shallow in correspondence to the horst. In this scenario, the NW-dipping fault would be a major structure. The Gumbardo Fault is associated with a gentle NW-oriented gravity gradient of ~ 0.34 mgal/km ($3.4 \mu\text{m}^*\text{s}^{-2}/\text{km}$). The Gumbardo Fault has no seismic expression through the lower crust and has been imaged as a shallow SE-dipping low angle reverse fault which affects only the upper crust. Similarly to other shallow structures within the Thomson Orogen, the shallowing of the upper basement along the Gumbardo Fault has limited effect on the magnetic profile.

The positive gravity (~ -34 mgal equating to $-340 \mu\text{m}^*\text{s}^{-2}$) Grenfield Uplift Zone shows a steeper NW-oriented gravity gradient (~ 0.93 mgal/km equating to $9.3 \mu\text{m}^*\text{s}^{-2}/\text{km}$) if compared to the Gumbardo Fault. This structure has been imaged as a steeply SE-dipping fault offsetting the lower crust. The Warrego - Grenfield Fault zone defines the southern extent of the Devonian rocks at the southern margin of the Adavale Basin. Deformation over the Gumbardo Fault and the Grenfield Fault significantly affects the Devonian sequences (Finlayson et al., 1988), which are displaced up to ~ 7 km. The seismic data indicate that the Gumbardo Fault had little significance in the deposition of the sedimentary rocks of the Adavale Basin but was active during the subsequent Carboniferous orogenesis. The Cothalow Arch is interpreted to be active as a strike-slip or normal fault during the Devonian deposition and then was reactivated and uplifted during the Carboniferous and the Cenozoic (Evans et al., 1992).

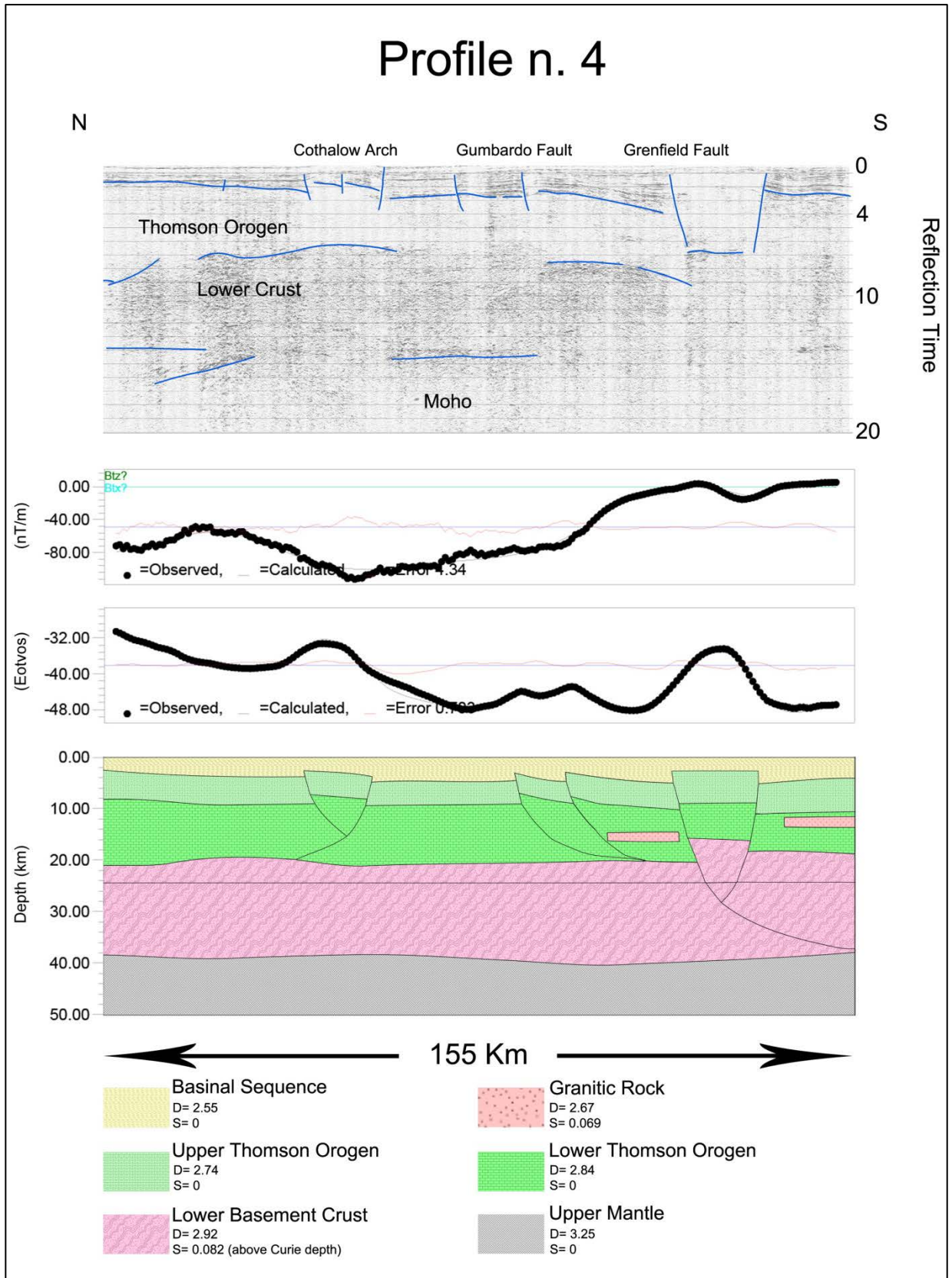


Fig. 5.13 Forward model n. 4 along the Deep Seismic Transects n. 11

5.8 Regional architecture of the Thomson Orogen

Forward modelling indicates that the lowest gravity anomalies reflect the distribution of the Devonian sedimentary succession. This interpretation is consistent with observations from seismic data and drill holes (Moss and Wake-Dyster, 1983; Pinchin and Senior, 1982).

Shallow basement rocks of the Thomson Orogen are reflected as positive gravity anomalies. On the contrary no obvious correlation occurs between the magnetic signature of the region and the morphology of the shallow basement. This may suggest that the shallow basement of the Thomson Orogen is non-magnetic or poorly magnetic if compared to the magnetized lower crust. Meta-sedimentary and meta-volcanic rocks of the Thomson Orogen (Murray, 1994; Murray and Kirkegaard, 1978) intersected by the drill holes may be representative of the non-magnetic to weakly magnetic upper basement crust extending from depths of 1 to 25 km.

The smooth texture and the long wavelength magnetic signature indicate deeply buried source bodies. The best fit model implies that the magnetic lower crust is responsible for the regional magnetic signature. In the geometrically constrained a-priori model, a range of magnetic susceptibility comprised between 0.025 and 0.088 SI above the Curie depth and densities of 2.92 - 2.95 g/cm³ fit the observed geophysical profiles.

The tectonic architecture of the region is characterized by major west-dipping and south-dipping high angle listric faults that control the architecture of the basement rocks and the regional distribution of the overlying infra-basins. Major high angle reverse faults penetrate the entire crust, with several extending to, and offsetting the Moho. These faults have a significant influence on the regional gravity and magnetic signature of the Thomson Orogen. Shallow faults do not affect the lower crust which implies that they terminate at the upper crust, possibly in an upper crustal detachment. Faults offsetting the upper crust result in positive gravity anomalies but have a minimal magnetic expression. Granitic intrusions at a shallow level within the upper basement have been modelled to take into account the short geophysical response along the profiles.

5.9 Crustal architecture of the Thomson Orogen

Understanding the nature of the basement crust of the Thomson Orogen is a fundamental issue that needs to be addressed to determine the potential connections with the surrounding north-western Proterozoic parts of the continent and the south-eastern Phanerozoic geological

provinces which preserve the evolution of the Gondwanan margin. Since the Thomson Orogen lies between these two very distinct geological regions of the Australian continent, this has major implications on reconstructing the post-Rodinia evolution of the continent as well as determining the time of amalgamation of the Tasmanides of Eastern Australia.

5.9.1 The Thomson Orogen as a single feature

A number of tectonic models suggest that the Thomson Orogen might not be a single feature (Glen et al., 2013; Harrington, 1974; Musgrave, 2013). Glen et al. (2013) indicated that the western part of the Thomson Orogen developed on Neoproterozoic to Early Cambrian oceanic crust. Their gravity models across the Olepoloko Fault (Fig. 5.1) suggest that meta-mafic or ultramafic rocks lie under the southern Thomson Orogen at a middle crustal level. In their view, this layer may represent oceanic crust which has been uplifted over mixed igneous and meta-sedimentary units overlying the upper mantle. They also indicated that the reflective lower crust of the Thomson Orogen may represent igneous oceanic crust extending from the western edge of the Tasmanides to the Quilpie Trough or the Cheepie Shelf. Adapting Harrington's work (1974), the Barcoo Basin is inferred to lie west of an eastwards-rifted Precambrian continental sliver represented by the Anakie Inlier and, less certainly, by the Nebine Ridge (Fig. 5.14a). Musgrave (2013) indicated that the Thomson Orogen may not be a single terrane. In his view, the magnetic signature of the region allows dividing the Thomson Orogen into separate crustal domains. In this interpretation, the Thomson Orogen formed as attenuated continental/arc crust to the east and accreted oceanic crust to the west (Fig. 5.14b).

However, the models presented in this study suggest that the crust of the eastern Thomson Orogen is petrophysically indistinguishable from the crust of the western Thomson Orogen. The long wavelength magnetic character does not change significantly across the region and major sutures within the region are not apparent in the geophysical grids. Our results support magnetotelluric studies, which indicate that the basement of the Thomson Orogen is generally isotropic and one dimensional resistivity model is appropriate for the region (Spence and Finlayson, 1983). The seismic fabric and the P-wave velocity pattern do not change across the Thomson Orogen (Finlayson et al., 1990a) except under the Canaway and the Nebine Ridges (Finlayson and Collins, 1987) further indicating that the Thomson Orogen is free of large lateral discontinuities. In the Lachlan Orogen, seismic velocity variations have been detected and might reflect crustal heterogeneity. However they are not apparent in the Thomson Orogen (Fishwick

and Reading, 2008). In light of all the supporting evidences we suggest that the Thomson Orogen represent a single crustal domain.

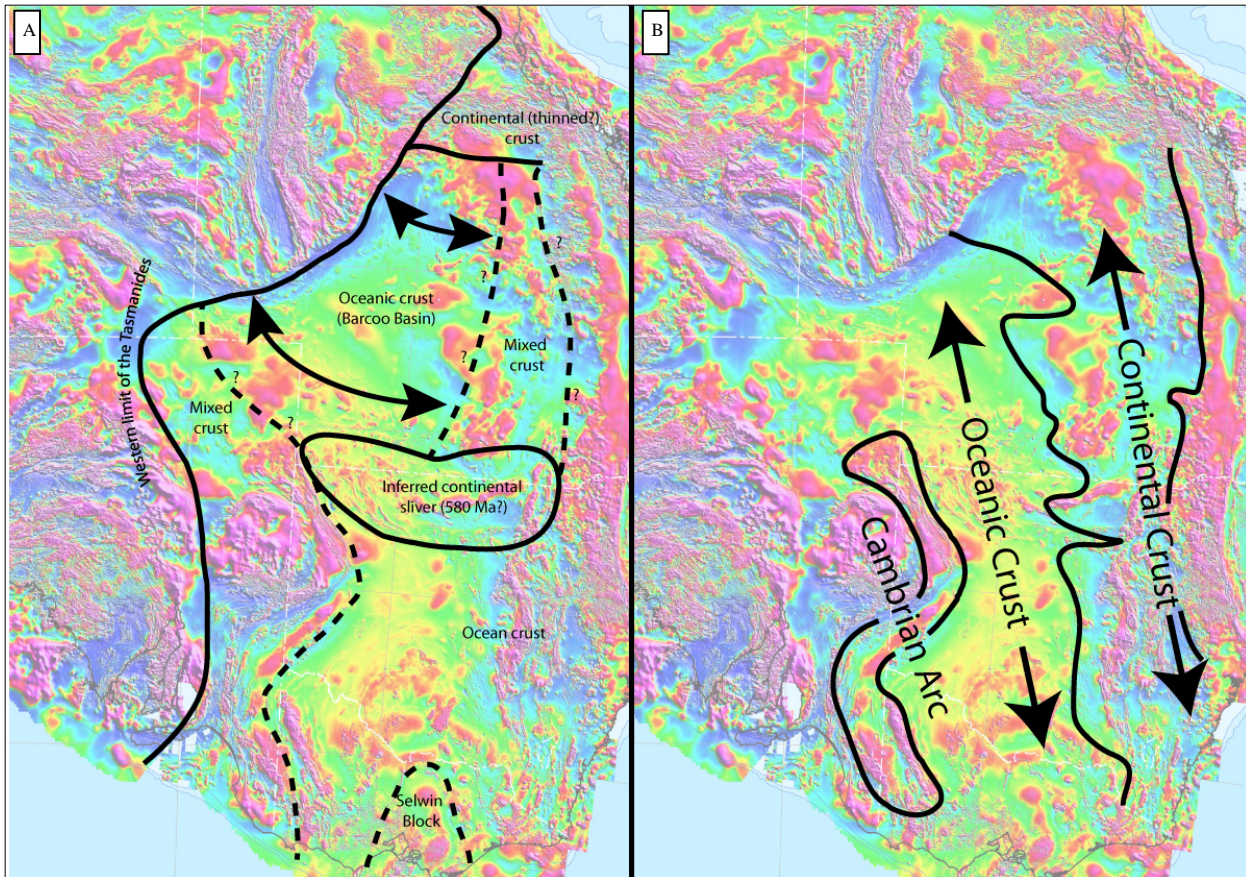


Fig. 5.14 Inferred nature of the crust under the Thomson and Lachlan orogens as proposed by A) Glen et al. (2013) and B) Musgrave (2013).

5.9.2 Thomson Orogen Vs. Lachlan Orogen

The Lachlan Orogen bounds the southern limit of the Thomson Orogen and represents the south-western extent of the Tasmanides (Fig. 5.1) (Glen, 2005). Most of the Lachlan Orogen is interpreted to have originated as Cambrian to Ordovician oceanic boninitic, MORB-type tholeiitic and island arc crust (Crawford et al., 1984; Crawford and Keays, 1987; Mathur, 1983). However, the province also includes isolated fragments of older continental crust (Cayley et al., 2011; Moresi et al., 2014).

Some authors envisaged that the Thomson and Lachlan orogens may represent a unique terrane (Burton, 2010; Glen et al., 2013; Musgrave, 2013). Burton (2010) suggested that the Lachlan Orogen continues into southern and central Queensland (the Thomson Orogen) based on

similarities in the gross magnetic response of the two regions. Glen et al. (2013) indicated that the reflective lower crust of the Thomson Orogen may represent igneous oceanic crust and may correlate with the oceanic crust inferred south of the Olepoloko Fault (Fig. 5.1) and in western and central Victoria (Cayley et al., 2011).

However, the crustal architecture and the seismic fabric of the Thomson and Lachlan orogens appear to be significantly different. The Thomson Orogen shows a thicker and more reflective lower crust if compared to the Lachlan Orogen (Glen et al., 2007a). The depth to the Moho is regionally shallower under the Thomson Orogen (36 - 42 km depth) if compared to the Lachlan Orogen (43 - 51 km depth) (Finlayson et al., 1984). The velocity increases at the seismic boundaries across the Thomson Orogen are sharp if compared to the transitional trend under the Lachlan Orogen (Finlayson et al., 1984). The Lachlan Orogen shows velocity decreases in the middle crust that are not detected in the Thomson Orogen (Finlayson, 1982). The Lachlan Orogen shows a regional north to northwest dominant trend whereas the structural grain of the Thomson Orogen is characterized by a set of prominent NE- (Murray and Kirkegaard, 1978; Wellman, 1992) and NW-trending (Spampinato et al., Unpublished results-b) structures. The Lachlan Orogen shows an imbricated tectonic style (Cayley et al., 2011), which is not apparent in the constrained forward modelled profiles. Combined, these differences suggest that the Thomson and the Lachlan orogens represent two distinct provinces having different crustal architecture.

5.9.3 Thomson Orogen Vs. Mount Isa terrane

The Mount Isa terrane (Fig. 5.1) forms a crustal fragment amalgamated to the North Australian Craton during the Palaeoproterozoic (Betts et al., 2006; Bierlein and Betts, 2004; Giles et al., 2006a; MacCready, 2006a; Spikings et al., 2001). Some authors suggested that a crust of Precambrian age lies in the subsurface of the Thomson Orogen (Fergusson et al., 2007a; Fergusson et al., 2009; Glen, 2005; Glen et al., 2006; Henderson, 1980; Murray, 1990; Wellman, 1990). Glen (2005) indicated that thinned continental crust underlies most of the Thomson Orogen. Fergusson et al. (2009) suggested that the Thomson Orogen is underlied by Precambrian crust while the Lachlan Orogen is formed by Early to Middle Palaeozoic accretionary orogens. Spampinato et al. (Unpublished results-a) indicated that the lower basement crust of the Thomson Orogen is petrophysically indistinguishable from the Mount Isa basement crust. This suggest that the Thomson orogen is floored by Proterozoic basement rocks. These correlations

further implies that the basement terranes of the Thomson and Lachlan orogens did not initiate as a single feature but rather as different entities and they amalgamated during the Palaeozoic (Glen et al., 2013; Spampinato et al., Unpublished results-b). However, the Mount Isa terrane and the Thomson Orogen appear to have a different crustal architecture. The Mount Isa terrane is characterized by weakly reflective and seismically homogeneous thick crust that extends to ~55 km depth (Korsch et al., 2012) whereas the Thomson Orogen shows two layered basement crust to ~42 km depth.

The Mount Isa terrane can be divided in two broad tectonic domains showing contrasting tectonic styles and heterogeneous depositional sequences (Betts et al., 2006). The Eastern Fold Belt accommodated west-directed tectonic transport above the crystalline basement rock during the Mesoproterozoic, whereas the Western Fold Belt shows east-directed deformations that affect the basement crust (Betts et al., 2006; MacCready, 2006a; O'Dea et al., 1997b). The Thomson Orogen instead is characterized by prominent west-dipping and south-dipping structures that affect the entire crust.

The correlation between the Mount Isa terrane and the Thomson Orogen is not apparent from both the seismic and the geophysical grids, which implies that either they represent two fundamentally different terranes or the Thomson Orogen underwent tectonic events that overprinted previous structures and resulted in a distinctive seismic fabric.

5.10 The crustal nature of the lower crust

The forward models and seismic profiles indicate that the lower crust has a considerable thickness (~20 km). The imbricated tectonic style which characterizes part of the Lachlan Orogen (Cayley et al., 2011) is not apparent in the Thomson Orogen thus the thickening cannot be ascribed to uplifting and doubling of the crust.

Tomography imaging highlighted a distinct high velocity feature in the Thomson Orogen suggesting that the lithosphere may have Precambrian affinities (Kennett et al., 2004). The high velocity character of the Thomson Orogen differs from lower velocities recorded across the rest of the Tasmanides which may mostly reflect younger oceanic lithosphere (Fishwick et al., 2008; Fishwick et al., 2005; Kennett et al., 2004). We interpret that the lower crust of the Thomson Orogen represents thinned and magnetized Precambrian continental crust at depth (Spampinato et al., Unpublished results-a). We support the early work of Finlayson et al. (1989) and we

suggest that extensional tectonics during the Neoproterozoic (Spampinato et al., Unpublished results-b) and the Early to Middle Phanerozoic (Finlayson, 1993; Finlayson and Leven, 1987; Finlayson et al., 1988; Finlayson et al., 1989; Leven et al., 1990; Murray and Kirkegaard, 1978; Spampinato et al., Unpublished results-b) resulted in thinning of the continental crust and enrichment of mafic content which is represented by increased reflectivity at mid- to low crustal level. Areas where the reflection characteristics of the deep crust differ from the rest of the Thomson Orogen such as under the Canaway and the Nebine ridges (Finlayson and Collins, 1987; Finlayson et al., 1990b; Mathur, 1983) may reflect regions where crustal extension was less intense.

5.11 Conclusions

Seismic profiles and forward models consistently indicate that the lower and upper basement crusts of the Thomson Orogen show different geophysical properties. The crust of the Thomson Orogen can be distinctly divided in a non-magnetic to weakly magnetic upper crust and a magnetic lower crust. The regional magnetic signature of the Thomson Orogen reflects the topography of the lower crust. Meta-sedimentary and meta-volcanic rocks of the Thomson Orogen may be representative of the upper crust while the lower crust may have a more mafic composition.

High angle reverse thrusts having listric form at depth displace the entire crust and appear to extend to the Moho. The amount of offset decreases towards the Eromanga Basin, which suggests multiple reactivation episodes.

The geophysical interpretation indicates that the western and eastern parts of the Thomson Orogen are petrophysically indistinguishable. It is inferred that the Thomson Orogen is free of large lateral discontinuities and may be a single terrane. The Thomson Orogen shows a fundamentally different structure than the Lachlan Orogen. Thinned Precambrian crust of the Thomson Orogen may be representative of an Early Palaeozoic continental margin or back-arc setting whereas the Lachlan Orogen formed via incorporation of arc type, oceanic and continental rocks.

Acknowledgement

Geoscience Australia is gratefully acknowledged for access to the Central Eromanga Basin Seismic Surveys (copyright Commonwealth of Australia – Geoscience Australia) which were

conducted by The Bureau of Mineral Resources. Potential field data and potential field grids (copyright Commonwealth of Australia – Geoscience Australia 2009) were acquired by the Queensland Geological Survey and are gratefully sourced from Geoscience Australia. Caroline Venn is thanked for proofreading the manuscript. Constructive comments by Robin Armit improved the manuscript and were greatly appreciated.

Declaration for Thesis Chapter 6

Monash University

Declaration for Thesis Chapter 6

Declaration by candidate

In the case of Chapter 6, the nature and extent of my contribution to the work was the following:

Nature of contribution	Extent of contribution (%)
Interpretation of gravity and magnetic data; 2D forward modelling; manuscript preparation	90

The following co-authors contributed to the work. If co-authors are students at Monash University, the extent of their contribution in percentage terms must be stated:

Name	Nature of contribution	Extent of contribution (%) for student co-authors only
Dr. Laurent Ailleres	Supervisory role; interpretation	5
Associate Professor Peter Betts	Supervisory role; assistance with 2D forward modelling	5

The undersigned hereby certify that the above declaration correctly reflects the nature and extent of the candidate's and co-authors' contributions to this work*.

**Candidate's
Signature**

Giovanni Pietro Tommaso Spampinato

Date

**Main
Supervisor's
Signature**

Dr. Laurent Ailleres

Date

Chapter 6: Imaging the basement architecture across the Cork Fault in Queensland using magnetic and gravity data

Giovanni P.T. Spampinato

PhD Candidate

Monash University - School of Earth, Atmosphere and Environment

PO Box 84

Building 28, room 242

Clayton Campus, Wellington Road

Clayton, Vic 3800



Peter G. Betts

Associate Professor

Monash University - School of Earth, Atmosphere and Environment

PO Box 16

Building 28, room 239

Clayton Campus, Wellington Road

Clayton, Vic 3800



Laurent Ailleres

Senior Research Fellow

Monash University - School of Earth, Atmosphere and Environment

PO Box 28E

Building 28, room 144

Clayton Campus, Wellington Road

Clayton, Vic 3800



ABSTRACT

The basement rocks in central Queensland are largely obscured by the Phanerozoic sedimentary succession and direct information comes only from sparse geological data. Forward modelling of regional aeromagnetic and Bouguer gravity data has been undertaken to unveil the crustal architecture at the junction of the Proterozoic Mount Isa terrane and the Phanerozoic Thomson Orogen in Queensland. The most prominent geophysical character is represented by the abrupt termination of positive NNW-trending geophysical features of the Mount Isa terrane against NE-trending low gravity and low magnetic anomalies of the Diamantina River Domain of the Thomson Orogen. The lower basement crust of the Thomson Orogen is petrophysically indistinguishable from the Proterozoic Mount Isa terrane. We interpret that the prominent gradients associated with the Cork Fault represent the displacement and burying of the Mount Isa terrane crust under the Thomson Orogen basement rocks. In this context, the Cork Fault is interpreted to represent a fundamental crustal break but does not represent the eastern margin of Rodinia because the Thomson Orogen is floored by Precambrian continental crust.

Initiation of the Cork Fault might have occurred as early as the Mesoproterozoic. At that time the Cork Fault was a major structure that developed during the separation of the Mount Isa terrane and the Curnamona Province. It is inferred that this break-up occurred during initial N-S to NNW extension. The Cork Fault formed part of a network of major north-dipping and south-dipping normal faults active at that time. The Cork Fault was repeatedly reactivated during the Neoproterozoic Rodinia break-up and during the Phanerozoic evolution of the Tasmanides. We suggest that the segment of the inferred ‘Tasman Line’ along the southern termination of the Mount Isa terrane should be regarded as a set of structures offsetting the Proterozoic crust rather than a simple lineament dividing the Proterozoic and the Phanerozoic Australian continent.

Key Words: *Mount Isa terrane, Thomson Orogen, Gravity, Magnetic, Phanerozoic Australia, Basement setting, Rodinia break-up, Cork Fault, Tasman Line.*

6.1 Introduction

The Cork Fault divides the Proterozoic Mount Isa terrane (Betts et al., 2006; Blake et al., 1984; O’Dea et al., 1997b) from the Phanerozoic Thomson Orogen (Finlayson et al., 1988; Glen, 2005;

Glen et al., 2010; Murray and Kirkegaard, 1978) in Queensland and is one of the most distinguishable geophysical features on the Australian continent (Fig. 6.1). Because of its prominence, the Cork Fault has been interpreted to represent a major feature associated with the Neoproterozoic break-up of Rodinia (Finlayson et al., 1988; Gunn et al., 1997; Murray and Kirkegaard, 1978; Shaw et al., 1996; Veevers, 2000a; Veevers and Powell, 1984). However, the architecture of the Cork Fault as well as the timing of its initiation is still poorly understood because the geological record of the fault is incomplete or sparsely preserved (Murray, 1994; Murray and Kirkegaard, 1978; Wellman, 1990).

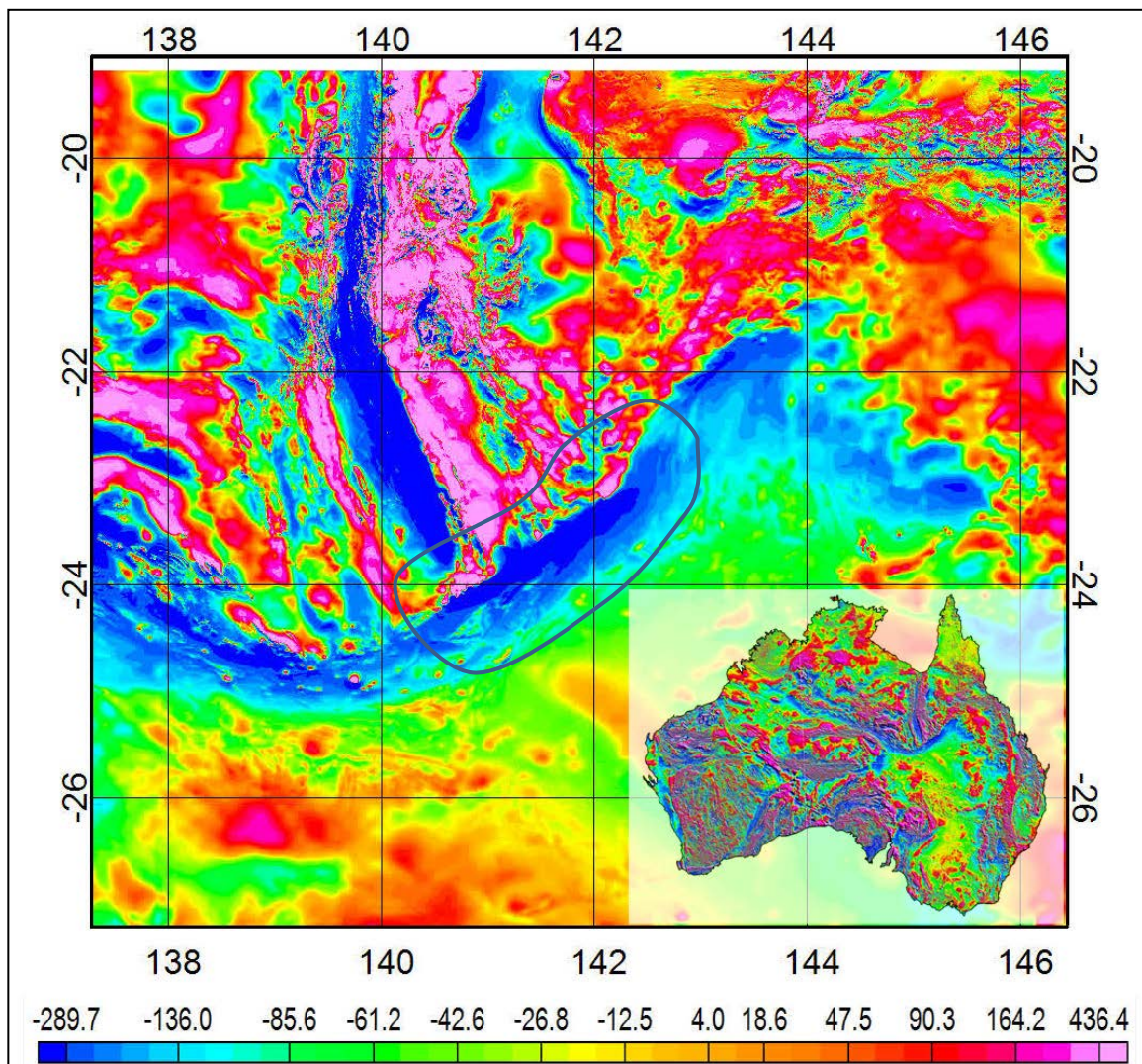


Fig. 6.1 Area of study over a TMI magnetic grid; on the bottom right, TMI magnetic map of the Australian continent. Values in the legend bar are in nT

In this study we use high resolution magnetic and gravity datasets to investigate the architecture of the Cork Fault to constrain the boundary between the Mount Isa terrane and the Thomson

Orogen. Regional potential field datasets have become increasingly used to unravel the crustal architecture of ancient tectonic systems in regions with little or no geological exposure (Betts et al., 2003a; McLean and Betts, 2003). The method, although ambiguous, provides insights into structural architecture and kinematics and can be used to map the geology of buried terranes (Gunn et al., 1997). Forward modelling technique has been undertaken to determine the architecture and kinematics of the Cork Fault and associated structures. The results provide insights in understanding the Precambrian tectonic evolution of the Eastern Australian continent and have implications for unraveling the nature of the deep crust of the Thomson Orogen.

6.2 Regional geology

6.2.1 The Mount Isa terrane

The Mount Isa terrane (Fig. 6.2) forms part of the Palaeoproterozoic North Australian Craton (Betts et al., 2006; Bierlein and Betts, 2004; Giles et al., 2006a; MacCready, 2006a; Spikings et al., 2001). The region has been repeatedly affected by Palaeoproterozoic superimposed rifting and subsidence (Betts et al., 2006; Blake et al., 1990; O'Dea et al., 1997a; O'Dea et al., 1997b) that occurred over basement rocks deformed during the ca. 1900 - 1870 Ma Barramundi Orogeny (Betts et al., 2006; Etheridge et al., 1987; Page and Williams, 1988). The ca. 1800 - 1600 Ma basinal evolution was subsequently ended and deformed by a Mesoproterozoic deformation event (Fig. 6.3) (Betts et al., 2006; Giles et al., 2006b). The exposed Mount Isa Inlier is divided in an Eastern and Western fold belts in which sedimentation and subsequent deformation have been heterogeneous in time and space (Betts et al., 2006; MacCready, 2006a; O'Dea et al., 1997b).

The ca. 1790 - 1730 Ma Ma Leichhardt Superbasin (Fig. 6.3) formed during an E-W crustal extension event (Betts et al., 2006; O'Dea et al., 1997a; O'Dea et al., 1997b) and was characterized by bimodal magmatism and clastic fluvial sedimentation (Jackson et al., 1990; O'Dea et al., 1997b). In the Western Fold Belt, basal deep marine to shallow marine clastic successions was followed by voluminous outpouring of continental flood basalt (Jackson et al., 2000). Overlying the continental basalt are clastic dominated sedimentary packages deposited in a rift environment during N-S extension (O'Dea et al., 1997b). The upper part of the Leichhardt Superbasin is represented by continental shelf and shoreline facies of quartzite – carbonate successions (Betts et al., 2006; O'Dea et al., 1997b).

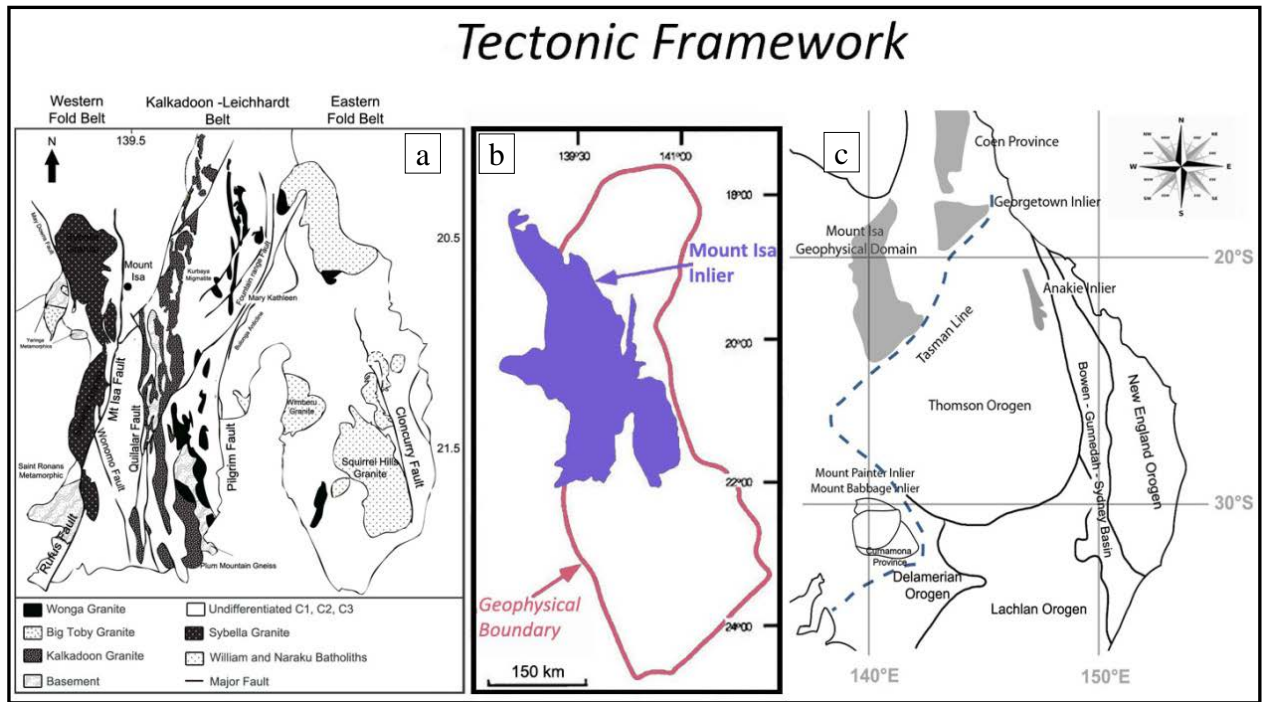


Fig. 6.2 a) Simplified tectonic setting of the exposed southern Mount Isa Inlier; modified from O’Dea et al. (1997b); b) Simplified tectonic map showing the position and extent of the Mount Isa Inlier along with its geophysical domain; c) Distribution of some of the central and eastern Australian orogens; modified from Glen (2005). The coast line is for location purpose only.

In the Eastern Fold Belt, basal felsic and mafic volcanics (Beardsmore et al., 1988; Betts et al., 2006) are overlain by conglomerates and carbonate successions reflecting near - shore depositional environment (O’Dea et al., 1997b). Basin inversion recorded in the Western Fold Belt ended the Leichardt Basin cycle and resulted in development of compressional structures and depositional hiatus (Betts et al., 1999).

A following ca. 1725 - 1690 Ma NW-directed extension marks the imposition of the Calvert Superbasin (Fig. 6.3) (Jackson et al., 2000). The Calvert Superbasin is well represented in the Western Fold Belt and was characterized by significant felsic magmatism and deposition of fluvial to shallow marine rocks on SE-thickening half graben (Betts et al., 1999; Southgate et al., 2000a). A mid-Calvert Superbasin inversion is recorded by uplift and erosion of sedimentary sequences (O’Dea et al., 1997b) and preceded a ca. 1700 to 1690 Ma second phase of NNE-SSW-directed extension (O’Dea et al., 1997b) which resulted in deposition of dominantly siliciclastic successions of conglomerates, sandstones and siltstones deposited in braided stream, alluvial fan to shallow marine environment (Blake et al., 1990; Derrick et al., 1980; Southgate et al., 2000a).

A ca. 1675 Ma switch in the regional extension direction resulted in the development of the Isa Superbasin. The Isa Superbasin is interpreted to reflect a period of thermal subsidence (Betts and Lister, 2001; Betts et al., 2001; Betts et al., 1999) and fault reactivation (Andrews, 1998; Betts, 2001; Krassay et al., 2000; Scott et al., 1998) during NNE-SSW-directed extension (Gibson et al., 2008). The lower part of the Isa Superbasin is represented by ca. 1676 to 1654 Ma (Foster and Austin, 2008) rift-related succession of marine to shallow marine carbonaceous shale, basalts, turbiditic sandstone and siltstone and quartzites successions (Betts et al., 2006; O'Dea et al., 1997b; Page and Sun, 1998). A ca. 1650 - 1630 Ma basin inversion occurred (McConachie and Dunster, 1998; Southgate et al., 2000b) prior to renewed deposition that represents the imposition of the ca. 1630 to 1595 Ma upper Isa Superbasin (Fig. 6.3) (Betts et al., 2006; Southgate et al., 2000a). This stage of the Isa Superbasin development marks the transition from extensional basin system to sag-phase sedimentation (Betts et al., 2006; Hutton et al., 2012) and is characterized by deposition of siltstone, shale, sandstone, conglomerate in the Western Fold Belt and carbonatic rocks, quartzite, sandstone and mafic volcanics in the Eastern Fold Belt (Foster and Austin, 2008; Southgate et al., 2000a).

The Isa Superbasin sedimentation was ended by the ca. 1600 - 1500 Ma Isan Orogeny (Figs. 6.3 and 6.4) (Bell, 1983; Betts et al., 2006; Blake, 1987; Giles et al., 2006b; O'Dea et al., 2006; O'Dea et al., 1997b; Page and Bell, 1986). This shortening event strongly overprinted previous tectonic fabrics and resulted in reactivation of existing normal faults as reverse thrusts (Giles et al., 2006b). The early stage of the Isan Orogeny occurred during a ca. 1600 - 1580 Ma N-S- to NW-directed crustal shortening (Betts et al., 2006; Giles et al., 2006b; O'Dea et al., 2006). The following ca. 1570 - 1540 Ma Middle Isan Orogeny developed through a major E-W crustal shortening event (Giles et al., 2006b; O'Dea et al., 1997b). Crustal-scale upright folds and major N-S-trending reverse faults and thrusts were imposed at this time (Giles et al., 2006b; MacCready et al., 1998). The subsequent wrenching tectonic stage defined the transition from ductile folding to brittle deformation (Giles et al., 2006b; O'Dea et al., 1997b). The ca. 1530 to 1500 Ma final stage of the Isan Orogeny is characterized by E-W- to ESE-directed deformation (Betts et al., 2006) and emplacement of A-type and I-type granites in the eastern part of the exposed inlier (Wyborn, 1998).

The Mount Isa terrane is considered to be cratonised after the Isan Orogeny and the architecture of the region has not changed since the Late Mesoproterozoic (Betts et al., 2006; O'Dea et al., 1997b).

6.2.2 *The Thomson Orogen*

Neoproterozoic to Ordovician meta-siltstone, quartzite, schist and igneous intrusive rocks of the adjacent Thomson Orogen (Figs. 6.2 and 6.3) (Draper, 2006; Murray, 1994; Murray and Kirkegaard, 1978; Withnall et al., 1995) are concealed by Middle Palaeozoic to Mesozoic sedimentary successions (Glen, 2005; Murray and Kirkegaard, 1978). The basement rocks of the Thomson Orogen deposited predominantly in a deep water environment (Murray, 1994). Initial deposition occurred during the Neoproterozoic to Middle Cambrian (Fig. 6.3) (Draper, 2006; Murray and Kirkegaard, 1978; Withnall et al., 1995). The rock package was subsequently deformed and metamorphosed by Middle to Late Cambrian tectonic event coeval with the Delamerian Orogeny (Draper, 2006; Murray and Kirkegaard, 1978). Renewed deposition and emplacement of volcanic rocks occurred during the Early to Middle Ordovician (Fig. 6.3) (Draper, 2006; Murray and Kirkegaard, 1978). At this time, rocks of north-eastern Australia have been interpreted to represent a back-arc igneous province associated with a convergent margin further east (Fergusson et al., 2007a). Middle Silurian (ca. 428 Ma) felsic magmatism occurred pervasively across the Thomson Orogen (Draper, 2006). The emplacement of intrusive bodies may have occurred during late Benambran contractional deformation (Champion et al., 2009; Draper, 2006) which has been recorded east (Fergusson et al., 2005; Fergusson et al., 2007b) and south (Foster and Gray, 2000; Glen, 2005; Glen et al., 2007b) of the Thomson Orogen. However, Spampinato et al. (Unpublished results-b) suggested that Middle Silurian felsic magmatism might reflect Early to Late Silurian extension due to the retreat of a congested plate margin located further southeast (Moresi et al., 2014). Early Ordovician volcanic rocks underlying the Adavale Basin appear underformed (Draper, 2006) further supporting that the Benambran Orogeny had little significance in the interior of the Thomson Orogen and the region instead might have been in a protracted Ordovician to Late Silurian back-arc setting.

Early Devonian intra-continental trans-tension resulted in the development of the widespread Adavale Basin (Fig. 6.3) (Evans et al., 1992; McKillop et al., 2007). During the Middle Carboniferous the Adavale Basin was deformed and exhumation took place (Finlayson et al., 1990c). The remnant synclinal structures reflecting the deepest sedimentary deposition and recorded in deep seismic surveys (Leven et al., 1990; Wake-Dyster et al., 1983) are termed - from west to east - the Warrabin, Quilpie, Cooladdi and Westgate troughs (Fig. 6.4) (Hoffmann, 1988; Mathur, 1983; Pinchin and Senior, 1982).

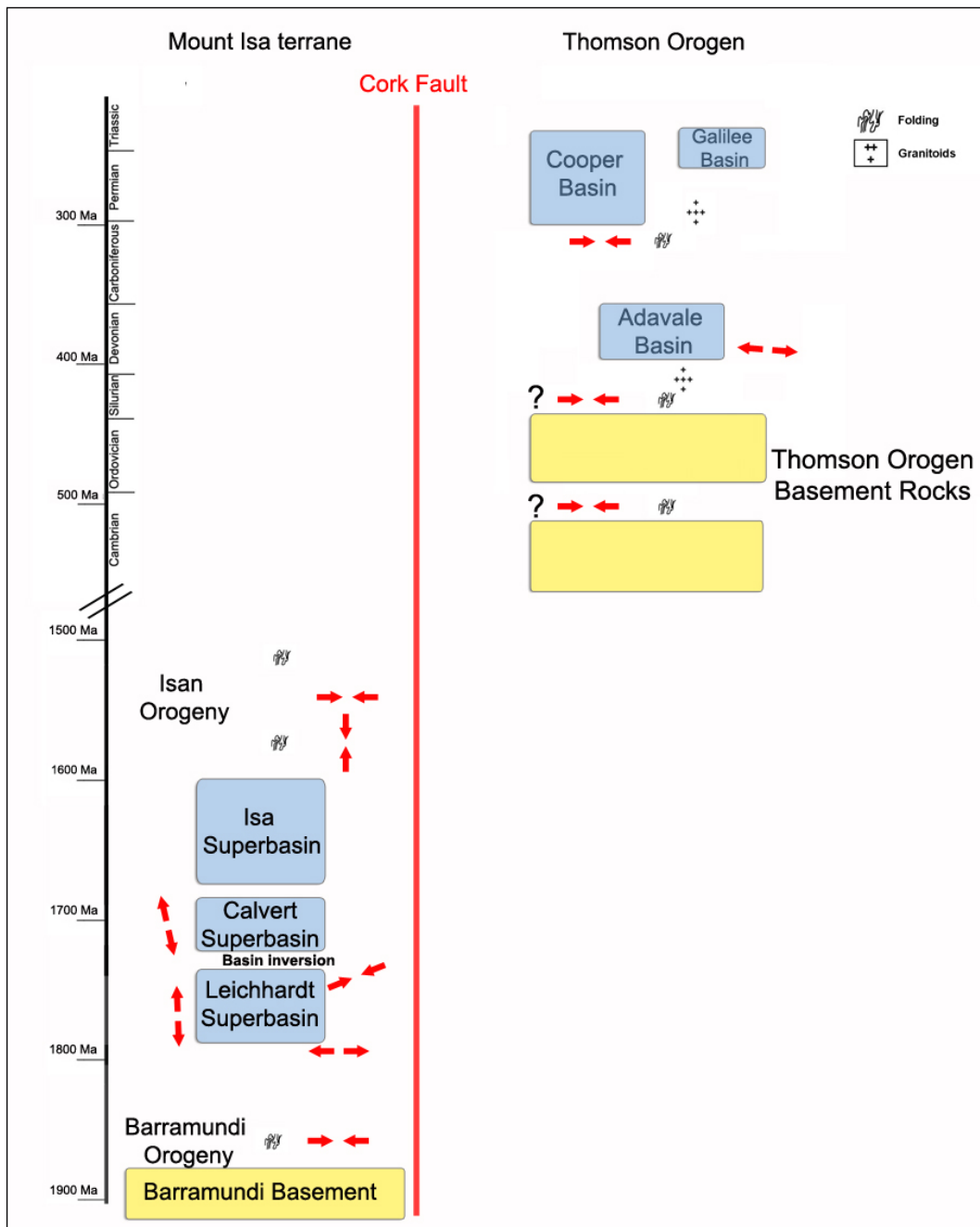


Fig. 6.3 Time - space diagram illustrating the major depositional sequences along the Mount Isa terrane and the Thomson Orogen from the Palaeoproterozoic to Late Palaeozoic; modified from Murray (1990).

A hiatus of ca. 70 Ma separates the Devonian sediments of the Adavale Basin from the Late Carboniferous – Middle Triassic Galilee Basin (Fig. 6.3) (Finlayson et al., 1988). The Galilee Basin is a large intra-cratonic basin which is predominantly filled by fluvial sediments. In the Lovelle Depression (Fig. 6.4) over 700 m of Permian and Triassic sediments accumulated over Precambrian and Early Palaeozoic metamorphic and granitic rocks (Hawkins and Harrison,

1978). The Galilee Basin was inverted during the Hunter-Bowen Orogeny which resulted in the development of large-scale thrust faults (Van Heeswijk, 2010).

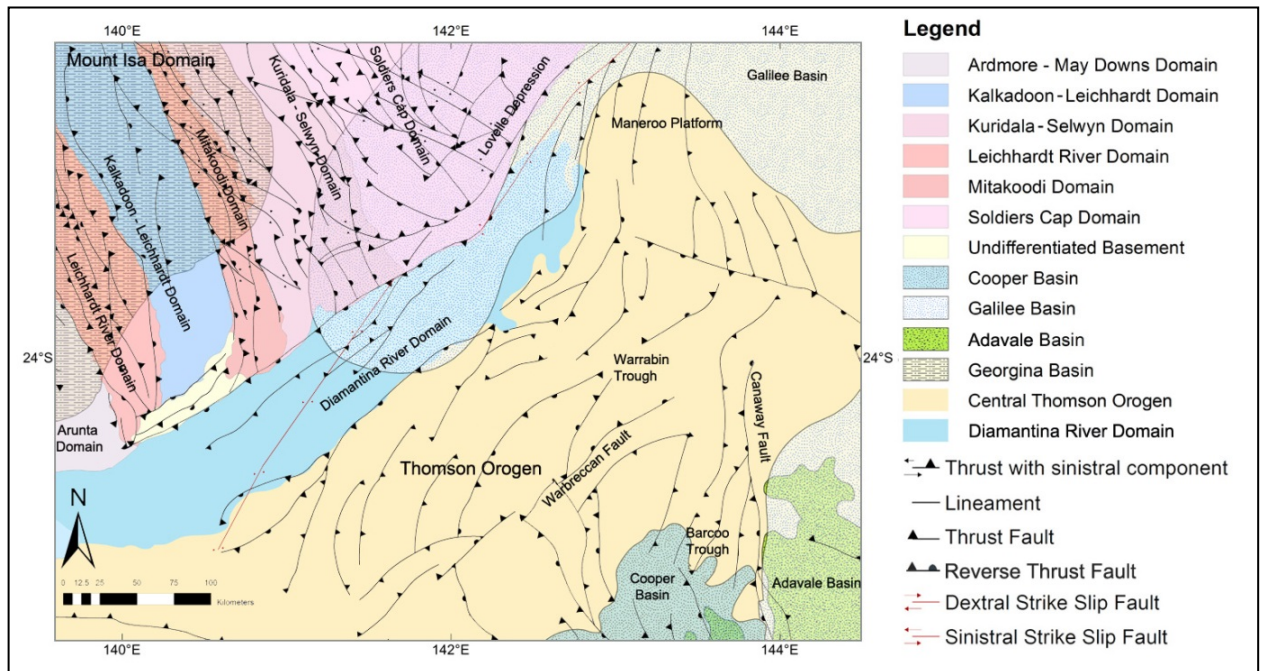


Fig. 6.4 Map of the geological domains and major structural features of the southern Mount Isa terrane and the Thomson Orogen

The Early Jurassic to Late Cretaceous Eromanga Basin unconformably overlies the northern part of the Mount Isa terrane, the basement rocks of the Thomson Orogen, the Devonian sedimentary sequences and the Galilee Basin (Finlayson et al., 1988; Mathur, 1983; Senior, 1978; Spence and Finlayson, 1983). Terrestrial to shallow marine sedimentary rocks of the Eromanga Basin extend over an area of approximately 1,200,000 km² and have been affected by minor deformations associated with Cenozoic compressive events which mostly reactivated the existing fault architecture (Leven et al., 1990; Moss and Wake-Dyster, 1983).

6.3 Previous geophysical surveys

6.3.1 The Mount Isa terrane

In 2006 deep crustal seismic reflection survey was undertaken along six transects across North Queensland (Fig. 6.7). The survey has been conducted by the Geological Survey of Queensland (GSQ), Geoscience Australia (GA), the Predictive Mineral Discovery Cooperative Research Centre and Zinifex Pty Ltd (now OZ Minerals). Signals were recorded to 20 seconds two-way

travel time equating to about 60 km in depth. The aim was to determine, among other goals, a geodynamic framework of the North Queensland (Murray, 2007). In addition, two previous transects from the Mount Isa deep seismic lines shot by the Australian Geological Survey Organisation in 1994 were reprocessed to standardize the methodology and uniform the available data.

The Mount Isa terrane is characterized by weakly reflective and seismically homogeneous crust extending to ~55 km depth (Korsch et al., 2012). The region can be divided in two broad tectonic domains having contrasting tectonic styles and regional vergences (Fig. 6.5) (Betts et al., 2006; MacCready, 2006a; O'Dea et al., 1997b). The Eastern Fold Belt is characterized by west-directed deformations located above the crystalline basement rock (MacCready, 2006a). The Western Fold Belt instead shows east-directed deformations that affect the basement rocks (MacCready, 2006a). Seismic data indicate that major fault zones - including the west-dipping Mount Isa, Rufus and Quilalar faults in the Western Fold Belt (Korsch et al., 2008; O'Dea et al., 1997a) and the east-dipping Pilgrim and Cloncurry faults (Austin and Blenkinsop, 2010; Blenkinsop et al., 2008) in the Eastern Fold Belt - controlled the architecture of the area (Figs. 6.2 and 6.5). They are interpreted to represent major structures that accommodated the Late Palaeoproterozoic basinal deposition and were reactivated as reverse thrusts during the Early Mesoproterozoic Isan Orogeny (Betts et al., 2006; Blenkinsop et al., 2008; Gibson et al., 2006; MacCready, 2006a; O'Dea et al., 1997b).

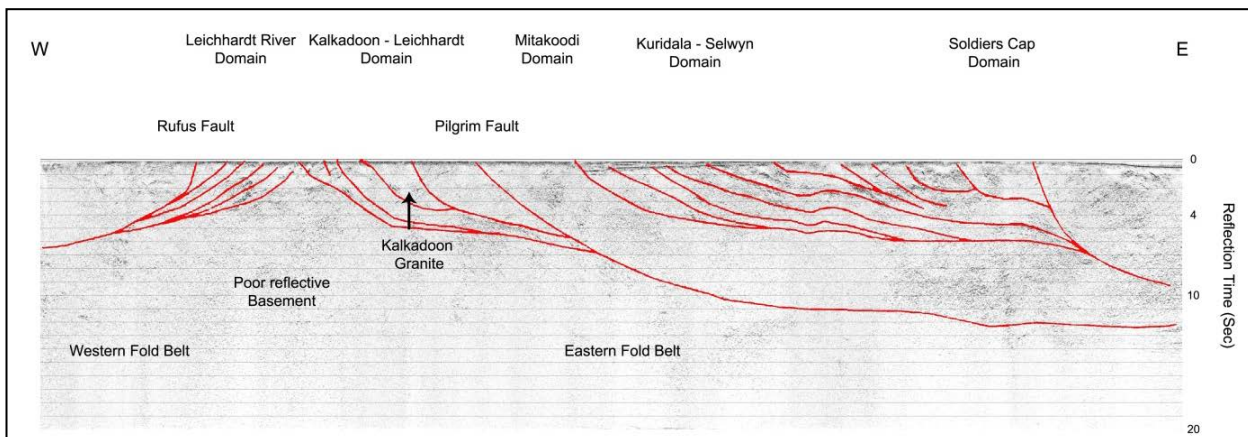


Fig. 6.5 interpreted seismic transects 06GA-M6; modified from Korsch et al. (2008)

6.3.2 The Thomson Orogen

Over the period 1980 - 1986 the Australian Bureau of Mineral Resources (BMR) recorded deep reflection surveys across the central part of the Eromanga Basin (Fig. 6.7). The results provided new insights into the crustal architecture of the Thomson Orogen (Fig. 6.6). 1,400 km of new seismic reflection data were obtained and 2,300 km of existing data over the Eromanga Basin were reprocessed (Moss and Wake-Dyster, 1983; Wake-Dyster et al., 1983).

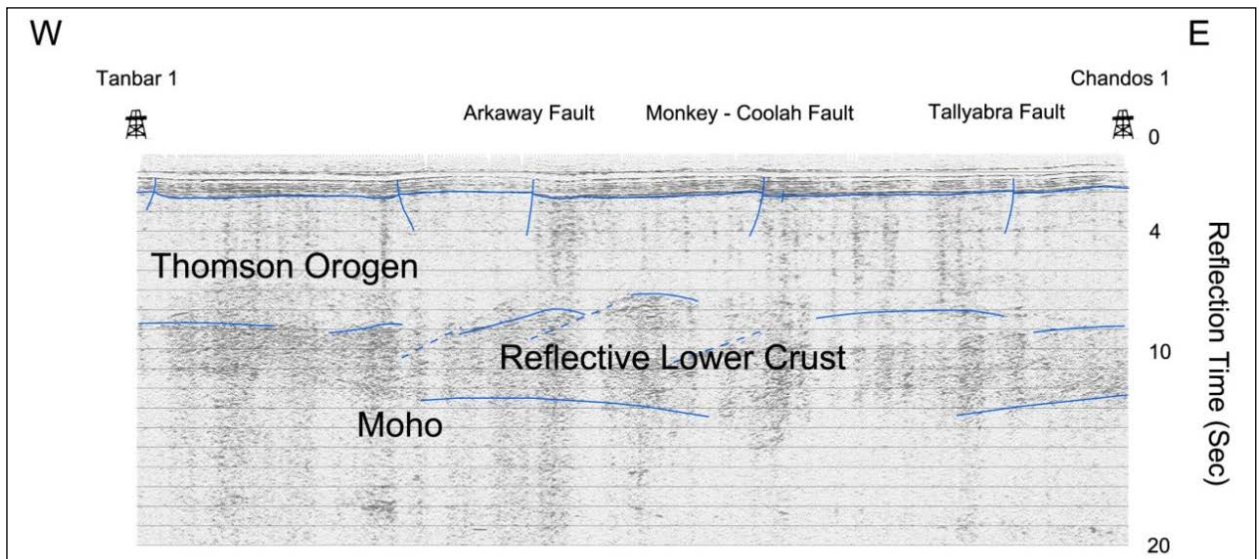


Fig. 6.6 Deep Seismic Traverse n. 3 of the BMR Central Eromanga deep seismic sections along with the main structures; modified from Finlayson et al. (1990b)

Seismic data indicate that high angle thrust faults form the dominant deformation style (Finlayson et al., 1988). The top reflective zone at 1-2 seconds represents the shallow sedimentary sequences (Fig. 6.6) (Pinchin and Senior, 1982). The underlying basement rocks show heterogeneous seismic fabric and have been divided in a non-reflective upper crust extending between 2.5 and 8 seconds and a reflective lower crust between 8 and 12 seconds (Fig. 6.6) (Finlayson et al., 1990b; Finlayson et al., 1990c; Mathur, 1983, 1984, 1987). The bottom zone with no reflections and refraction velocities of 8.2 km/s is interpreted to represent the seismically homogeneous upper mantle (Mathur, 1983). The non-reflective character of the upper crust may be due to the severe deformation of meta-sedimentary and meta-volcanic rocks (Lock et al., 1986; Mathur, 1983; Spence and Finlayson, 1983). Mathur (1983) and Finlayson (1983) suggested that the reflectivity in the lower crust may be due to mafic intrusions related to an extensional event in the Early and Middle Palaeozoic. Glen et al. (2013) suggested that the

lower crust may represent igneous oceanic crust that floors most of the Lachlan Orogen in the southern Tasmanides (Fig 6.2c).

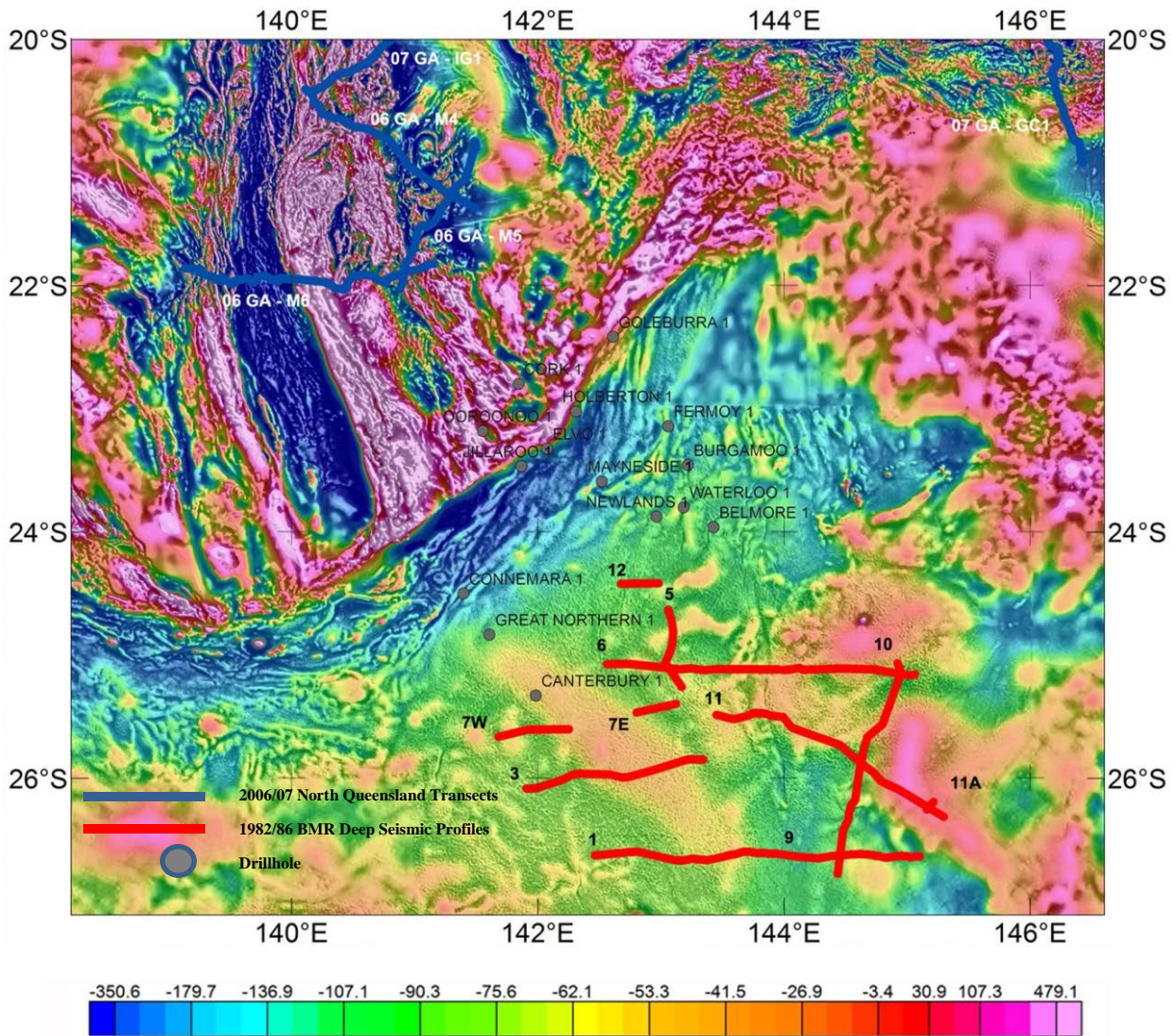


Fig. 6.7 Location of some of the 2006 Deep Seismic Transects crossing the Mount Isa terrane; 1980-1984 BMR Central Eromanga deep seismic reflection profiles crossing the Warbreccan structure, the Canaway Ridge and Devonian sedimentary sequences in the area of study; constraining drill holes over a composite RTP and tilt derivative magnetic map. Values in the legend bar are in nT; modified from Korsch et al. (2009).

6.3.3 The Cork Fault zone

The architecture of the deep crust along the Cork Fault zone is unresolved because there are no deep seismic transects crossing the structure. However, several 4 seconds two-way travel time

seismic surveys have been conducted in the region for oil exploration purpose and a number of them cross the Cork Fault, providing insights into the shallow tectonic setting of the fault.

In the 1980's, Esso Australia recorded 6,436 km of lines to investigate the Galilee Basin and the Maneroo Platform of the Thomson Orogen (Fig. 6.8). In the 1982, Crusader Ltd completed a series of seismic surveys across a portion of the Eromanga – Galilee basins on the down thrown side of the Cork Fault / Holberton Structure complex. Later they undertook seismic surveys in the Galilee – northern Eromanga basins over the plateau area formed by the Nisbet Range and Kangaroo Mountains (Fig. 6.8). The Opalton Seismic Survey operated by Minora Resources NL is located on the western flank of the northern Eromanga Basin, south of the Lovelle Depression within the Galilee Basin and covers an area of 5,990 km².

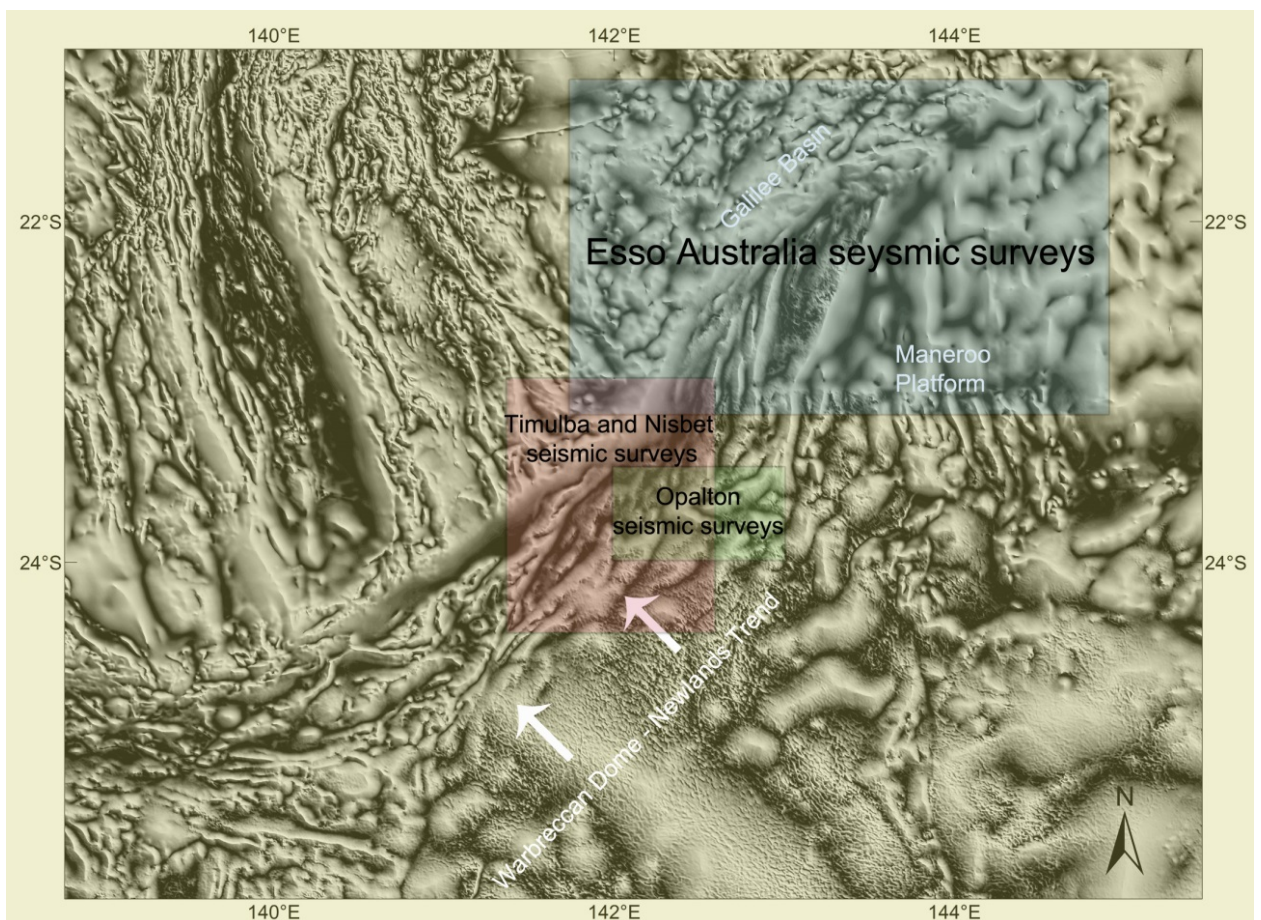


Fig. 6.8 Approximate location of 4 seismic surveys for oil exploration purpose

Within the Cork Fault zone - Diamantina River Domain, the dominant structural grain trends northeast. The faulting pattern is generally more complicated under the basement rocks. The overlying horizons are conformable to the basement but do not show such a high fault rate or

displacement. Faults are often terminated within the basement unit or show minor displacements in the overlying horizons, sometimes deforming last sediment packages through folding, which reflects reactivation episodes.

In the Maneroo Platform (Fig. 6.8), the basement is relatively shallower and is overlain by the Eromanga Basin. In the northern Central Thomson Orogen, the Warbreccan Dome and Newlands Trend (Fig. 6.8) form a prominent NE-trending structure and are flanked to the northwest by reverse faults. The Lovelle Depression is located along the junction of the Mount Isa terrane and the Maneroo Platform (Fig. 6.4) (Hawkins and Harrison, 1978). The NE-trending Cork Fault separates the Lovelle Depression from the Maneroo Platform (Esso_Australia_Limited, 1984). Major movements in Late Carboniferous determined a depocentre that accommodated sedimentation (Esso_Australia_Limited, 1984). The Cork Fault was interpreted to be active during the Early Permian and Late Permian and controlled the deposition of sedimentary sequences (Hawkins and Harrison, 1978). The Cork Fault along with the associated Holberton and Wetherby structures are reflected at surface as westerly-dipping monoclines, which reflects protracted fault reactivation (Esso_Australia_Limited, 1984).

6.4 Methods

6.4.1 Image interpretation

Aeromagnetic and gravity data interpretation is a powerful tool for regional geology and large-scale characterization in regions with little or no geological exposure (Aitken and Betts, 2009; Stewart and Betts, 2010b). The method provides insights into structural architecture and kinematics although it does not have unique solution (Betts et al., 2003b; Stewart and Betts, 2010b). However, geological and geophysical constraints such as seismic data, drill holes, geochemical data and observations in the surrounding areas may reduce significantly the ambiguity.

In 2006 the Geological Survey of Queensland started new acquisition of high resolution gravity and airborne geophysics data throughout Queensland including the Mount Isa terrane and Galilee/Thomson regions. Over 50% of Queensland has been covered by high resolution gravity data having 2 to 4 km station spacing. Aeromagnetic data were collected at a line spacing of 400 m and a ground clearance of 80 m (Chopping and Henson, 2009).

Magnetic and gravity datasets have been processed in order to enhance the geophysical signal and to assist in the geological interpretation. Image processing has been carried out using Oasis Montaj™ which allows viewing and processing of potential field datasets, grids and images within one integrated environment. In a total magnetic intensity grid, the shape of the magnetic anomalies is function of the geometrical and petrophysical properties of the source bodies as well as the inclination and declination of the main magnetic field (the Earth's magnetic field). We have firstly applied a reduced to the pole filter to the TMI grid. This filter reconstructs the magnetic field of a given region as if it were at the pole. As a result, anomalies are brought over their source bodies and their shape can be associated with geometries or variation of magnetic susceptibility of the source bodies. Then we applied a number of filters to the resulted spectrum to enhance the geophysical signal and identify source bodies at different crustal levels. The vertical derivative filter has been applied to better determine the geometries of the source bodies. This filter calculates the vertical rate of change in the magnetic signal. As a result, boundaries between source bodies have been sharpened and have been identified more accurately. The tilt derivative filter calculates the ratio of the vertical gradient and the total horizontal gradient irrespective of the amplitude or wavelength of the magnetic field. This filter was applied to enhance weak magnetic anomalies. The tilt filtered grid has been superimposed onto the vertical derivative grid in order to highlight the structural architecture of the region and to interpret overprinting relationships. Low pass filter has been used to remove the noise that may arise when derivative filters are applied and to retain the longest wavelengths. Structural and lithological maps from image interpretation have been created in ArcGIS environment.

6.4.2 Forward modelling

Forward modelling technique allows testing the validity of the interpretation in 2–2.5 dimensions (Gunn et al., 1997). Geological models have been built using GM-SYS™ Profile Modelling which allows checking the accuracy in real time by comparing the model's gravity and magnetic responses to observed measurements. Cross sections are extracted along selected profiles. Rock packages are then divided in geological units and are assigned unique geometrical and petrophysical properties (McLean and Betts, 2003; McLean et al., 2008). This generates a calculated magnetic and gravity profiles along the cross section which are compared to the observed geophysical response. The parameters are adjusted until the calculated and observed geophysical profiles show an acceptable correlation (Blakely, 1995).

Total magnetic and Bouguer gravity data have been extracted along two selected profiles crossing the Cork Fault. Profile n. 3 lies entirely within the Thomson Orogen (Fig. 6.13). The forward models cover a total linear distance of ~725 km and have been modelled to 50 km depth. The Curie depth varies from ~40 km in the southern Mount Isa terrane to ~24 km in the northern Thomson Orogen (Maule et al., 2009).

Profile n. 3 has been built along the Central Eromanga Deep Seismic Surveys n. 7E and 7W (Fig. 6.13). This constrains the interpretation and provides a-priori structuring of the region. Although the forward models n. 1 and 2 are unconstrained, sparse data provided by drill holes and 4 seconds seismic profiles can be used to gain information about the geometries of the sedimentary succession and the upper basement rocks. Furthermore, the southern ending of the forward model n. 1 intersects the constrained forward model n. 3. The intersection point can be used as a constrained reference point. We have chosen to extend the forward model n. 2 through the Warbreccan – Newlands trend and the Canaway Ridge because the architecture of the latter are well known from seismic imaging (Fig. 6.7), which further constrain the geometries in the forward models.

6.5 Geophysical signature of the region

The magnetic signature of the Thomson Orogen has been described in details by Spampinato et al. (Unpublished results-b) while geophysical interpretation of the southern Mount Isa Geophysical Domain has been carried out by Spampinato et al. (Unpublished results-c).

The Mount Isa terrane shows the highest amplitude geophysical signature (up to 2200 nT and $450 \mu\text{m}^*\text{s}^{-2}$) if compared to the surrounding regions. The adjacent Thomson Orogen is characterized instead by lower magnetic (between 180 and -350 nT) and Bouguer gravity (between 200 and -500 $\mu\text{m}^*\text{s}^{-2}$) amplitudes and smoother texture. The Mount Isa terrane shows a prominent N-S- to NNW-trending structural grain while the Thomson Orogen is characterized by a network of NE- and NW-trending anomalies mostly evident in the Bouguer gravity grid (Fig. 6.10). The steep NW-oriented gradients (~150 nT/km and 5 mgal/km) that define the boundary between the two provinces form a prominent feature in both the magnetic and gravity grids (Figs. 9, 10 and 11).

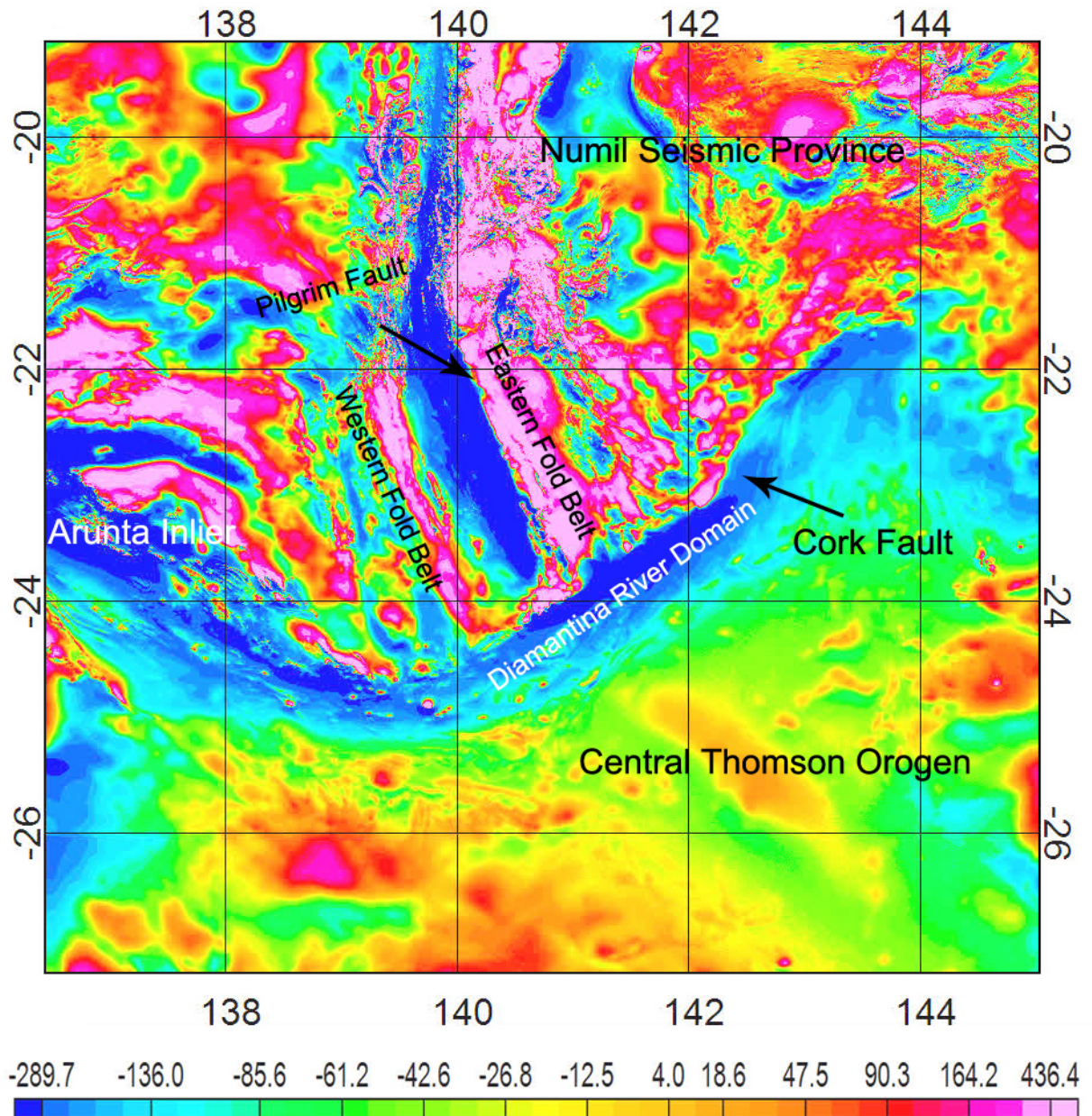


Fig. 6.9 RTP magnetic map of Central Queensland. Values in the legend bar are in nT

Regionally the Diamantina River Domain of the Thomson Orogen shows a persistent low magnetic signature comprised between -100 nT and -350 nT and Bouguer gravity anomalies of up to $200 \mu\text{m}*\text{s}^{-2}$ that decrease to $\sim -350 \mu\text{m}*\text{s}^{-2}$ towards the southeast (Figs. 6.9 and 6.10).

Short wavelength ENE- to NE-trending elongated low density source bodies appear to be discontinuously confined at the southern termination of the Mount Isa Geophysical Domain. They appear to be focused along the northern flank of the Cork Fault (Fig. 6.11). An arcuate NE-trending high gravity belt having amplitudes between 40 and $-60 \mu\text{m}*\text{s}^{-2}$ lies in the northern

Diamantina River Domain and appears to bound the southern flank of the Cork Fault (Figs. 6.10 and 6.11).

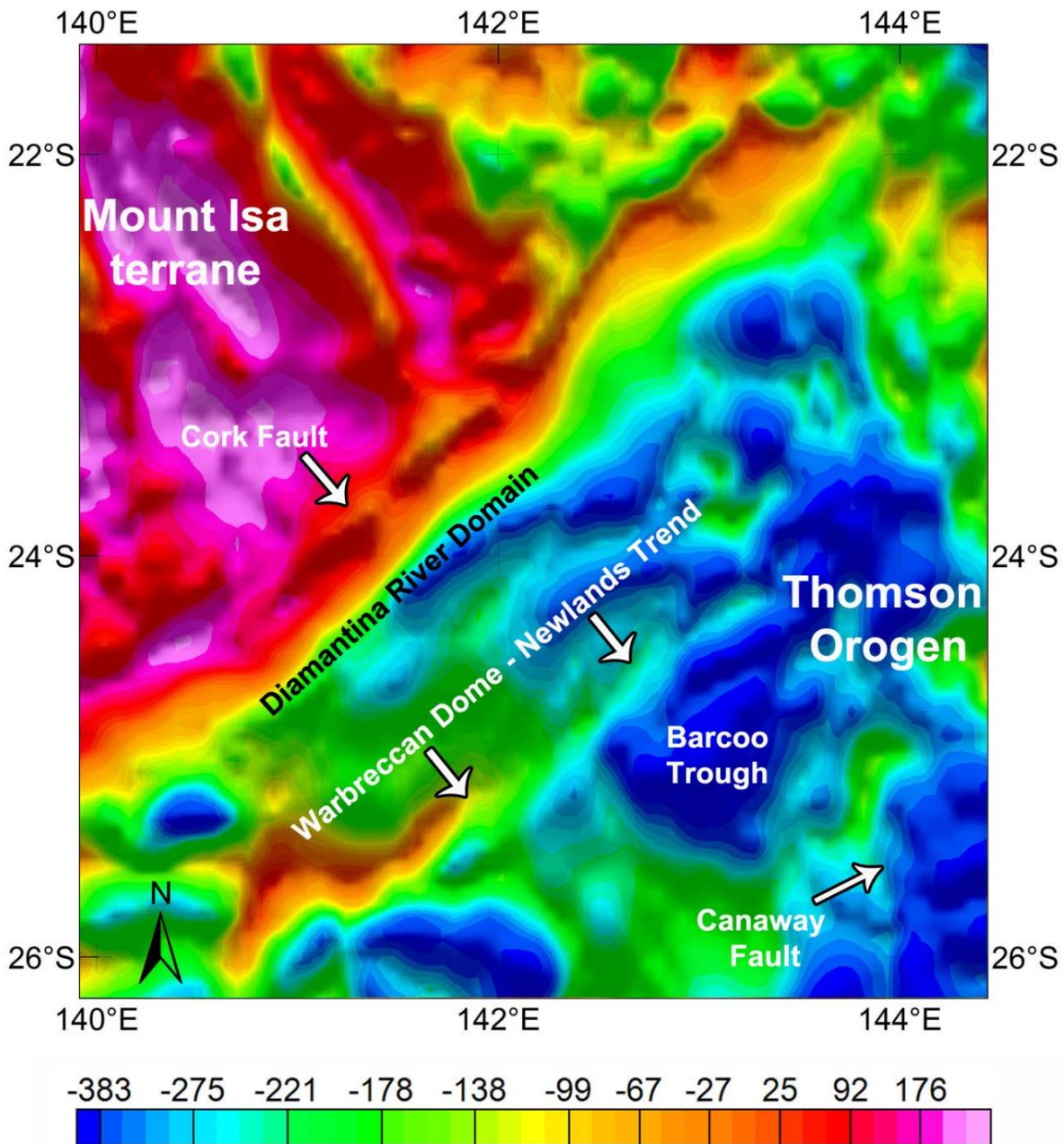


Fig. 6.10 Bouguer gravity map of the boundary between the Mount Isa terrane and the Thomson Orogen. Values in the legend bar are in $\mu\text{m}\cdot\text{s}^{-2}$

Further south, NE-trending structures including the Warbreccan Dome - Newlands Trend are defined by positive Bouguer gravity anomalies with gravity amplitude values between -20 and -260 $\mu\text{m}\cdot\text{s}^{-2}$. On the RTP map, the Warbreccan Dome - Newlands Trend is less well defined and corresponds to increased positive regional magnetic anomalies above -100 nT. The long

wavelength magnetic signature of the Thomson Orogen is punctuated by short wavelength high magnetic and low gravity anomalies reflecting source bodies at shallow crustal level.

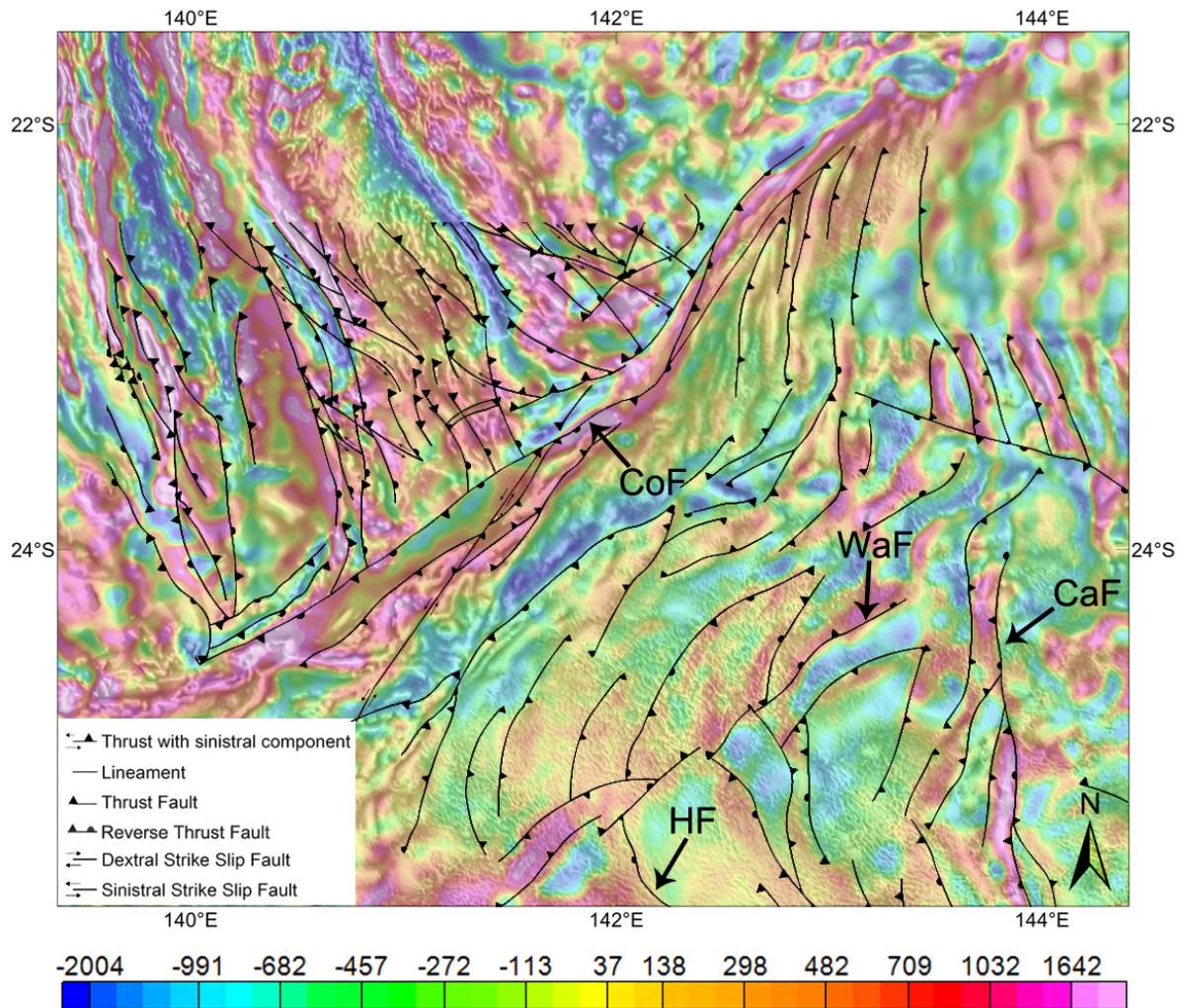


Fig. 6.11 Vertical derivative Bouguer gravity map over a grey tilt and vertical derivative magnetic map of the boundary between the Mount Isa terrane and the Thomson Orogen. CoF= Cork Fault; WaF= Warbreccan Fault; CaF=Canaway Fault; HF=Harkaway Fault. Values in the legend bar are in $\mu\text{m}\cdot\text{s}^{-2}/\text{m}$

6.6 Regional interpretation

Positive stippled geophysical anomalies located to the north of the Cork Fault might represent magnetic rocks of the Mount Isa terrane, which have been intersected by several drillholes at a shallow depth (~1 – 2 km). Spampinato et al. (Unpublished results-c) suggested that the positive magnetic responses of the Mount Isa terrane is mostly due to Barramundi-aged basement rocks and meta-volcanic and meta-sedimentary rocks deposited or emplaced during the Leichhardt Superbasin phase. Regions showing lower magnetic and gravity anomalies may reflect the

distribution of the Calvert and Isa superbasins or shallow granitic intrusions (Spampinato et al., Unpublished results-c). The N-S to NNW structural grain that characterizes the Mount Isa terrane well correlate with major N-S- to NNW-trending fault zones interpreted to accommodate the Palaeoproterozoic deposition and subsequently reactivated as reverse thrusts during the ca. 1600 - 1500 Ma Isan Orogeny (Betts et al., 2006; Giles et al., 2006a; Giles et al., 2006b; O'Dea et al., 2006; Spampinato et al., Unpublished results-c).

The Thomson Orogen is characterized by lower amplitudes and long wavelength anomalies suggesting thicker sedimentary sequences and deeper magnetic source bodies if compared to the Mount Isa terrane. Spampinato et al. (Unpublished results-b) indicated that the lowest gravity response (below $-300 \mu\text{m}^*\text{s}^{-2}$) outlines the distribution of the Devonian basinal sequences while the long wavelength magnetic signature reflects the topography of a magnetized lower crust above the Curie depth.

The steep regional gradients characterizing the Cork Fault reflect high petrophysical contrast between the Mount Isa terrane and the Thomson Orogen. The prominent geophysical signature representing the boundary of the two terranes is likely to reflect either two fundamentally different juxtaposed terranes or the burial of a magnetic crust beneath younger basinal successions. In both cases, the Cork Fault marks a tectonic boundary between the cratonised Proterozoic Mount Isa terrane (Betts et al., 2006) and the Thomson Orogen which was a tectonically active region until the Carboniferous (Murray and Kirkegaard, 1978). ENE- to NE-trending short wavelength positive magnetic and low gravity anomalies bounding the northern flank of the Cork Fault are interpreted to represent granitic intrusions (Fig. 6.12). The source bodies do not trend N-S as does the main architecture of the Mount Isa terrane and it is likely that their emplacement occurred at the time of initiation or reactivation of the Cork Fault. K-Ar analysis on granitic rocks in drill holes CPC Ooroonoo 1 yielded a isotopic age of ca. 858 Ma (Murray and Kirkegaard, 1978), further supporting that post-Mesoproterozoic tectonics affected the southern termination of the Mount Isa terrane, although post-Isan Orogenic events did not change significantly the architecture of the region. The NE-trending high gravity feature lying immediately to the south of the Cork Fault might reflect a belt of shallow basement rocks. The positive gravity belt shows poor magnetic expression, thus it is inferred that the shallow basement of the Diamantina River Domain must be formed by weakly magnetized rocks if compared to the basement rocks of the Mount Isa terrane. The belt of high density rock bounds the prominent Cork Fault and this suggests that the two structures may be related. The positive

regional gravity signature associated with the Warbreccan Dome - Newlands Trend is interpreted to represent shallowing of basement rocks of the Thomson Orogen.

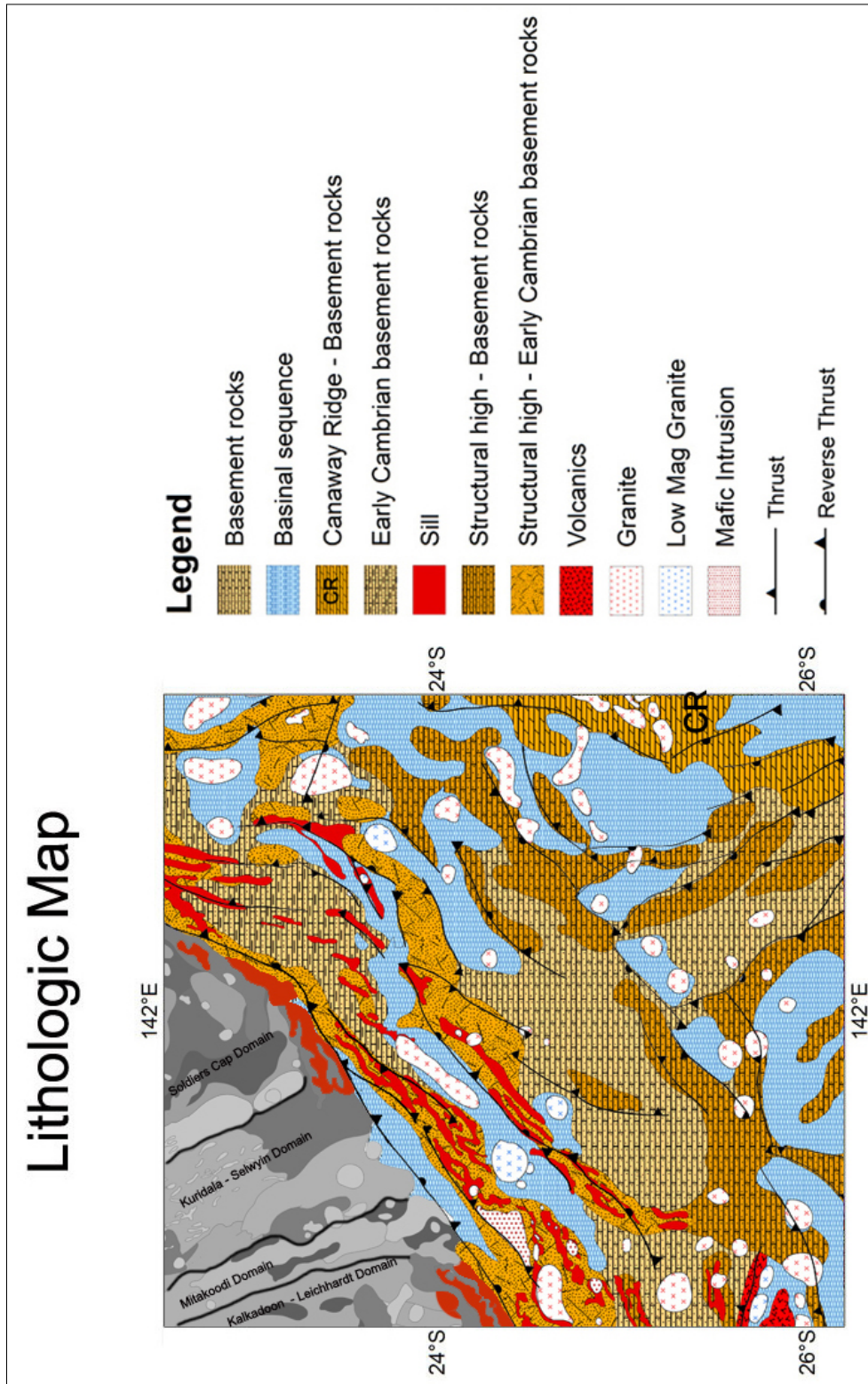


Fig. 6.12 Lithological map at the junction of the Proterozoic Mount Isa terrane and the Phanerozoic Thomson Orogen

Variation in the regional magnetic signature suggests that the latter may represent a major structure within the Thomson Orogen. The NE-trending Warbreccan Dome - Newlands Trend shows the same orientation as the Cork Fault suggesting correlations. Short wavelength positive magnetic and low gravity anomalies focused along NE-trending structures are interpreted to represent granitic intrusions (Fig. 6.12). The orientation of the intrusions suggests that their geometries are controlled by the structural pattern of the area.

6.7 Forward models

The crust and the upper mantle are modelled as six discrete layers. The shallowest geological unit is represented by the sedimentary sequence of the reflective Eromanga, Cooper and Galilee basins (Pinchin and Senior, 1982). Regions showing significant thickening of the sedimentary rocks are inferred to contain remnants of the Devonian sedimentary sequence.

In the Mount Isa terrane, the underlying basement rocks has been sparsely drilled at a shallow level and has been modelled to extend from approximately 1 km to approximately 42 km. The Mount Isa terrane basement crust includes the Barramundi-aged crystalline basement as well as Palaeo- to Mesoproterozoic meta-sedimentary and meta-volcanic rocks, which have been mapped in the exposed inlier (Beardsmore et al., 1988; Blake et al., 1984; O'Dea et al., 1997b) and imaged in the 2006 Deep Seismic Transects (Korsch et al., 2008; MacCready, 2006a). In the Thomson Orogen, the non-reflective layer underlying the sedimentary rocks (Finlayson et al., 1990b; Finlayson et al., 1990c; Mathur, 1983, 1984, 1987) corresponds to the upper basement which extends from ~1 - 4 km depth to a maximum depth of ~20 km. The transition to the lower crust is defined by an increase in reflectivity and seismic velocities (Finlayson et al., 1990b; Finlayson et al., 1990c; Mathur, 1983, 1984, 1987) and has been imaged to extend to approximately 39 - 45 km depth. The underlying upper mantle shows poor reflectivity in both the Mount Isa terrane (Korsch et al., 2012; MacCready, 2006a) and the Thomson Orogen (Mathur, 1983). Deep seismic profiles show that the Moho under the Mount Isa terrane is deeper (~ 42 - 45 km depth) (Korsch et al., 2012; MacCready, 2006a) than beneath the Thomson Orogen (~ 38 - 42 km depth) (Mathur, 1983). NW-oriented forward models n. 1 and n. 2 were created to intersect orthogonally the Cork Fault (Fig. 6.13). The forward model n. 3 is oriented ENE and has been extracted along the 1983 BMR Deep Seismic Transects n. 7E and 7W (Fig. 6.13).

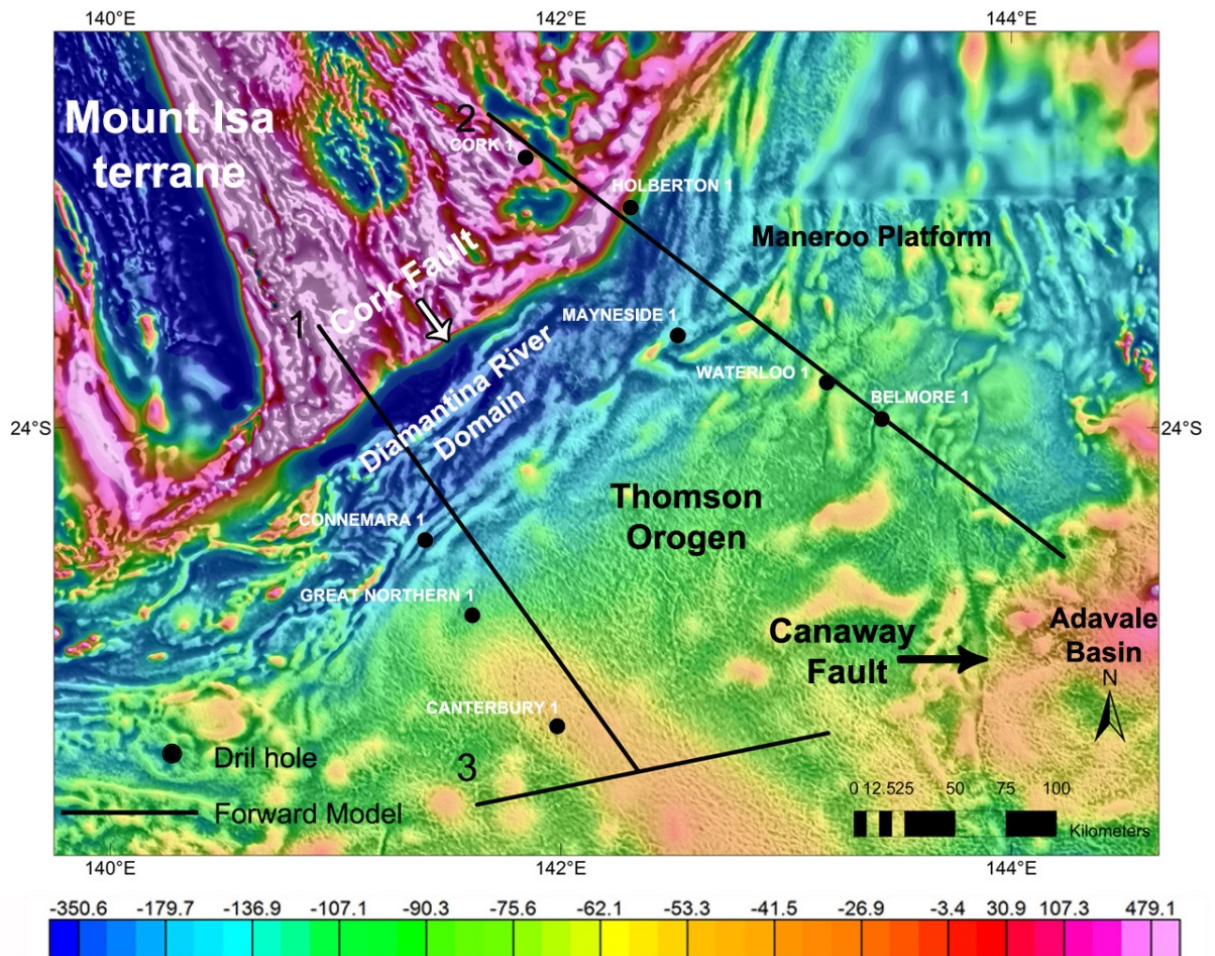


Fig. 6.13 Location of the forward models and constraining drill holes over a composite RTP and vertical derivative map. Values in the scale bar are in nT

6.7.1 Forward model n. 1

Profile n. 1 is ~260 km long and extends across the Cork Fault to intersect the Mitakoodi Domain of the Mount Isa terrane, the Diamantina River Domain and the Warbreccan Dome - Newlands Trend of the Central Thomson Orogen. Drillholes GSQ Connemara 1, AEI Great Northern 1, IOR Canterbury 1 and the 1983 BMR Deep Seismic Transects n. 7E and 7W (Figs. 6.7 and 6.13) constrain the profile.

Regional Bouguer gravity anomalies comprised between 26 and -27 mgal (260 to $-270 \mu\text{m}^*\text{s}^{-2}$) decrease towards the southeast with a gradient of ~ 0.5 mgal/km ($5 \mu\text{m}^*\text{s}^{-2}/\text{km}$) and correspond to the burying at depth of a dense crust beneath the Thomson Orogen. Relative high wavelength (~ 20 km wide) low gravity signature reflects the thickening of the sedimentary deposition that extends to a max depth of ~ 3.2 km. Major shallowing of the upper basement is located under

positive gravity anomalies and is associated - from south to north - with the Warbreccan Structure (~ -14 mgal equating to $-140 \mu\text{m}^2\text{s}^{-2}$), NE-trending structures in the Diamantina River Domain (~ 7 mgal equating to $70 \mu\text{m}^2\text{s}^{-2}$) and the shallow Mount Isa terrane crust (~ 25 mgal equating to $250 \mu\text{m}^2\text{s}^{-2}$) north of the Cork Fault. The regional magnetic anomalies show a prominent amplitude peak of ~ 820 nT under the Mount Isa terrane. To the immediate south, a steep gradient of ~ 33 nT/km decreasing towards the southeast is interpreted to represent the termination of the Mount Isa terrane crust against the adjacent Thomson Orogen. Beneath the Thomson Orogen, the observed magnetic profile shows amplitudes values of ~ 10 nT and a smooth magnetic signature. Best fit reconstruction suggests that the prominent gradient and the smooth texture represent the displacement and the burying at depth of a magnetic crust, which is petrophysically indistinguishable from the Mount Isa terrane crust.

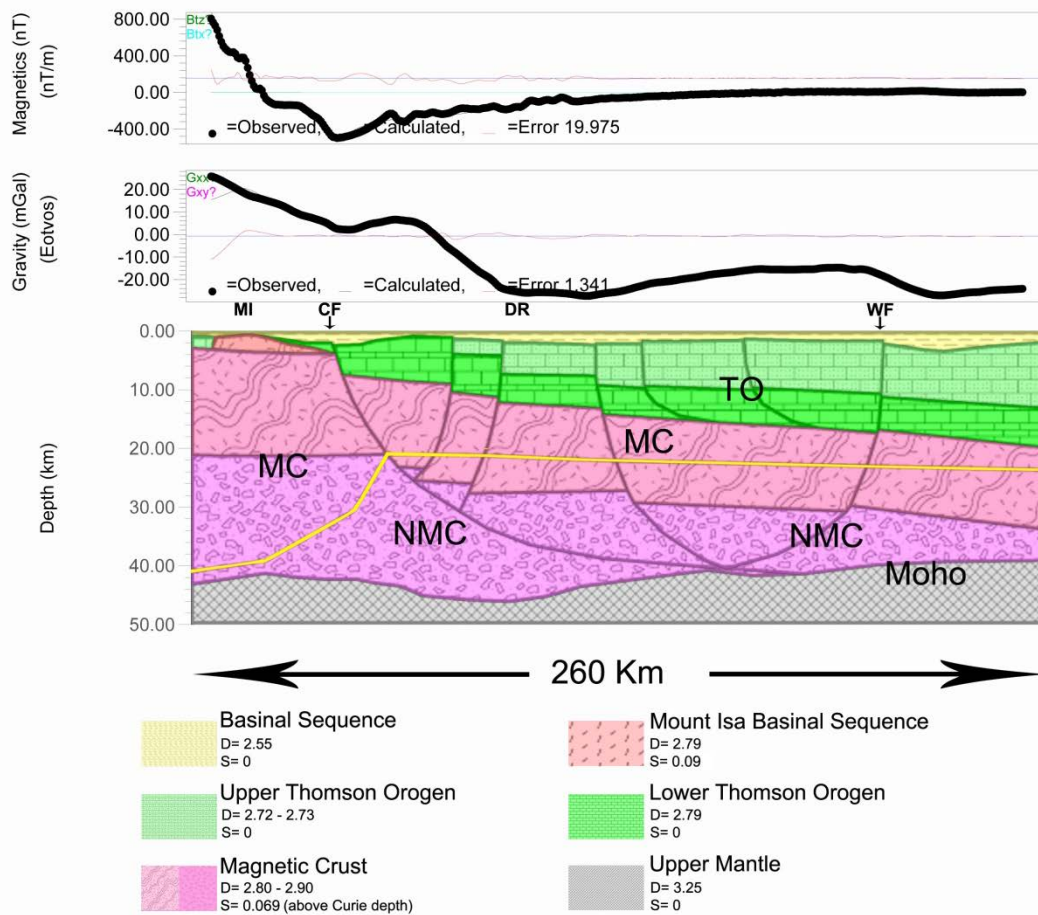


Fig. 6.14 Forward model n. 1; MI= Mount Isa terrane; CF= Cork Fault; DR= Diamantina River Domain; WF= Warbreccan Fault; TO = Thomson Orogen basement; MC= Magnetic crust; NMC= Non-magnetic crust; Yellow Line= Curie depth

Shallowing of the upper basement crust beneath the Thomson Orogen is well represented in the observed gravity profile but show little magnetic expression, suggesting that the upper basement along the profile may be poorly magnetized. The shallowest unit is represented by non-magnetic sedimentary sequences ($D= 2.55 \text{ g/cm}^3$) which conceal the basement rocks. The basement crust under the Mount Isa terrane extends until $\sim 42 \text{ km}$ depth and is magnetized above the Curie depth (0.069 SI). The basement rocks of the Thomson Orogen may be divided in a non - magnetic upper crust ($D= 2.72 - 2.79 \text{ g/cm}^3$), which thickens to the south and extend to a maximum depth of $\sim 19 \text{ km}$ and a magnetized lower crust ($D= 2.80 - 2.90 \text{ g/cm}^3$; $S=0.069 \text{ SI}$) overlying the Moho. The non-reflective upper mantle ($D= 3.25 \text{ g/cm}^3$) is non-magnetic being well under the Curie depth. The Moho regionally deepens from the Thomson Orogen ($\sim 39 \text{ km}$ depth) towards the Mount Isa terrane ($\sim 42 \text{ km}$ depth).

The Cork Fault is modelled as a major high angle south-dipping listric fault. Major high angle structures, including the Warbreccan Fault, displace the entire crust and are modelled to connect into a major detachment surface. Shallow thrusts offset the upper basement of the Thomson Orogen which is reflected as positive gravity anomalies. They have been modelled to lie into the upper crust because they do not appear to affect the regional magnetic signature of the region.

6.7.2 Forward model n. 2

Profile n. 2 is $\sim 310 \text{ km}$ long and it is oriented northwest to intersect the Mount Isa terrane, the Lovelle Depression of the Galilee Basin, the Cork Fault, the Diamantina River Domain, the Adavale Basin and the Canaway Fault within the Thomson Orogen. The drillholes EAL Cork 1, EHN Holberton 1, AAP Mayneside 1, MAN Waterloo 1 and LOL Belmore 1 constrain the geometries of the shallow basement rocks (Fig. 6.13). Although the profile is unconstrained, the Central Eromanga deep seismic profiles n. 2, 5 and 6 (Fig. 6.7) and shallow seismic surveys provide information about the geometries of the Lovelle Depression, Warbreccan Fault, Barcoo Trough and Canaway Ridge and allow a-priori structuring of the region.

The observed gravity profile shows a peak of 15 mgal ($150 \mu\text{m}*\text{s}^{-2}$) under the Mount Isa terrane which regionally decreases towards the Diamantina River Domain with gradients of $\sim 0.3 \text{ mgal/km}$ ($3 \mu\text{m}*\text{s}^{-2}/\text{km}$). This trend is associated with the deepening of the Mount Isa terrane crust towards the southeast. To the south of the Diamantina River Domain, the Thomson Orogen shows gravity anomalies with amplitude values comprised between -13 and -42 mgal (-130 to $-420 \mu\text{m}*\text{s}^{-2}$). The lowest amplitude values reflect regions where the sedimentary sequences are

thicker. The Devonian Barcoo Trough is characterized by gravity anomalies below -30 mgal (-300 $\mu\text{m}\cdot\text{s}^{-2}$). By inference we interpret that regions characterized by low gravity anomalies up to -42 mgal (-420 $\mu\text{m}\cdot\text{s}^{-2}$) reflect significant thickening (up to 4.5 km) of the sedimentary sequences and might contain remnants of the Devonian sedimentary deposition. Positive structures or shallowing of the upper basement under the depositional sequences are associated with positive gravity anomalies with amplitude values comprised between -30 and -13 mgal (-300 to -130 $\mu\text{m}\cdot\text{s}^{-2}$). Positive regional magnetic anomalies having peak amplitudes of ~620 nT decrease towards the southeast. The Cork Fault is associated with a steep gradient of ~20 nT/km decreasing towards the southeast. Such as the profile n. 1, the observed magnetic profile shows smoother magnetic responses under the Thomson Orogen. The forward model indicates that displacement and deepening of a magnetic crust to depth in the Thomson Orogen is appropriate for the geophysical response of the region.

The topography of the upper basement in the Thomson Orogen is well represented by the observed gravity profile but poorly correlate to the magnetic signature along the profile, indicating that its magnetic contribution might be negligible. The shallower unit has been modelled as a non-magnetic depositional sequence ($D= 2.55 \text{ g/cm}^3$) extending up to 3.7 km depth. The shallow basement crust of the Mount Isa terrane (~2 km) extends until ~44 km being magnetized above the Curie depth (0.069 SI). To the southeast, the upper basement rocks of the Thomson Orogen ($D= 2.73$ to 2.79 g/cm^3) have assigned no magnetization and regionally thicken towards the southeast. The magnetic lower crust ($D= 2.80$ - 2.90 g/cm^3 ; $S=0.069$ SI) extends to a maximum depth of ~41 km. Similar to the profile n.1, the lower crust of the Thomson Orogen cannot be petrophysically distinguished from the basement crust of the Mount Isa terrane. High wavelength (~25 km wide) positive geophysical anomalies under the Diamantina River Domain might be due to volcanic intrusions. Our preferred interpretation is that they represent the remnants of the magnetized Proterozoic meta-sedimentary and meta-volcanic rocks of the Mount Isa terrane. The upper mantle ($D= 3.25 \text{ g/cm}^3$) has been modelled to shallow under the Thomson Orogen and is non-magnetic because it lies well under the Curie depth.

Prominent SE- and NW-dipping listric structures are modelled to connect into a major detachment zone possibly extending to the Moho (Fig. 6.15). The Cork Fault is modelled as a high angle SE-dipping fault having listric geometry at depth (Fig. 6.15). Shallow thrusts deform the sedimentary sequence and uplift the upper basement rocks which is reflected as positive gravity anomalies. High angle structures penetrating and offsetting the magnetized crust are

associated with variation in the regional magnetic and gravity signature (Fig. 6.15). Positive gravity anomalies showing poor magnetic expression represent shallow features deforming the non-magnetic upper basement. The connection between the west-dipping Canaway Fault (Finlayson et al., 1988) and a major SE-dipping fault is only apparent in the profile. Uplift of the upper basement and deformation of the sedimentary sequences are interpreted to reflect reactivation of structures that accommodated the deposition. The sedimentary rocks progressively thin towards the Canaway Ridge which is inferred to have been a structural high during the Devonian (Hoffmann, 1989) dividing the depositional sequences of the Barcoo Trough from those in the Adavale Basin.

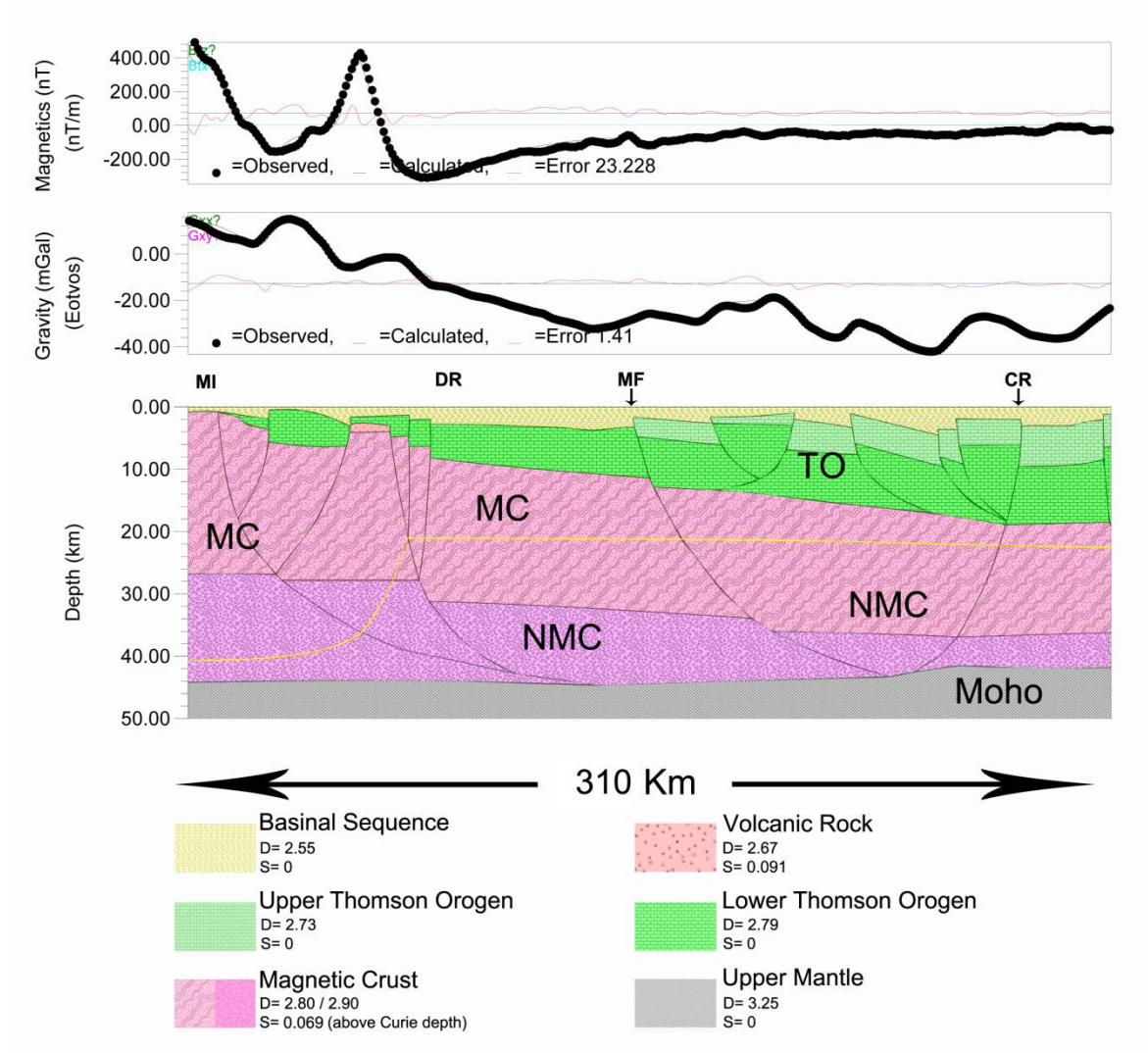


Fig. 6.15 Forward model n. 2; MI= Mount Isa terrane; DR= Diamantina River Domain; MF= Major SE-dipping fault; CR= Canaway Fault; TO = Thomson Orogen basement; MC= Magnetic crust; NMC= Non-magnetic crust; Yellow line= Curie depth

6.7.3 Forward model n. 3

Profiles n. 3 (Fig. 6.16) is ~155 km long and it is oriented east - west to intersect the northern part of the Cooper Basin, the Harkaway and Windorah-Ingella faults. In its eastern part, the profile intersects also the Moothandella Fault, which represents the eastern limit of the Devonian Barcoo Trough. This profile lies entirely within the Thomson Orogen and crosses a major NW-trending magnetic anomaly that is prominent in the RTP magnetic grid (Fig. 6.9). The Deep Seismic Profiles n.7E and 7W have been used as constraints. The Central Eromanga Deep Seismic Transect n. 3 (Fig. 6.6) is located further south and runs parallel to the orientation of the forward model. The seismic profile n. 3 intersects the southern continuation of NW-oriented structures crossing the forward model thus providing additional constraints.

The observed gravity profile shows amplitude values comprised between -16 and -33 mgal (-160 to $-330 \mu\text{m}^*\text{s}^{-2}$) decreasing from west to east with a regional gradient of ~ 0.10 mgal/km ($1 \mu\text{m}^*\text{s}^{-2}/\text{km}$). The regional gravity trend correlates with the deepening of the Moho from 37 to 39 km eastward. Regions showing thicker sedimentary sequences ($D= 2.55 \text{ g/cm}^3$) are associated with lower gravity signature (up to -33 mgal equating to $-330 \mu\text{m}^*\text{s}^{-2}$) while shallowing of the upper basement rocks ($D= 2.73 \text{ g/cm}^3$) are reflected by short wavelength positive gravity anomalies which reflect uplifting occurring along the Harkaway, Windorah-Ingella and Moothandella faults.

The observed magnetic profile (Fig. 6.16) shows a prominent peak with amplitude values of ~ 30 nT having a wavelength of ~ 100 km, decreasing towards the east and west with a gradient of $\sim 1.3 - 1.4$ nT/Km. The seismic profile shows that the lower crust, which extends from $\sim 19 - 22$ km to $\sim 37 - 39$ km, is shallower beneath this prominent magnetic source body. Best fit reconstruction suggests that a magnetized lower crust having a density of 2.82 to 2.92 g/cm^3 and susceptibility of 0.069 SI above the Curie depth is appropriate.

The observed gravity and magnetic profiles show poor correlation. In the western part of the profile, major shallowing of the upper basement is associated with positive gravity signature but corresponds to the lowest magnetic amplitude values. To the centre of the profile, the upper crust appears almost flat, which is reflected by flat trend of the observed gravity profile but regional peak anomalies in the magnetic profile occur. Thus it is inferred that the upper crust has a significantly lower magnetization if compared to the magnetic lower crust and do not contribute to the regional magnetic signature of the region. Positive magnetic shallow granitic rocks ($D=$

2.67 g/cm³; S= 0.037 - 0.069 SI) lying at ~6 to 14 km depth have been modelled to take into account short wavelength variations in the observed magnetic profile. They are associated with low gravity anomalies.

The Harkaway, Windorah-Ingella and Moothandella faults are imaged as high angle west-dipping major structures. They displace the entire crust which is reflected in variation of the gravity and magnetic anomalies and they seem to control the architecture of the region. Minor east-dipping faults have been imaged to connect into major west-dipping faults including the Windorah-Ingella and Moothandella faults, resulting in positive flower structures, which are reflected as relative short wavelength positive gravity anomalies.

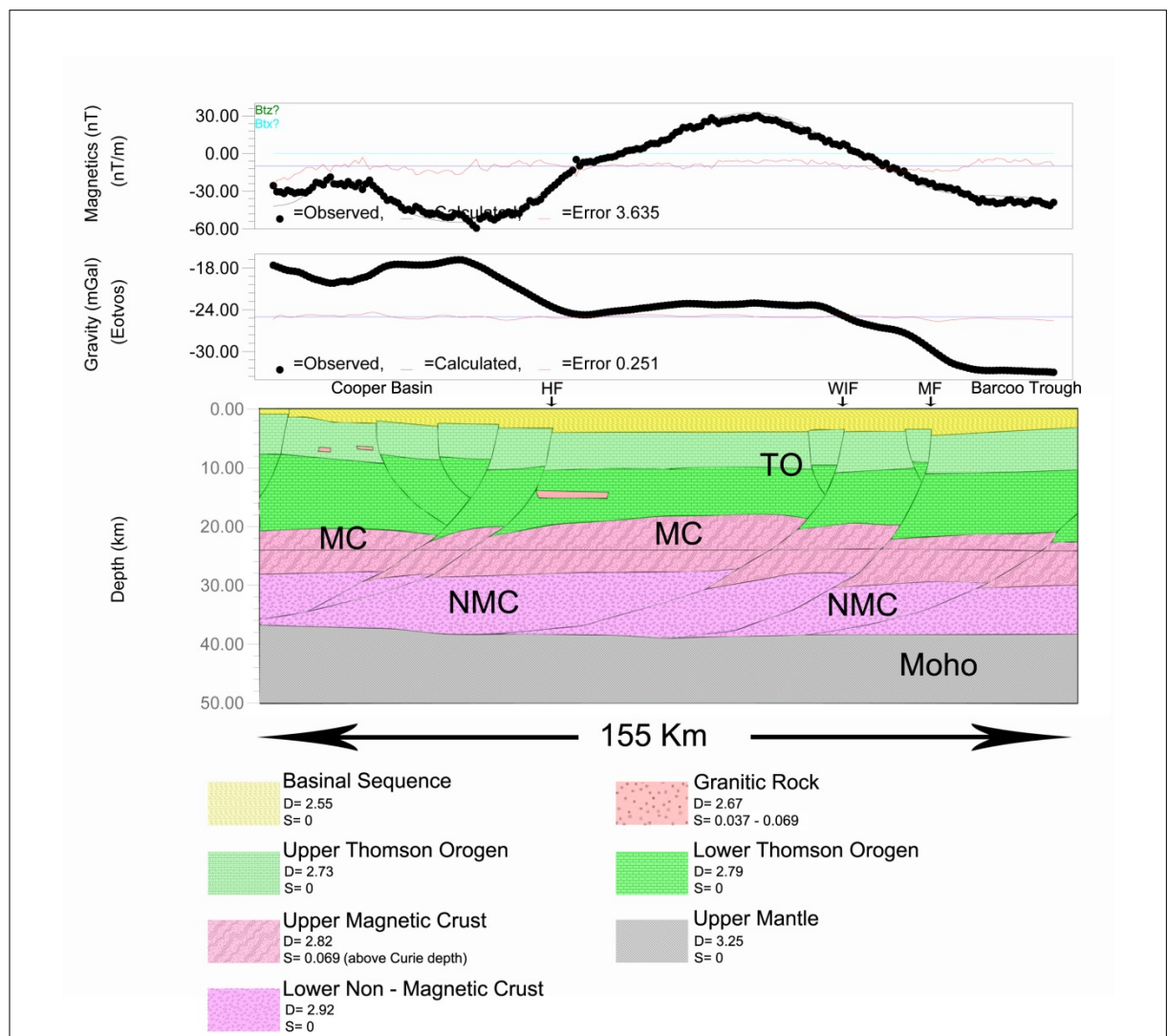


Fig. 6.16 Forward model n. 3; AF= Harkaway Fault; WIF= Windorah-Ingella Fault; MF= Moothandella Fault; TO = Thomson Orogen basement; MC= magnetic crust; NMC= Non-magnetic crust; Curie depth= 24 km

6.8 Validity of the interpretation

The petrophysical properties assigned to the basement crust flooring the Mount Isa terrane and the Thomson Orogen are consistent with previous studies (Goodwin, 1991, 1997, Spampinato et al. in prep. -a,b). The forward models indicate that the basement rocks of the Mount Isa terrane and the lower crust of the Thomson Orogen are petrophysically indistinguishable. The Cork Fault is interpreted to belong to a network of major NE-trending north-dipping and south-dipping listric faults that displace the magnetized Mount Isa terrane crust at depth. The steep magnetic gradients that characterize the Cork Fault result from dislocation of the shallowest portion of the magnetic crust. The burying at depth of the magnetic crust in the Thomson Orogen is inferred to be responsible for the regional smoother magnetic signature of the region. It is thus inferred that the Mount Isa terrane crust is represented under the Thomson Orogen by the lower crust imaged in the Deep Seismic Transects.

The observed magnetic profiles across the Thomson Orogen show poor correlation with the observed gravity profiles. In the Thomson Orogen, variation in depth and displacement of the upper crust does not seem to affect the magnetic trend and has therefore been interpreted to be not significantly magnetic if compared to the Mount Isa terrane crust. The high gravity structural belt that continuously bounds the southern termination of the Mount Isa terrane might represent a NW-dipping fault zone that connects into a major SE-dipping detachment surface. This detachment seems to control the architecture of the area.

The NE-trending Warbreccan Dome - Newlands Trend is interpreted to be a major NW-dipping listric fault that connects into a major detachment surface. This structure is associated with variation of gravity and magnetic anomalies thus it is inferred that displacement of both the upper and lower crust occurs. Geophysical interpretation along with forward modelling suggests that the Warbreccan Dome - Newlands Trend and the Cork Fault might be related.

The crust is concealed by less dense and non-magnetic shallow depositional sequence of the Eromanga, Galilee and Adavale Basin as confirmed by the sparse geological record. The major listric faults appear to control the architecture of the area and have been repeatedly reactivated resulting in vertical variation of offset, which decreases towards the top units as imaged in the seismic data.

6.9 Discussion

The configuration of the Proterozoic supercontinent Rodinia as well as palaeogeographical reconstructions of the Australian continent are based on common geological character, tectonic elements and crustal age of nowadays divided geological provinces (Betts et al., 2008; Karlstrom et al., 2001; Li et al., 1995; Wingate et al., 2002). However, the lack of exposed piercing points along with the intense reworking that the Australian continent underwent adds ambiguities to the Precambrian geodynamic evolution.

6.9.1 Timing of initiation and reactivation of the Cork Fault

The Cork Fault has been interpreted to represent a segment of the much debated Tasman Line (Direen and Crawford, 2003) which broadly divides the Proterozoic provinces of the Australian continent from Phanerozoic rocks of the Tasmanides (Fig. 6.2) (Fergusson et al., 2007a; Glen, 2005; Murray and Kirkegaard, 1978; Veevers, 2000a). Even though the Cork Fault is widely inferred to play a major role during the Neoproterozoic Rodinia break-up (Finlayson et al., 1988; Gunn et al., 1997; Murray and Kirkegaard, 1978; Shaw et al., 1996; Veevers and Powell, 1984) most geodynamic reconstructions of the Proterozoic Australian continent envisage that the Cork Fault was an active feature (Betts and Giles, 2006; Gibson et al., 2008; Giles et al., 2004; Henson, 2011; Williams et al., 2010).

1.6.9.1 Time of initiation: the Palaeoproterozoic Mount Isa – Curnamona Province link

Lithologic, metamorphic and metallogenic similarities as well as common geophysical features recorded in the Mount Isa terrane and part of the Gawler Craton (Fig. 6.17) indicate that the former and the latter - or part of them - might have shared the same tectonic history during the Palaeoproterozoic (Betts and Giles, 2006; Betts et al., 2002; Giles et al., 2004; Henson, 2011). The ca. 1850 Ma Donington Suite recorded in the eastern Gawler Craton forms a huge N-S-trending granitoid belt (Hand et al., 2007) and temporally correlates with the Kalkadoon Batholith (Blake et al., 1990; Page, 1983; Page and Sun, 1998) of the Mount Isa terrane. Giles et al. (2004) argued that the Donington Suite could have formed a continuous belt with the Kalkadoon Batholith. The Palaeoproterozoic superimposed basinal evolution recorded in the Mount Isa terrane can be correlated with sedimentary successions preserved in the Curnamona Province, Georgetown-Yambo-Coen Inliers, Gawler Craton and McArthur Basin (Betts and

Giles, 2006; Giles et al., 2004). The ca. 1700 - 1600 Ma Willyama and Maronan supergroups show remarkable similarities in timing, processes and sedimentary facies (Giles et al., 2004). Both successions were followed by a ca. 1600 - 1580 Ma major tectono-thermal event (Page and Laing, 1992; Page and Sun, 1998) that preceded the Isan Orogeny in the Mount Isa terrane and the Olarian Orogeny in the Curnamona Province respectively (Giles et al., 2004). The timing and the deformation style of the Isan Orogeny and the Olarian Orogeny show striking analogies as well (Giles et al., 2004; O'Dea et al., 1997b).

To honour the geological similarities between the two provinces, Giles et al. (2004) and Betts and Giles (2006) proposed a reconstruction in which the South Australian Craton was rotated 52° counterclockwise about an Euler pole located at 136°E 25°S relative to its current position (Fig. 6.17a). Their reconstruction aligns the Proterozoic orogenic belts occurred respectively during the ca. 1800 - 1700 Ma Strangways - Kimban orogenies (Collins and Shaw, 1995; Parker, 1993), the ca. 1700 - 1600 Ma Early Kararan - Leibig events in the western Gawler Craton and in the southern Arunta Inlier (Daly et al., 1998) and the ca. 1610 - 1500 Ma Olarian and Isan orogenies (Betts et al., 2002; Betts et al., 2006; Giles et al., 2004).

Henson et al. (2011) observed that the shape of the boundaries that truncate the southern Mount Isa terrane - Arunta Province and northern Curnamona Province are superimposable. They inferred that a N-S structural grain characterizes both provinces and suggested that the Curnamona Province can be simply translated and restored next to the Mount Isa terrane (Fig 6.17b). In their reconstruction, the Curnamona Province and the Mount Isa terrane are not directly juxtaposed since it is inferred that the two provinces may have been separated by attenuated crust. However, structures that reflect the V-shaped geophysical signature may belong to different tectonic processes. The north-western structural grain of the southern Arunta Inlier might have been imposed during the Aileron Event and Alice Springs Orogeny (Collins and Shaw, 1995; Floettmann et al., 2004; Lechler and Greene, 2006; Shaw et al., 1984). The Cork Fault may represent a long-lived tectonic element and might have played a major role during the Rodinia break-up (Draper, 2006; Finlayson et al., 1988; Glen et al., 2010; Murray and Kirkegaard, 1978). NE-trending faults that characterize part of the Thomson-Lachlan Orogen might have been imposed during the Late Neoproterozoic to Early Cambrian and were possibly reactivated during the Phanerozoic (Apak et al., 1997; Gatehouse, 1986; Greenfield et al., 2011; Sun, 1997).

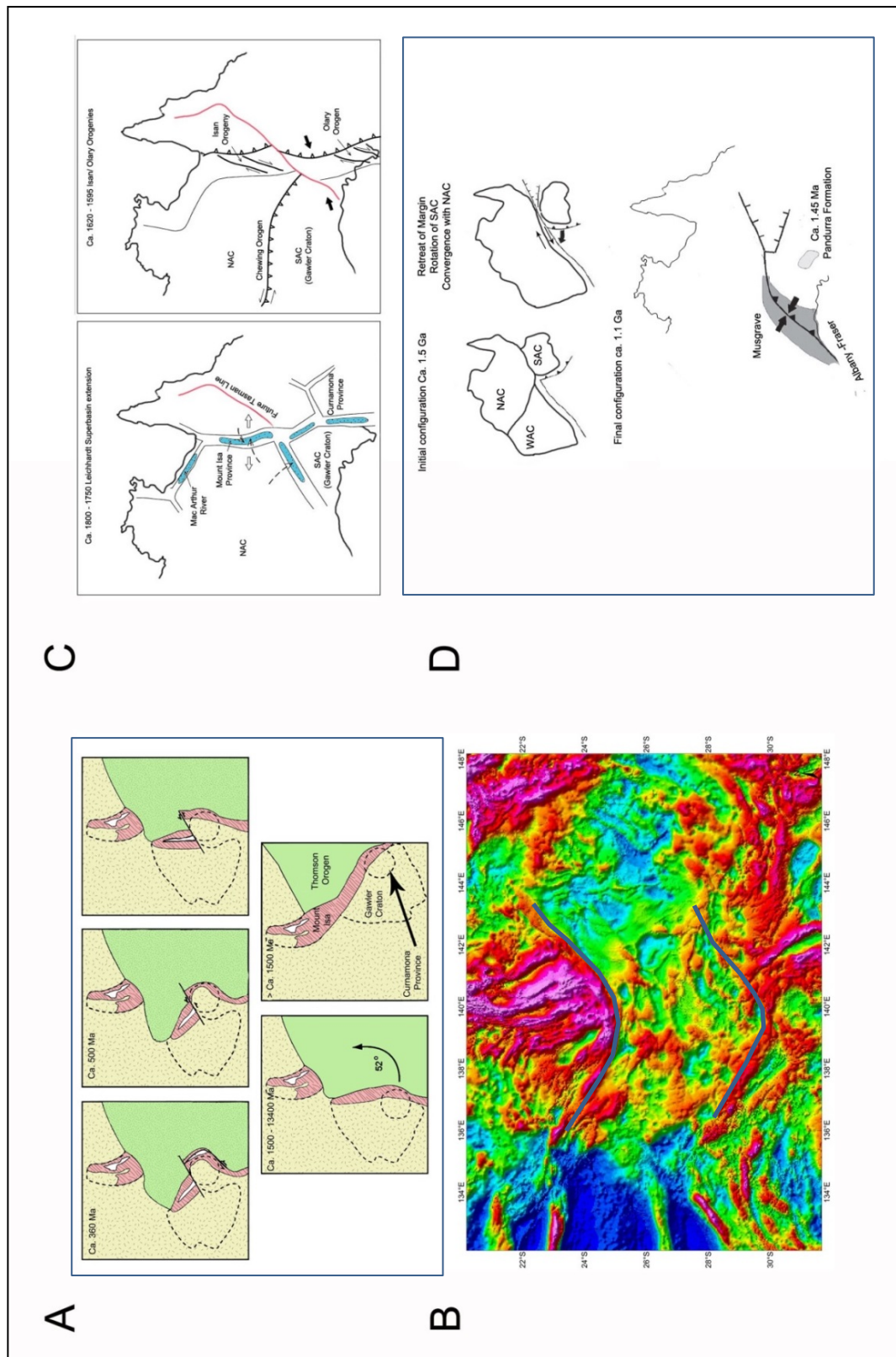


Fig. 6.17 Mid-Proterozoic Reconstruction of the Australian continent after a) Giles et al. (2004); modified from Williams et al. (2010); b) Henson (2011) c) Gibson et al. (Gibson et al., 2008) d) Betts & Giles (2006)

Gibson et al. (2008) indicated that there is no need for the Mount Isa terrane and the Curnamona Province to be contiguous during the Palaeoproterozoic and suggested that the two terranes occupied different part of a single continental scale rift system that extended from northern to southern Australia from ca. 1800 Ma to 1640 Ma (Fig. 6.17c). In this scenario, the Cork Fault acted as a transfer fault and was an active feature during the Mesoproterozoic Isan Orogeny.

Although the three models contemplate different kinematics, the Cork Fault is inferred to represent a major feature active at the time of the Middle Proterozoic continental reorganization. Our interpretation supports the model proposed by Betts & Giles (2006). In this context, the Cork Fault initiated as an extensional fault dipping to the south (Fig. 6.17d). Initial N-S to NNW-SSE Crustal separation between the two provinces led to burying of the continental crust at depth and crustal attenuation within the Thomson Orogen (e.g., Spampinato et al., in prep.-a, b). Independent support to this model are given from recent detrital zircon ages, Hf and Nd isotopic data on the ca. 1760 - 1700 Ma cover sequences from the northern and western Gawler Craton which have found that source characteristics are likely to be derived from the North Australian Craton (Howard et al., 2011). That implies that the SAC and the NAC were physically connected at the time of deposition (Howard et al., 2011). Palaeomagnetic data also support Betts & Giles (2006) model, although Wingate and Evans (2003) suggested that the Euler pole should be positioned west of the proposed position. Williams et al. (2010) correlated the interpreted suture along the eastern margin of the Curnamona Province to the Pilgrim Fault of the Mount Isa terrane (Fig. 6.9) where allochthonous crusts were amalgamated to the Australian margin at ca. 2200 - 1850 Ma further supporting Betts & Giles (2006) model.

2.6.9.1 Neoproterozoic reactivation

Geological evidence indicates that the Thomson Orogen was a tectonically active area during the Rodinia break - up (Fergusson et al., 2007a; Glen, 2005; Murray and Kirkegaard, 1978). Early to Middle Cambrian deposition is recorded in the adjacent Anakie Inlier (Anakie Metamorphic Group) and Charters Towers Province (Wynyard Metamorphic) (Fergusson et al., 2001; Fergusson et al., 2007a; Withnall et al., 1995). Middle Cambrian deformation occurred in the northern Thomson Orogen and post-dates deposition of pre-Delamerian sedimentary successions (Draper, 2006; Murray and Kirkegaard, 1978; Spampinato et al., Unpublished results-b). Finlayson et al. (1988) suggested that the major NE-trending structures of the Thomson Orogen - including the Cork Fault - initiated during the Late Neoproterozoic and are associated with SE-

directed rifting. Spampinato et al. (Unpublished results-b) correlated the Neoproterozoic architecture of the western Thomson Orogen and the south-eastern Arunta Inlier (Greene, 2010) and indicated that the Rodinia break-up might have occurred further east to the Thomson Orogen, which instead recorded the interior extensional architecture in response to a NE-directed extensional event. In their model, the Cork Fault might have been reactivated as a Neoproterozoic strike-slip fault. If this model is correct, the NW-trending structural grain in the western Thomson Orogen reflecting west-dipping structures imaged in the forward models and the BMR Deep Seismic Surveys, might have occurred at this time.

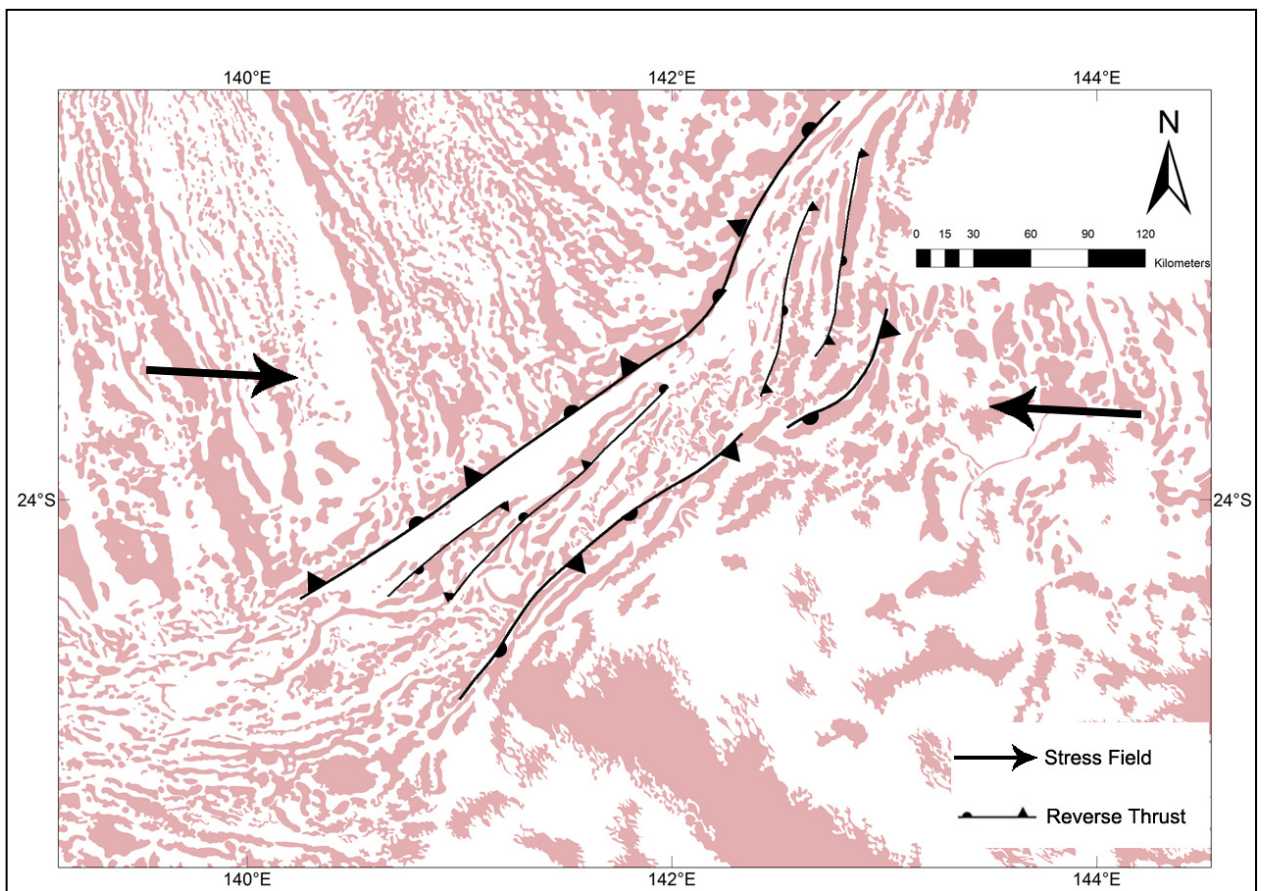


Fig. 6.18 Sketch showing the inferred Early Cambrian shortening event within the Diamantina River Domain

Steeply dipping slate, phyllite and quartzite were intersected in several wells located over the NE-trending high gravity belt associated with the Warbreccan - Newland Structure and in the Maneroo Platform (Murray and Kirkegaard, 1978). Rb – Sr and K – Ar isotopic date on basement phyllite in AAP Fermoy 1 gave Cambrian age (Harding, 1969; Murray and Kirkegaard, 1978). Late Cambrian crustal shortening is recorded in the Anakie Inlier and Charters Tower Province

further to the east (Fergusson et al., 2001; Fergusson et al., 2007a; Withnall et al., 1995; Withnall et al., 1996). This suggests that a deformational episode coeval to the Delamerian Orogeny affected the northern Thomson Orogen (Draper, 2006; Spampinato et al., Unpublished results-b). This tectonic event is interpreted to have initiated or reactivated north-dipping faults that connect to the Cork Fault. The Neoproterozoic to Early Cambrian sedimentary sequences might have been uplifted and deformed resulting in a high gravity belt bounding the Cork Fault. However, the Benambran (?) and Kanimblan orogenies are also likely to have reactivated the existing fault architecture and contributed to the uplift of meta-sedimentary basement rocks of the Thomson Orogen.

6.10 Conclusions

Geophysical interpretation and forward modelling technique across the Cork Fault indicate that the boundary between the Mount Isa terrane and the Thomson Orogen is not sharp. High angle listric faults displace the magnetic crust which gradually deepens toward the southeast. The lower crust of the Thomson Orogen is petrophysically indistinguishable from the continental crust of the Mount Isa terrane. We suggest that the lower crust of the Thomson Orogen is attenuated continental crust with Precambrian affinities.

The timing of initiation of the Cork Fault might be dated to the Mesoproterozoic and may be related to the continental re-organization of the Australian continent that led to the separation of the Mount Isa terrane from the Curnamona Province. The mechanism of separation involves initial N-S to NNW-SSE extension and development of normal faults. During the Rodinia break-up, the Cork Fault might have been reactivated as a strike-slip fault, being in a favourable orientation and formed part of the NE-striking strike-slip faults and NW-oriented normal faults that accommodated the deposition of the Late Neoproterozoic to Early Cambrian stratigraphy. The northern part of the central Thomson Orogen was affected by Early Palaeozoic deformational events. Deformation was controlled by the existing fault network and resulted in the formation of a positive gravity belt that bound the southern termination of the Mount Isa terrane.

The protracted tectonic history of the Cork Fault results in a variety of geophysical responses that should be regarded as the expression of a complex interaction between several geological elements.

Acknowledgement

The 2006 Mount Isa Deep Crustal Seismic Survey (copyright Commonwealth of Australia – Geoscience Australia 2009) was acquired by Geoscience Australia under the Onshore Energy Security Program, in collaboration with the Queensland Geological Survey, the pmd*CRC and Zinifex which are gratefully acknowledged. Geoscience Australia is thanked and acknowledged for access to the Central Eromanga Basin Seismic Surveys (copyright Commonwealth of Australia – Geoscience Australia) which were conducted by The Bureau of Mineral Resources. TMI magnetic and Bouguer gravity grids (copyright Commonwealth of Australia – Geoscience Australia 2009) were thankfully obtained from Geoscience Australia.

Chapter 7: Synthesis and Conclusion

The tectonic evolution of the Mount Isa terrane and the Thomson Orogen spans the Early Palaeoproterozoic to the Late Carboniferous and preserves geological records of a major Palaeoproterozoic continental reorganization as well as the assembly and dispersal of the supercontinents Rodinia and Gondwana. The protracted and poly-cyclic tectonic events have led to a complex structural architecture which is preserved in the basement rocks undercover.

The aims of this research project were to use potential field data to establish a tectonic framework of the southern Mount Isa terrane and the Thomson Orogen, to understand the tectonic processes responsible for the current configuration of the area and to define the architecture and the tectonic significance of the boundary that divides the two regions. Understanding the architecture of the Cork Fault and the nature of the basement crust of the Thomson Orogen has major implications in determining the potential connections of the orogen with north-western Proterozoic regions of the continent, reconstructing the Rodinia break-up and determining the tectonic evolution and time of amalgamation of the Tasmanides of Eastern Australia.

Analysis of potential field data led to a series of interpretations and models. This provided insights into the crustal architecture and kinematics of the region and allowed interpretation of discrete tectonic events.

7.1 Chapter 3 – Tectonic evolution of the southern Mount Isa terrane

The regional N-S- to NNW-trending geophysical anomalies of the Mount Isa terrane extend for ~250 km south of the exposed inlier and are abruptly terminated by the NE-trending Cork Fault. The Palaeoproterozoic depositional sequences and the bipartite regional architecture of the exposed Mount Isa Inlier are interpreted to continue southward under the Palaeozoic cover.

Palaeoproterozoic deposition occurred onto an Early Palaeoproterozoic basement. Polycyclic sedimentary successions were controlled by NNW-trending structures in half graben setting resulting in complex superimposed and stacked basins. Petrophysically constrained geophysical interpretation indicate that the prominent regional magnetic and gravity anomalies of the

southern Mount Isa Geophysical Domain reflect the shallowing of the Pre-1800 Ma crystalline basement and the distribution of metamorphosed sedimentary and volcanic rocks deposited during the development of the ca. 1790 Ma to 1730 Ma Leichhardt Superbasin. Regional low magnetic and gravity responses are inferred to represent the sedimentary successions of the ca. 1725 – 1690 Ma Calvert Superbasin and the ca. 1675 – 1595 Ma Isa Superbasin. The geophysical signature of the region is mostly determined by the distribution of the Eastern Creek Volcanics in the Leichhardt River Domain, the Kalkadoon Batholith, the Mount Guide Quartzite and the Corella Formation in the Kalkadoon - Leichhardt Domain, the Bulonga, Marraba and Argylla Volcanics in the Mitakoodi Domain, the Kuridala Group in the Kuridala - Selwyn Domain, the Soldiers Cap Group and the Numil sedimentary sequences in the Soldiers Cap Domain. Constrained geophysical interpretation suggests that in the Western Fold Belt the sedimentary deposition occurred in half graben and was focussed into the Leichhardt Rift defined by NNW- to N-S-trending west-dipping faults. This structure is interpreted to have been up to 60 km wide and 300 km long and is now preserved in the Leichhardt River Fault Trough. In the Eastern Fold Belt, thick sedimentary and volcanic successions were controlled by major NNW-trending east-dipping normal faults. The geophysical expression of the east-dipping Pilgrim, Overhang, and Cloncurry fault zones extend undercover to the south of the Mount Isa Inlier. They form major structures that controlled the basinal deposition and represent major geological boundaries.

The Isan Orogeny reactivated the existing extensional fault network and determined the current regional architecture which is reflected by the prominent geophysical trend. N-S- to NE-trending thrust faults active during the Early Isan Orogeny are not apparent in the study area, except for the northernmost part of the Kuridala - Selwyn Domain. This suggests that deformations during the Early Isan Orogeny might have been confined to the central and northern part of the Mount Isa terrane. The Middle Isan Orogeny recorded the inversion of major NNW-trending rift faults in a favourable orientation and resulted in regional scale culminations which are reflected in positive NNW-trending gravity and magnetic anomalies. The wrenching phase of the Middle Isan Orogeny is represented by the activation of NW- and NE-oriented strike-slip faults overprinting the prominent N-S- to NNW-oriented structures. The emplacement of NNW-trending low density batholiths is interpreted to be coeval with the ca. 1600 – 1500 Ma Isan Orogeny and may represent the southern extension of the Williams Supersuite.

In the Eastern Fold Belt, the geophysical grids highlight a prominent gravity and magnetic feature that continue undercover and might represent the southern continuation of the suturing between the Mount Isa terrane and the Numil Seismic Province. ENE- to NE-trending geophysical anomalies at the southern termination of the Mount Isa terrane reflect the deposition of rock packages and emplacement of volcanic intrusions. They appear to overprint the prominent NNW trend and it is inferred that they resulted from post-Isan tectonics. The inferred ENE- to NE-trending granitic intrusions and meta-sedimentary sequences focused along the northern side of the Cork Fault are likely to be related to the time of initiation or reactivation of the latter.

7.2 Chapter 4 – Tectonic evolution of the Thomson Orogen

Combined potential field and seismic interpretation indicates that the Thomson Orogen is characterized by prominent regional NE- and NW-trending structural grain with increasing deformation grade eastward. The N-S-trending Canaway Fault appears to divide the Thomson Orogen in two distinctive domains showing different structural grain. The eastern Thomson Orogen is characterized by a prominent NE-trending structural grain and orthogonal faults and fold interference patterns resulting in a series of troughs and highs. The western portion appears as a series of NW-trending structures interpreted to represent reverse thrust faults. The negative gravity anomalies reflect mostly the distribution of the basinal sequences inferred from drill holes and deep seismic surveys. Positive geophysical anomalies correlate with the shallower parts of the basement and are associated with the Warbreccan Dome - Newlands Trend, Maneroo Platform, Yaraka Shelf, Cheepie Shelf and Warrego - Grenfield Structure. They appear to delimit the regional distribution of the Devonian sedimentary rocks which are defined by Bouguer gravity anomalies below -30 mgal and regionally thicken against NE- and NW-trending structures in half graben setting.

The steep regional gradients characterizing the Cork Fault and the persistent low magnetic signature of the Diamantina River Domain reflect high petrophysical contrast between the two regions. Hence, the geophysical signature of the region is likely to reflect either two fundamentally different juxtaposed terranes or the burial of a magnetic crust beneath younger basinal successions. The smooth magnetic signature of the Thomson Orogen is interpreted to reflect significant depths to magnetic sources beneath the non-magnetic Eromanga, Cooper, and

Adavale basins. Short wavelength positive magnetic features that correlate with negative gravity anomalies are interpreted to represent shallower granitic intrusions. They appear to be focused along major faults that might have controlled the locus for magmatism.

Sedimentation and basin development may have initiated during the Neoproterozoic to Early Cambrian in response to a NE- to E-W-directed extension possibly related to the Rodinia break-up. Constrained geophysical interpretation indicates that the Neoproterozoic extension in the Thomson Orogen might have been controlled by NW-oriented rift segments. At this time, it is inferred that the Thomson Orogen was in a continental setting and extension occurred as a distal response to the NE- to E-W-directed Rodinia Break-up which has been recorded further east in the Anakie Inlier and south in the Koonenberry Belt and the Adelaide Fold Belt. This model implies that the Thomson Orogen records the interior extensional architecture during the Rodinia break-up. At this time, the Cork Fault might have been active as a strike-slip fault system. By the Late Neoproterozoic to Middle Cambrian, the Thomson Orogen may have transitioned from a passive margin setting to a continental back-arc setting driven by the roll-back of a NW-dipping subduction zone. This extensional event was followed by Middle to Late Cambrian shortening recorded in the Maneroo Platform and Diamantina River Domain, possibly correlated with the Delamerian Orogeny. The Delamerian Orogeny affected the northern interior of the Thomson Orogen and deformations might have resulted in a dextral shear zone to the immediate south of the Cork Fault. The sparse geological data do not allow determining the effects of the Delamerian Orogeny in the rest of the Thomson Orogen. Renewed deposition and volcanism occurred during the Ordovician that may have continued into the Late Silurian, resulting in thinned Proterozoic basement crust and extensive basin systems that formed in a distal continental back-arc environment. This period of crustal extension correlates with extensional basins that formed in the southern Lachlan Orogen. The intrusion of mid-Silurian granitic bodies, which are reflected in the geophysical grids as short wavelength low gravity and high magnetic anomalies, might have occurred during the retreating of an Early to Late Silurian transitional plate margin. The Devonian Adavale Basin initiated as an extensional basin in a continental setting. At this time, the extension resulted from the interaction of major pre-existing NW- and NE-oriented structures that accommodated the sedimentary sequence. The architecture was shaped by Carboniferous deformation events which resulted in regional-scale folds and widespread erosion.

7.3 Chapter 5 – Nature of the lower crust of the Thomson Orogen

Deep seismic reflections and forward modelling of aeromagnetic and gravity data indicate that the Thomson Orogen can be distinctly divided in a non-reflective and non-magnetic upper basement which underlies the sedimentary sequences and a seismically reflective and magnetized lower basement. The magnetic grid shows smooth texture punctuated by short wavelength positive anomalies which indicate magnetic contribution at different crustal levels. Constrained forward modelling indicates that the regional magnetic signature of the region reflects the topography of the boundary between the upper and lower crusts. It is interpreted that meta-sedimentary and meta-volcanic rocks of the Thomson Orogen may be representative of the upper crust while the lower crust may have a more mafic composition. Best fit reconstruction suggests that the lowest Bouguer gravity anomalies (below -30 mgal) define the distribution of the Devonian sedimentary rocks of the Adavale Basin and the Colladi, Quilpie, Warrabin and Barcoo troughs. The Devonian sequences are bounded by positive gravity anomalies that reflect shallowing of the basement rocks and define NE-trending structures associated with the Maneroo Platform, Warbreccan Dome - Newlands Trend, the Yaraka Shelf, the Warrego Fault and the Nebine Ridge. No obvious correlation occurs between the magnetic signature of the region and the morphology of the upper basement. Short wavelength magnetized source bodies characterized by negative gravity signature are interpreted to represent shallow granitic intrusions.

The tectonic architecture of the region is characterized by major west-dipping and south-dipping high angle listric faults that control the architecture of the basement rocks and the regional distribution of the overlying infra-basins. Major high angle reverse faults penetrate the entire crust, with several extending to, and offsetting the Moho. These faults have a significant influence on the regional gravity and magnetic signature of the Thomson Orogen. Shallow faults do not affect the lower crust, which implies that they terminate at the upper crust, possibly in an upper crustal detachment. Faults offsetting the upper crust result in positive gravity anomalies but have a minimal magnetic expression. The amount of offset decreases towards the shallower Eromanga Basin sequence and suggests multiple reactivation episodes.

The geophysical interpretation indicates that the western and eastern parts of the Thomson Orogen are petrophysically indistinguishable. Forward modelling suggests that the Thomson

Orogen might be a single terrane which shows a fundamentally different structure and seismic character than the southern Lachlan Orogen. Thinned Precambrian crust of the Thomson Orogen may be representative of an Early Palaeozoic continental margin or back-arc setting whereas the Lachlan Orogen formed via incorporation of arc type, oceanic and continental rocks. We interpret that lower basement consists of attenuated Precambrian and mafic enriched continental crust which differs from the oceanic crust of the Lachlan Orogen further south.

7.4 Chapter 6 – The tectonic significance of the Cork Fault

The prominent NE-trending geophysical anomalies that characterize the Cork Fault define one of the major geophysical structures in the Australian continent. The prominent geophysical character is represented by the abrupt termination of positive NNW-trending geophysical features of the Mount Isa terrane against NE-trending low gravity and low magnetic anomalies of the Diamantina River Domain of the Thomson Orogen. The different structural grain of the Mount Isa terrane and the Thomson Orogen suggests a different crustal structure.

Geophysical interpretation and forward modelling technique across the Cork Fault indicates that the boundary between the Mount Isa terrane and the Thomson Orogen is not sharp. Best fit reconstruction suggests that high angle listric faults, including the Cork Fault, displace the magnetic crust which gradually deepens toward the southeast in the Thomson Orogen. The NE-trending Warbreccan Dome - Newlands Trend is interpreted to be a major north-dipping listric fault that connects into a detachment surface. This structure is associated with variation of gravity and magnetic anomalies, thus it is inferred that displacement of both the upper and lower crusts occurs.

The lower basement crust of the Thomson Orogen is petrophysically indistinguishable from the Proterozoic Mount Isa terrane. A structural framework is proposed in which the Cork Fault belongs to a network of major NE-trending north-dipping and south-dipping listric faults that displace the magnetized Mount Isa crust at depth. The prominent gradient associated with the Cork Fault and the persistent low magnetic signature of the Diamantina River Domain may represent the thinning and burying at depth of a magnetic crust with Precambrian affinities under the Thomson Orogen.

Supporting geophysical data indicate that the timing of initiation of the Cork fault might be dated to the Mesoproterozoic. It may be related to the continental re-organization of the Australian

continent that led to the separation of the Mount Isa terrane from the Curnamona Province. It is inferred that the Mesoproterozoic Mount Isa break-up developed through initial N-S to NNW extension. The Cork Fault formed part of a network of north-dipping and south-dipping normal faults active at that time. During the Rodinia break-up, the Cork Fault might have been reactivated as a strike-slip fault system, being in a favourable orientation and formed part of the NE-striking strike-slip faults and NW-oriented normal faults that accommodated the deposition of the Late Neoproterozoic to Early Cambrian stratigraphy. In this context, the Cork Fault is interpreted to represent a fundamental crustal break but does not represent the eastern margin of Rodinia.

The northern part of the Thomson Orogen was affected by Early Palaeozoic deformational events that were controlled by the existing network of major structures. This resulted in uplift of the shallow basement rock in the Diamantina River Domain of the Thomson Orogen. The protracted tectonic history of the Cork Fault results in a variety of geophysical responses that should be regarded as the expression of a complex interaction between several geological elements rather than a simple lineament dividing the Proterozoic and the Phanerozoic Australian continent.

Aeromagnetic and gravity dataset has been proved to be an effective tool to unravel the regional geology of the concealed southern Mount Isa terrane and the Thomson Orogen. Interpretation of potential field data has non-unique solution, however the ambiguity can be significantly reduced when integrating geological data are available. Nevertheless, the method is very effective at constraining the crustal architecture over large areas and no other method provides such a high density data on a regional scale.

In this thesis, high resolution aeromagnetic and gravity data have been successfully applied to unveil the regional geology (chapters 3 and 4), the structural architecture of ancient tectonic systems (chapters 3, 4 and 5) and continental scale structures (chapter 6), the structural setting and associated kinematics (chapters 3 and 4), the basement nature (chapters 4 and 5) and potential geological links (chapters 3, 4, 5 and 6) in regions with little or no geological exposure.

The results of this study established or supported potential links between the basement crusts of the Mount Isa terrane and the Thomson Orogen and provided insights in understanding the Precambrian tectonic evolution of the Eastern Australian continent during the transition from the

Neoproterozoic break-up of Rodinia and the subsequent Phanerozoic evolution of east Gondwana.

Overall, the prominent NNW-trending geophysical anomalies of the southern Mount Isa terrane reflect a complex tectonic evolution that involved poly-cyclic tectonic events including intra-continental rift evolution, basin inversions, intra-plate igneous activity, and poly-phase orogenesis. The architecture and the depositional sequences recorded in the exposed Mount Isa Inlier continue southward in the concealed southern Mount Isa terrane. Palaeoproterozoic sedimentary successions deposited onto an Early Palaeoproterozoic basement. Deposition was controlled by NNW-trending structures in half graben setting, resulting in complex superimposed and stacked basins. The Isan Orogeny reactivated the existing extensional fault network and determined the current regional architecture which is reflected by the prominent geophysical trend.

The NE- and NW-trending structural grain of the Thomson Orogen reflects a different crustal architecture which has been determined from the Neoproterozoic to the Carboniferous. Combined geophysical interpretation and constraining drill holes indicate that meta-sedimentary and meta-volcanic rocks of the Thomson Orogen may be representative of the upper basement. The lower basement may have a more mafic composition and may be formed by thinned Precambrian crust.

Our interpretation places the Thomson Orogen to the west of the Neoproterozoic passive margin, which occurred in the Anakie Inlier. The region is likely to represent the interior extensional architecture during the Rodinia break-up that has been subsequently extensively modified by multiple extensional basin forming events and transient episodes of crustal shortening and basin inversions. In this scenario, the Cork Fault does not define the zone of break-up as has been previously proposed nor is required to represent the boundary between the Proterozoic crust and the Phanerozoic crust of the Australian continent. This implies that the Thomson Orogen differs from the rest of the Tasmanides and the Thomson and the Lachlan orogens are two fundamentally different terranes. Geophysical data show that the Thomson Orogen and the Lachlan Orogen differs in terms of seismic fabric, crustal architecture, crustal nature and deformation style. Amalgamation between the two terrane might have occurred in the Middle Palaeozoic.

REFERENCES

- Aitken, A.R.A., Betts, P.G., 2009. Multi-scale integrated structural and aeromagnetic analysis to guide tectonic models: An example from the eastern Musgrave Province, Central Australia. *Tectonophysics* 476, 418-435.
- Ambrose, G.J., Kruse, P.D., Putnam, P.E., 2001. Geology and hydrocarbon potential of the southern Georgina Basin, Australia. *APPEA Journal* 41, 139-163.
- Andrews, S.J., 1998. Stratigraphy and depositional setting of the upper McNamara Group, Lawn Hills region, Northwest Queensland. *Economic Geology and the Bulletin of the Society of Economic Geologists* 93, 1132-1152.
- Apak, S.N., Stuart, W.J., Lemon, N.M., Wood, G., 1997. Structural evolution of the Permian-Triassic Cooper basin, Australia: Relation to hydrocarbon trap styles. *AAPG Bulletin* 81, 533-555.
- Arkani-Hamed, J., 1988. Differential reduction-to-the-pole of regional magnetic anomalies. *Geophysics* 53, 1592-1600.
- Arnold, G.O., Fawckner, J.F., 1980. The Broken River and Hodgkinson provinces, in: Henderson, R.A., Stephenson, P.J. (Eds.), *The geology and geophysics of northeastern Australia*. Geol. Soc. Aust., Queensl. Div., Brisbane, Queensl., Australia, pp. 175-189.
- Austin, J.R., Blenkinsop, T.G., 2008. The Cloncurry Lineament; geophysical and geological evidence for a deep crustal structure in the Eastern Succession of the Mount Isa Inlier. *Precambrian Research* 163, 50-68.
- Austin, J.R., Blenkinsop, T.G., 2010. Cloncurry fault zone: Strain partitioning and reactivation in a crustal-scale deformation zone, mt isa inlier. *Australian Journal of Earth Sciences* 57, 1-21.
- Australian_Aquitaine_Petroleum_PTY, 1965. Aquitaine Mayneside n.1 Well Completion Report.
- Barlow, M.A., 2004. Density and susceptibility characterization of major rock units and rock types of Mount Isa Inlier. I1 & I2 Projects PMD*CR.
- Battersby, D.G., 1976. Cooper Basin gas and oil fields. *Monograph Series - Australasian Institute of Mining and Metallurgy*, 321-368.
- Beardsmore, T.J., Newbery, S.P., Laing, W.P., 1988. The Maronan Supergroup: an inferred early volcanosedimentary rift sequence in the Mount Isa Inlier, and its implications for ensialic rifting in the Middle Proterozoic of northwest Queensland. *Precambrian Research* 40-41, 487-507.
- Bell, T.H., 1983. Thrusting and duplex formation at Mount Isa, Queensland, Australia. *Nature* 304, 493-497.
- Betts, P.G., 1999. Palaeoproterozoic mid-basin inversion in the northern Mt Isa terrane, Queensland. *Australian Journal of Earth Sciences* 46, 735-748.
- Betts, P.G., 2001. Three-dimensional structure along the inverted Palaeoproterozoic Fiery Creek fault system, Mount Isa Terrane, Australia. *Journal of Structural Geology* 23, 1953-1969.
- Betts, P.G., Armit, R.J., Stewart, J., Aitken, A.R.A., Ailleres, L., Donchak, P., Hutton, L., Withnall, I., Giles, D., in press. *Australia and Nuna*. Geological Society of London Special publication.

- Betts, P.G., Giles, D., 2006. The 1800-1100 Ma tectonic evolution of Australia. *Precambrian Research* 144, 92-125.
- Betts, P.G., Giles, D., Foden, J., Schaefer, B.F., Mark, G., Pankhurst, M.J., Forbes, C.J., Williams, H.A., Chalmers, N.C., Hills, Q., 2009. Mesoproterozoic plume-modified orogenesis in eastern Precambrian Australia. *Tectonics* 28.
- Betts, P.G., Giles, D., Lister, G.S., 2003a. Tectonic environment of shale-hosted massive sulfide Pb-Zn-Ag deposits of Proterozoic northeastern Australia. *Economic Geology and the Bulletin of the Society of Economic Geologists* 98, 557-576.
- Betts, P.G., Giles, D., Lister, G.S., 2004. Aeromagnetic patterns of half-graben and basin inversion: Implications for sediment-hosted massive sulfide Pb-Zn-Ag exploration. *Journal of Structural Geology* 26, 1137-1156.
- Betts, P.G., Giles, D., Lister, G.S., Frick, L.R., 2002. Evolution of the Australian lithosphere. *Australian Journal of Earth Sciences* 49, 661-695.
- Betts, P.G., Giles, D., Mark, G., Lister, G.S., Goleby, B.R., Aillères, L., 2006. Synthesis of the proterozoic evolution of the Mt. Isa Inlier. *Australian Journal of Earth Sciences* 53, 187-211.
- Betts, P.G., Giles, D., Schaefer, B.F., 2008. Comparing 1800-1600 Ma accretionary and basin processes in Australia and Laurentia: Possible geographic connections in Columbia. *Precambrian Research* 166, 81-92.
- Betts, P.G., Giles, D., Schaefer, B.F., Mark, G., 2007. 1600-1500 Ma hotspot track in eastern Australia: Implications for Mesoproterozoic continental reconstructions. *Terra Nova* 19, 496-501.
- Betts, P.G., Lister, G.S., 2001. Comparison of the "strike-slip" versus the "episodic-rift-sag" models for the origin of the Isa Superbasin. *Australian Journal of Earth Sciences* 48, 265-280.
- Betts, P.G., Lister, G.S., Giles, D., 2001. Tectonic environment of shale-hosted massive sulphide Pb-Zn mineralisation in the Western fold belt, Mount Isa Terrane. *Contributions of the Economic Geology Research Unit* 59, 20-21.
- Betts, P.G., Lister, G.S., Pound, K.S., 1999. Architecture of a Palaeoproterozoic Rift System: Evidence from the Fiery Creek Dome region, Mt Isa terrane. *Australian Journal of Earth Sciences* 46, 533-534.
- Betts, P.G., Valenta, R.K., Finlay, J., 2003b. Evolution of the Mount Woods Inlier, northern Gawler Craton, southern Australia; an integrated structural and aeromagnetic analysis. *Tectonophysics* 366, 83-111.
- Bierlein, F.P., Betts, P.G., 2004. The Proterozoic Mount Isa fault zone, northeastern Australia; is it really a ca. 1.9 Ga terrane-bounding suture? *Earth and Planetary Science Letters* 225, 279-294.
- Bierlein, F.P., Black, L.P., Hergt, J., Mark, G., 2008. Evolution of Pre-1.8 Ga basement rocks in the western Mt Isa Inlier, northeastern Australia--Insights from SHRIMP U-Pb dating and in-situ Lu-Hf analysis of zircons. *Precambrian Research* 163, 159-173.
- Bierlein, F.P., Maas, R., Woodhead, J., 2011. Pre-1.8 Ga tectono-magmatic evolution of the Kalkadoon-Leichhardt Belt: Implications for the crustal architecture and metallogeny of the

- Mount Isa Inlier, northwest Queensland, Australia. *Australian Journal of Earth Sciences* 58, 887-915.
- Blake, D.H., 1987. Geology of the Mount Isa Inlier and environs, Queensland and Northern Territory. *Bulletin - Bureau of Mineral Resources, Geology & Geophysics, Australia* 225.
- Blake, D.H., 1996. Structural interpretations of the Wonga Belt in the Proterozoic Mount Isa Inlier of northwest Queensland - a review. *AGSO Journal of Australian Geology and Geophysics* 16, 609-619.
- Blake, D.H., Bultitude, R.J., Donchak, P.J.T., Wyborn, L.A.I., Hone, I.G., 1984. Geology of the Duchess-Urandangi region, Mount Isa Inlier, Queensland. Australian Geological Survey Organization, Canberra, A.C.T., Australia.
- Blake, D.H., Etheridge, M.A., Page, R.W., Stewart, A.J., Williams, P.R., Wyborn, L.A.I., 1990. Mount Isa Inlier; regional geology and mineralisation. *Monograph Series - Australasian Institute of Mining and Metallurgy* 14, 915-925.
- Blake, D.H., Stewart, A.J., 1992. Stratigraphic and tectonic framework, Mount Isa Inlier. *AGSO Bulletin*, 1-12.
- Blakely, R.J., 1995. *Potential Theory in Gravity and Magnetic Applications*. Cambridge University Press, New York.
- Blakely, R.J., Simpson, R.W., 1986. Approximating edges of source bodies from magnetic or gravity anomalies. *Geophysics* 51, 1494-1498.
- Blenkinsop, T., Hutton, L., Bressan, G., Brown, A., Shah, A., Josey, J., in prep. Collection of rock properties along the Mount Isa seismic transects.
- Blenkinsop, T.G., Huddleston-Holmes, C.R., Foster, D.R.W., Edmiston, M.A., Lepong, P., Mark, G., Austin, J.R., Murphy, F.C., Ford, A., Rubenach, M.J., 2008. The crustal scale architecture of the Eastern Succession, Mount Isa: The influence of inversion. *Precambrian Research* 163, 31-49.
- Bonini, M., Sani, F., Antonielli, B., 2012. Basin inversion and contractional reactivation of inherited normal faults: A review based on previous and new experimental models. *Tectonophysics* 522-523, 55-88.
- Brown, D., Purdy, D., Carr, P., Cross, A., Kositcin, N., 2014. New isotopic data from the Thomson Orogen basement cores: a possible link with the Centralian Superbasin. *Geological Society of Australia Abstracts* 110, 243-244.
- Burton, G.R., 2010. New structural model to explain geophysical features in northwestern New South Wales: Implications for the tectonic framework of the Tasmanides. *Australian Journal of Earth Sciences* 57, 23-49.
- Burton, G.R., Dadd, K.A., Vickery, N.M., 2008. Volcanic arc-type rocks beneath cover 35 km to the northeast of Bourke. *Quarterly Notes of the Geological Surveys of New South Wales*, 1-23.
- Carr, P., Purdy, D., Brown, D., 2014. Peeking under the covers: undercover geology of the Thomson Orogen. *Geological Society of Australia Abstracts* 110, 244-245.

- Cawood, P.A., Wang, Y., Xu, Y., Zhao, G., 2013. Locating South China in Rodinia and Gondwana: A fragment of greater India lithosphere? *Geology* 41, 903-906.
- Cayley, R.A., 2011. Exotic crustal block accretion to the eastern Gondwanaland margin in the Late Cambrian-Tasmania, the Selwyn Block, and implications for the Cambrian-Silurian evolution of the Ross, Delamerian, and Lachlan orogens. *Gondwana Research* 19, 628-649.
- Cayley, R.A., Korsch, R.J., Moore, D.H., Costelloe, R.D., Nakamura, A., Willman, C.E., Rawling, T.J., Morand, V.J., Skladzien, P.B., O'Shea, P.J., 2011. Crustal architecture of central Victoria: Results from the 2006 deep crustal reflection seismic survey. *Australian Journal of Earth Sciences* 58, 113-156.
- Chakravarthi, V., Ramamma, B., Venkat Reddy, T., 2013. Gravity anomaly modeling of sedimentary basins by means of multiple structures and exponential density contrast-depth variations: A space domain approach. *Journal of the Geological Society of India* 82, 561-569.
- Chakravarthi, V., Sundararajan, N., 2004. Automatic 3-D gravity modeling of sedimentary basins with density contrast varying parabolically with depth. *Computers and Geosciences* 30, 601-607.
- Champion, D.C., Kositcin, N., Huston, D.L., Mathews, E., Brown, C., 2009. Geodynamic synthesis of the Phanerozoic of eastern Australia and implications for metallogeny. Geoscience Australia, Canberra, A.C.T., Australia.
- Cheng, J.H., Yin, B.X., 2011. A study of application of gravity and magnetic information for the west foot of moon mountain to ore exploration prospect forecast in ningxia province. *Wutan Huatan Jisuan Jishu* 33, 45-50.
- Chopping, R., Henson, P.A.E., 2009. 3D map and supporting geophysical studies in the north Queensland region. Geoscience Australia, Canberra, A.C.T., Australia.
- Clark, D.A., 1981. A system for regional lithofacies mapping. *Bulletin of Canadian Petroleum Geology* 29, 197-208.
- Clark, D.A., Emerson, D.W., 1991. Notes on rock magnetization characteristics in applied geophysical studies. *Exploration Geophysics* 22, 547-555.
- Clark, D.A., Schmidt, P.W., 1982. Theoretical analysis of thermomagnetic properties, low-temperature hysteresis and domain structure of titanomagnetites. *Physics of the Earth and Planetary Interiors* 30, 300-316.
- Collins, C.D.N., Lock, J., 1983. A seismic refraction study of the Quilpie Trough and adjacent basement highs, Eromanga Basin, eastern Australia. *Tectonophysics* 100, 185-198.
- Collins, W.J., Shaw, R.D., 1995. Geochronological constraints on orogenic events in the Arunta Inlier; a review. *Precambrian Research* 71, 315-346.
- Connors, K.A., Page, R.W., 1995. Relationships between magmatism, metamorphism and deformation in the western Mount Isa Inlier, Australia. *Precambrian Research* 71, 131-153.
- Crawford, A.J., Cameron, W.E., Keays, R.R., 1984. The association of boninite low-Ti andesite-tholeiite in the Heatcote Greenstone Belt, Victoria; ensimatic setting for the early Lachlan fold belt. *Australian Journal of Earth Sciences* 31, 161-175.

- Crawford, A.J., Keays, R.R., 1987. Petrogenesis of Victorian Cambrian tholeiites and implications for the origin of associated boninites. *Journal of Petrology* 28, 1075-1109.
- Crawford, A.J., Stevens, B.P.J., Fanning, M., 1997. Geochemistry and tectonic setting of some Neoproterozoic and Early Cambrian volcanics in western New South Wales. *Australian Journal of Earth Sciences* 44, 831-852.
- Crawford, B.L., Betts, P.G., Aillères, L., 2010. An aeromagnetic approach to revealing buried basement structures and their role in the Proterozoic evolution of the Wernecke Inlier, Yukon Territory, Canada. *Tectonophysics* 490, 28-46.
- Daly, S.J., Fanning, C.M., Fairclough, M.C., 1998. Tectonic evolution and exploration potential of the Gawler Craton, South Australia. *AGSO Journal of Australian Geology and Geophysics* 17, 145-168.
- Derrick, G.M., 1982. A Proterozoic rift zone at Mount Isa, Queensland, and implications for mineralisation (Australia). *BMR Journal of Australian Geology & Geophysics* 7, 81-92.
- Derrick, G.M., Wilson, I.H., Hill, R.M., Mitchell, J.E., 1971. Geology of the Marraba 1:100 000 sheet area Qld. Geoscience Australia, Canberra, A.C.T., Australia.
- Derrick, G.M., Wilson, I.H., Sweet, I.P., 1980. The Quilalar and Surprise Creek Formations - new Proterozoic units from the Mount Isa Inlier (Australia): their regional sedimentology and application to regional correlation. *BMR Journal of Australian Geology & Geophysics* 5, 215-223.
- Direen, N.G., Crawford, A.J., 2003. The Tasman Line: Where is it, what is it, and is it Australia's Rodinian breakup boundary? *Australian Journal of Earth Sciences* 50, 491-502.
- Draper, J.J., 2006. The Thomson fold belt in Queensland revisited. *Abstracts - Geological Society of Australia* 82, 6.
- Drummond, B.J., Goleby, B.R., Goncharov, A.G., Wyborn, L.A.I., Collins, C.D.N., MacCready, T., 1998. Crustal-scale structures in the Proterozoic Mount Isa Inlier of north Australia: Their seismic response and influence on mineralisation. *Tectonophysics* 288, 43-56.
- Dunster, J., Kruse, P., Duffett, M., Ambrose, G., Muegge, A., 2003. Resource potential of the southern Georgina Basin. *Geological Survey Record*.
- Edmiston, M.A., Lepong, P., Blenkinsop, T.G., 2008. Structure of the Isan Orogeny under cover to the east of the Mount Isa Inlier revealed by multiscale edge analysis and forward and inverse modelling of aeromagnetic data. *Precambrian Research* 163, 69-80.
- Eriksson, K.A., Simpson, E.L., Jackson, M.J., 1994. Stratigraphical evolution of a Proterozoic syn-rift to post-rift basin: constraints on the nature of lithospheric extension in the Mount Isa Inlier, Australia. *Tectonic controls and signatures in sedimentary successions*, 203-221.
- Ervin, C.P., 1976. Reduction to the magnetic pole using a fast Fourier series algorithm. *Computers & Geosciences* 2, 211-217.
- Esso_Australia_Limited, 1984. A-P 166P, W80A & W81A SEISMIC SURVEYS, FINAL REPORT. Esso Australia Limited.
- Etheridge, M.A., Rutland, R.W.R., Wyborn, L.A.I., 1987. Orogenesis and tectonic process in the early to middle Proterozoic of northern Australia. *Geodynamics Series* 17, 131-147.

- Evans, P.R., Hoffmann, K.L., Remus, D.A., Passmore, V.L., 1992. Geology of the Eromanga sector of the Eromanga-Brisbane Geoscience Transect. Bulletin - Bureau of Mineral Resources, Geology & Geophysics, Australia 232, 83-104.
- Fergusson, C.L., 2010. Plate-driven extension and convergence along the east Gondwana active margin; Late Silurian-Middle Devonian tectonics of the Lachlan fold belt, southeastern Australia. Australian Journal of Earth Sciences 57, 627-649.
- Fergusson, C.L., Carr, P.F., Fanning, C.M., Green, T.J., 2001. Proterozoic-Cambrian detrital zircon and monazite ages from the Anakie Inlier, Central Queensland: Grenville and Pacific-Gondwana signatures. Australian Journal of Earth Sciences 48, 857-866.
- Fergusson, C.L., Henderson, R.A., 2013. Chapter 3 Thomson Orogen. P. A. Jell (Eds.), Geology of Queensland. Geological Survey of Queensland, 113-224.
- Fergusson, C.L., Henderson, R.A., Fanning, C.M., Withnall, I.W., 2007a. Detrital zircon ages in Neoproterozoic to Ordovician siliciclastic rocks, northeastern Australia: Implications for the tectonic history of the East Gondwana continental margin. Journal of the Geological Society 164, 215-225.
- Fergusson, C.L., Henderson, R.A., Lewthwaite, K.J., Phillips, D., Withnall, I.W., 2005. Structure of the Early Palaeozoic Cape River Metamorphics, Tasmanides of north Queensland: Evaluation of the roles of convergent and extensional tectonics. Australian Journal of Earth Sciences 52, 261-277.
- Fergusson, C.L., Henderson, R.A., Withnall, I.W., Fanning, C.M., 2007b. Structural history of the Greenvale Province, north Queensland; early Palaeozoic extension and convergence on the Pacific margin of Gondwana. Australian Journal of Earth Sciences 54, 573-595.
- Fergusson, C.L., Offler, R., Green, T.J., 2009. Late Neoproterozoic passive margin of East Gondwana: Geochemical constraints from the Anakie Inlier, central Queensland, Australia. Precambrian Research 168, 301-312.
- Ferraccioli, F., Bozzo, E., Armadillo, E., 2002. A high-resolution aeromagnetic field test in Friuli: towards developing remote location of buried ferro-metallic bodies, 8th Workshop on Geo-Electromagnetism, 10-12 Oct. 2000, 2 ed. Editrice Compositori, Italy, pp. 219-232.
- Fichtner, A., Kennett, B.L.N., Igel, H., Bunge, H.P., 2009. Full seismic waveform tomography for upper-mantle structure in the Australasian region using adjoint methods. Geophysical Journal International 179, 1703-1725.
- Finlayson, D.M., 1982. Geophysical differences in the lithosphere between Phanerozoic and Precambrian Australia. Tectonophysics 84, 287-312.
- Finlayson, D.M., 1990. Basin and Crustal evolution along the Eromanga-Brisbane Geoscience Transect: Precambrian and analogues. Bulletin - Bureau of Mineral Resources, Geology & Geophysics, Australia 232, 253-261.
- Finlayson, D.M., 1993. Crustal architecture across Phanerozoic Australia along the Eromanga-Brisbane Geoscience Transect: evolution and analogues. Tectonophysics 219, 191-200, 205-211.

- Finlayson, D.M., Collins, C.D.N., 1987. Crustal differences between the Nebine Ridge and the central Eromanga Basin from seismic data (Queensland, Australia). *Australian Journal of Earth Sciences* 34, 251-259.
- Finlayson, D.M., Collins, C.D.N., Lock, J., 1984. P-wave velocity features of the lithosphere under the Eromanga Basin, Eastern Australia, including a prominent MID-crustal (Conrad?) discontinuity. *Tectonophysics* 101, 267-291.
- Finlayson, D.M., Collins, C.D.N., Wright, C., 1990a. Seismic velocity models of the crust and upper mantle under the basins of southern Queensland. *Bulletin - Bureau of Mineral Resources, Geology & Geophysics, Australia* 232, 189-202.
- Finlayson, D.M., Leven, J.H., 1987. Lithospheric structures and possible processes in Phanerozoic eastern Australia from deep seismic investigations. *Tectonophysics* 133, 199-215.
- Finlayson, D.M., Leven, J.H., Etheridge, M.A., 1988. Structural styles and basin evolution in Eromanga region, eastern Australia. *American Association of Petroleum Geologists Bulletin* 72, 33-48.
- Finlayson, D.M., Leven, J.H., Wake-Dyster, K.D., 1989. Large-scale lenticles in the lower crust under an intra-continental basin in eastern Australia. *Geophysical Monograph* 51, 1-16.
- Finlayson, D.M., Leven, J.H., Wake-Dyster, K.D., Johnstone, D.W., 1990b. A crustal image under the basins of southern Queensland along the Eromanga-Brisbane geoscience transect. *Bulletin - Australia, Bureau of Mineral Resources, Geology and Geophysics* 232, 153-175.
- Finlayson, D.M., Wake-Dyster, K.D., Leven, J.H., Johnstone, D.W., Murray, C.G., Harrington, H.J., Korsch, R.J., Wellman, P., 1990c. Seismic imaging of major tectonic features in the crust of Phanerozoic eastern Australia. *Tectonophysics* 173, 211-230.
- Fishwick, S., Heintz, M., Kennett, B.L.N., Reading, A.M., Yoshizawa, K., 2008. Steps in lithospheric thickness within eastern Australia, evidence from surface wave tomography. *Tectonics* 27.
- Fishwick, S., Kennett, B.L.N., Reading, A.M., 2005. Contrasts in lithospheric structure within the Australian craton - Insights from surface wave tomography. *Earth and Planetary Science Letters* 231, 163-176.
- Fishwick, S., Reading, A.M., 2008. Anomalous lithosphere beneath the Proterozoic of western and central Australia: A record of continental collision and intraplate deformation? *Precambrian Research* 166, 111-121.
- Floettmann, T., Hand, M., Close, D., Edgoose, C., Scrimgeour, I., 2004. Thrust tectonic styles of the intracratonic Alice Springs and Petermann Orogenies, central Australia. *AAPG Memoir* 82, 538-557.
- Foden, J., Elburg, M.A., Dougherty-Page, J., Burt, A., 2006. The timing and duration of the Delamerian orogeny: Correlation with the Ross Orogen and implications for Gondwana assembly. *Journal of Geology* 114, 189-210.
- Foster, D.A., Gray, D.R., 2000. Evolution and structure of the Lachlan Fold Belt (Orogen) of eastern Australia, pp. 47-80.

- Foster, D.R.W., Austin, J.R., 2008. The 1800-1610 Ma stratigraphic and magmatic history of the Eastern Succession, Mount Isa Inlier, and correlations with adjacent Paleoproterozoic terranes. *Precambrian Research* 163, 7-30.
- Gatehouse, C.G., 1986. The geology of the Warburton Basin in South Australia. *Australian Journal of Earth Sciences* 33, 161-180.
- Geological_Survey_of_Queensland, 2010. Proterozoic Mount Isa Synthesis. Report for the Queensland Government Section I: Mount Isa Inlier Geodynamic Synthesis.
- Gibson, G.M., Hutton, L.J., Korsch, R.J., Huston, D.L., Murphy, F.C., Withnall, I.W., Jupp, B., Stewart, L., 2010. Deep seismic reflection imaging of a Paleoproterozoic–Early Mesoproterozoic rift basin succession and related Pb-Zn mineral province: the Mount Isa Inlier. Finlayson, D.F. (Ed.) 14th International symposium on deep seismic profiling of the continents and their margins: Geoscience Australia Record.
- Gibson, G.M., Neumann, N.L., Southgate, P.N., Hutton, L.J., Foster, D., 2006. Geodynamic evolution of the Mount Isa Inlier and its influence on the formation, timing and localisation of fluid flow. *Record - Geoscience Australia*, 36-40.
- Gibson, G.M., Rubenach, M.J., Neumann, N.L., Southgate, P.N., Hutton, L.J., 2008. Syn- and post-extensional tectonic activity in the Palaeoproterozoic sequences of Broken Hill and Mount Isa and its bearing on reconstructions of Rodinia. *Precambrian Research* 166, 350-369.
- Giles, D., Aillères, L., Jeffries, D., Betts, P., Lister, G., 2006a. Crustal architecture of basin inversion during the Proterozoic Isan Orogeny, Eastern Mount Isa Inlier, Australia. *Precambrian Research* 148, 67-84.
- Giles, D., Betts, P., Lister, G., 2002. Far-field continental backarc setting for the 1.80-1.67 Ga basins of northeastern Australia. *Geology* 30, 823-826.
- Giles, D., Betts, P.G., Aillères, L., Hulscher, B., Hough, M., Lister, G.S., 2006b. Evolution of the Isan Orogeny at the southeastern margin of the Mt. Isa Inlier. *Australian Journal of Earth Sciences* 53, 91-108.
- Giles, D., Betts, P.G., Lister, G.S., 2004. 1.8-1.5-Ga links between the North and South Australian Cratons and the Early-Middle Proterozoic configuration of Australia. *Tectonophysics* 380, 27-41.
- Giles, D., Nutman, A.P., 2002. SHRIMP U-Pb monazite dating of 1600-1580 Ma amphibolite facies metamorphism in the southeastern Mt Isa Block, Australia. *Australian Journal of Earth Sciences* 49, 455-465.
- Gilmore, P.J., Greenfield, J.E., Reid, W.J., Mills, K.J., 2008. Metallogenesis of the Koonenberry Belt, northwestern New South Wales. *Abstracts - Geological Society of Australia* 89, 111.
- Glen, R.A., 2005. The Tasmanides of eastern Australia. *Geological Society Special Publications* 246, 23-96.
- Glen, R.A., Crawford, A.J., Percival, I.G., Cooke, D., Meffre, S., Scott, R., Barron, L.M., 2009. Key features of the Macquarie Arc, eastern Lachlan Orogen; a 2007 summary. *Abstracts - Geological Society of Australia* 92, 78.
- Glen, R.A., Djomani, Y.P., Korsch, R.J., Costelloe, R.D., Dick, S., 2007a. 2007 Thomson-Lachlan seismic project Results and implications. *Mines and Wines*.

- Glen, R.A., Korsch, R.J., Costelloe, R.D., Poudjom Djomani, Y., Mantaring, R., 2006. Preliminary results from the Thomson-Lachlan Deep Seismic Survey, northwest New South Wales. . Lewis, P., editor, Mineral exploration geoscience in New South Wales, Extended Abstracts Mines and Wines Conference, Cessnock, NSW. SMEDG, Sydney, , 105-109. .
- Glen, R.A., Korsch, R.J., Hegarty, R., Saeed, A., Djomani, Y.P., Costelloe, R.D., Belousova, E., 2013. Geodynamic significance of the boundary between the Thomson Orogen and the Lachlan Orogen, northwestern New South Wales and implications for Tasmanide tectonics. *Australian Journal of Earth Sciences* 60, 371-412.
- Glen, R.A., Meffre, S., Scott, R.J., 2007b. Benambran Orogeny in the eastern Lachlan Orogen, Australia. *Australian Journal of Earth Sciences* 54, 385-415.
- Glen, R.A., Saeed, A., Hegarty, R., Percival, I.G., Bodorkos, S., Griffin, W.L., 2010. Preliminary zircon data and tectonic framework for the Thomson Orogen, northwestern NSW, pp. 1-26.
- Gray, D.R., Gregory, R.T., 2003. Fault geometry as evidence for inversion of a former rift basin in the eastern Lachlan Orogen. *Australian Journal of Earth Sciences* 50, 513-523.
- Greco, F., Currenti, G., D'Agostino, G., Germak, A., Napoli, R., Pistorio, A., Del Negro, C., 2012. Combining relative and absolute gravity measurements to enhance volcano monitoring. *Bulletin of Volcanology* 74, 1745-1756.
- Greene, D.C., 2010. Neoproterozoic rifting in the southern Georgina Basin, central Australia: Implications for reconstructing Australia in Rodinia. *Tectonics* 29.
- Greenfield, J.E., Musgrave, R.J., Bruce, M.C., Gilmore, P.J., Mills, K.J., 2011. The Mount Wright Arc: A Cambrian subduction system developed on the continental margin of East Gondwana, Koonenberry Belt, eastern Australia. *Gondwana Research* 19, 650-669.
- Gunn, P.J., Maidment, D., Milligan, P.R., 1997. Interpreting aeromagnetic data in areas of limited outcrop. *AGSO Journal of Australian Geology and Geophysics* 17, 175-185.
- Hamdi-Nasr, I., Hédi Inoubli, M., Ben Salem, A., Tlig, S., Mansouri, A., 2009. Gravity contributions to the understanding of salt tectonics from the Jebel Cheid area (dome zone, Northern Tunisia). *Geophysical Prospecting* 57, 719-728.
- Hand, M., Reid, A., Jagodzinski, L., 2007. Tectonic framework and evolution of the Gawler craton, Southern Australia. *Economic Geology* 102, 1377-1395.
- Harding, R.R., 1969. Catalogue of age determinations on Australian rocks, 1962-65. Australian Geological Survey Organisation, Canberra, A.C.T., Australia.
- Harrington, H.J., 1974. The Tasman Geosyncline in Australia, The Tasman Geosyncline; A Symposium. Geol. Soc. Aust. Inc., Queensl. Div., Brisbane, Queensland, pp. 383-409.
- Hawkins, P.J., Harrison, P.L., 1978. Stratigraphic and seismic investigations in the Lovelle Depression, western Galilee Basin. *Queensland Government Mining Journal* 79(926), 623 - 650.
- Henderson, R.A., 1980. Structural outline and summary geological history for northeastern Australia, in: Henderson, R.A., Stephenson, P.J. (Eds.), *The geology and geophysics of northeastern Australia*. Geol. Soc. Aust., Queensl. Div., Brisbane, Queensl., Australia, pp. 1-26.

- Henderson, R.A., 1986. Geology of the Mt Windsor subprovince - a Lower Palaeozoic volcano-sedimentary terrane in the northern Tasman orogenic zone. *Australian Journal of Earth Sciences* 33, 343-364.
- Henson, P.K., N. ; Huston, D. , 2011. Broken Hill and Mount Isa: linked but not rotated. *AusGeo News* June 2011
- Hill, D., 1951. Geology, in: *Handbook of Queensland*. Australian Association for the Advancement of Science, Brisbane., pp. 13-24.
- Hinze, W.J., 1960. Application of the gravity method to iron ore exploration. *Economic Geology* 55, 465-484.
- Hoffmann, K.L., 1988. Revision of the limits of the Adavale Basin and Warrabin Trough, southwest Queensland. Queensland Department of Mines Record 1988/18.
- Hoffmann, K.L., 1989. Tectonic setting and structural analysis of the southern Eromanga Basin, Queensland. Queensland Department of Mines Record 1989/15.
- Holcombe, R.J., Pearson, P.J., Oliver, N.H.S., 1991. Geometry of a Middle Proterozoic extensional décollement in northeastern Australia. *Tectonophysics* 191, 255-274.
- Hone, I.G., Carberry, V.P., Reith, H.G., 1987. Physical property measurements on rock samples from the Mount Isa Inlier, northwest Queensland (Australia). Report - Bureau of Mineral Resources, Geology & Geophysics, Australia 265.
- Hood, P., Dods, D., Kornik, L.J., Olson, D., Sawatzky, P., Teskey, D., 1982. Aeromagnetic Gradiometer Program of the Geological Survey of Canada; a progress report. *Geophysics* 47, 441.
- Houseman, G.A., Hegarty, K.A., 1987. Did rifting on Australia's southern margin result from tectonic uplift? *Tectonics* 6, 515-527.
- Howard, K.E., Hand, M., Barovich, K.M., Payne, J.L., Cutts, K.A., Belousova, E.A., 2011. U-Pb zircon, zircon Hf and whole-rock Sm-Nd isotopic constraints on the evolution of Paleoproterozoic rocks in the northern Gawler Craton. *Australian Journal of Earth Sciences* 58, 615-638.
- Hutton, L.J., Denaro, T.J., Dhnaram, C., Derrick, G.M., 2012. Mineral systems in the Mount Isa Inlier. *Episodes* 35, 120-130.
- Hutton, L.J., Korsch, R.J., 2008. Deep seismic reflection interpretations, Mount Isa and Isa-Georgetown surveys. *Digging Deeper 6 Seminar Extended Abstracts: Queensland Geological Record*.
- Jackson, K.S., Horvath, Z., Hawkins, P.J., 1981. Assessment of the petroleum prospects for the Galilee Basin, Queensland. *APEA journal* 21, 172-186.
- Jackson, M.J., Scott, D.L., Rawlings, D.J., 2000. Stratigraphic framework for the Leichhardt and Calvert superbasins: Review and correlations of the pre-1700 Ma successions between Mt Isa and McArthur River. *Australian Journal of Earth Sciences* 47, 381-403.

- Jackson, M.J., Simpson, E.L., Eriksson, K.A., 1990. Facies and sequence stratigraphic analysis in an intracratonic, thermal-relaxation basin: the early Proterozoic, Lower Quilalar Formation and Ballara Quartzite, Mount Isa Inlier, Australia. *Sedimentology* 37, 1053-1078.
- Jessell, M., 2001. Three-dimensional geological modelling of potential-field data. *Computers and Geosciences* 27, 455-465.
- Karlstrom, K.E., Ahall, K.-I., Harlan, S.S., Williams, M.L., McLelland, J., Geissman, J.W., 2001. Long-lived (1.8-1.0 Ga) convergent orogen in southern Laurentia, its extensions to Australia and Baltica, and implications for refining Rodinia. *Precambrian Research* 111, 5-30.
- Kennett, B.L.N., Fishwick, S., Reading, A.M., Rawlinson, N., 2004. Contrasts in mantle structure beneath Australia: Relation to Tasman Lines? *Australian Journal of Earth Sciences* 51, 563-569.
- Kirkegaard, A.G., 1974. Structural elements of the northern part of the Tasman Geosyncline, The Tasman Geosyncline; A Symposium. Geol. Soc. Aust. Inc., Queensl. Div., Brisbane, Queensland, pp. 47-63.
- Kivior, I., Boyd, D., 1998. The contribution of high quality aeromagnetic survey data to hydrocarbon exploration. *Exploration Geophysics (Melbourne)* 29, 462-466.
- Kohn, S.B., Bonet, C., DiFrancesco, D., Gibson, H., 2011. Geothermal exploration using gravity gradiometry - A Salton Sea example, *Transactions - Geothermal Resources Council*, pp. 1699-1702.
- Korsch, R., Henson, P., Gibson, G., Withnall, I., Hutton, L., Saygin, E., Jones, L., Stewart, L., Huston, D., Maidment, D., 2008. Results from the central and southern Mt Isa Inlier (Lines 06GA-MI6 and 94AGS-MTI1). Mt Isa Seismic Workshop 24 June 2008.
- Korsch, R.J., Huston, D.L., Henderson, R.A., Blewett, R.S., Withnall, I.W., Fergusson, C.L., Collins, W.J., Saygin, E., Kositcin, N., Meixner, A.J., Chopping, R., Henson, P.A., Champion, D.C., Hutton, L.J., Wormald, R., Holzschuh, J., Costelloe, R.D., 2012. Crustal architecture and geodynamics of North Queensland, Australia: Insights from deep seismic reflection profiling. *Tectonophysics* In Press.
- Korsch, R.J., Struckmeyer, H.I.M., Kirkby, A., Hutton, L.J., Carr, L.K., Hoffmann, K.L., Chopping, R., Roy, I.G., Fitzell, M., Totterdell, J.M., Nicoll, M.G., Talebi, B., 2011. Energy potential of the Millungera Basin; a newly discovered basin in north Queensland. *APPEA Journal* 51, 295-332.
- Korsch, R.J., Withnall, I.W., Hutton, L.J., Henson, P.A., Blewett, R.S., Huston, D.L., Champion, D.C., Meixner, A.J., Nicoll, M.G., Nakamura, A., 2009. Geological interpretation of the deep seismic reflection line 07GA-IG1: the Cloncurry to Croydon transect. *Australian Institute of Geoscientists* 49, 153 - 158.
- Kositcin, N., Champion, D.C., Huston, D.L., 2009. Geodynamic synthesis of the north Queensland region and implications for metallogeny. *Geoscience Australia*, Canberra, A.C.T., Australia.
- Krassay, A.A., Bradshaw, B.E., Domagala, J., Jackson, M.J., 2000. Siliciclastic shoreline to growth-faulted, turbiditic sub-basins: The Proterozoic River Supersequence of the upper McNamara group on the Lawn Hill Platform, northern Australia. *Australian Journal of Earth Sciences* 47, 533-562.

- Lechler, A.R., Greene, D.C., 2006. Fault reactivation during intracontinental deformation; the Toko syncline and Toomba fault, Georgina Basin, central Australia. *Abstracts with Programs - Geological Society of America* 38, 11.
- Letouzey, J., Werner, P., Marty, A., 1990. Fault reactivation and structural inversion. Backarc and intraplate compressive deformations. Example of the eastern Sunda shelf (Indonesia). *Tectonophysics* 183, 341-362.
- Leven, J.H., Finlayson, D.M., 1986. Basement thrusts in the southern Adavale Basin. *Abstracts - Geological Society of Australia* 15, 123-124.
- Leven, J.H., Finlayson, D.M., 1987. Lower crustal involvement in upper crustal thrusting. *Geophysical Journal - Royal Astronomical Society* 89, 415-422.
- Leven, J.H., Finlayson, D.M., Wake-Dyster, K., 1990. Mid-crustal detachments controlling basin deformation: ramp synforms in southwestern Queensland. *Tectonophysics* 173, 231-234,239-246.
- Li, X.H., Li, Z.X., Li, W.X., 2014. Detrital zircon U-Pb age and Hf isotope constrains on the generation and reworking of Precambrian continental crust in the Cathaysia Block, South China: A synthesis. *Gondwana Research* 25, 1202-1215.
- Li, Z.X., Powell, C.M., 2001. An outline of the palaeogeographic evolution of the Australasian region since the beginning of the Neoproterozoic. *Earth-Science Reviews* 53, 237-277.
- Li, Z.X., Zhang, L., Powell, C.M., 1995. South China in Rodinia; part of the missing link between Australia-East Antarctica and Laurentia? *Geology (Boulder)* 23, 407-410.
- Lillie, R.J., 1999. *Whole Earth Geophysics; an introductory textbook for geologists and geophysicists*. Printice Hall, Upper Saddle River, NJ, United States.
- Lister, G.S., O'Dea, M.G., Somaia, I., 1999. A tale of two synclines: Rifting, inversion and transpressional popouts at Lake Julius, northwestern Mt Isa terrane, Queensland. *Australian Journal of Earth Sciences* 46, 233-250.
- Lock, J., Collins, C.D.N., Finlayson, D.M., 1986. Basement structure and velocities under the central Eromanga Basin from seismic refraction studies (Australia). *Contributions to the geology and hydrocarbon potential of the Eromanga Basin*, 155-162.
- Lowrie, W., 1997. *Fundamentals of geophysics*. Cambridge University Press, Cambridge, United Kingdom.
- MacCready, T., 2006a. Structural cross-section based on the Mt. Isa Deep Seismic Transect. *Australian Journal of Earth Sciences* 53, 5-26.
- MacCready, T., 2006b. Structural evolution of the southern Mt. Isa Valley. *Australian Journal of Earth Sciences* 53, 27-40.
- MacCready, T., Goleby, B.R., Goncharov, A., Drummond, B.J., Lister, G.S., 1998. A framework of overprinting orogens based on interpretation of the Mount Isa deep seismic transect. *Economic Geology* 93, 1422-1434.

- Maidment, D.W., Gibson, G.M., Giddings, J.W., 2000. Regional structure and distribution of magnetite; implications for the interpretation of aeromagnetic data in the Broken Hill region, New South Wales. *Exploration Geophysics* (Melbourne) 31, 8-16.
- Mathur, S.P., 1983. Deep crustal reflection results from the central Eromanga Basin, Australia. *Tectonophysics* 100, 163-173.
- Mathur, S.P., 1984. Tectonic evolution of the central Eromanga basin area from reflection data. *Bureau Mineral Resources* 1984/28:25-29.
- Mathur, S.P., 1987. Deep seismic reflection data suggest major compressional deformation of the crust in the central Eromanga Basin area during the mid-Carboniferous. *Tectonophysics* 134, 311-321.
- Maule, C.F., Purucker, M.E., Olsen, N., 2009. Inferring magnetic crustal thickness and geothermal heat flux from crustal magnetic field models. *Danish Climate Centre Report* 09.
- McConachie, B.A., Dunster, J.N., 1998. Regional stratigraphic correlations and stratiform sediment-hosted base-metal mineralisation in the northern Mt Isa Basin. *Australian Journal of Earth Sciences* 45, 83-88.
- McDonald, G.D., Collerson, K.D., Kinny, P.D., 1997. Late Archean and early Proterozoic crustal evolution of the Mount Isa Block, Northwest Queensland, Australia. *Geology* (Boulder) 25, 1095-1098.
- McKillop, M.D., McKellar, J.L., Draper, J.J., Hoffmann, K.L., 2007. The Adavale Basin; stratigraphy and depositional environments. *Special Publication - Northern Territory Geological Survey*, 82-107.
- McLean, M.A., Betts, P.G., 2003. Geophysical constraints of shear zones and geometry of the Hiltaba Suite granites in the western Gawler Craton, Australia. *Australian Journal of Earth Sciences* 50, 525-541.
- McLean, M.A., Morand, V.J., Cayley, R.A., 2010. Gravity and magnetic modelling of crustal structure in central Victoria; what lies under the Melbourne Zone? *Australian Journal of Earth Sciences* 57, 153-173.
- McLean, M.A., Rawling, T.J., Betts, P.G., Phillips, G., Wilson, C.J.L., 2008. Three-dimensional inversion modelling of a Neoproterozoic basin in the southern Prince Charles Mountains, East Antarctica. *Tectonophysics* 456, 180-193.
- McLean, M.A., Wilson, C.J.L., Boger, S.D., Betts, P.G., Rawling, T.J., Damaske, D., 2009. Basement interpretations from airborne magnetic and gravity data over the Lambert Rift region of East Antarctica. *Journal of Geophysical Research* 114.
- Meixner, A.J., 2009. Rock property data (densities and magnetic susceptibilities) of the Mount Isa region. *Geoscience Australia / OEMD*.
- Meixner, A.J., Boucher, R.K., Yeates, A.N., Frears, R.A & Gunn, P.J., 1999. Interpretation of Geophysical and Geological Data Sets, Cooper Basin Region, South Australia. . Australian Geological Survey Organisation, Canberra. Record 1999/022.
- Miller, H.G., Singh, V., 1994. Potential field tilt - a new concept for location of potential field sources. *Journal of Applied Geophysics* 32, 213-217.

- Milsom, J., 2003. Field geophysics. John Wiley & Sons, Chichester, United Kingdom.
- Moresi, L., Betts, P.G., Miller, M.S., Cayley, R.A., 2014. Dynamics of continental accretion. 508, 245-248.
- Moss, F.J., Wake-Dyster, K.D., 1983. The Australian central Eromanga Basin project: An introduction. *Tectonophysics* 100, 131-145.
- Murray, C., 2007. Deep crustal seismic reflection profiling. *Queensland Government Mining Journal* 2007, 92-94.
- Murray, C.G., 1990. Summary of geological developments along the Eromanga-Brisbane Geoscience Transect. *Bulletin - Bureau of Mineral Resources, Geology & Geophysics, Australia* 232, 11-20.
- Murray, C.G., 1994. Basement cores from the Tasman Fold Belt System beneath the Great Artesian Basin in Queensland. Department of Minerals and Energy, Brisbane, Queensl., Australia.
- Murray, C.G., Kirkegaard, A.G., 1978. The Thomson Orogen of the Tasman orogenic zone. *Tectonophysics* 48, 299-325.
- Musgrave, R., 2013. Long-wavelength magnetic anomalies as a guide to the deep crustal composition and structure of eastern Australia. *ASEG Extended Abstracts* 2013, 1-4.
- Musgrave, R.J., 2013. Long-wavelength magnetic anomalies as a guide to the deep crustal composition and structure of eastern Australia. . *ASEG Extended Abstracts*, 1-4.
- Mutton, A.J., Almond, R.A., 1979. Geophysical mapping of buried Precambrian rocks in the Cloncurry area, northwest Queensland. *Australia Bureau of Mineral Resources and Geophysics, Report* 210.
- Nabighian, M.N., Ander, M.E., Grauch, V.J.S., Hansen, R.O., LaFehr, T.R., Li, Y., Pearson, W.C., Peirce, J.W., Phillips, J.D., Ruder, M.E., 2005a. Historical development of the gravity method in exploration. *Geophysics* 70, 63ND-89ND.
- Nabighian, M.N., Grauch, V.J.S., Hansen, R.O., LaFehr, T.R., Li, Y., Peirce, J.W., Phillips, J.D., Ruder, M.E., 2005b. The historical development of the magnetic method in exploration. *Geophysics* 70, 33ND-61ND.
- Neef, G., 2004. Stratigraphy, sedimentology, structure and tectonics of Lower Ordovician and Devonian strata of south Mootwingee Darling Basin, western New South Wales. *Australian Journal of Earth Sciences* 51, 15-29.
- Neef, G., Bottrill, R.S., 1991. Early Devonian (Gedinnian) nonmarine strata present in a rapidly subsiding basin in far western New South Wales, Australia. *Sedimentary Geology* 71, 195-212.
- Neumann, N.L., Fraser, G.L., 2007. Geochronological synthesis and time-space plots for Proterozoic Australia. *Geoscience Australia, Canberra, A.C.T., Australia*.
- Neumann, N.L., Kositcin, N., 2011. New SHRIMP U-Pb zircon ages from north Queensland, 2007-2010. *Geoscience Australia, Canberra, A.C.T., Australia*.
- Neumann, N.L., Southgate, P.N., Gibson, G.M., Hutton, L.J., Foster, D., 2006a. Regional scale correlations; sequencing the SHRIMP detrital record. *Record - Geoscience Australia*, 82-86.

- Neumann, N.L., Southgate, P.N., Gibson, G.M., McIntyre, A., 2006b. New SHRIMP geochronology for the Western Fold Belt of the Mt Isa Inlier: Developing a 1800 - 1650 Ma event framework. *Australian Journal of Earth Sciences* 53, 1023-1039.
- O'Dea, M.G., Betts, P.G., MacCready, T., Aillères, L., 2006. Sequential development of a mid-crustal fold-thrust complex: Evidence from the Mitakoodi Culmination in the eastern Mt. Isa Inlier, Australia. *Australian Journal of Earth Sciences* 53, 69-90.
- O'Dea, M.G., Lister, G.S., Betts, P.G., Pound, K.S., 1997a. A shortened intraplate rift system in the Proterozoic Mount Isa terrane, NW Queensland, Australia. *Tectonics* 16, 425-441.
- O'Dea, M.G., Lister, G.S., MacCready, T., Betts, P.G., Oliver, N.H.S., Pound, K.S., Huang, W., Valenta, R.K., 1997b. Geodynamic evolution of the Proterozoic Mount Isa terrain, pp. 99-122.
- Olgers, F., 1969. The geology of the Drummond Basin, Queensland. Geoscience Australia, Canberra, A.C.T., Australia.
- Page, R.W., 1983. Timing of superposed volcanism in the Proterozoic Mount Isa Inlier, Australia. *Precambrian Research* 21, 223-245.
- Page, R.W., 1998. Links between Eastern and Western fold belts in the Mount Isa Inlier, based on SHRIMP U-Pb studies. *Abstracts - Geological Society of Australia* 49, 349.
- Page, R.W., Bell, T.H., 1986. Isotopic and structural responses of granite to successive deformation and metamorphism (Australia). *Journal of Geology* 94, 365-379.
- Page, R.W., Laing, W.P., 1992. Felsic metavolcanic rocks related to the Broken Hill Pb-Zn-Ag orebody, Australia: geology, depositional age, and timing of high- grade metamorphism. *Economic Geology* 87, 2138-2168.
- Page, R.W., Sun, S., Carr, G., 1994. Proterozoic sediment- hosted lead-zinc-silver deposits in northern Australia — U-Pb zircon and Pb isotope studies. *Precambrian Research*, 21-36.
- Page, R.W., Sun, S.S., 1998. Aspects of geochronology and crustal evolution in the Eastern Fold Belt, Mt Isa Inlier. *Australian Journal of Earth Sciences* 45, 343-361.
- Page, R.W., Williams, I.S., 1988. Age of the barramundi orogeny in northern Australia by means of ion microprobe and conventional U-Pb zircon studies. *Precambrian Research* 40-41, 21-36.
- Parker, A.J., 1993. The geology of South Australia; Volume 1, The Precambrian. Geological Survey of South Australia, Adelaide, South Aust., Australia.
- Passmore, V.L., Sexton, M.J., 1984. Structural development and hydrocarbon potential of Palaeozoic source rocks in the Adavale Basin region. *APEA journal* 24, 393-411.
- Pinchin, J., Senior, B.R., 1982. The Warrabin Trough, western Adavale Basin, Queensland. *Journal Geological Society of Australia* 29, 413-424.
- Pinto, V., Casas, A., Rivero, L., Torné, M., 2005. 3D gravity modeling of the Triassic salt diapirs of the Cubeta Alavesa (northern Spain). *Tectonophysics* 405, 65-75.
- Potma, W.A., Betts, P.G., 2006. Extension-related structures in the Mitakoodi Culmination: Implications for the nature and timing of extension, and effect on later shortening in the eastern Mt. Isa Inlier. *Australian Journal of Earth Sciences* 53, 55-67.

- Powell, C.M., Preiss, W.V., Gatehouse, C.G., Krapez, B., Li, Z.X., 1994. South Australian record of a Rodinian epicontinental basin and its mid-neoproterozoic breakup (~700 Ma) to form the Palaeo-Pacific Ocean. *Tectonophysics* 237, 113-140.
- Preiss, W.V., 2000. The Adelaide Geosyncline of South Australia and its significance in Neoproterozoic continental reconstruction. *Precambrian Research* 100, 21-63.
- Prieto, C., Morton, G., 2003. New insights from a 3D earth model, deepwater gulf of Mexico. *Leading Edge (Tulsa, OK)* 22, 356-360.
- Roest, W.R., Pilkington, M., 1993. Identifying remanent magnetization effects in magnetic data. *Geophysics* 58, 653-659.
- Roest, W.R., Verhoef, J., Pilkington, M., 1992. Magnetic interpretation using the 3-D analytic signal. *Geophysics* 57, 116-125.
- Rubenach, M.J., Foster, D.R.W., Evins, P.M., Blake, K.L., Fanning, C.M., 2008. Age constraints on the tectonothermal evolution of the Selwyn Zone, Eastern Fold Belt, Mount Isa Inlier. *Precambrian Research* 163, 81-107.
- Sampath, N., Ogilvy, R.D., 1974. Cloncurry area geophysical survey, Queensland, 1972. Bureau of Mineral Resources, Australia Record 1974/135.
- Scott, D.L., Bradshaw, B.E., Tarlowski, C.Z., 1998. The tectonostratigraphic history of the Proterozoic northern Lawn Hill Platform, Australia; an integrated intracontinental basin analysis. *Tectonophysics* 300, 329-358.
- Senior, B.R.M., A.; Harrison, P. L., 1978. Geology of the Eromanga Basin. Australian Geological Survey Organization, Canberra, A.C.T., Australia.
- Shaw, R.D., Etheridge, M.A., Lambeck, K., 1991. Development of the late Proterozoic to mid-Paleozoic, intracratonic Amadeus Basin in central Australia; a key to understanding tectonic forces in plate interiors. *Tectonics* 10, 687-721.
- Shaw, R.D., Stewart, A.J., Black, L.P., 1984. The Arunta inlier: a complex ensialic mobile belt in central Australia. Part 2: tectonic history. *Australian Journal of Earth Sciences* 31, 457-484.
- Shaw, R.D., Wellman, P., Gunn, P., Whitaker, A.J., Tarlowski, C.Z., Morse, M., 1996. Guide to using the Australian crustal elements map. AGSO - Australian Geological Survey Organisation, Canberra, A.C.T., Australia.
- Shoffner, J.D., Li, Y., Sabin, A., Lazaro, M., 2011. Understanding the utility of gravity and gravity gradiometry for geothermal exploration in the southern Walker Lake Basin, Nevada, *Transactions - Geothermal Resources Council*, pp. 1747-1751.
- Simons, F.J., Zielhuis, A., Van Der Hilst, R.D., 1999. The deep structure of the Australian continent from surface wave tomography, pp. 17-43.
- Skeels, D.C., 1947. Ambiguity in gravity interpretation. *Geophysics* 12, 43-56.
- Smith, B.D., McCafferty, A.E., McDougal, R.R., 2000. Utilization of airborne magnetic, electromagnetic, and radiometric data in abandoned mine land investigations. Open-File Report - U. S. Geological Survey, 86-91.

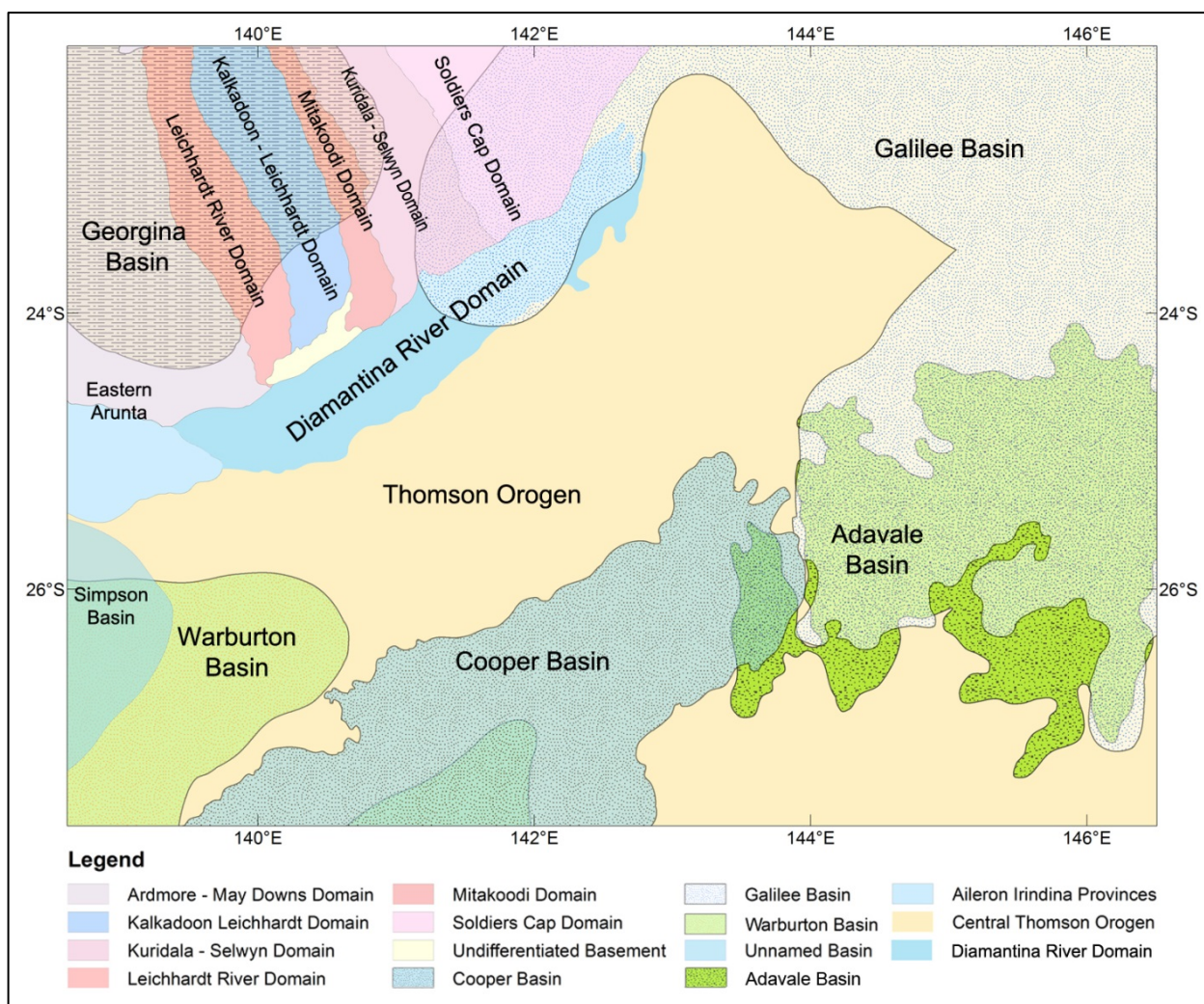
- Smith, D.V., Pratt, D., 2003. Advanced processing and interpretation of the high-resolution aeromagnetic survey data over the central Edwards Aquifer, Texas. *Proceedings - Symposium on the Application of Geophysics to Engineering and Environmental Problems (SAGEEP) 2003*, 374-384.
- Smith, R.P., Grauch, V.J.S., Blackwell, D.D., 2002. Preliminary results of a high-resolution aeromagnetic survey to identify buried faults at Dixie Valley, Nevada. *Transactions - Geothermal Resources Council* 26, 543-546.
- Smith, W.D., 1969. Penecontemporaneous faulting and its likely significance in relation to Mt Isa ore deposition. *Special Publication - Geological Society of Australia* 2, 225-235.
- Soengkono, S., Bromley, C., Reeves, R., Bennie, S., Graham, D., 2013. Geophysical techniques for low enthalpy geothermal exploration in New Zealand. *Exploration Geophysics* 44, 215-227.
- Southgate, P.N., Bradshaw, B.E., Domagala, J., Jackson, M.J., Idnurm, M., Krassay, A.A., Page, R.W., Sami, T.T., Scott, D.L., Lindsay, J.F., McConachie, B.A., Tarlowski, C., 2000a. Chronostratigraphic basin framework for Palaeoproterozoic rocks (1730-1575 Ma) in northern Australia and implications for base-metal mineralisation. *Australian Journal of Earth Sciences* 47, 461-483.
- Southgate, P.N., Scott, D.L., Sami, T.T., Domagala, J., Jackson, M.J., James, N.P., Kyser, T.K., 2000b. Basin shape and sediment architecture in the Gun Supersequence: A strike-slip model for Pb-Zn-Ag ore genesis at Mt Isa. *Australian Journal of Earth Sciences* 47, 509-531.
- Spaldin, N., 2010. *Magnetic materials : fundamentals and applications (2nd ed.)*. Cambridge: Cambridge University Press.
- Spampinato, G.P.T., Betts, P.G., Ailleres, L., Unpublished results-a. Imaging the basement architecture across the Cork Fault in Queensland using Magnetic and Gravity data. *Precambrian Research*.
- Spampinato, G.P.T., Betts, P.G., Ailleres, L., Armit, R.J., Unpublished results-b. Early tectonic evolution of the Thomson Orogen in Queensland inferred from constrained magnetic and gravity data. *Tectonophysics*.
- Spampinato, G.P.T., Betts, P.G., Ailleres, L., Armit, R.J., Unpublished results-c. Structural architecture of the southern Mount Isa terrane in Queensland inferred from magnetic and gravity data. *Precambrian Research*.
- Spence, A.G., Finlayson, D.M., 1983. The resistivity structure of the crust and upper mantle in the central Eromanga Basin, Queensland, using magnetotelluric techniques (Australia). *Journal Geological Society of Australia* 30, 1-16.
- Spikings, R.A., Foster, D.A., Kohn, B.P., Lister, G.S., 2001. Post-orogenic (< 1500 Ma) thermal history of the proterozoic Eastern Fold Belt, Mount Isa Inlier, Australia. *Precambrian Research* 109, 103-144.
- Spikings, R.A., Foster, D.A., Kohn, B.P., Lister, G.S., 2002. Post-orogenic (< 1500 Ma) thermal history of the Palaeo-Mesoproterozoic, Mt. Isa province, NE Australia. *Tectonophysics* 349, 327-365.

- Stewart, J.R., Betts, P.G., 2010a. Implications for Proterozoic plate margin evolution from geophysical analysis and crustal-scale modeling within the western Gawler Craton, Australia. *Tectonophysics* 483, 151-177.
- Stewart, J.R., Betts, P.G., 2010b. Late Paleo-Mesoproterozoic plate margin deformation in the southern Gawler Craton: Insights from structural and aeromagnetic analysis. *Precambrian Research* 177, 55-72.
- Sun, X., 1997. Structural style of the Warburton Basin and control in the Cooper and Eromanga basins, South Australia. *Exploration Geophysics* 28, 333-339.
- Thornton, R.C.N., 1979. Regional stratigraphic analysis of the Gidgealpa Group, southern Cooper Basin, Australia. Geological Survey of South Australia, Adelaide, South Aust., Australia.
- Tsokas, G.N., Papazachos, C.B., 1992. Two-dimensional inversion filters in magnetic prospecting: application to the exploration for buried antiquities. *Geophysics* 57, 1004-1013.
- Van Heeswijck, A., 2010. Late paleozoic to early Mesozoic deformation in the northeastern Galilee Basin, Australia. *Australian Journal of Earth Sciences* 57, 431-451.
- VandenBerg, A.H.M., Willman, C.E., Maher, S., Simons, B.A., Cayley, R.A., Taylor, D.H., Morand, V.J., Moore, D.H., Radojkovic, A., 2000. The Tasman Fold Belt System in Victoria: geology and mineralisation of Proterozoic to Carboniferous rocks, p. 463.
- Veevers, J.J., 2000a. Billion-year earth history of Australia and neighbours in Gondwanaland. GEMOC Press, Sydney, N.S.W., Australia.
- Veevers, J.J., 2000b. Neoproterozoic-Paleozoic Australia and neighbours in Gondwanaland, in: Veevers, J.J. (Ed.), Billion-year earth history of Australia and neighbours in Gondwanaland. GEMOC Press, Sydney, N.S.W., Australia, pp. 253-282.
- Veevers, J.J., Powell, C.M., 1984. Comparative tectonics of the transverse structural zones of Australia and North America. Oxford geological sciences series ; no. 2 J.J. Veevers, Phanerozoic earth history of Australia.
- Vos, I.M.A., Bierlein, F.P., Barlow, M.A., Betts, P.G., 2006. Resolving the nature and geometry of major fault systems from geophysical and structural analysis: The Palmerville Fault in NE Queensland, Australia. *Journal of Structural Geology* 28, 2097-2108.
- Wake-Dyster, K.D., Moss, F.J., Sexton, M.J., 1983. New seismic reflection results in the central Eromanga Basin, Queensland, Australia: The key to understanding its tectonic evolution. *Tectonophysics* 100, 147-162.
- Wellman, P., 1990. A tectonic interpretation of the gravity and magnetic anomalies in southern Queensland. *Bulletin - Australia, Bureau of Mineral Resources, Geology and Geophysics* 232, 21-35.
- Wellman, P., 1992. Structure of the Mount Isa region inferred from gravity and magnetic anomalies. *Detailed studies of the Mount Isa Inlier*, 15-27.
- White, S.H., Bretan, P.G., Rutter, E.H., 1986. Fault-zone reactivation: kinematics and mechanisms. *Philosophical Transactions - Royal Society of London, Series A* 317, 81-97.

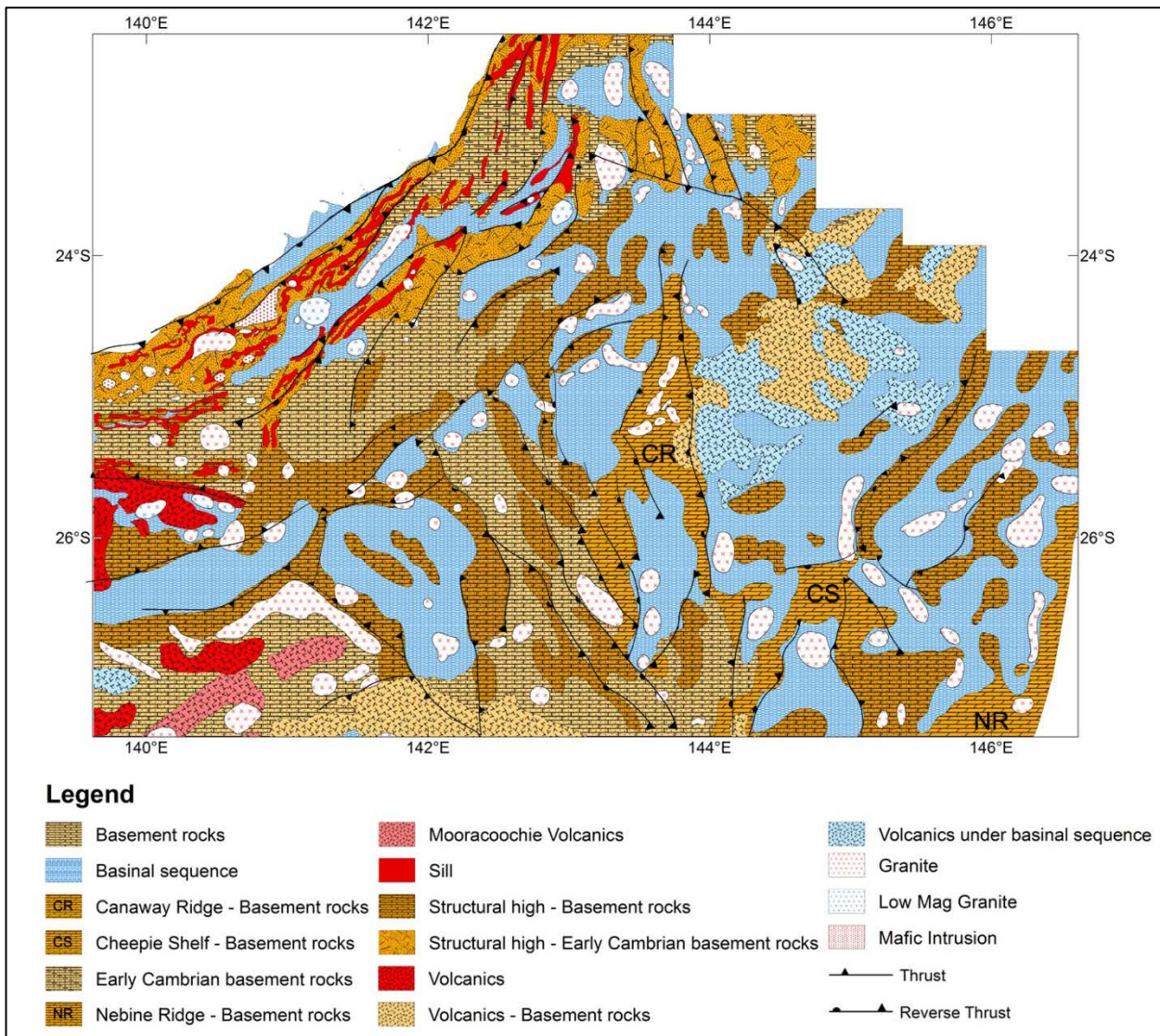
- Williams, H.A., Betts, P.G., Ailleres, L., 2009. Constrained 3D modeling of the Mesoproterozoic Benagerie Volcanics, Australia. *Physics of the Earth and Planetary Interiors* 173, 233-253.
- Williams, H.A., Betts, P.G., Ailleres, L., Burt, A., 2010. Characterization of a proposed Palaeoproterozoic suture in the crust beneath the Curnamona Province, Australia. *Tectonophysics* 485, 122-140.
- Williams, I.S., Goodge, J.W., Myrow, P., Burke, K., Kraus, J., 2002. Large scale sediment dispersal associated with the late Neoproterozoic assembly of Gondwana. *Abstracts - Geological Society of Australia* 67, 238.
- Wilson, I.H., 1987. Geochemistry of Proterozoic Volcanics, Mount Isa Inlier, Australia, pp. 409-423.
- Wingate, M.T.D., Campbell, I.H., Compston, W., Gibson, G.M., 1998. Ion microprobe U-Pb ages for Neoproterozoic basaltic magmatism in south-central Australia and implications for the breakup of Rodinia. *Precambrian Research* 87, 135-159.
- Wingate, M.T.D., Evans, D.A.D., 2003. Palaeomagnetic constraints on the Proterozoic tectonic evolution of Australia, pp. 77-91.
- Wingate, M.T.D., Pisarevsky, S.A., Evans, D.A.D., 2002. Rodinia connections between Australia and Laurentia: No SWEAT, no AUSWUS? *Terra Nova* 14, 121-128.
- Withnall, I.W., Blake, P.R., Crouch, S.B.S., Woods, K.T., Grimes, K.G., Hayward, M.A., Lam, J.S., Garrad, P., Rees, I.D., 1995. Geology of the southern part of the Anakie Inlier, central Queensland. Department of Resource Industries, Brisbane, Australia.
- Withnall, I.W., Golding, S.D., Rees, I.D., Dobos, S.K., 1996. K-Ar dating of the Anakie Metamorphic Group; evidence for an extension of the Delamerian Orogeny into central Queensland. *Australian Journal of Earth Sciences* 43, 567-572.
- Withnall, I.W., Mackenzie, D.E., Denaro, T.J., Bain, J.H.C., Oversby, B.S., Knutson, J., Donchak, P.J.T., Champion, D.C., Wellman, P., Cruikshank, B.I., Sun, S.S., Pain, C.F., 1997. North Queensland Geology. *Bulletin of the Australian Geological Survey Organisation*, 19-69.
- Wyborn, L., 1998. Younger ca 1500 Ma granites of the Williams and Narku batholiths, Cloncurry District, eastern Mt Isa Inlier; geochemistry, origin, metallogenic significance and exploration indicators. *Australian Journal of Earth Sciences* 45, 397-411.
- Wyborn, L.A.I., Page, R.W., Parker, A.J., 1987. Geochemical and Geochronological Signatures in Australian Proterozoic Igneous Rocks. Geological Society, London, Special Publications 33, 377-394.
- Xstrata, 2004. Physical property measurements on rock samples from the Mount Isa Inlier. Xstrata Corporate petrophysical database.
- Zerbini, S., Richter, B., Negusini, M., Romagnoli, C., Simon, D., Domenichini, F., Schwahn, W., 2001. Height and gravity variations by continuous GPS, gravity and environmental parameter observations in the Southern Po Plain, near Bologna, Italy. *Earth and Planetary Science Letters* 192, 267-279.

Appendix A

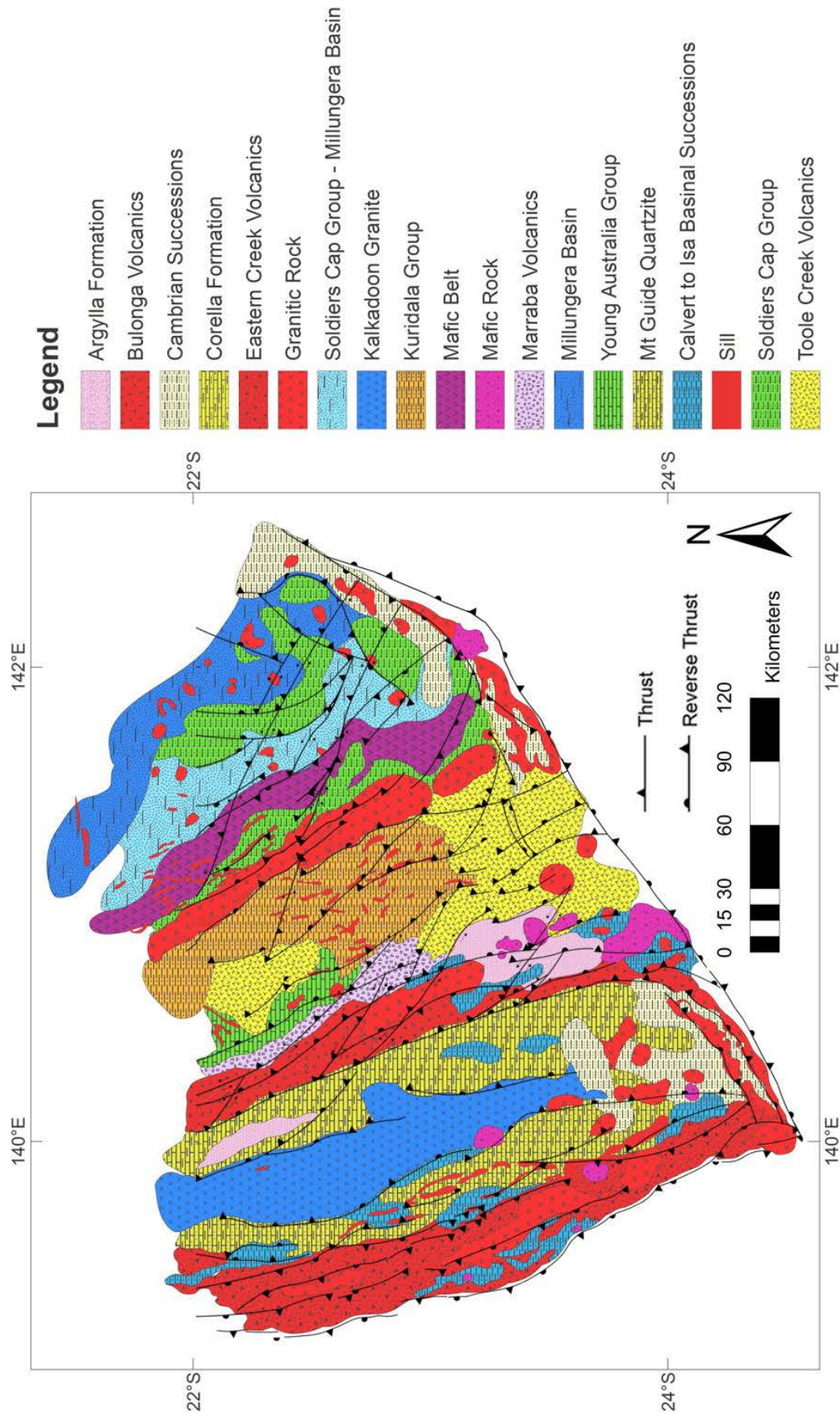
Compilation of maps of the southern Mount Isa terrane and the Thomson Orogen



Map of the geological and geophysical domains of the southern Mount Isa terrane and the Thomson Orogen

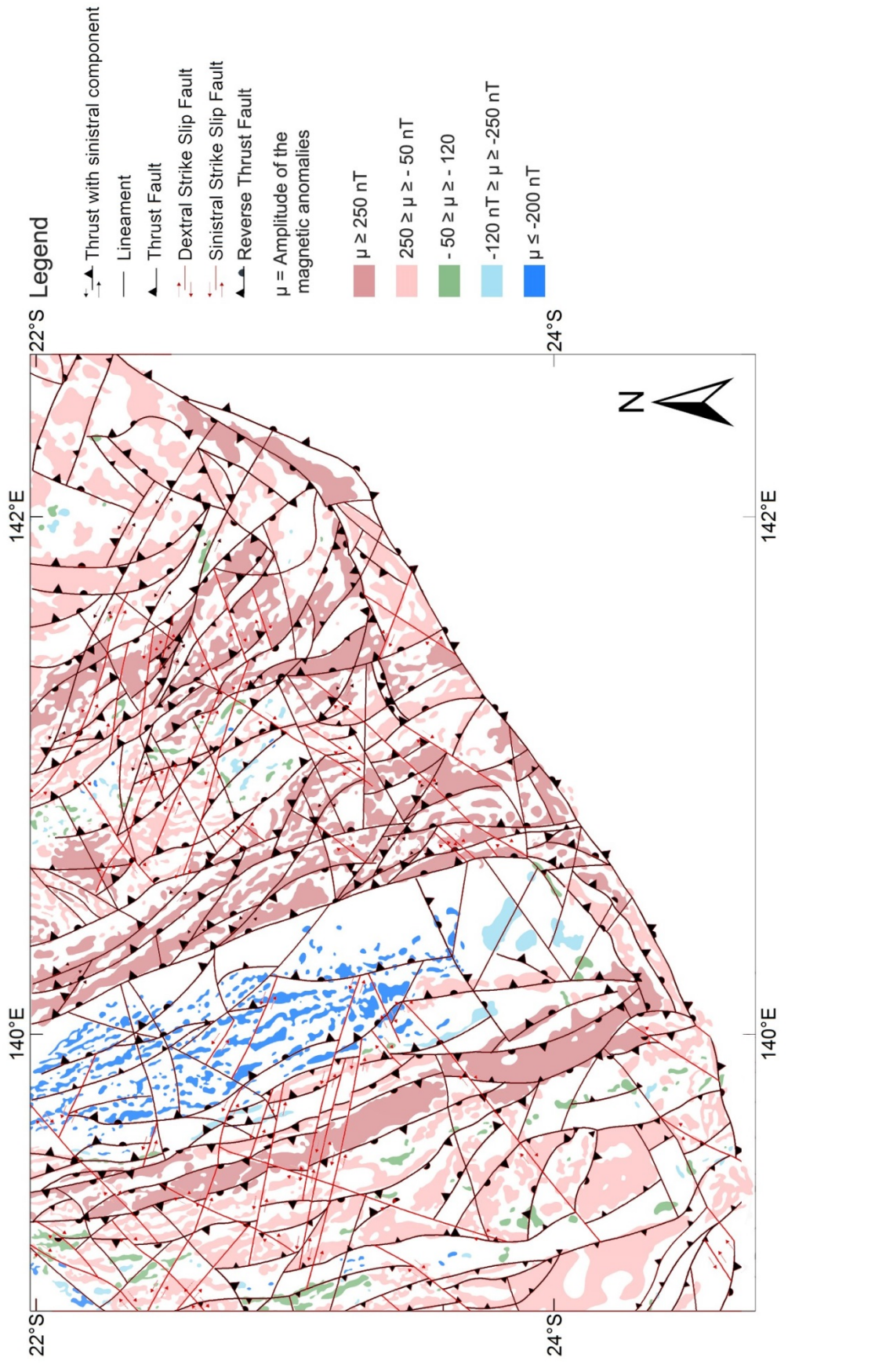


Lithological map and major structures of the Thomson Orogen

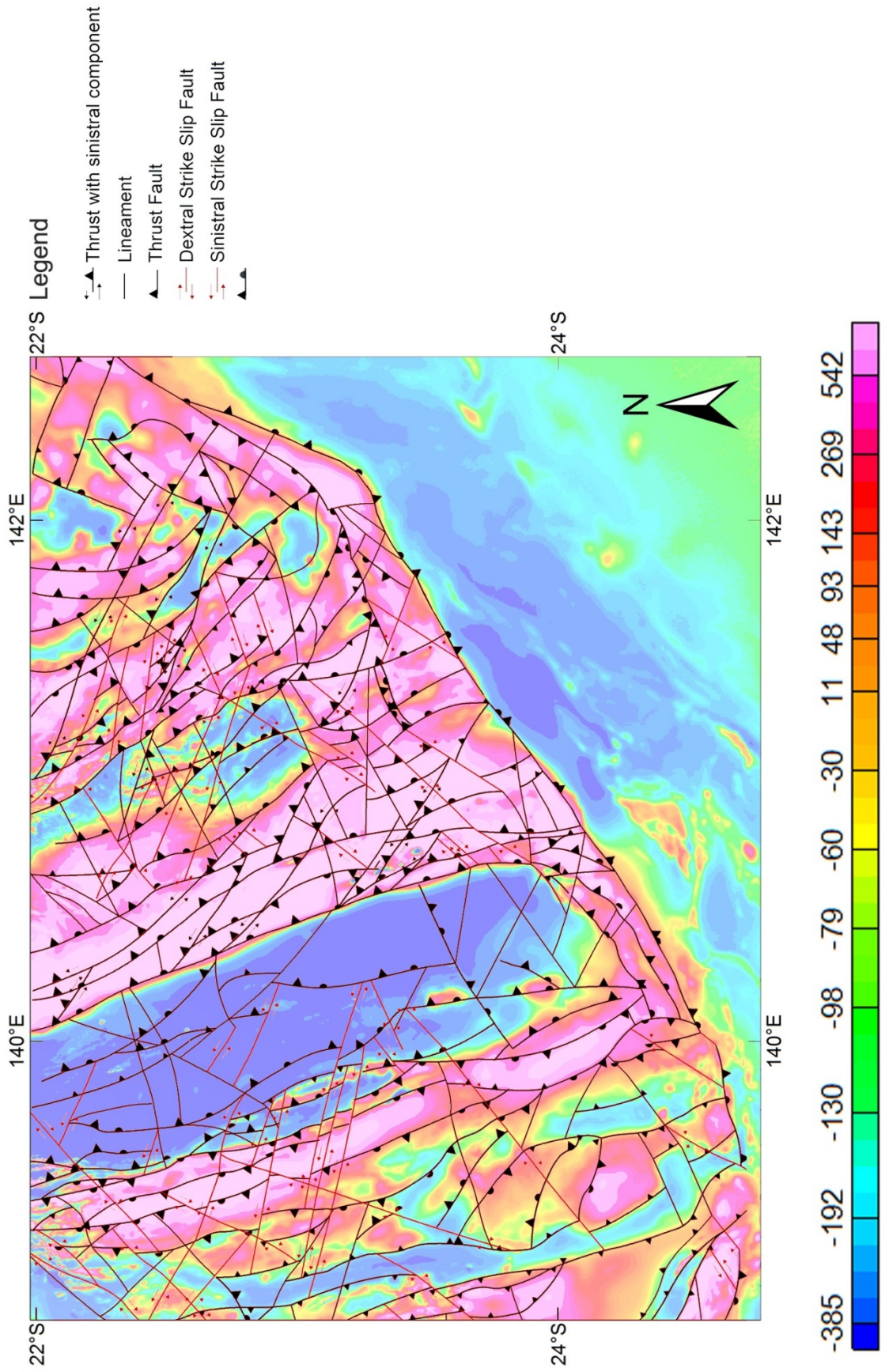


Lithological map and major structures of the southern Mount Isa terrane

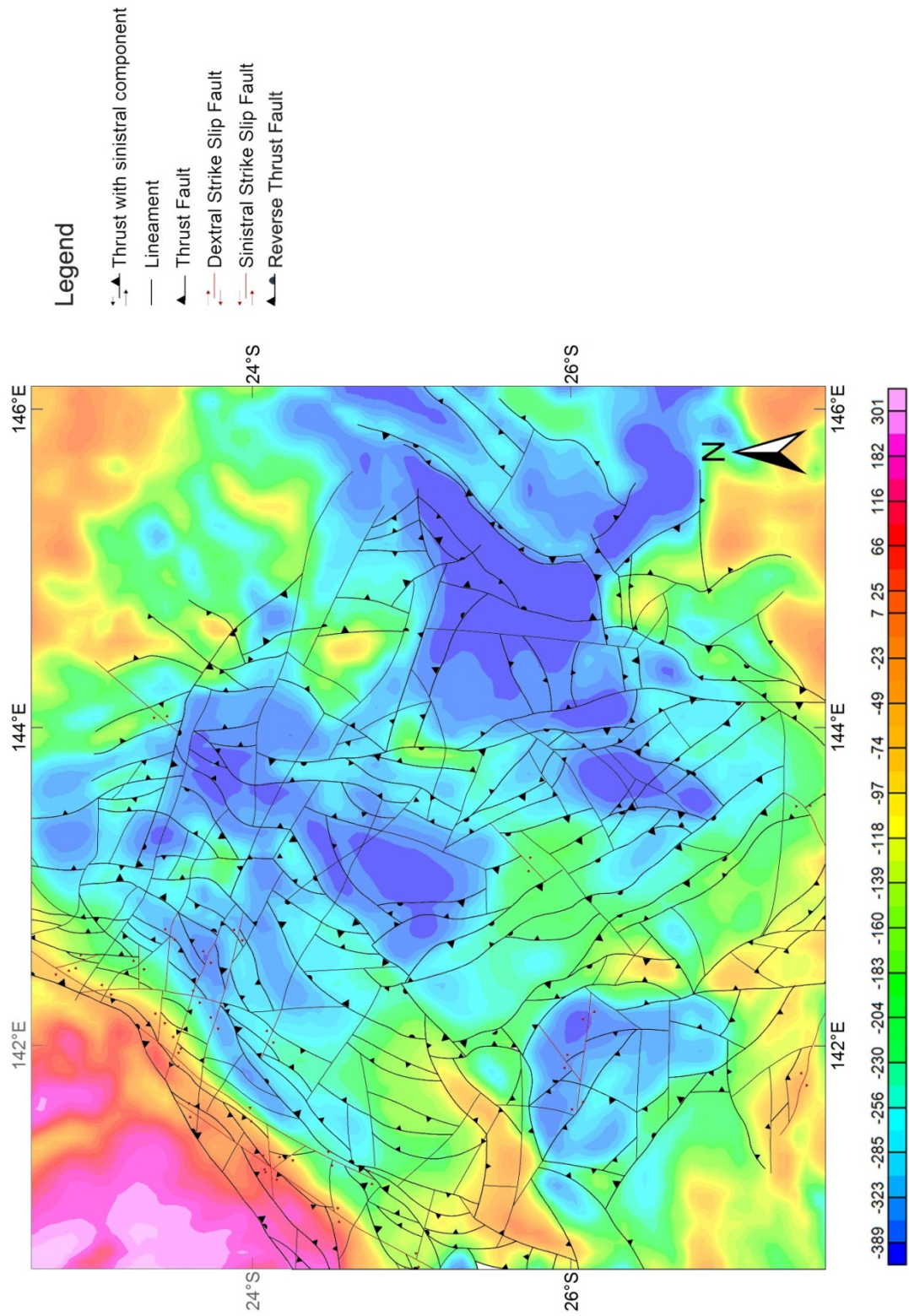
Structural map of the southern Mount Isa terrane



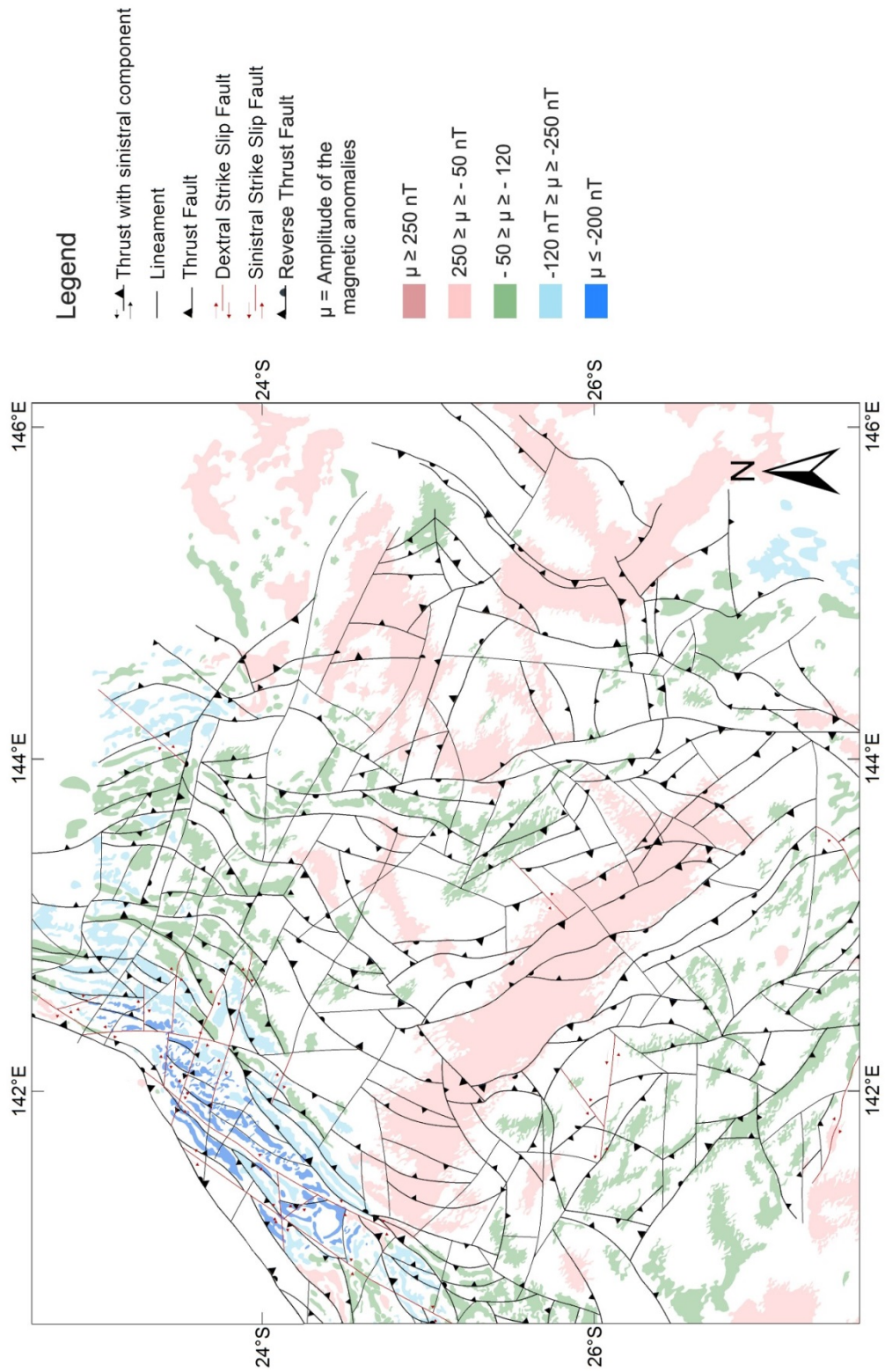
Structural map of the southern Mount Isa terrane



Structural map of the Central Thomson Orogen



Structural map of the Central Thomson Orogen



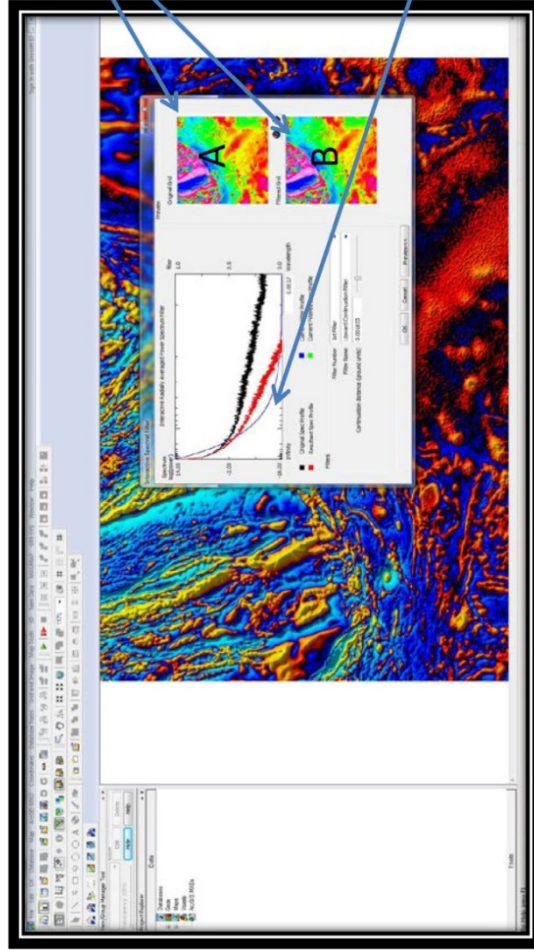
Appendix B

MAGMAP Filters

With Oasis Montaj™ Interactive
Filtering tool

A quick look at the parameters

Oasis Montaj™ Interactive Filtering tool: Useful and easy tool to understand and fully control the filtering parameters during image processing



Preview windows:

A: Original (unfiltered) grid

B: Interactive image view of the filtered grid

Radially averaged power spectrum profile from the original input spectrum file (black line), filtered profile (red line) and filter profile (blue line)

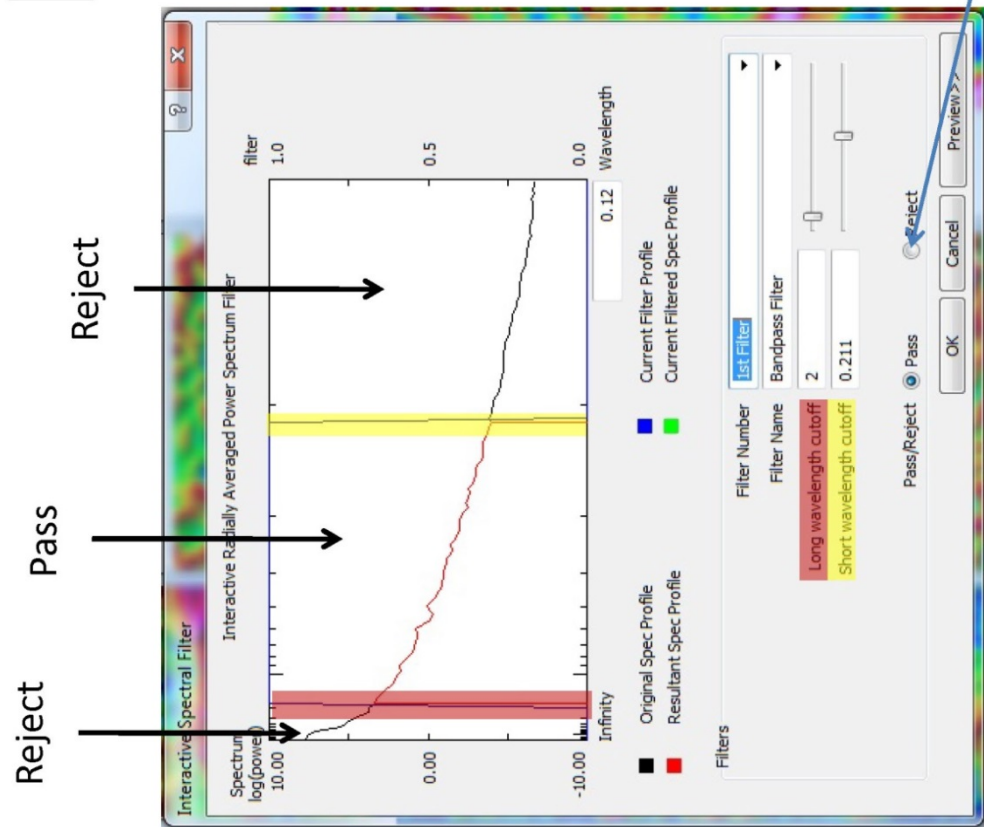
Modify the parameters by moving the parameters sliders or typing values in fields. As changes are made to the filter parameters, the results are iteratively displayed in the preview windows 'B'.

When using the Butterworth filter, the Cosine Roll-off filter or the Gaussian filter, select either the regional or residual button to specify if a residual (high pass filter) or a regional (low pass filter) is required. By default, the system applies a regional filter.

Band-Pass Filter

Features: ideal BPF → abrupt transition at cut-off frequency

Preserve or reject selected wavelengths from the spectrum by scrolling the long and short wavelengths cut-off.



Long wavelength cut-off

When this parameter is set to "infinity"* the longest wavelengths are preserved. Reject undesired long wavelengths (which represent the regional geophysical signal) by scrolling the long wavelength cut-off. A vertical bar (highlighted in red) shows the parts of the spectrum that will be rejected (black line) and preserved (red line).

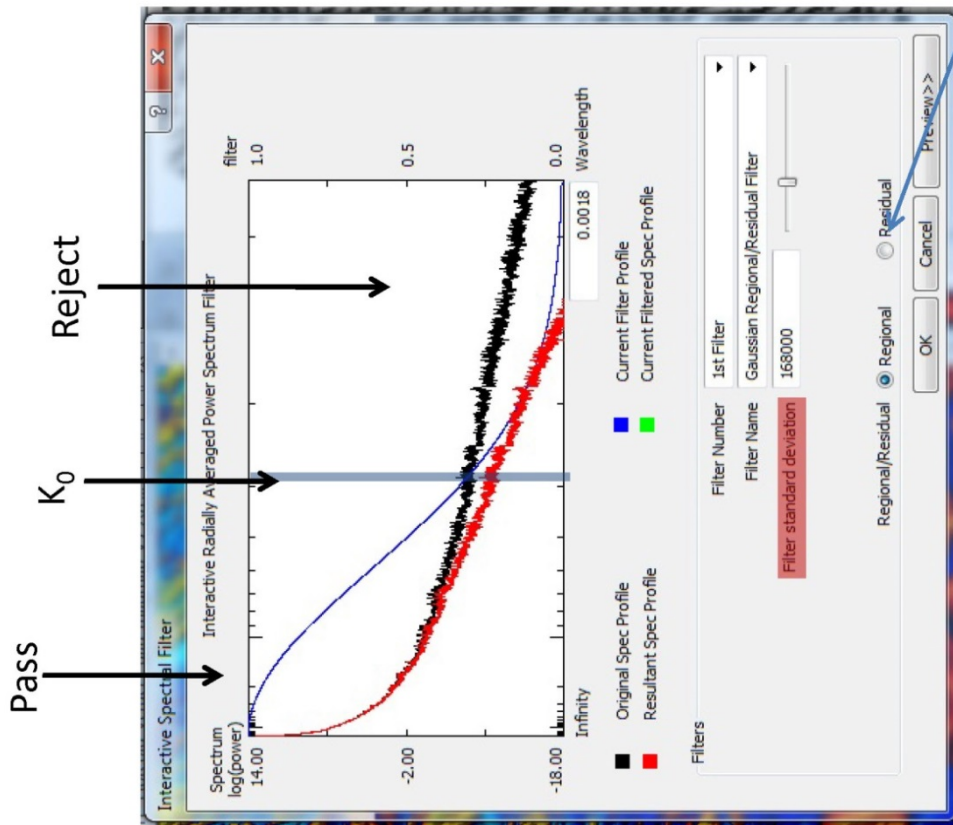
Short wavelength cut-off

If this parameter is set to the lowest wavelength amplitude, the highest wavelengths (which represent the residual geophysical signal) are preserved from the spectrum and the filter behaves as a high pass filter. Reject undesired high wavelengths by scrolling the short wavelength cut-off. A vertical bar (highlighted in yellow) shows the wavelengths that will be rejected (black line) or preserved (red line) from the original spectrum profile.

*The option 'pass' is selected by default and allows preserving the part of the spectrum profile comprised between the long wavelength cut-off and the short wavelength cut-off. On the contrary if the option 'reject' is selected, the filter will reject the part comprised between the long and short wavelengths cut-off, preserving the lowest and highest wavelengths from the spectrum profile.

Gaussian Filter

Features: smooth transition



Filter Standard Deviation

K_0 = Standard deviation of the Gaussian function. It is similar to a cut-off frequency.

The degree of smoothing (therefore the steepness of the filter) is a function of the filter standard deviation

By scrolling the 'filter standard deviation' bar from the lowest values towards 'infinity' the filter cuts the residual signal first, then the regional signal. The steepness increase for increasing standard deviation values.

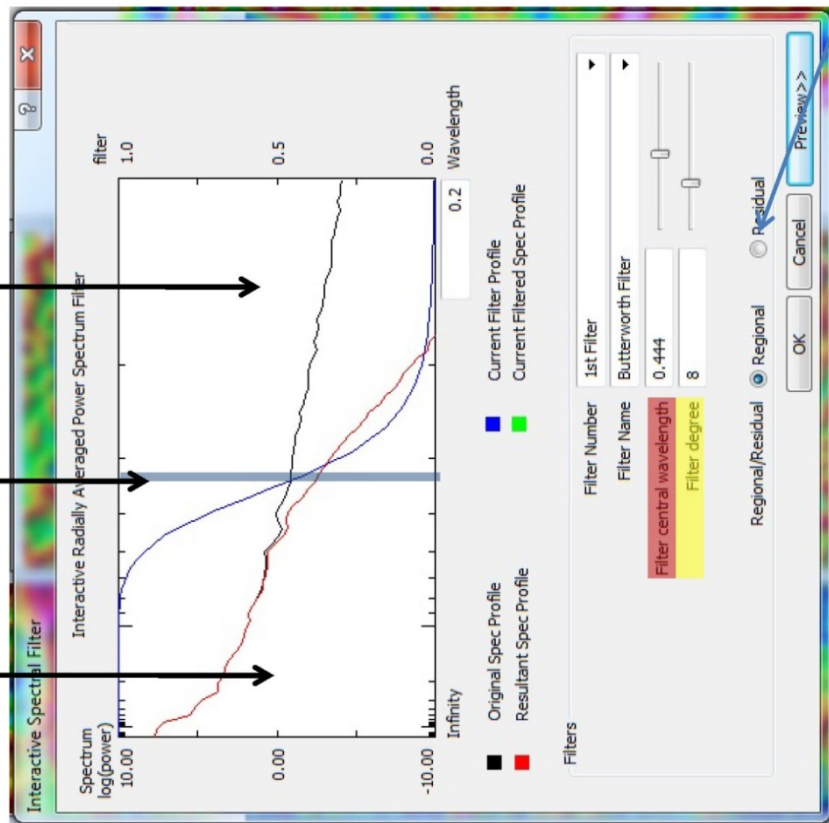
By selecting the option 'regional' the filter behaves as a low pass filter. Select 'residual' is a high pass filter is required.

Butterworth Filter

Features: variable steepness and smooth transition at cut-off frequency

Pass █ **Cut-off frequency**

Reject █



K_0 represents the central wavenumber of the filter

With a low pass filter setting ('regional' button selected), by scrolling the 'filter central wavelength' bar from the lowest wavelengths towards 'infinity', the filter will cut the residual response, then the regional signal.

Filter degree

This parameter is the expression of the steepness at the cut-off frequency and varies from 0 (flat) to 30 (nearly vertical). Scroll the filter degree bar to adjust the steepness of the filter.

For small filter degrees ($n=2,3$) the Butterworth filter resembles a Gaussian filter. Advantage over the Gaussian filter: the cut-off frequency can be set independently from the filter order.

For increasing filter degrees ($n>10$) the Butterworth filter looks like an ideal LPF (and ringing might arise)

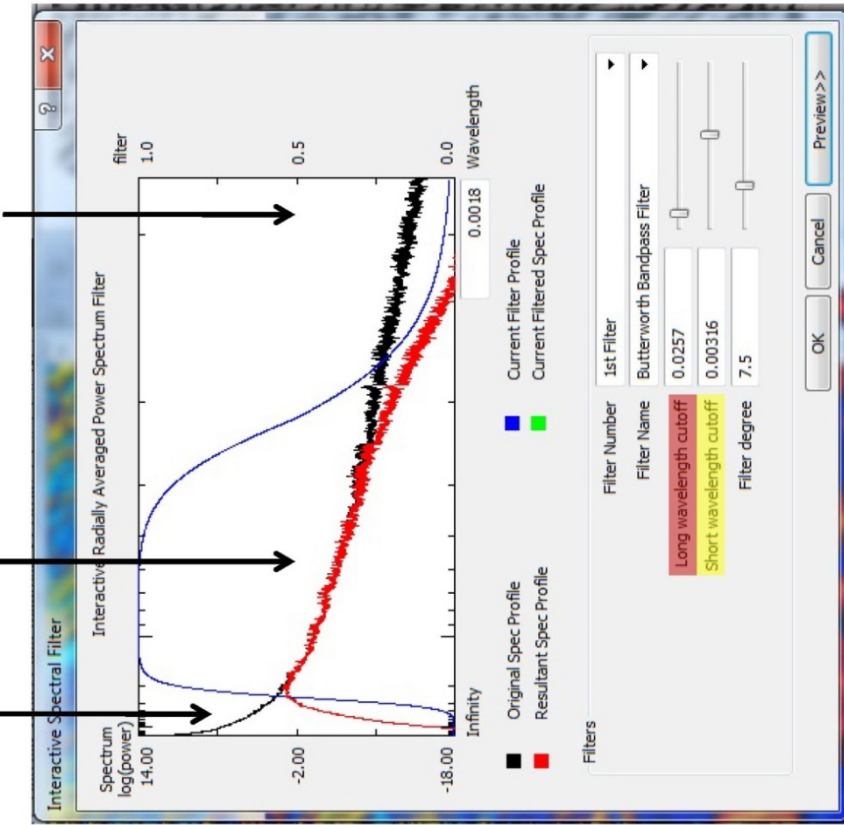
*In this example the option 'regional' is selected by default. The filter preserves the regional geophysical signal from the spectrum profile. By selecting "residual" the filter will reject the longest wavelengths from the spectrum profile preserving the residual signals.

Butterworth Band-Pass Filter

Features: variable steepness and smooth transition at cut-off

frequency

Reject Pass Reject



The parameters are the same as previously described for the Butterworth filter. The Butterworth band-pass filter enables to preserve or reject selected wavelengths from the spectrum profile while adjusting the filter degree.

Long wavelength cut-off

The long wavelength cut-off cuts the regional responses from the spectrum.



Short wavelength cut-off

The short wavelength cut-off cuts the residual signal from the spectrum

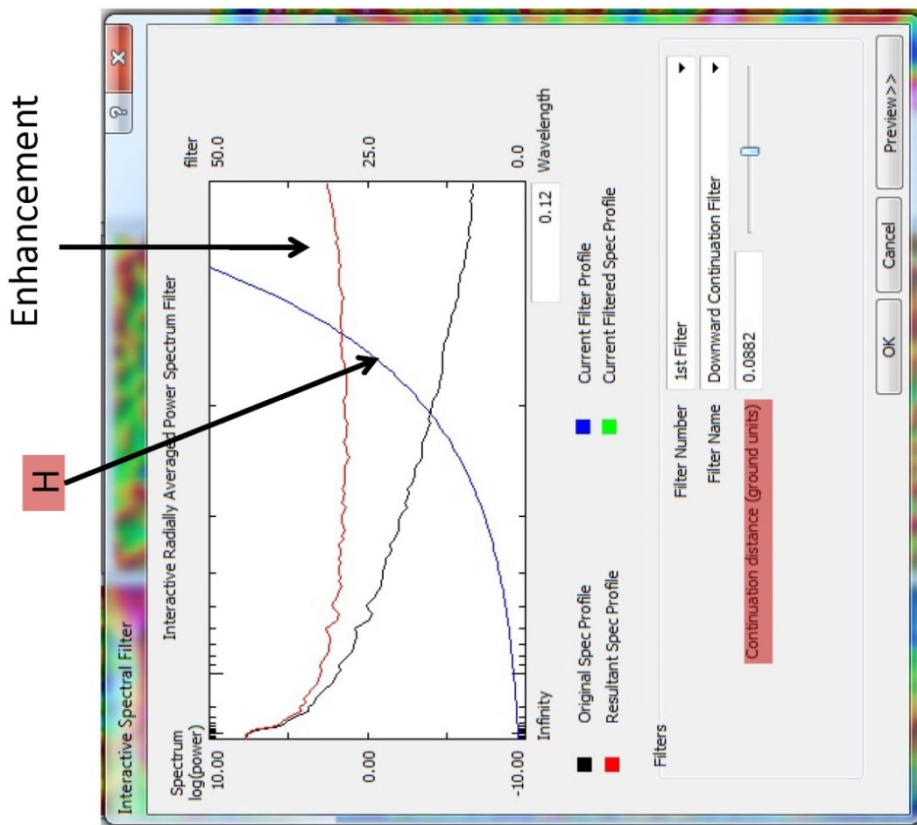


The steepness can be tuned by adjusting the filter degree.

By controlling the degree of roll-off ringing (Gibb's phenomena) can be avoided.

Downward Continuation Filter

Features: it enhances the response from shallow sources by bringing the plane of measurement closer to the source



Continuation distance (H):

This parameter represents the distance in ground units (usually meters) to continue down relative to the plane of observation.

For increasing values the downward continuation filter enhances the high frequency content of the data (see the resultant spectrum profile).

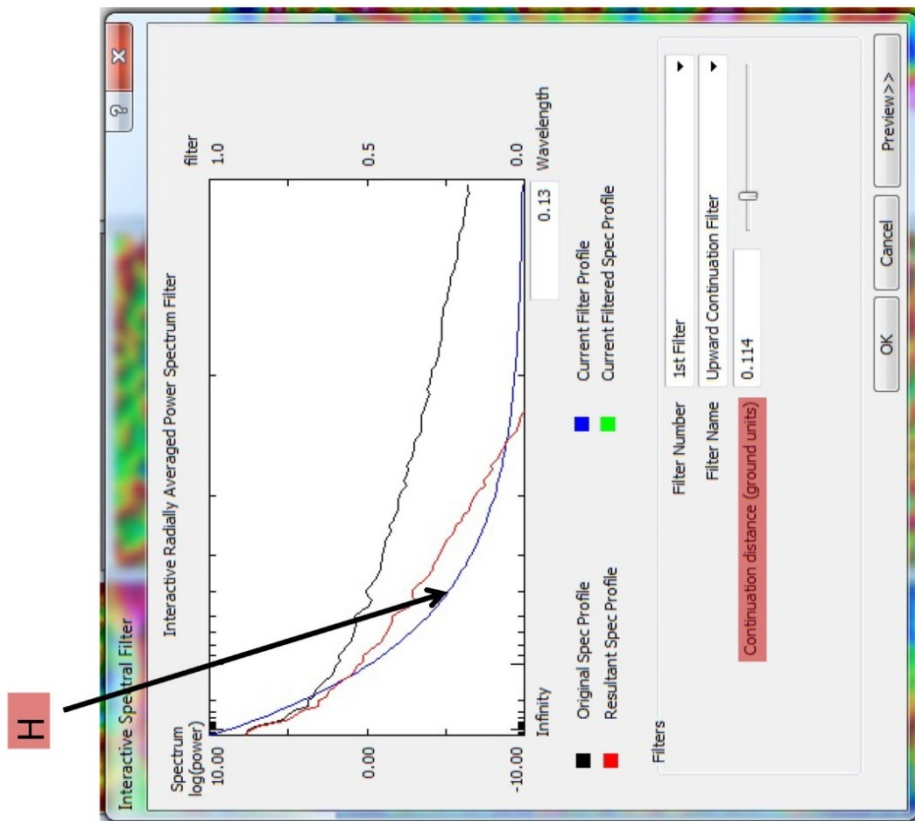
The downward continuation filter is unstable filter and can introduce noise to the grid.

To prevent noise it is recommended to use a low pass filter (i.e. a Gaussian or Butterworth filter) to prevent high magnitude and short wavelength noise in the processed data.

Note: If the plane of continuation is located below the actual potential field sources the results become erratic.

Upward Continuation Filter

Features: it enhances the response from source at a depth by bringing the plane of measurement farther to the source



Continuation distance (H):

This parameter represents the distance in ground units (usually meters) to continue up relative to the plane of observation. For increasing values the filter enhances the regional signal from the spectrum profile (see the resultant spectrum profile).

The upward continuation filter is a low pass filter and do not introduce noise. It extracts the longest wavelengths from the spectrum and minimizes the geophysical response of shallower source bodies.

The upward continuation filter can be used to estimate the regional trends of the geophysical data.

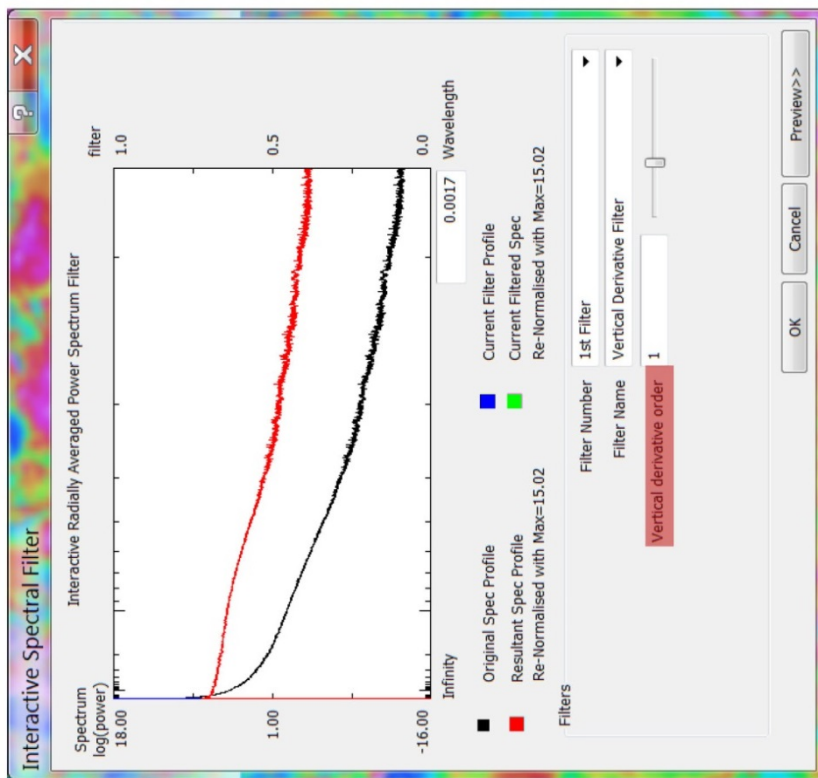
Vertical Derivative Filter

Features: shallow anomalies are enhanced, the shape of source bodies are sharpened

Vertical derivative order

The order of differentiation

The vertical derivative filter is commonly applied to enhance shallow geophysical signal and improve the geometries and boundaries between the source bodies.



Cosine Roll-off Filter

Features: variable steepness, smooth shape, more degrees of freedom if compared to the butterworth and the Gaussian filters

